

**THE PHOTOCHEMISTRY OF ARYLDISILANES
AND THE REACTIVITY OF TRANSIENT SILENES**

by

GREGORY WILTON SLUGGETT, B.Sc.

A Thesis

Submitted to the School of Graduate Studies

in Partial Fulfilment of the Requirements

for the Degree

Doctor of Philosophy

McMaster University

(c) Copyright by Gregory Wilton Sluggett, October 1993

**THE PHOTOCHEMISTRY OF ARYLDISILANES
AND THE REACTIVITY OF TRANSIENT SILENES**

DOCTOR OF PHILOSOPHY (1993)
(Chemistry)

McMASTER UNIVERSITY
Hamilton, Ontario

TITLE: **The Photochemistry of Aryldisilanes and
the Reactivity of Transient Silenes**

AUTHOR: Gregory Wilton Sluggett, B.Sc. (Queen's University)

SUPERVISOR: Professor William J. Leigh

NUMBER OF PAGES: xvii, 200

ABSTRACT

The photochemistry of a homologous series of arylsilanes (**9**, **12**, **34**, and **35**) has been studied in detail by steady state and nanosecond laser flash photolysis (NLFP) techniques. Direct irradiation in hydrocarbon or acetonitrile solution results in competitive formation of the corresponding transient simple silenes by concerted dehydrosilylation, 1,3,5-(1-sila)hexatrienes (silatrienes) by [1,3]-silyl migration, and silyl free radicals by Si-Si bond homolysis. Simple silenes and silatrienes are derived from rearrangements in the disilane lowest excited singlet state and are the major products in hydrocarbon solvents. Silyl free radicals are triplet-derived and are the major products in polar solvents such as acetonitrile. Steady-state photolysis in the presence of acetone affords two products consistent with addition of acetone to the corresponding silatriene: a silyl ether (**56**) from a formal ene reaction, and a 1,2-siloxetane (**57**) from formal [2+2]-cycloaddition. Products consistent with ene reaction of the corresponding simple silenes with acetone are also detected. Arylsilane photolysis in the presence of 2,3-dimethyl-1,3-butadiene (DMB) affords both formal ene- and [2+2]- or [2+4]-addition products of the corresponding silatrienes, while irradiation of oxygen-saturated disilane solutions results in the formation of phenyltrimethylsilane and silanone oligomers. Steady-state photolysis in the presence of methanol affords complex mixtures of at least five primary products, four of which are isomeric products consistent with addition of the trapping reagent to the corresponding silatriene, while the other is the simple-silene adduct. Analogous complex product mixtures are obtained upon photolysis in the presence of a series of other alcohols and methoxytrimethylsilane.

Nanosecond laser flash photolysis of deoxygenated acetonitrile (ACN), isooctane (OCT), or tetrahydrofuran (THF) solutions of aryl-disilanes affords readily detectable transient absorptions in the 300-340 and 400-540 nm ranges which have been assigned to the corresponding silyl radicals (and simple silenes in some cases), and silatrienes, respectively. Silyl radical absorptions are significantly more intense in polar solvents such as ACN compared to hydrocarbons. Simple silenes, silyl radicals, and silatrienes can be detected *selectively* by the addition of the appropriate combination of trapping reagents to the disilane solutions. Increasing phenyl substitution at the silenic silicon atom results in red-shifts in the silatriene absorption maxima consistent with increasing conjugation in the chromophore. The silatrienes form complexes with THF solvent molecules; the equilibrium constant for complex formation is dependent upon the degree of phenyl substitution in the chromophore.

Absolute rate constants for reactions of several silatrienes with carbonyl compounds, alkenes, dienes, oxygen, alkyl halides, dimethyl sulfoxide, and alcohols have been determined by NLFP techniques. Silatriene reactions with acetone, DMB, and oxygen occur via stepwise mechanisms involving rate-determining formation of biradical intermediates which undergo subsequent decomposition to afford the detected products. Silatriene quenching by water, methanol, ethanol, *tert*-butanol, 1-pentanol, and ethylene glycol affords curved quenching plots, while the analogous plots for quenching by 2,2,2-trifluoroethanol, acetic acid, and 1,3-propanediol are linear. The addition of water and methanol are subject to deuterium kinetic isotope effects (KIE's) of 1.7 and 1.9, respectively, while silatriene quenching by acetic acid-*O_d* does not exhibit an observable KIE. These results are consistent with a mechanism which involves rapid, reversible formation of an alcohol/silatriene complex followed by competing, rate-determining, intra- and intermolecular proton transfer.

Direct photolysis of 1,2-di-*tert*-butyl-1,1,2,2-tetraphenyldisilane (**40**) affords *tert*-butyldiphenylsilyl radicals (**41**) exclusively. Bimolecular rate constants for the reactions of *tert*-butyldiphenylsilyl radicals with a variety of alkyl halides, alkenes, dimethyl sulfoxide, and acetone have been determined.

ACKNOWLEDGEMENTS

I would like to take this opportunity to thank several people who have contributed to this thesis:

I would like to thank my supervisor, Professor William Leigh, first and foremost. Willie has always made himself available for assistance, and could always be counted on to provide timely guidance and inspiration in this work. I am proud to say that Willie has been my mentor for the past four years. I hope our professional and personal association continues.

I would like to thank the members of my supervisory committee, Professor Nick Werstiuk and Professor Michael Brook, who gave of their time to attend committee meetings and read this thesis.

Thanks to Mr. Brian Sayer and Dr. Don Hughes for assistance with the operation of the NMR spectrometers and for help with a few experiments, all of which came in the last eight months.

Thanks to NSERC for providing me with a scholarship which made life as a graduate student somewhat less of a financial burden.

Thanks to my former lab-mate, Dr. Mark Workentin, for his help in the lab when I was a "rookie" photochemist and for some electrochemical measurements performed at NRC, Ottawa. But most of all, thanks for your friendship and sharing some extracurricular activities: golf, baseball, beer, etc.

Thanks to Dr. Scott Mitchell for the elemental analysis and also partaking in the extracurriculars.

Al Postigo. Thanks for the "lively" discussions and the Spanish lessons. I'll miss them.

Thanks also to all other current and former labmates in ABB-467: Jo-Ann, Michael, Christine, Johnathan, Nien, Laura, and K.C. who managed to survive my rants and get some chemistry done.

Mom, Dad, Gill, and Gram. Thanks so much for your love and unquestioned support in everything I pursue!

Finally, thanks to my wife, Michele. You know how important all of this is to me. It will work out. I love you, Mich.

TABLE OF CONTENTS

List of Schemes	x	
List of Figures	xi	
List of Tables	xv	
CHAPTER 1: INTRODUCTION		
1.1	Silicon Reactive Intermediates	1
1.2	The Chemistry of Silenes	2
1.2.1	The Physical Properties of Silenes	2
1.2.2	The Generation of Silenes	3
1.2.3	Silene Reactions	7
1.3	The Chemistry of Silyl Radicals	15
1.3.1	Silyl Radical Generation	15
1.3.2	Silyl Radical Reactions	16
1.4	The Photochemistry of Aryldisilanes	18
1.4.1	Photophysical Studies of Phenylidisilanes	18
1.4.2	Mechanistic Aspects of Silene Generation and Reactivity	28
1.5	Objectives of this Work	36
CHAPTER 2: REINVESTIGATION OF THE PHOTOCHEMISTRY OF METHYLPENTAPHENYLDISILANE		
2.1	Introduction	40
2.2	Results	41
2.3	Discussion	64
CHAPTER 3: SOLVENT AND SUBSTITUENT EFFECTS ON THE PHOTOREACTIVITY OF PHENYLDISILANES		
3.1	Introduction	75

3.2	Results	77
3.2.1	The Photochemistry of Phenyldisilanes in Non-Polar and Polar Solvents	77
3.2.2	Triplet Quenching and Sensitization Experiments	81
3.2.3	The Photochemistry of 1,2-Di- <i>tert</i> -butyl-1,1,2,2-tetraphenyldisilane and Hexaphenyldisilane	87
3.3	Discussion	98
 CHAPTER 4: SOLVENT AND SUBSTITUENT EFFECTS ON THE REACTIVITY OF SILATRIENES		
4.1	Introduction	109
4.2	Results	111
4.2.1	Silatriene UV Absorption and THF Complexation	111
4.2.2	Silatriene Reactions with Carbonyl Compounds	114
4.2.3	Reactions with Alkenes and Dienes	122
4.2.4	Reactions with Oxygen	125
4.2.5	Reactions with Alkyl Halides	127
4.2.6	Reactions with Methoxytrimethylsilane (MTMS)	130
4.2.7	Silatriene Reactions with Alcohols	131
4.3	Discussion	142
 CHAPTER 5: SUMMARY AND CONCLUSIONS		
5.1	Contributions of the Study	166
5.2	Future Work	175
 CHAPTER 6: EXPERIMENTAL		
6.1	General	176
6.2	Commercial Solvents and Reagents	177
6.3	Nanosecond Laser Flash Photolysis	179
6.4	Preparation and Characterization of Compounds	180
6.5	Steady-State Photolysis	184

6.5.1	General Methods	184
6.5.2	Quantum Yield Determinations	185
6.5.3	Photoproduct Identification	185
REFERENCES		191

LIST OF SCHEMES

1.1	Silicon Reactive Intermediates	1
1.2	Silene Addition Reactions with σ-Bonded Nucleophiles	9
1.3	Silene Reactions with Dienes and Alkenes	13
1.4	Silene Reactions with Carbonyl Compounds	14
1.5	Molecular Orbital Energies and Correlation Diagram of σ-π Mixing	20
1.6	Schematic Representation of the OICT State in Phenylidisilanes	22
1.7	Conformational Changes Involved in Population of TICT States	23
1.8	Schematic Representation of the $(2p\pi^*, 3d\pi(\text{Si}))^1$ CT State in Phenylidisilanes	23
1.9	Bimolecular Charge-Transfer Reactions of Disilanes	27
1.10	The Photogeneration and Reactivity of Silatrienes	29
1.11	Possible Silatriene Adducts with Unsaturated Compounds	31
1.12	The Photoreactivity of Phenylidisilanes	35
2.1	The Photochemical Reactivity of Methylpentaphenylidisilane in Hydrocarbon Solution	67
2.2	Electron Transfer Quenching of Methylpentaphenylidisilane	70
2.3	Effects of π-Donor and π-Acceptor Substituents on the HOMO and LUMO Energies of Silenes	73
3.1	Phenylidisilane Photochemical Partitioning in Non-Polar Solvents	100
4.1	Biradical Conformational Effects on Silatriene/Acetone Adduct Yields	147
4.2	Silatriene Conformational Effects on Silatriene/Acetone Adduct Yields	148
5.1	The Photoreactivity of Arylidsilanes.	168

LIST OF FIGURES

1.1	Fluorescence emission spectra of 12 in (a) isooctane and (b) acetonitrile solution at 23 ± 2 °C.	21
2.1	^1H NMR spectra of crude mixtures from the photolysis of deoxygenated 0.02 M solutions of 9 in cyclohexane- d_{12} , in the presence of (a) 0.05 M acetone and 0.05 M chloroform, and (b) 0.05 M methanol, at 23 °C to <i>ca.</i> 30% and 40% conversion, respectively. Resonances due to the various products are labelled in the spectra.	43
2.2	Photolysis of deoxygenated cyclohexane solutions of 9 (0.01 M) containing acetone (0.05 M) and varying concentrations of chloroform. (a) Stern-Volmer plot for product 10 . (b) Plot of relative quantum yield for formation of 46 versus chloroform concentration.	48
2.3	(a) Ultraviolet absorption spectrum and (b) fluorescence emission and excitation spectra of 9 in isooctane solution at 23 ± 2 °C.	50
2.4	Stern-Volmer plots for quenching of fluorescence of 9 in cyclohexane solution at 23 ± 2 °C by chloroform (■) and carbon tetrachloride (●).	50
2.5	Time-resolved UV absorption spectra recorded (a) 70-90 ns and (b) 2.8-3.2 μs after 248 nm nanosecond laser flash photolysis of a deoxygenated 1.8×10^{-4} M solution of 9 in acetonitrile at 23 ± 2 °C.	52
2.6	Transient decay traces recorded at (a) 330 nm and (b) 490 nm from 248 nm nanosecond laser flash photolysis of a 1.8×10^{-4} M solution of 9 in acetonitrile at 23 ± 2 °C.	52
2.7	Transient absorption spectra of (a) triphenylsilyl- (33) and (b) methyl-diphenylsilyl radicals (44), from nanosecond laser flash photolysis (337 nm) of solutions of triphenylsilane (10) and methyl-diphenylsilane (43), respectively in 1:4 BOOB/isooctane at 23 ± 2 °C.	54
2.8	Time-resolved absorption spectrum recorded 120-160 ns following NLFP (248 nm) of a 1.7×10^{-4} M solution of 9 in ACN containing 0.1 M 2-bromopropane.	55

2.9	Transient absorption spectrum recorded 40-80 ns following laser excitation from NLFP of an oxygen saturated 3.1×10^{-3} M ACN solution of 1,1-diphenylsilacyclobutane at 23 ± 2 °C.	55
2.10	Transient absorption spectra recorded by NLFP, 10-200 ns after 248 nm laser excitation of deoxygenated OCT (a-c) and ACN (d-f) solutions of 12, 34, and 35.	58
2.11	Transient decay traces recorded at (a) 320 and (b) 460 nm following NLFP (248 nm) of a <i>ca.</i> 0.001 M solution of 34 in deoxygenated acetonitrile at 23 ± 2 °C.	59
2.12	Transient absorption spectrum recorded 160-320 ns after laser excitation (248 nm) from NLFP of a deoxygenated 1.3×10^{-4} M solution of 39 in isooctane at 23 ± 2 °C.	59
2.13	Transient UV absorption spectra, recorded by nanosecond laser flash photolysis of 1.8×10^{-4} M solutions of 9 in OCT under the following conditions: (a) deoxygenated solution; (b) partially oxygenated solution containing 0.05 M chloroform; (c) oxygenated solution; (d) deoxygenated solution containing 0.06 M acetone. The spectra were recorded 100-500 ns after 248 nm laser excitation, and were corrected for minor, long-lived residual absorption at $\lambda < 320$ nm.	63
3.1	Fluorescence emission spectra recorded from (a) OCT and (b) ACN solutions of 34 at 23 ± 2 °C.	78
3.2	Transient absorption spectra recorded 0-40 ns after 248 nm laser excitation of deoxygenated 5.5×10^{-4} M THF solutions of 35 in the absence (—) and presence (.-.-) of <i>trans</i> -piperylene (0.067 M). The absorption bands due to silatriene 38 and triphenylsilyl radical 33 are labelled. The latter spectrum is actually <i>ca.</i> 3.5 times less intense than is shown, but this is accounted for by screening of the excitation light by the diene.	85
3.3	Stern-Volmer quenching plot of the yield of triphenylsilyl radicals (33), measured by the relative initial optical densities at 328 nm and 490 nm, obtained by NLFP of THF solutions of 35 containing different	86

	concentrations of <i>trans</i> -piperylene.	
3.4	Stern-Volmer quenching plot from the photolysis ($\lambda > 265$ nm) of deoxygenated 0.01 M solutions of 40 in cyclohexane containing 0.1 M chloroform and <i>trans</i> -piperylene (0-0.1 M).	90
3.5	(a) Transient absorption spectrum, recorded 40-80 ns after the laser pulse, from NLFP of a deoxygenated 1.2×10^{-4} M solution of 40 in isooctane solution at 23 ± 2 °C. (b) A representative transient decay trace recorded at 305 nm under the same conditions.	91
3.6	Plots of k_{decay} of radical 41 versus quencher concentration, for reaction of several alkyl halides listed in Table 3.5: A, CCl ₄ ; B, <i>tert</i> -butyl bromide; C, 2-bromopropane; D, chloroform.	94
3.7	(a) Transient absorption spectrum, recorded 150-400 ns after the laser pulse, from NLFP of a deoxygenated 8×10^{-5} M solution of hexaphenyldisilane (32) in isooctane at 23 ± 2 °C. (b) Transient absorption spectrum recorded under similar conditions in the presence of 0.07 M acetone.	97
4.1	Transient absorption spectra recorded by NLFP, 10-200 ns after 248 nm laser excitation of deoxygenated THF solutions of (a) 12 , (b) 34 , and (c) 35 .	112
4.2	Transient absorption spectra from NLFP of deoxygenated solutions of 12 in ACN, THF, and 5% THF/ACN at 23 ± 2 °C.	113
4.3	¹ H NMR spectrum (500 MHz; δ -0.4-6.4 region) of a crude mixture from photolysis of a deoxygenated, 0.05 M solution of 35 in cyclohexane containing 0.05 M acetone to <i>ca.</i> 50% conversion, after evaporation of solvent and redissolution in CDCl ₃ . Resonances due to protons in 35 (•), 56c (↓), and 57c (⋈) are labelled. The spectrum has been expanded to reveal the weak signals in the δ 2.9-6.0 region.	116
4.4	¹ H- ¹³ C Heteronuclear shift correlation NMR spectrum of the same photolysis sample used in Figure 4.3. Resonances due to carbons in 35 (•), 56c (↓), and 57c (⋈) are labelled.	117
4.5	Plots of k_{decay} versus quencher concentration for reactions of silatrienes	120

	13, 37, and 38 with acetone in isooctane (OCT) solution at 23 ± 2 °C.	
4.6	Plots of k_{decay} versus quencher concentration for reactions of silatrienes 13 and 37 with CCl_4 in acetonitrile (ACN) solution at 23 ± 2 °C.	128
4.7	^1H NMR spectrum of the crude mixture from photolysis of a deoxygenated 0.05 M C_6D_{12} solution of 35 containing 0.05 M methanol to <i>ca.</i> 50% conversion.	135
4.8	Plots of k_{decay} versus quencher concentration for quenching of 38 with acetic acid (HOAc) and trifluoroethanol (TFE) in acetonitrile (ACN) solution at 23 ± 2 °C.	136
4.9	Plots of k_{decay} versus quencher concentration for reactions of 37 with methanol (MeOH) and methanol- <i>Od</i> (MeOD) in acetonitrile (ACN) solution at 23 ± 2 °C.	137

LIST OF TABLES

1.1	A Comparison of the Physical Properties of Silene and Ethylene.	3
1.2	Relative Rates of Diels-Alder Additions of Dienes to $\text{Me}_2\text{Si}=\text{C}(\text{SiMe}_3)_2$.	12
1.3	Bond Dissociation Energies of Substituted Alkanes and Silanes.	16
1.4	UV Absorption Data of Mono- and Disilanes.	18
2.1	Product Yields from the Photolysis of Methylpentaphenyldisilane (9) in the Presence of 0.05 M Acetone and Various Additives.	44
2.2	Relative Quantum Yields for Formation of 10, 45, 46, and 47 from the Photolysis of Deoxygenated Solutions of 9 in Chloroform/Cyclohexane Mixtures Containing 0.05 M Acetone.	47
2.3	Rate Constants for Bimolecular Quenching of Silatrienes 13 and 50 by Oxygen, Acetone, Ethyl Acetate, Cyclohexene, DMB, 1,1,1-Trifluoroethanol, and Acetic Acid in ACN Solution at 23 ± 2 °C	62
3.1	Charge-Transfer Fluorescence Emission Maxima from OCT and ACN Solutions of 12, 34, and 35 at 23 ± 2 °C.	78
3.2	Product Yields from the Photolysis of 0.05 M Cyclohexane-d_{12} Solutions of Disilanes 12, 34, and 35 in the Presence of Acetone (0.05 M).	79
3.3	Product Yields from Photolysis of 0.05 M ACN-d_3 Solutions of 12, 34, and 35 Containing 0.05 M Acetone in the Presence and Absence of Chloroform.	82
3.4	Product Yields from Acetone- and Benzene-Sensitized Photolyses of 1,1,1-Trimethyl-2,2,2-triphenyldisilane (35).	83
3.5	Bimolecular Rate Constants for Quenching of <i>tert</i>-Butyldiphenylsilyl (41), Triethylsilyl, and Triphenylsilyl (33) Radicals by Alkyl Halides, Alkenes, and Acetone in Deoxygenated Isooctane (OCT) solution at 23 ± 2 °C.	95

4.1	Rate Constants for Reaction of Silatrienes 13 , 13-<i>d</i>₅ , 37 , and 38 with Acetone, Acetone- <i>d</i> ₆ , and Ethyl Acetate (EtOAc) in Acetonitrile (ACN), Tetrahydrofuran (THF), and Isooctane (OCT) solution at 23 ± 2°C.	121
4.2	Product Yields from the Photolysis of 0.05 M Cyclohexane- <i>d</i> ₁₂ Solutions of Disilanes 12 , 34 , and 35 in the Presence of DMB (0.06 M) to <i>ca.</i> 80% Conversion.	123
4.3	Rate Constants for Reaction of Silatrienes 13 , 13-<i>d</i>₅ , 37 , and 38 with DMB and Cyclohexene in Tetrahydrofuran (THF), and Isooctane (OCT) solution at 23 ± 2°C.	124
4.4	Rate Constants for Reaction of Silatrienes 13 , 13-<i>d</i>₅ , 37 , and 38 with Oxygen in Acetonitrile (ACN), Tetrahydrofuran (THF), and Isooctane (OCT) solution at 23 ± 2°C.	126
4.5	Rate Constants for Reaction of Silatrienes 13 , 37 , and 38 with Carbon Tetrachloride (CCl ₄) and Chloroform (CHCl ₃) in Acetonitrile (ACN) and Isooctane (OCT) Solution at 23 ± 2°C.	129
4.6	Rate Constants for Reaction of Silatrienes 13 , 37 , and 38 with Methanol (MeOH), Methanol- <i>Od</i> (MeOD), Trifluoroethanol (TFE), Acetic Acid (HOAc), and Acetic Acid- <i>d</i> (DOAc) in ACN Solution at 23 ± 2 °C.	138
4.7	Rate Constants for Quenching of Silatrienes 13 and 50 with H ₂ O, D ₂ O, Methanol (MeOH), Ethanol (EtOH), and <i>tert</i> -Butyl Alcohol (<i>t</i> -BuOH) in Acetonitrile (ACN) Solution at 23 ± 2 °C.	139
4.8	Rate Constants for Reaction of Silatrienes 13 , 37 , and 38 with MeOH, 1-Pentanol (C ₅ H ₁₁ OH), Trifluoroethanol (TFE), and Acetic Acid (HOAc) in THF and OCT Solution.	140
4.9	Rate Constants for Reaction of Silatriene 13 with Ethylene Glycol and 1,3-Propanediol in Acetonitrile (ACN) and Tetrahydrofuran (THF) Solution at 23 ± 2 °C.	141
4.10	Rate Constants for Quenching of Silatriene 13 with Methanol (MeOH) in Acetonitrile (ACN) Solution in the Presence of Trifluoroacetic Acid (TFA) or Triethylamine at 23 ± 2 °C.	141

5.1	Chemical Yields of Silatrienes, Simple Silenes, and Silyl Radicals from the Photolysis of Disilanes 9, 12, 34, 35 and 40 in Hydrocarbon Solution.	171
------------	--	------------

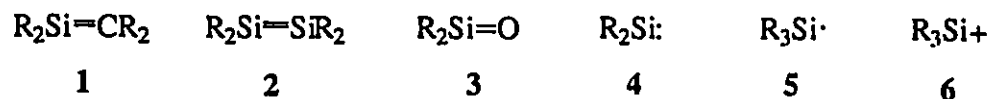
CHAPTER 1

INTRODUCTION

1.1 Silicon Reactive Intermediates

One of the most prominent areas of organosilicon chemistry over the past two decades has been the study of silicon reactive intermediates such as silenes (1),¹⁻⁷ disilenes (2),^{1,8,9} silanones (3),^{1,3,7,10-12} silylenes (4),¹²⁻¹⁴ silyl radicals (5),¹⁵⁻¹⁹ and silyl cations (6)²⁰ (Scheme 1.1). The photolysis of oligosilanes is the most important method for the generation of these short-lived species under mild conditions because it allows the direct examination of their properties by time-resolved techniques and the investigation of their subsequent reactions by chemical trapping experiments.

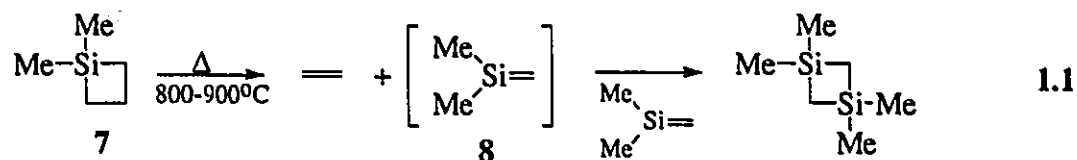
Scheme 1.1 Silicon Reactive Intermediates



1.2 The Chemistry of Silenes

1.2.1 The Physical Properties of Silenes

Prior to the 1967 report by Gusel'nikov and Flowers of the generation of 1,1-dimethylsilene (**8**) from the thermolysis of 1,1-dimethylsilacyclobutane (**7**) (eq 1.1),²¹ many chemists were skeptical of the possible existence of compounds with a silicon-carbon double bond. It was suggested that if silenes could be formed at all they would be highly reactive species.²² The π bond was predicted to be very weak because of poor orbital overlap, differences in energy, and the longer bond distances between adjacent $3p$ and $2p$ orbitals of silicon and carbon, respectively. Most silenes are indeed short-lived reactive intermediates, and over the past 25 years have frequently been postulated as reactive intermediates in the photolysis and thermolysis of organosilicon compounds, usually on the basis of chemical trapping experiments or matrix isolation spectroscopy.



The inherently high reactivity of simple silenes becomes evident upon comparison of the physical properties of the parent silene with those of ethylene (Table 1.1). The silene Si=C bond is considerably longer than the C=C bond which, in addition to its lower infrared stretching frequency and π ionization potential, demonstrates that π bonds of silenes are much weaker than alkene π bonds. The calculated dipole moment indicates that the Si=C bond is polar with partial positive charge on the silicon atom. Silenes also

exhibit dramatic red-shifts in their UV absorption maxima compared to those of alkenes, indicative of a small separation between the highest occupied molecular orbital (HOMO) and the lowest unoccupied molecular orbital (LUMO). These properties of the Si=C bond account for their significantly higher reactivity than alkenes and leads to many reactions which are not characteristic of the C=C bond.

Table 1.1 A Comparison of the Physical Properties of Silene and Ethylene.^a

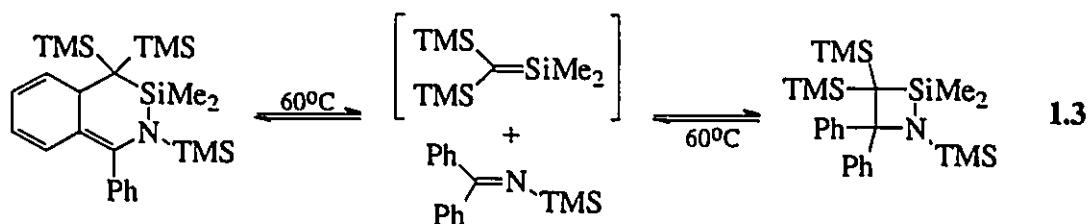
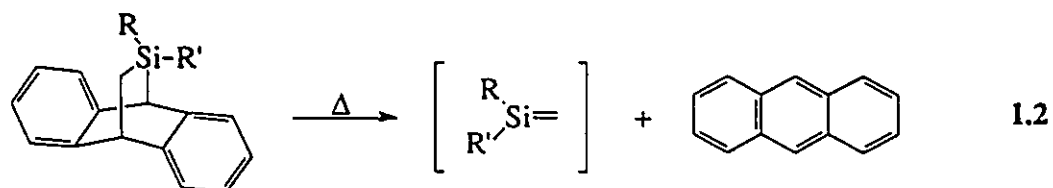
	H ₂ C=CH ₂	H ₂ Si=CH ₂
Bond Length (Å)	1.33	1.70
D	0	0.84
E _π (kcal/mol)	65	38
ν _{X=C} (cm ⁻¹)	1640	985
λ _{max} (nm)	165	258
π-IP (eV)	10.5	8.8

a. Data from reference 1.

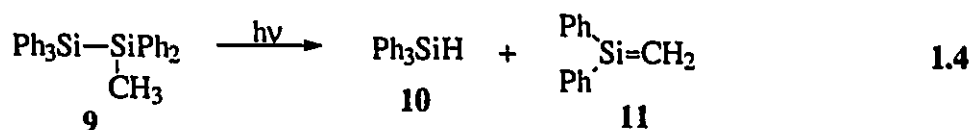
1.2.2 The Generation of Silenes

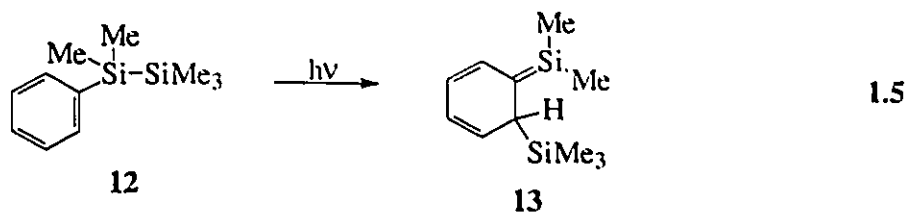
One the most useful thermal and photochemical routes to silenes is [2+2] and [4+2] cycloreversion. Silacyclobutanes are silene sources under pyrolytic (eq 1.1) and photochemical conditions,^{21,23-28} allowing the generation of a wide variety of simple silenes by changing the substitution at silicon. More mild methods include the thermal

retro-Diels-Alder reaction of substituted bicyclo-[2.2.2]-octadienes (eq 1.2),²⁹⁻³⁴ and some [2+2] and [4+2] cycloreversions reported by Wiberg and coworkers (eq 1.3).^{2,35}

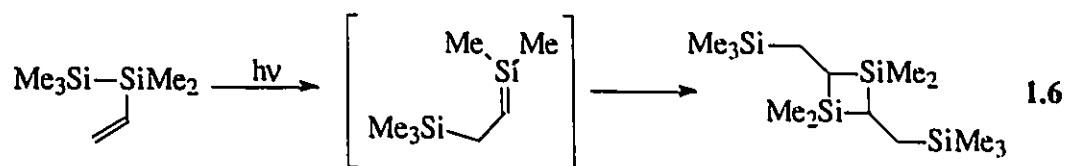


Another class of convenient photochemical precursors to silenes is arylsilylanes. The photolysis of methylpentaphenyldisilane (**9**) yields triphenylsilane (**10**) and 1,1-diphenylsilene (**11**) (eq 1.4),³⁶ while irradiation of pentamethylphenyldisilane (**12**) generates a conjugated 1,3,5-(1-sila)-hexatriene (**13**) (eq 1.5).^{4,14,37-41} The formation of these transient silenic compounds was suggested on the basis of chemical trapping experiments.

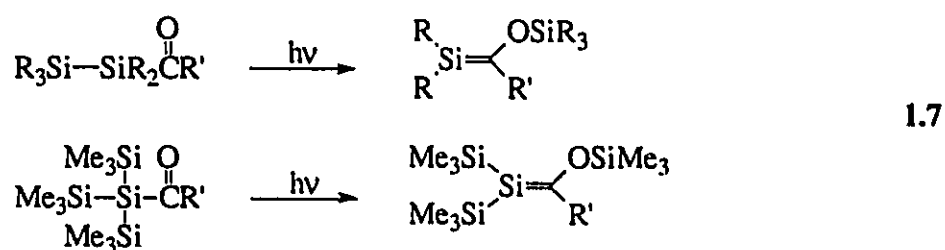




The photolysis of simple alkyl vinyldisilanes, such as pentamethylvinylidisilane (eq 1.6), results in a [1,3]-Si shift to the remote carbon atom of the alkenyl group to form a reactive silene which, in the absence of silene trapping agents, undergoes head-to-tail dimerization.⁴²⁻⁴⁴

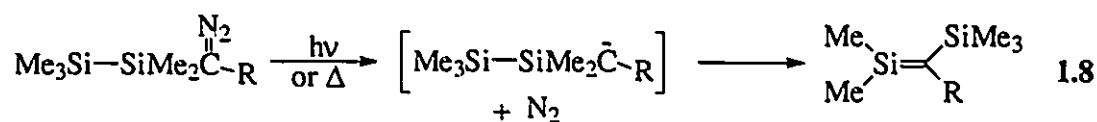


Brook and coworkers have reported that acyldisilanes and acylpolysilanes are photochemical precursors to stabilized silenes.⁴⁵⁻⁴⁸ Upon irradiation, these compounds undergo clean [1,3]-Si shifts to the oxygen atom to yield silenes (eq 1.7). The silenes are stable when R' is a bulky substituent such as 1-adamantyl or mesityl.

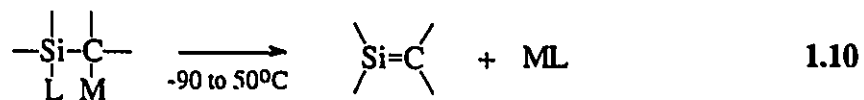


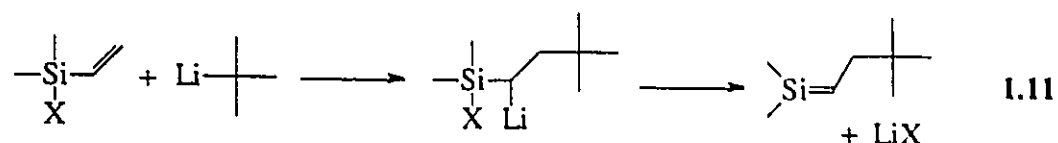
Another important route to silenes is the thermal or photochemical isomerization of silylcarbenes and alkylsilylenes. Ando and coworkers have demonstrated that the

photolysis or thermolysis of substituted silyldiazoalkanes yields α -silylcarbenes which thermally rearrange to silenes (eq 1.8).^{49,50} Michl and West have reported that the 450 nm photolysis of dimethylsilylene (**15**), generated from the 254 nm photolysis of dodecamethylcyclohexasilane (**14**) at 35 K, causes a [1,2]-H shift to yield 1-methylsilene (**16**) (eq 1.9).⁵¹



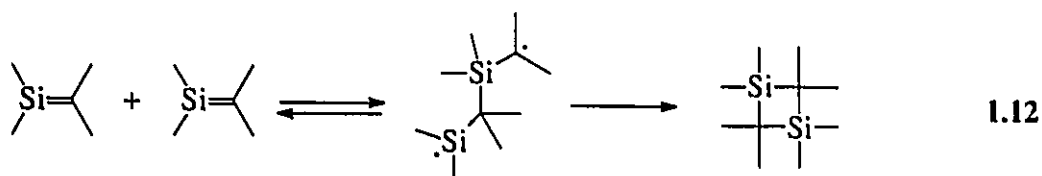
Silenes are also generated by 1,2-elimination reactions from adjacent silicon and carbon atoms. The precursor molecule usually has a metal atom (usually M = lithium) attached to carbon and a leaving group (e.g. L = halide, sulfide, phosphate) attached to silicon (eq 1.10). Wiberg has studied the reaction in detail and has used this method to prepare stabilized silenes.^{2,35,52,53} Jones and coworkers have reported the generation of silenes by addition of *tert*-butyl lithium to vinylchloro- or vinylfluorosilanes followed by 1,2-elimination of LiX (eq 1.11).^{30,33,54}



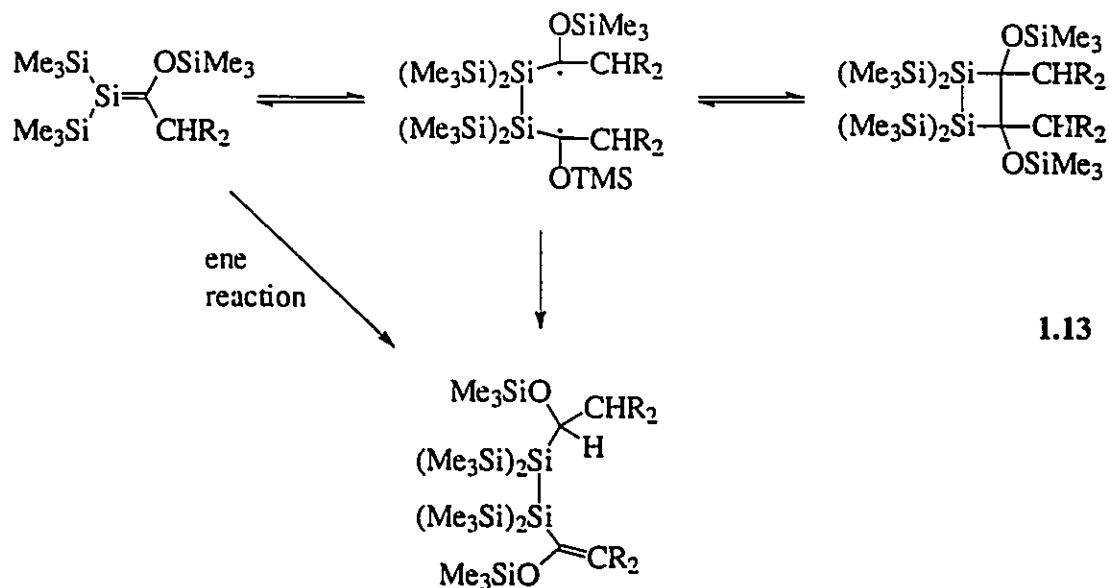


1.2.3 Silene Reactions

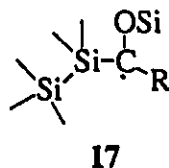
In the absence of trapping reagents, silenes undergo dimerization and oligomerization. The dimerization of 1,1-dimethylsilene (8) was the first known silene reaction as reported by Gusev'nikov and Flowers (eq 1.1).²¹ Head-to-tail dimers are normally observed for simple silenes due to the polarized nature of the silicon-carbon double bond. The dimerization of the parent silene has recently been reported to occur via a stepwise mechanism involving a 1,4-biradical analogous to the dimerization of ethylene (eq 1.12).⁵⁵



Head-to-head silene dimerization occurs for silenes which contain particularly polar or bulky substituents. For example, Brook has reported that stabilized silenes undergo head-to-head dimerization when the alkyl substituent is relatively small to yield 1,2-disilacyclobutanes (eq 1.13).⁵ If the alkyl group contains an allylic hydrogen, linear dimers are also formed; these are formally the products of an ene type cycloaddition reaction. No dimers are formed at all when the alkyl substituent is sufficiently bulky (e.g. 1-adamantyl, CEt₃, 1-methylcyclohexyl); i.e. these silenes are "stable".



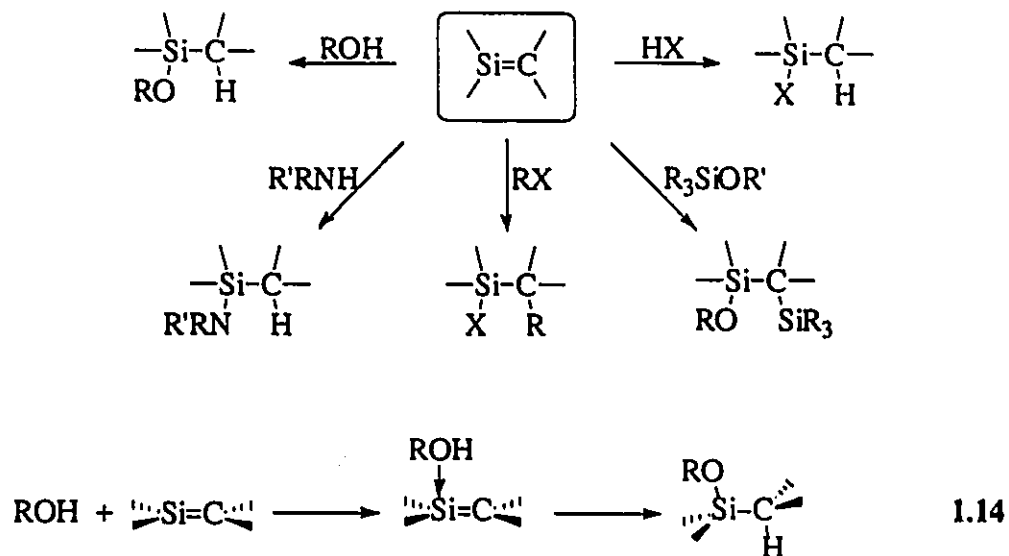
It has been suggested that the siloxy substituent reduces the overall polarization of the Si=C bond in these compounds, leading to predominant head-to-head dimerization via a biradical pathway.^{5,56} Support for this biradical mechanism is provided by the observation of a persistent ESR signal consistent with a carbon centred radical of structure **17** for each of these "stable" monomeric silenes.⁵⁷

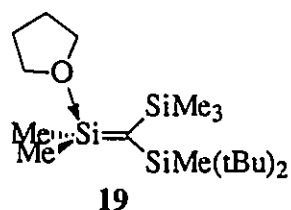


Nucleophilic σ -bonded reagents such as alcohols, hydrogen halides, alkyl halides, amines, and alkoxy silanes undergo addition to silenes as outlined in Scheme 1.2. Wiberg has reported that the rate of the reaction of 1,1-dimethyl-2,2-bis(trimethylsilyl)silene (**18**)

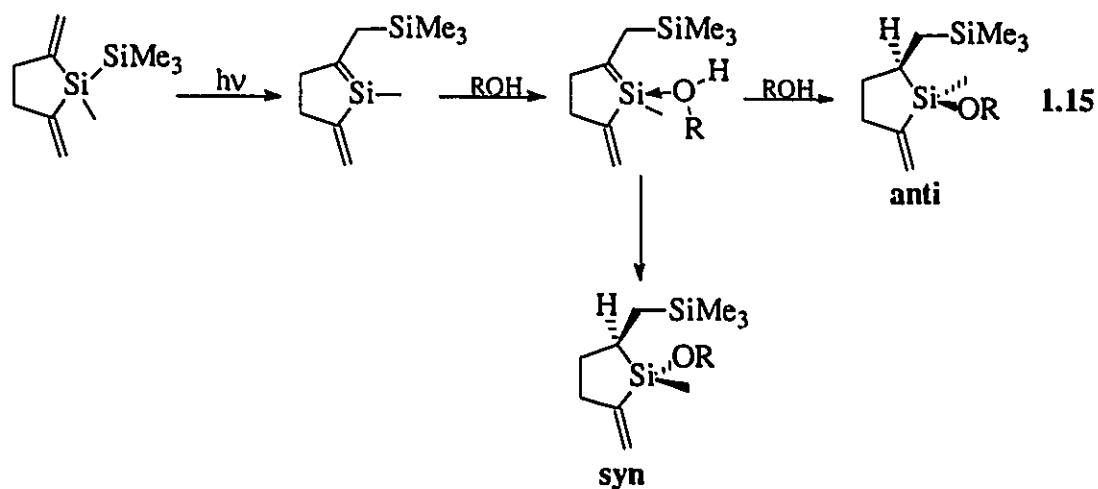
with alcohols depends on the nucleophilicity and steric bulk of the alcohol: methanol > ethanol > 2-propanol > *tert*-butanol > 1-pentanol > cyclohexanol > phenol.² Similar trends were observed for a series of substituted amines; the relative rate of addition was proportional to the nucleophilicity of the amine. It was also shown that for Lewis bases of equal steric bulk, the reagent with the higher nucleophilicity reacts more rapidly; e.g. 2-propylamine reacts twice as fast as 2-propanol. Wiberg has also noted that methanol-*O**d* adds at the same rate as methanol.² These results led to the conclusion that the mechanism of alcohol addition involves nucleophilic attack of the alcohol molecule to form a complex, in which the oxygen atom acts as a Lewis base and the silicon atom acts as the Lewis acid, followed by fast proton-transfer to the carbon atom (eq 1.14). Additional evidence for this mechanism was obtained with the isolation and crystal structure of a stable silene/tetrahydrofuran (THF) adduct (19).⁵²

Scheme 1.2 Silene Addition Reactions with σ -Bonded Nucleophiles



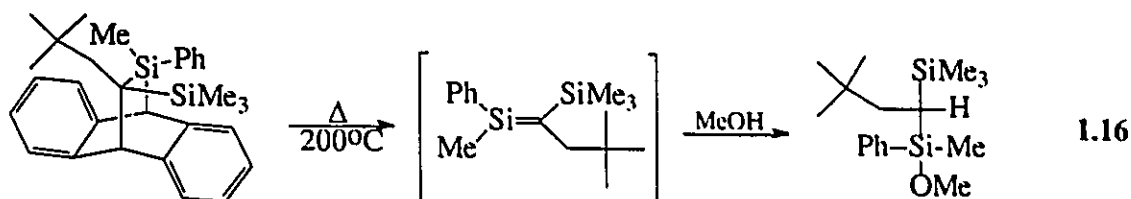


Recently, Sakurai and coworkers have also suggested a two-step mechanism for the addition of alcohols to a cyclic silene (eq 1.15).⁵⁸ They explained the *syn/anti* ratio of product alkoxy-silanes in terms of competition between intracomplex proton transfer and proton transfer assisted by a second alcohol molecule. Intracomplex proton transfer would be expected to yield the *syn* isomer while bimolecular proton transfer would yield the *anti* isomer.



The stereochemistry of alcohol addition to silenes appears to vary from system to system. Brook has reported that the addition of methanol to "stable" silenes gives a mixture of two diastereomers⁵⁹ consistent with the two-step addition mechanism outlined in eq 1.14. Sakurai also has suggested a stepwise non-stereospecific alcohol addition mechanism (eq 1.15).⁵⁸ However, Jones and coworkers have reported the stereospecific

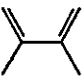
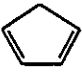
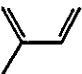
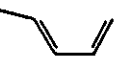
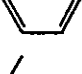
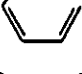
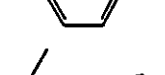
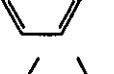
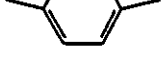
additions of methanol and Me_3SiOMe to Z-1-methyl-1-phenyl-2-neopentylsilene (eq 1.16), suggesting a concerted mechanism in this case.³⁰



Another classic silene reaction is [4+2] cycloaddition to dienes to generate Diels-Alder and ene adducts (Scheme 1.3). Wiberg has studied the effects of diene structure on the relative rate of Diels-Alder addition to **18** (Table 1.2) and on the relative yields of the Diels-Alder and ene adducts.² Electron-rich dienes such as 2,3-dimethyl-1,3-butadiene (DMB) react more rapidly than electron-poor ones. Steric effects are also important since the presence of terminal methyl groups slows down the Diels-Alder reaction. Only the ene adduct is observed in the reaction of 2,5-dimethyl-2,4-hexadiene with **18**. The data suggest that silene reactions with dienes may proceed in a concerted manner.

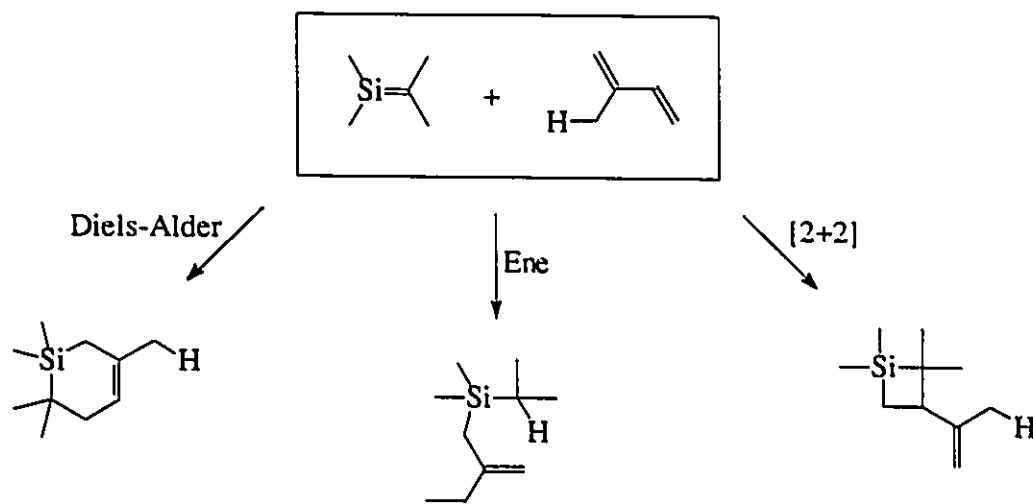
Silenes react with monoolefins to yield ene and [2+2] adducts (Scheme 1.3). For example, **18** reacts with isobutene to produce the corresponding ene product while 1,1-dimethyl-2-neopentylsilene and "stable" 2-siloxy-silenes undergo [2+2] and [4+2] cycloaddition with butadiene. Brook has reported examples of stabilized silenes which react with alkynes in a [2+2] manner.⁵ The [2+2] cycloadducts of "stable" silenes are likely formed via a stepwise mechanism involving biradical intermediates.

Table 1.2 Relative Rates of Diels-Alder Additions of Dienes to $\text{Me}_2\text{Si}=\text{C}(\text{SiMe}_3)_2^{\text{a}}$

Diene	Relative Rate
	100
	77
	66
	42
	27
	2
	2
	0.2
	~0

a. Data from reference 2.

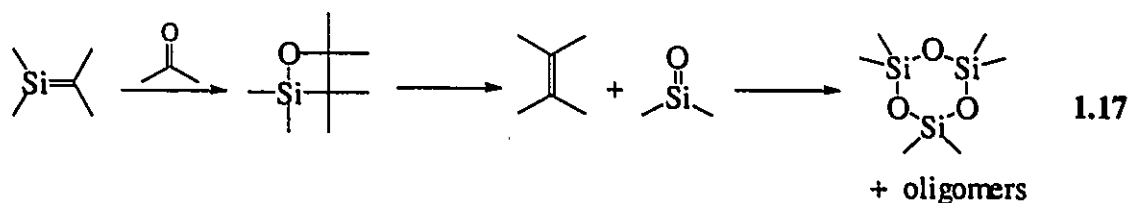
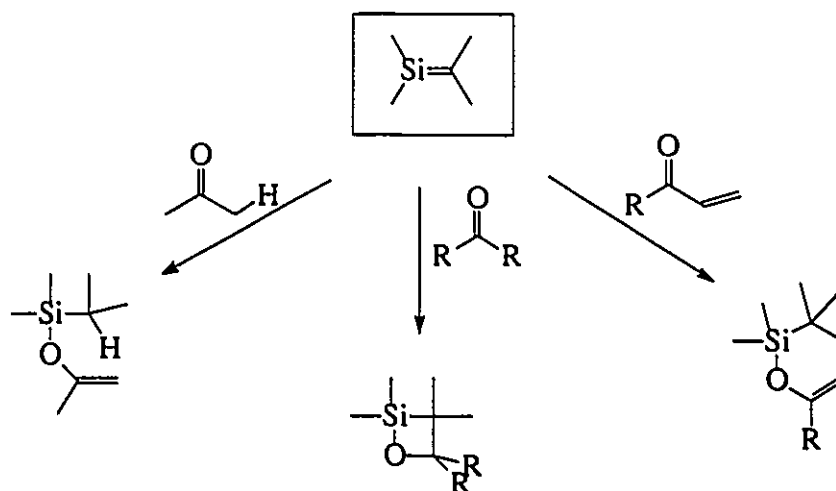
Scheme 1.3 Silene Reactions with Dienes and Alkenes



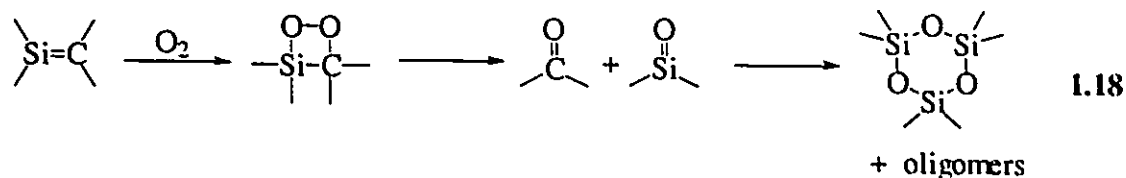
Simple silenes undergo ene reactions with carbonyl compounds possessing α -hydrogens, and formal [2+2]- and [4+2]-cycloadditions with carbonyl compounds which do not (Scheme 1.4).^{1,2,5} Sommer first reported that the trapping of pyrolytically generated silenes with carbonyl compounds yields an olefin and silanone oligomers.^{24,60,61} The silanone oligomers (normally the cyclic trimer) were suggested to arise from the decomposition of a highly unstable 2-siloxetane intermediate formed from formal [2+2]-addition of the carbonyl compound to the silene (eq. 1.17). The isolation of siloxetanes proved elusive until recently when Brook⁶² and Wiberg² independently reported convincing spectroscopic and crystallographic data in support of siloxetane derivatives of several stabilized silenes. The mechanism of the reaction of silenes with carbonyl compounds is thought to involve nucleophilic attack by the lone-pair of electrons on the oxygen atom but it is not known for certain whether these reactions are stepwise or concerted. Leigh and coworkers have recently reported that ene reactions of 1,1-

diphenylsilene (**11**) with carbonyl compounds follow a concerted but asynchronous mechanism in which Si-O bond formation precedes H-atom transfer.⁶³

Scheme 1.4 Silene Reactions with Carbonyl Compounds



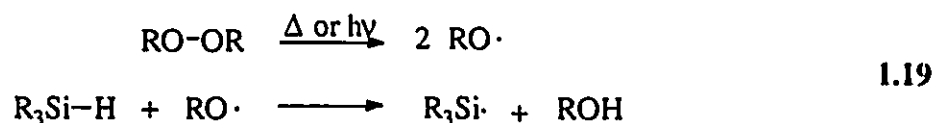
Silenes react with molecular oxygen to yield cyclic siloxanes and carbonyl compounds (eq 1.18).^{46,64-66} The reaction is thought to involve a siladioxetane intermediate which decomposes thermally to the corresponding carbonyl compound and silanone which oligomerizes.



1.3 The Chemistry of Silyl Radicals

1.3.1 Silyl Radical Generation

The most common method for silyl radical synthesis is hydrogen atom abstraction by a thermally or photochemically generated radical initiator such as benzoyl peroxide or di-*tert*-butyl peroxide (BOOB) (eq 1.19).^{18,19} Ketone triplets also abstract silane hydrogen atoms efficiently.⁶⁷ These reactions are highly exothermic ($\Delta H \sim -15$ kcal/mol) and occur rapidly due mainly to the weak Si-H bond⁶⁸ (BDE ~ 90 kcal/mol; see Table 1.3). The absolute rate constants for the reaction of *tert*-butoxy radicals with silanes, measured by nanosecond laser flash photolysis (NLFP) techniques, are in the 10^6 - 10^7 $\text{M}^{-1}\text{s}^{-1}$ range.⁶⁷ Ingold and coworkers have also employed this technique in the measurement of absolute rate constants for the reactions of trialkylsilyl radicals with alkyl halides,⁶⁹ carbonyl compounds,⁷⁰ and alkenes.⁷¹



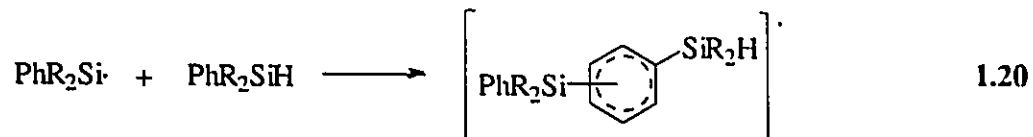
1.3.2 Silyl Radical Reactions

Silyl radicals react rapidly with alkyl halides, carbonyl compounds, alkenes, aromatics, and other unsaturated compounds. Several excellent reviews of silyl radical reactions are available.¹⁵⁻¹⁹ In the absence of radical quenchers, trialkylsilyl radicals undergo diffusion controlled second-order recombination ($2k_t \sim 10^{10} \text{ M}^{-1}\text{s}^{-1}$)⁶⁹ to yield dimerization and disproportionation products. Aryl substituted silyl radicals, on the other hand, decay with first-order kinetics with the rate constants proportional to the concentration of the phenylsilane precursor.⁷² Thus, the major mode of decay of arylsilyl radicals is addition to the aromatic ring of the precursor (eq 1.20).

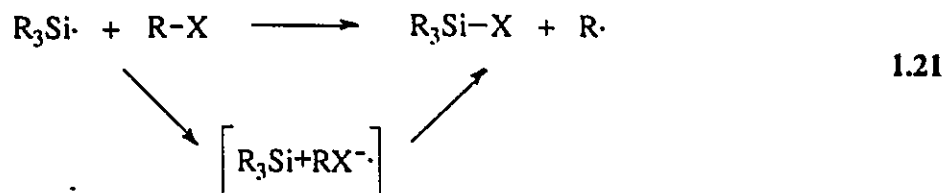
Table 1.3 Bond Dissociation Energies of Substituted Alkanes and Silanes (kcal/mol)^a

X	H ₃ C-X	Me ₃ Si-X
H	105	90
CH ₃	90	90
SiMe ₃	84	84
OMe	92	114
Cl	84	113
Br	71	96

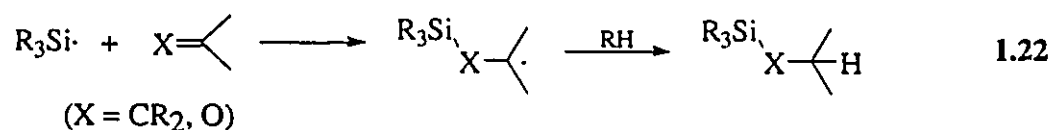
a. Data from reference 68.



The driving force for reactions of silyl radicals with alkyl halides is the formation of strong Si-X bonds (see Table 1.3). In some cases electron transfer processes may be involved (eq 1.21). Ingold and coworkers have reported that for a particular R group, the rate constants decrease along the series $X = \text{I} > \text{Br} > \text{Cl} > \text{F}$, while for a given X, the rate constants decrease along the series $R = \text{allyl} > \text{benzyl} > \text{tert-alkyl} > \text{sec-alkyl} > \text{primary alkyl} > \text{cyclopropyl} > \text{phenyl}$.⁶⁹ Thus, the rate of reaction is determined by the bond strength of the silyl halide and the thermodynamic stability of the incipient alkyl radical.



The addition of silyl radicals to carbonyl compounds and alkenes (eq 1.22) is exothermic and, generally, proceeds with rate constants in the 10^5 - $10^9 \text{ M}^{-1}\text{s}^{-1}$ range.⁷⁰ These free radical hydrosilylation reactions are among the most important Si-C and Si-O bond forming reactions and have been applied in the syntheses of many organosilicon compounds.^{73,74} Hydrosilylation reactions are now more commonly carried out thermally in the presence of transition metal catalysts such as chloroplatinic acid (H_2PtCl_6).⁷⁴



1.4 The Photochemistry of Aryldisilanes

1.4.1 Photophysical Studies of Phenyldisilanes

The replacement of a hydrogen atom in benzene with a disilanyl group causes a red-shift and increase in extinction coefficient in the lowest energy 1L_a absorption band.⁷⁵⁻⁷⁸ Increasing phenyl substitution in aryldisilanes results in increasing bathochromic shifts and extinction coefficients for this absorption (Table 1.4). The lack of intense 1L_a absorption above 215 nm for monosilanes such as phenyl- and vinyltrimethylsilane indicates that the chromophore involves the Si-Si bond and the π system of the phenyl or vinyl groups.

Table 1.4 UV Absorption Data of Mono- and Disilanes.^a

Silane	λ_{max} (nm)	ϵ ($\text{M}^{-1}\text{cm}^{-1}$)
$\text{Me}_3\text{Si-SiMe}_3$	199.5	7230
$\text{PhMe}_2\text{Si-SiMe}_3$	231.0	10900
$\text{PhMe}_2\text{Si-SiMe}_2\text{Ph}$	238.0	18500
$\text{Ph}_2\text{MeSi-SiMePh}_2$	240.0	25900
PhSiMe_3	211.0	9300
$\text{CH}_2=\text{CH-SiMe}_2\text{-SiMe}_3$	223.2	5200
$\text{CH}_2=\text{CH-SiMe}_3$	202.0	1470

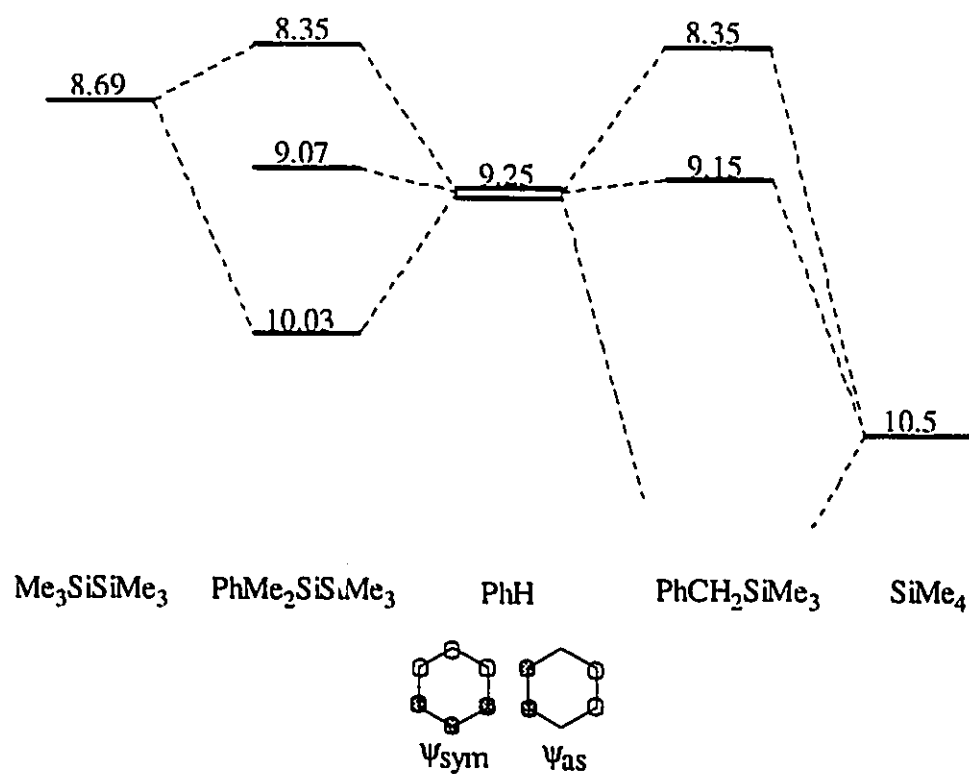
a. Data from reference 40.

The conjugation between the Si-Si bond and the π system was originally explained in terms of an interaction of the vacant $3d$ orbitals on the silicon atoms with the phenyl or vinyl π orbitals in the excited state.⁷⁵⁻⁷⁸ However, ground state interactions between the Si-Si σ bond and the π system have been demonstrated on the basis of photoelectron spectroscopy (PES),⁷⁹ and stereoelectronic effects on the UV absorption spectra of phenyldisilanes.^{80,81}

In 1972 Pitt and Bock reported evidence for σ - π mixing in **12** based on its PE spectrum.⁷⁹ Three low energy bands were observed at 8.35, 9.07, and 10.03 eV in the PE spectrum (Scheme 1.5). The band at 9.07 eV was assigned to ψ_{is} of the originally degenerate e_{1g} MO's of benzene since it should be only weakly perturbed by substitution at the nodal ipso position. The bands at 8.35 and 10.03 eV were assigned to linear combinations of the ψ_{SiSi} and ψ_{sym} orbitals. Remarkably, benzyltrimethylsilane has an identical IP to **12** but does not exhibit 1L_a absorption above 220 nm due to the lack of σ - π conjugation.

The configurational assignment of the lowest excited singlet states in aryldisilanes is a controversial subject. Although it is not addressed explicitly in this study, it is worthwhile to review what is known about this topic. Dual fluorescence emission from aryldisilanes such as **12** has been reported by Shizuka's^{38,82-88} and Sakurai's^{37,81,89} groups; in addition to normal emission from an aromatic $(\pi,\pi^*)^1$ (LE, locally excited) state, a broad band at longer wavelengths has been observed in hydrocarbon solvents (see Figure 1.1). In acetonitrile solution, only the long wavelength band is observed. While Shizuka and Sakurai agree that the lower energy emission band is due to emission from an intramolecular charge-transfer (CT) excited state, they do not agree on the direction of this charge-transfer or on the geometrical requirements in this excited state.

Scheme 1.5 Molecular Orbital Energies and Correlation Diagram of σ - π Mixing



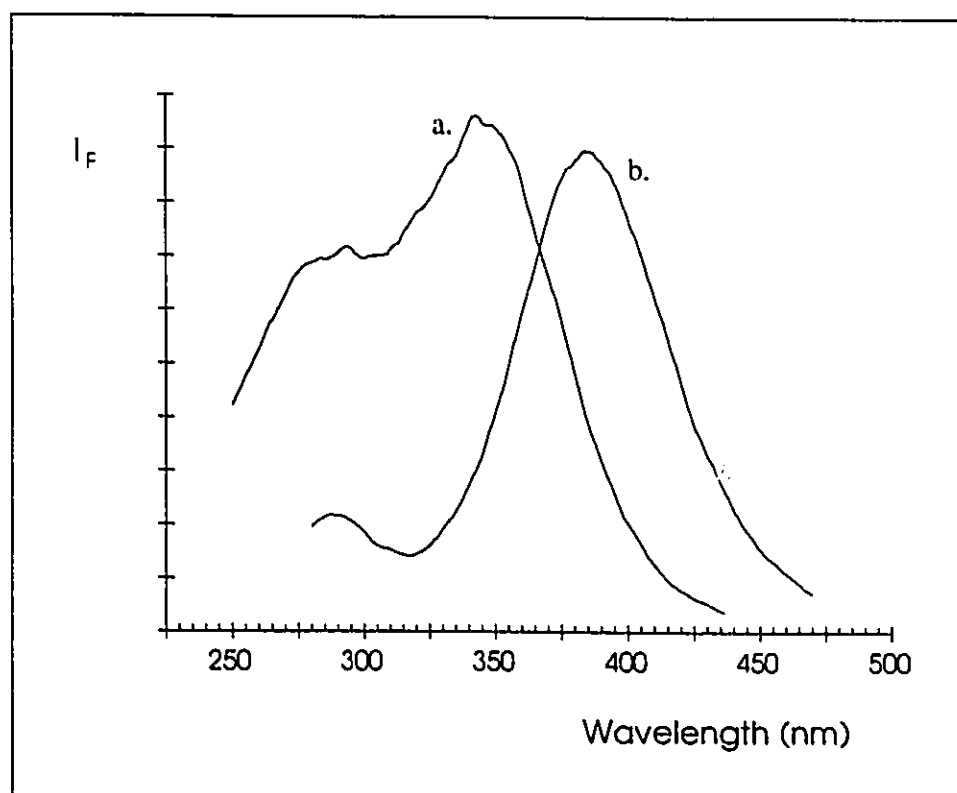
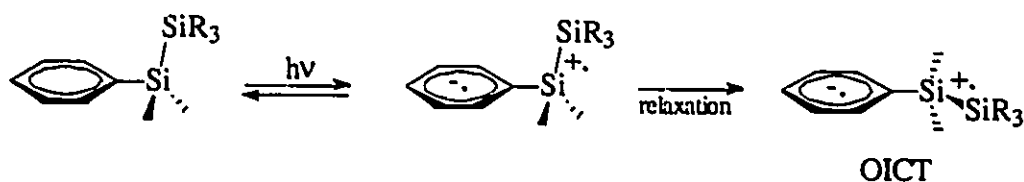


Figure 1.1 Fluorescence emission spectra of **12** in (a) isoctane and (b) acetonitrile solution at 23 ± 2 °C.

Sakurai and coworkers have assigned the phenyldisilane CT state to the orthogonal intramolecular charge transfer (OICT) (σ, π^*)¹ excited state on the basis of a study of substituent and solvent effects on the dual fluorescence of **12**.^{37,81,89} This mechanism involves CT from the disilanyl group to the aromatic π system followed by rapid relaxation to a mutually orthogonal orientation of the $\sigma(\text{Si-Si})$ and aromatic π orbitals (Scheme 1.6). Thus, in the OICT state, the $\sigma(\text{Si-Si})$ bond is proposed to lie in the same plane as the phenyl ring.

Scheme 1.6 Schematic Representation of the OICT State in Phenyldisilanes



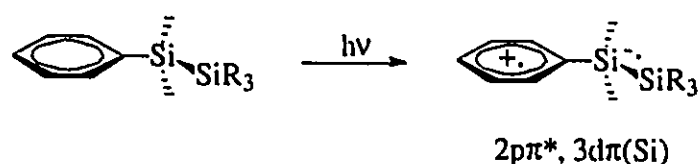
OICT is conceptually similar to twisted intramolecular charge transfer (TICT) employed to explain the dual fluorescence emission of *N,N*-dialkylaminobenzonitriles and *N,N*-dialkylaminobenzoate esters.⁹⁰ In these cases (n, π^*)¹ charge transfer is followed by relaxation via a 90° twist in the molecular framework such that the n and π^* orbitals are mutually perpendicular (Scheme 1.7). This conformation lowers the energy of the CT state since reverse charge-transfer is prevented, and results in the red-shift of the CT emission versus the LE emission band. The TICT state is inherently dipolar and is stabilized in polar solvents, causing the TICT emission to shift to lower energy with increasing solvent polarity.

Scheme 1.7 Conformational Changes Involved in Population of TICT States



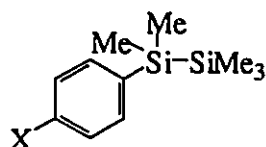
Shizuka^{38,88} has assigned the phenyldisilane CT state as $(2p\pi^*, 3d\pi(\text{Si}))^1$. In this model charge-transfer occurs from the aromatic π^* orbital to the vacant $3d\pi(\text{Si})$ orbital. In order for this CT interaction to occur, the disilane must be able to adopt a ground state conformation in which the aromatic π orbital is able to overlap with the attached silicon $3d\pi$ orbital. In this case the $2p\pi^*-3d\pi(\text{Si})$ conjugation is greatest when the disilane has a planar structure as shown in Scheme 1.8.

Scheme 1.8 Schematic Representation of the $(2p\pi^*, 3d\pi(\text{Si}))^1$ CT State in Phenyldisilanes



Evidence for the OICT (σ, π^*)¹ state has come from the fluorescence emission spectra of a series of para-substituted phenylpentamethyldisilanes (12, 20-23) and a series of disilane geometric isomers⁸¹ (24-27) in a variety of solvents. All of these compounds, except for the two disilanes with electron donating para-substituents (21, 22), exhibit dual fluorescence in medium polarity solvents such as tetrahydrofuran (THF). The intensity of the low energy CT emission is enhanced at the expense of the LE emission and the CT emission shifts to longer wavelengths with increasing solvent polarity. This indicates that

the lower energy emitting states are polar and the efficiency of conversion to the CT state is enhanced by increasing the solvent polarity. Monosilanes, such as phenyltrimethylsilane and benzyltrimethylsilane, exhibit fluorescence emission from the LE state exclusively in all solvents, indicating the importance of the disilanyl group in the CT state.



12: X = H

20: X = Me

21: X = OMe

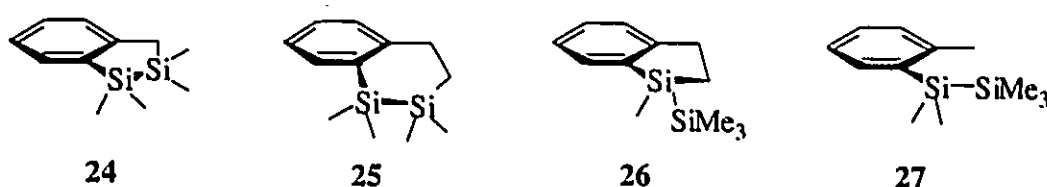
22: X = NMe₂

23: X = MeC=CH₂

In acetonitrile solution, a blue shift in the CT emission band was observed from **23** to **12** to **20**, whereas **21** and **22** do not exhibit CT fluorescence at room temperature.⁸¹ This provides evidence in favour of the $(\sigma, \pi^*)^1$ CT state over the $(2p\pi^*, 3d\pi(\text{Si}))^1$ assignment of Shizuka and coworkers. The energy of the CT state is raised by the introduction of an electron donating group (such as *p*-OMe, *p*-Me, *p*-NMe₂) on the phenyl ring as a result of a decrease in electron affinity (E_A). Electron withdrawing substituents, such as MeC=CH₂, facilitate CT from the disilanyl group into the aromatic system and lower the energy of the CT emission. According to Shizuka's model, the energy of the CT band should correlate with the IP rather than the E_A of the substituted benzene and prominent CT emission would be expected from **21** and **22**.

Sakurai and coworkers have investigated stereoelectronic effects on the UV absorptions and emissions of phenyldisilanes (**24-27**).^{80,81} 1,1,2,2-Tetramethyl-3,4-benzo-1,2-disilacyclopentene-3 (**24**) has a ground state conformation in which the Si-Si bond is in the nodal plane of the π system so that σ - π^* conjugation is not possible. Such interactions require coplanarity of the p_{π} -axis and the interacting σ bond (see Scheme 1.6)

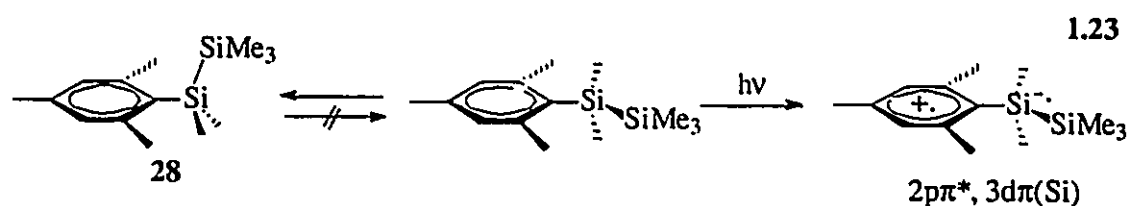
and, as expected, intense 1L_a absorption was not observed for this compound. Disilane **25**, in which the dihedral angle between the $\sigma(\text{Si-Si})$ and π orbitals is over 60° at the half-chair conformation, exhibits a weak shoulder 1L_a absorption at 232 nm. Disilanes **26** and **27**, which have dihedral angles of 80.3° and ca. $80-90^\circ$, respectively, have strong 1L_a absorptions. These experiments provide convincing evidence of $\sigma-\pi^*$ conjugation involvement in the charge-transfer type 1L_a absorptions of phenyldisilanes.



The fluorescence emission spectra of **24-27** in acetonitrile reveal significant stereoelectronic effects similar to those observed in the UV absorption spectra of these compounds.⁸¹ Compounds **25**, **26**, and **27** exhibit exclusive CT emission while **24** shows weak CT emission compared to the LE emission band. The CT emission maxima of **24** and **25** are identical and are at the lowest energy in the series. A blue shift in the emission maximum occurs from **24** and **25** to **27** to **26**. This indicates that the favoured geometry of the CT state is the form in which the $\sigma(\text{Si-Si})$ bond is in the plane of the phenyl ring. Therefore, **24** and **25** exhibit the lowest energy CT emission since their ground state conformations are closest to the required OICT geometry. The weak CT emission observed for **24**, which does not exhibit 1L_a absorption, may be due to internal conversion of the 1L_b state.

Shizuka has based much of his argument in favour of the $(2p\pi^*, 3d\pi(\text{Si}))^1$ assignment on the disilane structure as well. The fact that mesitylpentamethyldisilane (**28**) does not exhibit CT fluorescence emission in acetonitrile solution at room temperature has

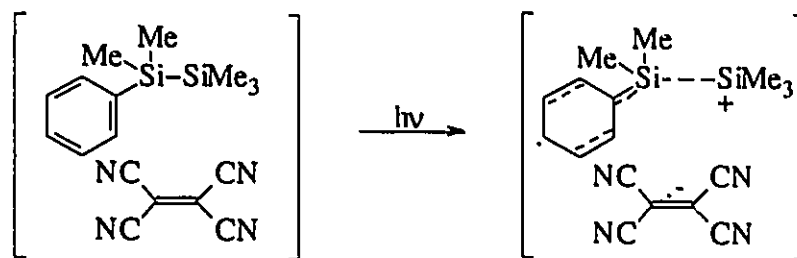
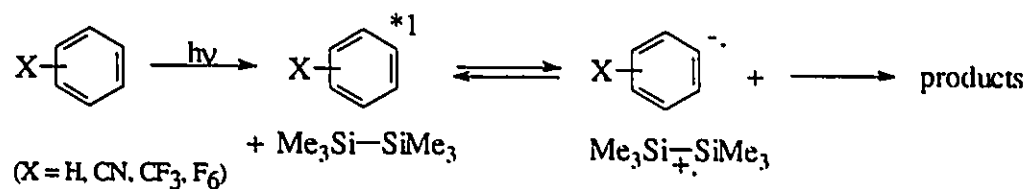
been explained as due to the inability of this disilane to adopt the required planar geometry for $2p\pi^*-3d\pi(\text{Si})$ overlap owing to the presence of the two ortho methyl groups on the phenyl ring^{38,88} (eq 1.23). On the other hand, pentamethylphenyldisilane (**12**), can easily attain the necessary conformation for this CT interaction and, as a result, relatively strong CT emission is observed.



Another significant piece of evidence in favour of this mechanism was the observation of double exponential CT emission from **12** at 77 K in a frozen matrix ($\tau_{\text{CT(fast)}} = 300 \text{ ps}$; $\tau_{\text{CT(slow)}} = 3.2 \text{ ns}$).^{38,88} Similarly the growth of the CT emission occurred within 10 ps indicating that rotation of the C(ipso)-Si bond during the lifetime of the excited state is not necessary for CT state formation, this is quite different from the OICT model, in which the disilane must relax to a planar geometry following excitation (Scheme 1.6). Shizuka has determined that the CT fluorescence emission from **12** is polarized parallel to the molecular long axis which is consistent with the $(2p\pi^*, 3d\pi(\text{Si}))^1$ mechanism. The CT emission would be expected to be polarized perpendicular to the molecular plane of the phenyl ring if the $(\sigma, \pi^*)^1$ OICT mechanism were operative. Disilane **12** also shows a positive magnetic circular dichroism (MCD) spectrum consistent with the disilanyl group acting as an electron withdrawing group. Shizuka has also observed CT emission in poly(vinyl alcohol) film at 77 K from two disilanes, *p*-tert-butylphenylpentamethyldisilane and *p*-methoxyphenylpentamethyldisilane (**21**), which do not show CT emission at room temperature in acetonitrile solution. One problem with

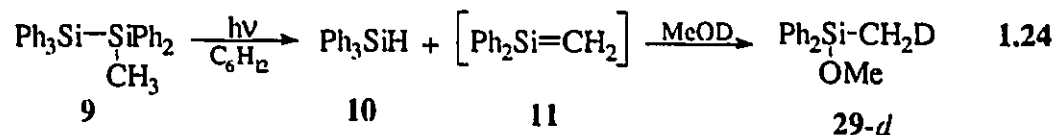
Shizuka's model, in which charge transfer occurs from the aromatic π system to the disilanyl group, is that it is incompatible with the well documented electron-donating nature of the $\sigma(\text{Si-Si})$ bond in bimolecular processes such as electron transfer quenching of electron-deficient benzenes⁹¹ and charge-transfer complex formation with tetracyanoethylene^{92,93} (Scheme 1.9).

Scheme 1.9 Bimolecular Charge-Transfer Reactions of Disilanes



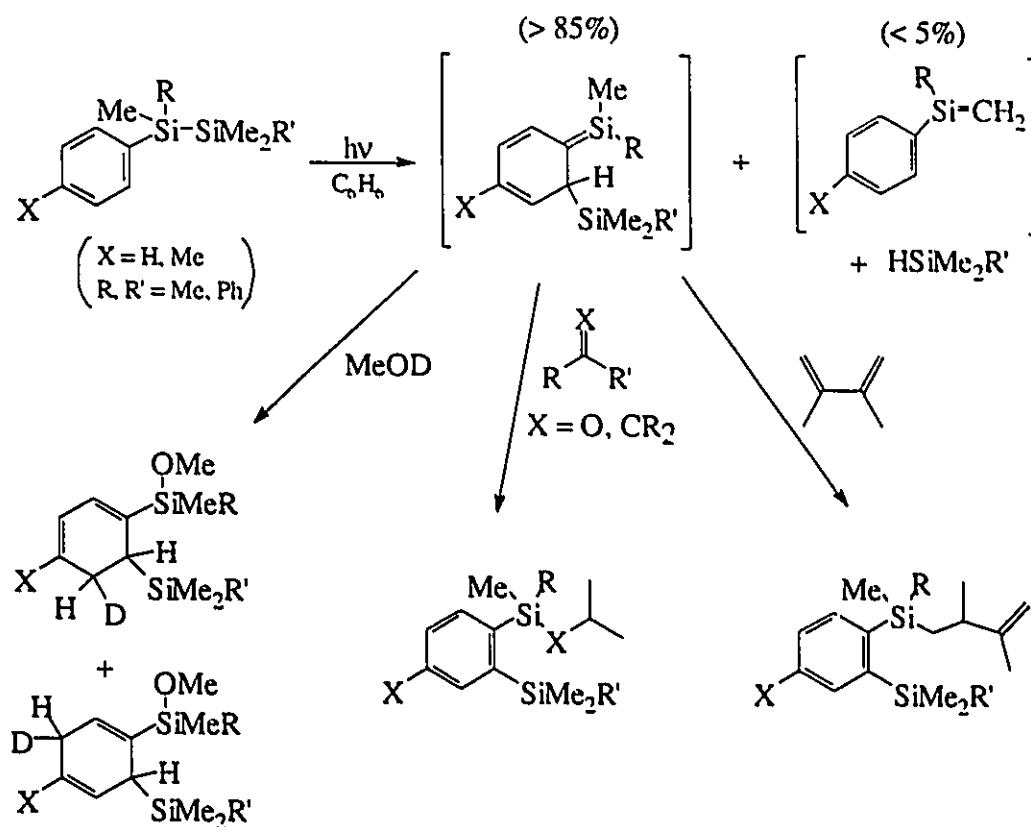
1.4.2 Mechanistic Aspects of Silene Generation and Reactivity

The photolysis of phenyldisilanes allows the generation and characterization of a variety of silicon reactive intermediates and has received a great deal of attention in the last twenty years.^{4,37,39-41} In their seminal 1972 report, Sommer and coworkers showed that the photolysis of methylpentaphenyldisilane (**9**) in the presence of methanol-*Od* in cyclohexane yields triphenylsilane (**10**) and methoxymethyldiphenylsilane-*d* (**29**).³⁶ The latter is formed by nucleophilic trapping of 1,1-diphenylsilene (**11**) with methanol-*Od* (eq 1.24). In the absence of methanol, an insoluble yellow polymer, formed from the oligo- and polymerization of **11**, and triphenylsilane are produced.

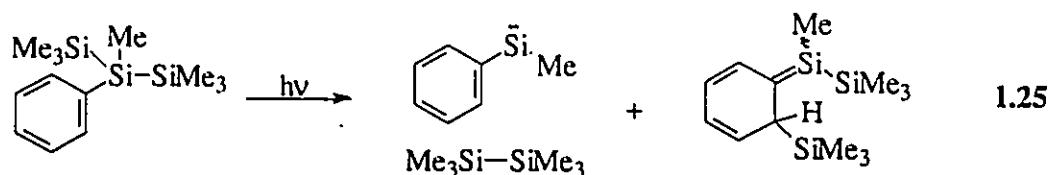


The photochemical behaviour of **9** is contrasted by that of other phenyldisilanes, such as **12**, which, upon photolysis, appear to rearrange predominantly to silatrienes (eq 1.5) on the basis of trapping experiments with alcohols,⁹⁴⁻⁹⁶ alkenes,⁹⁶⁻⁹⁸ alkynes,⁹⁹ dienes,^{97,100,101} carbonyl compounds,^{96,102} and organometallic reagents¹⁰³ (Scheme 1.10). In all cases, the major products are consistent with the predominant formation of a silatriene intermediate upon irradiation of these disilanes. Simpler silenes analogous to those formed in the photolysis of **9** are apparently formed in very low yields. In the absence of added quenchers, products consistent with silatriene di-, oligo- and polymerization are detected.^{104,105}

Scheme 1.10 The Photogeneration and Reactivity of Silatrienes

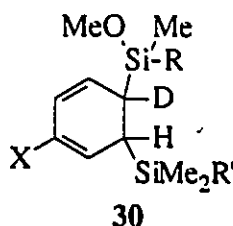


Silatrienes are also produced in the direct photolysis of aryl-substituted trisilanes;¹⁴ however, silylene extrusion is usually the predominant process. Ishikawa and coworkers have shown that when less bulky groups are attached to the central silicon atom, silatriene formation can compete effectively with silylene extrusion (eq 1.25).¹⁰¹



Despite the large number of reports of the chemical trapping of photochemically generated silatrienes, surprisingly little is known about the mechanisms of these reactions other than what can be inferred from the isolated products. In a review article, Brook has suggested that silatrienes are anomalous in their reactions with known silene trapping agents.⁵

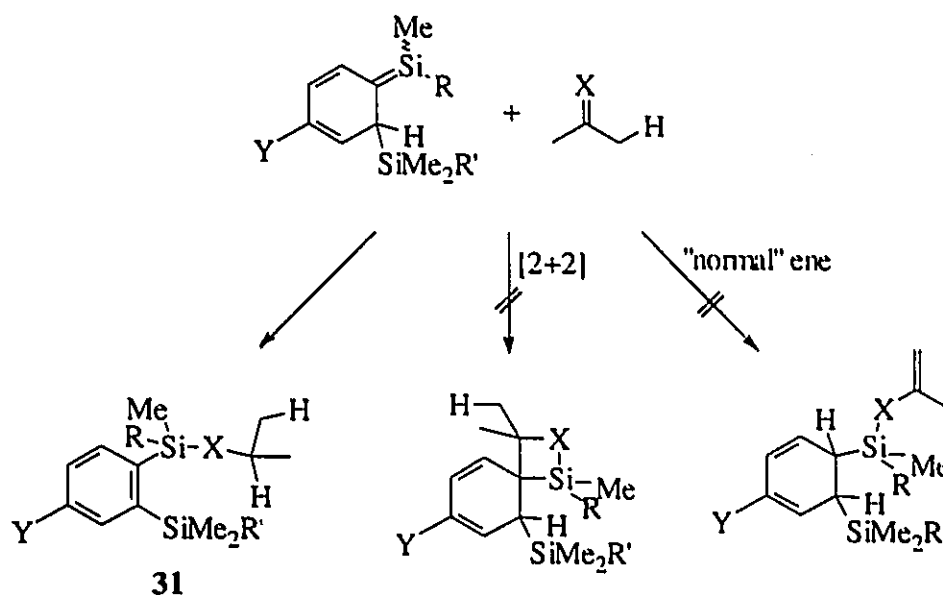
The reaction of silatrienes with alcohols is reported to yield two isomeric addition products formally derived from 1,4- and 1,6-addition. The 1,2-addition isomer (30), analogous to the product of alcohol addition to simple silenes, was not detected.⁹⁴⁻⁹⁶ The two isolated isomers indicate that the reaction is likely to be stepwise, as was first suggested by Wiberg (eq 1.14).²



Silatrienes also appear to react atypically with carbonyl compounds, alkenes, and dienes. In each case the *only* detected products (31) were those of formal ene addition involving the allylic hydrogen atom of the silatriene. Products consistent with [2+2]-cycloaddition or "normal" ene reaction, involving the alpha or allylic hydrogens of the trapping reagent, were *not* detected (Scheme 1.11). In the case of dienes, no products of

Diels-Alder addition to the silatrienes were detected.^{97,100,101} The driving force for the production of adducts **31** may be the rearomatization of the phenyl ring which accompanies their formation. Although Ishikawa has suggested that these reactions may be stepwise involving biradical intermediates,¹⁰² no conclusive evidence in favour of a concerted or stepwise mechanism (involving biradicals or zwitterionic intermediates) has been reported.

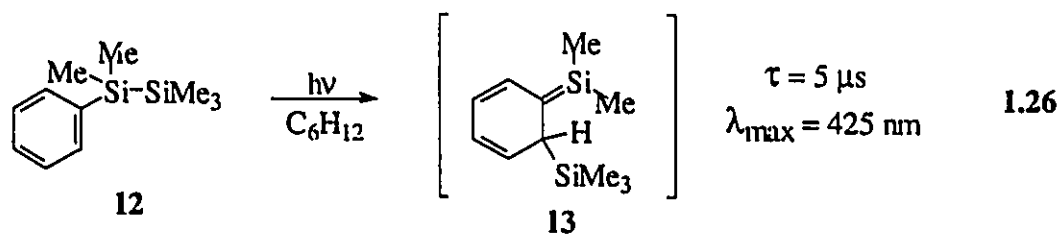
Scheme 1.11 Possible Silatriene Adducts with Unsaturated Compounds



A possible complication in these steady-state product studies is the question of whether the kinetic or thermodynamic products have been isolated. It is certainly conceivable, in the case of the alcohol reaction with silatrienes, that the 1,2-addition product (**30**) is the initial product, but it isomerizes to the more thermodynamically stable 1,4- and 1,6-adducts. Likewise, it is possible that the [2+2]- and/or "normal" ene

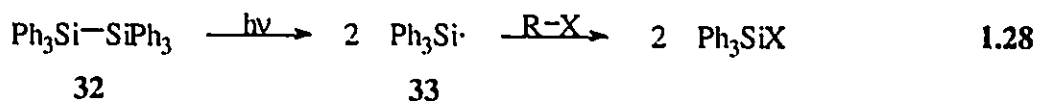
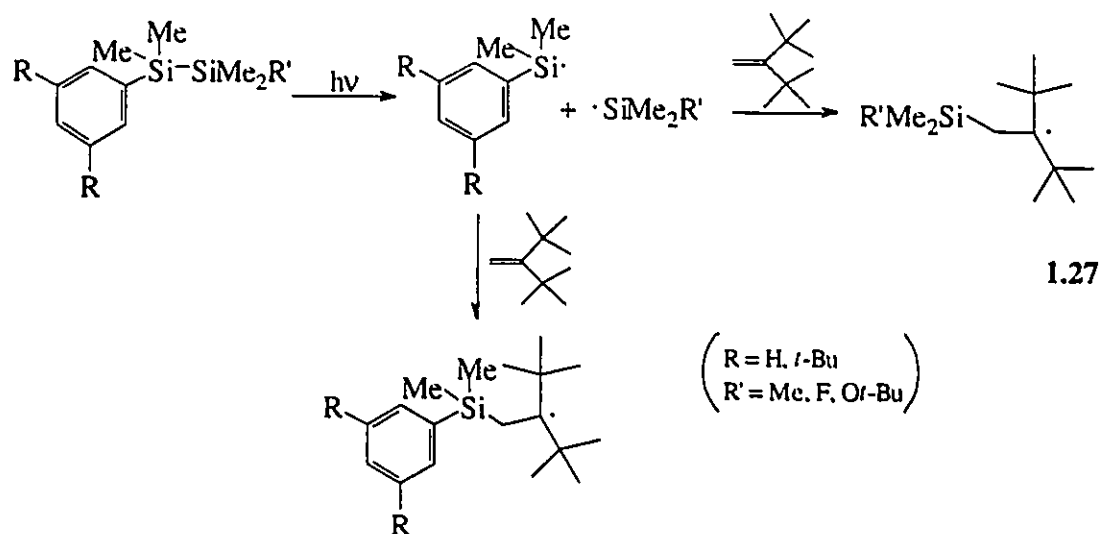
cycloadducts may be the primary products in the reactions with carbonyl compounds, alkenes, and dienes, but isomerize rapidly to the observed adducts **31** under the experimental conditions employed. In these studies, the products were quantitated and isolated by gas chromatography, conditions which could facilitate thermal equilibration of the products. Thus, it would be instructive if a more mild analytical technique, such as (nuclear magnetic resonance) NMR, were employed for product characterization since the identification of the kinetic products of these reactions is necessary to obtain any meaningful mechanistic information from these experiments.

Silatriene **13** has been detected directly using nanosecond laser flash photolysis (NLFP) techniques (eq 1.26);^{14,82} however, only rate constants for its reaction with three silene trapping agents (oxygen, ethanol, and 2,3-dimethyl-1,3-butadiene (DMB)) have been reported in a review article by Gaspar and coworkers.¹⁴ Other than indicating that conjugated silenes such as **13** react rapidly ($k_q \approx 10^8$ - $10^9 \text{ M}^{-1}\text{s}^{-1}$) with these reagents, this study did not provide any mechanistic information on these reactions. The product(s) from the reaction of oxygen with **13** have not been reported, so this rate constant is of minimal value.



Considering the large number of reports of the photolysis of arylsilanes, the mechanistic aspects of arylsilane photochemistry have similarly received little attention. The excited state(s) responsible for silene and silatriene production are the subject of

controversy, primarily because of that involved in the assignment of the aryldisilane CT state. Shizuka *et al* have employed picosecond time resolved spectroscopy to monitor the CT fluorescence decay of **12**.⁸² The rate of growth of a new transient centred at 425 nm, assigned to the corresponding silatriene (**13**), matched the fluorescence decay kinetics. This indicated that silatriene formation occurs via a direct [1,3]-silyl migration in the disilane CT excited state. Sakurai has suggested that silatriene formation occurs in a phenyldisilane single excited state due to the apparent lack of quenching of products by *trans*-piperylene.³⁷ More recently, Sakurai and coworkers have suggested that silatriene formation occurs via rearrangement in the $(\pi,\pi^*)^1$ LE excited state while the CT state yields products consistent with nucleophilic cleavage of the Si-Si bond.⁸⁹ Silyl radicals have been detected from aryldisilane photolyses but their role in silene and silatriene formation has not been determined conclusively. Sakurai and coworkers have detected free silyl radicals from the photolysis of phenyldisilanes in the presence of 1,1-di-*tert*-butylethylene as a spin trap (eq 1.27) by electron spin resonance (ESR) spectroscopy.¹⁰⁶ The chemical yield of silyl radicals has not been reported, however. Ito and coworkers have detected triphenylsilyl radicals (**33**) from the photolysis of hexaphenyldisilane (**32**) and have measured rate constants for their reactions with alkyl halides using flash photolysis techniques (eq 1.28).¹⁰⁷ The detection of free silyl radicals has led several groups to conclude that silenes and silatrienes arise from the disproportionation and recombination, respectively, of these radicals (Scheme 1.12).^{5,40} However, the excited state(s) responsible for silyl radical formation have not been identified. Likewise, the involvement of phenyldisilane triplet excited states in product formation has not been investigated.

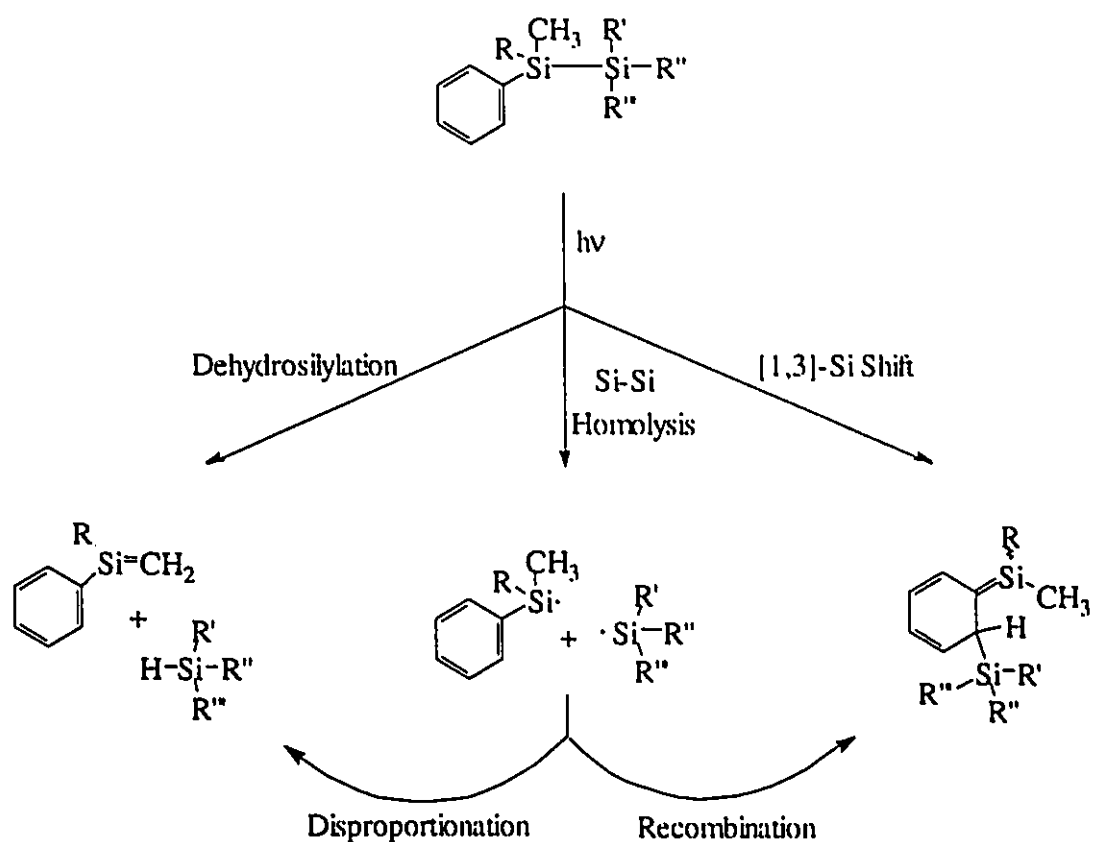


The role of solvent polarity on the photochemistry of phenyldisilanes and silatriene reactivity has not been investigated. The majority of Ishikawa's steady-state photolysis studies were carried out in benzene solution under conditions where the solvent is the primary absorber of the 254 nm irradiation.³⁹ Typical disilane concentrations employed were in the 0.01-0.05 M range; concentrations high enough to quench the singlet excited state of benzene quantitatively. Thus, the majority of the information about phenyldisilane photochemistry has been obtained under conditions of singlet sensitization. Little is known about the behaviour of these disilanes under direct photolysis in solvents of different polarity.

The general scheme for the photochemistry of phenyldisilanes involves the formation of three distinct transient intermediates: free silyl radicals by Si-Si bond homolysis, simple

silenes by concerted dehydrosilylation (or silyl radical disproportionation), and silatrienes by concerted [1,3]-silyl migration (or silyl radical recombination) into one of the phenyl rings (Scheme 1.12). The relative yields of the three types of reactive intermediates depends on the structure of the disilane.

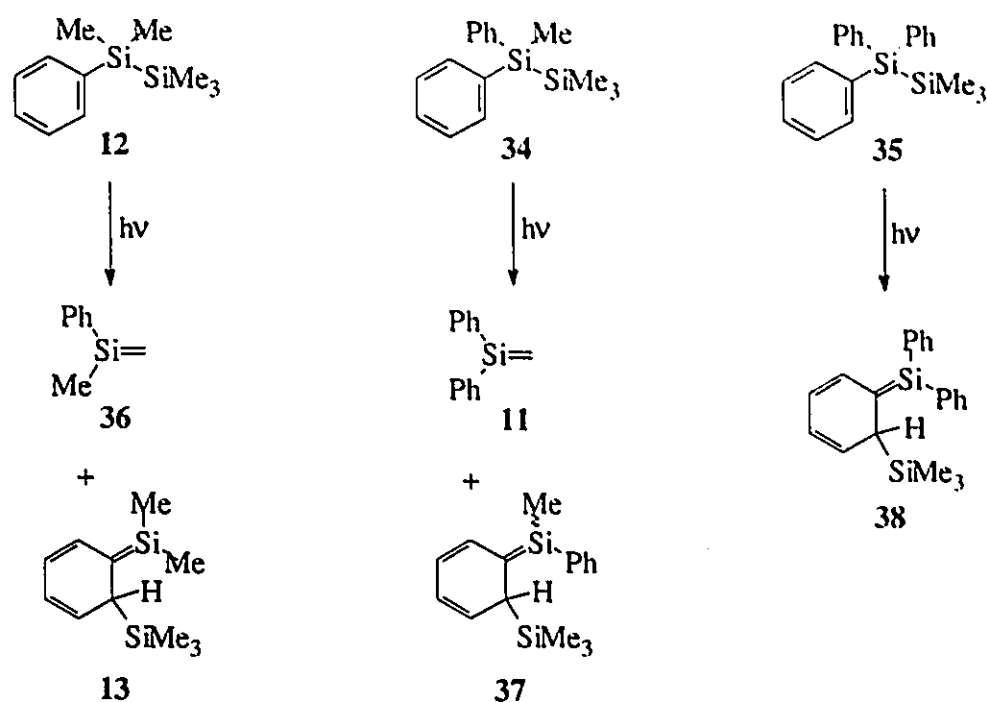
Scheme 1.12 The Photoreactivity of Phenyldisilanes



1.5 **Objectives of this Work**

The majority of silene assignments have been based on chemical trapping experiments, which can only yield qualitative information about their mechanisms of generation and their reactivity. While there are now several reports of the synthesis and reactions of "stable" silenes, there are only a few recent studies which have employed transient spectroscopic techniques to characterize smaller *reactive* silenes which are more common in the reactions of organosilicon compounds in fluid solution at room temperature.¹ There exists only *one* reported transient absorption spectrum of a reactive conjugated silene (**13**) obtained from flash photolysis of **12**⁸² and until very recently, there were no reports at all of absorption spectra of simple silenes such as 1,1-diphenylsilene (**11**) in solution. Thus, the original goal of this work was to employ NLFP techniques to directly detect simple and more highly conjugated silenes such as **11** and **13**.

A comparison of the photochemistry of methylpentaphenyldisilane (**9**) and pentamethylphenyldisilane (**12**) reveals a significant dependence of disilane structure on the yield and type of silicon reactive intermediate produced on photolysis. The photolysis of **9** yields the simple silene **11**, while **12** yields silatriene **13**. Phenyldisilanes **34** and **35** have been synthesized in addition to **12** and their photoreactivities have been investigated in detail in non-polar and polar solvents. NLFP techniques have been employed in attempts to detect directly the simple (**36** and **11**) and conjugated silenes (**13**, **37**, **38**), and the corresponding arylsilyl radicals produced from the photolysis of **12**, **34**, and **35**. Hexaphenyldisilane (**32**) and 1,2-dimethyl-1,1,2,2-tetraphenyldisilane (**39**) have been examined briefly by NLFP techniques to aid in the assignments of silatrienes (**37**, **38**) and to estimate the relative yields of the three possible reactive intermediates.



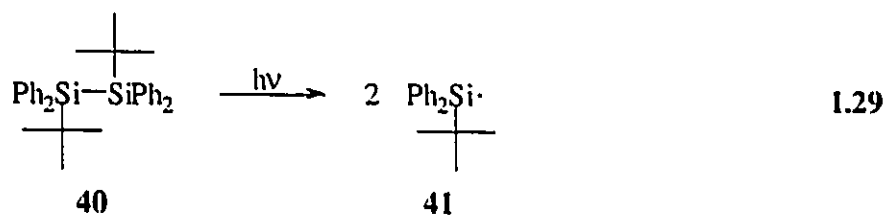
Although numerous silene and silatriene reactions have been reported, there is surprisingly little mechanistic information available. Thus, mechanistic studies of the reactivity of these silatrienes towards known silene trapping agents such as alcohols, methoxytrimethylsilane (MTMS), carbonyl compounds, dienes, alkenes, sulfoxides, alkyl halides, and oxygen have been undertaken by noting solvent and substituent effects on the kinetics of these reactions. Pentamethyl(pentadeuteriophenyl)disilane (**12-d₅**) has been prepared and examined by NLFP techniques to determine the kinetic deuterium isotope effects on the addition of carbonyl compounds, alkenes, dienes, and oxygen to silatrienes. Steady-state product studies of the photolysis of these disilanes in the presence of each trapping agent have been performed in order to confirm the original reports, where applicable, and to uncover any new reactions. This study represents the first systematic examination of the effects of phenyl substitution and solvent on the photochemistry of phenyldisilanes and on the reactivity of silatrienes.

While Sakurai has detected free silyl radicals from the photolysis of phenyldisilanes (eq 1.27),¹⁰⁶ the role of these intermediates in silene and silatriene formation is not known. Thus, the mechanism of silatriene and simple silene formation (concerted rearrangement in the excited state versus stepwise formation from silyl radicals) has been examined by photolysis of disilanes **9**, **12**, **34**, and **35** in the presence of acetone *and* chloroform as silene and silyl radical trapping agents, respectively. These experiments have provided the chemical yields of simple silene, silatriene, and silyl radical-derived products. Any decreases in yields of the silene and silatriene-derived products compared to those obtained in the absence of chloroform indicate the extent of silyl radical involvement in their formation.

Shizuka has reported that silatriene **13** is produced via a concerted [1,3]-Si migration in a singlet CT excited state of **12**;⁸² however, the excited states responsible for the formation of simple silenes and silyl radicals are not known. An examination of singlet versus triplet state reactivity of **35** has been undertaken through triplet quenching and sensitization experiments. Although this study allowed the determination of the excited state multiplicity (singlet or triplet) responsible for the generation of each type of silicon reactive intermediate, it did not attempt to assign the specific type of singlet state(s) (LE or CT) involved.

One of the ultimate goals of this work was the elucidation of the factors, such as structure and solvent, which affect the photoreactivity of phenyldisilanes, and, with this knowledge in hand, to design systems with controlled reactivity or which test these theories. Disilane **40** was synthesized as a potential high yield source of silyl radicals. In this case, Si-Si bond homolysis would be expected to predominate (yielding arylsilyl radicals **41**) since silatriene formation would be blocked by the steric bulk at each silicon atom and formal dehydrosilylation is prevented by the absence of an available H-atom α to

the silicon atom (eq 1.29). The reactivity of **41** towards known silyl radical trapping agents such as alkyl halides, alkenes, and carbonyl compounds has been investigated using NLFP techniques. The clean formation of **41** in a single step from the direct photolysis of **40** would be advantageous to the indirect techniques for silyl radical generation and characterization which require the use of thermally or photochemically generated radical initiators (eq 1.19).

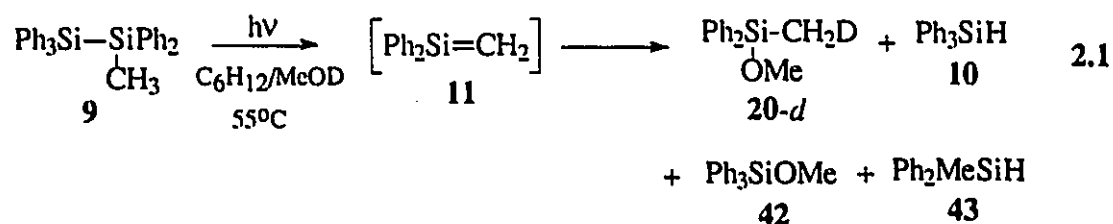


CHAPTER 2

REINVESTIGATION OF THE PHOTOCHEMISTRY OF METHYLPENTAPHENYLDISILANE

2.1 Introduction

In 1972, Sommer and coworkers reported that the photolysis of methylpentaphenyl-disilane (**9**) in cyclohexane containing methanol-*Od* at 55 °C yields a product (**20-d**) consistent with the formation of 1,1-diphenylsilene (**11**) and triphenylsilane (**10**) in approximately 60% yield.³⁶ Two other products, methoxytriphenylsilane (**42**) and methyl-diphenylsilane (**43**), were also detected as minor products, and were suggested to arise from Si-Si bond homolysis followed by silyl radical attack on the solvents (eq 2.1).



Although it was proposed that **11** is formed via concerted dehydrosilylation in a disilane excited state,³⁶ silene formation by disproportionation of triphenylsilyl- (**33**) and

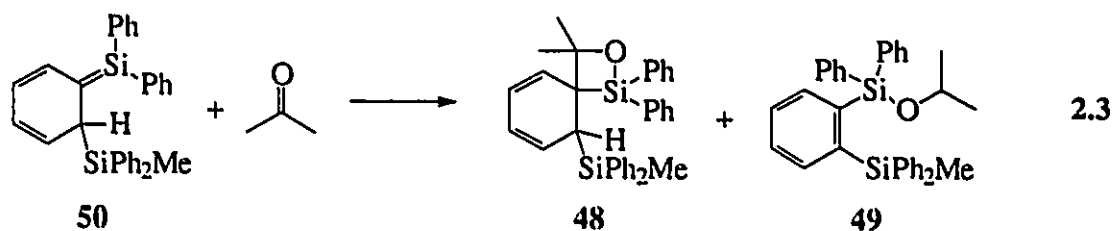
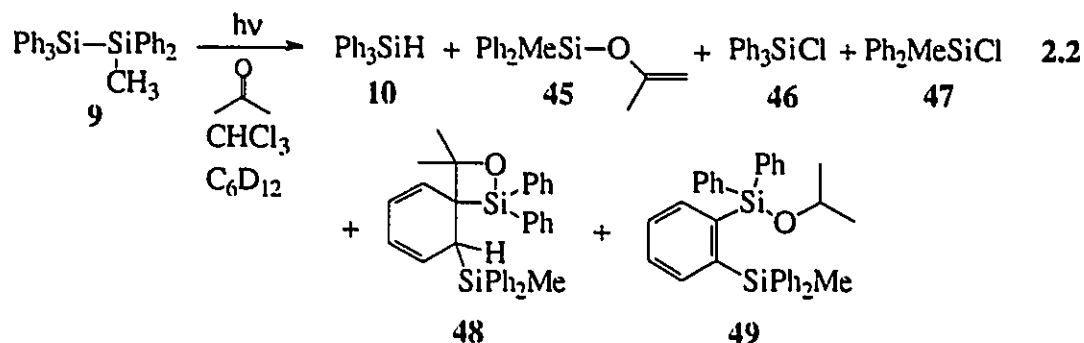
methyldiphenylsilyl radicals (**44**) could not be ruled out. The role of silyl free radicals in silene formation from the photolysis of **9** and the photochemical partitioning between simple silene, silatriene, and silyl free radical formation has been investigated by steady-state photolysis experiments which employed acetone and chloroform as silene and silyl radical trapping reagents, respectively. The photochemistry of **9** in the presence of methanol has been reinvestigated briefly. Methylpentaphenyldisilane (**9**) was also studied by nanosecond laser flash photolysis (NLFP) techniques with the goal of characterization of **11** by its UV absorption spectrum and reactivity with various silene trapping agents.

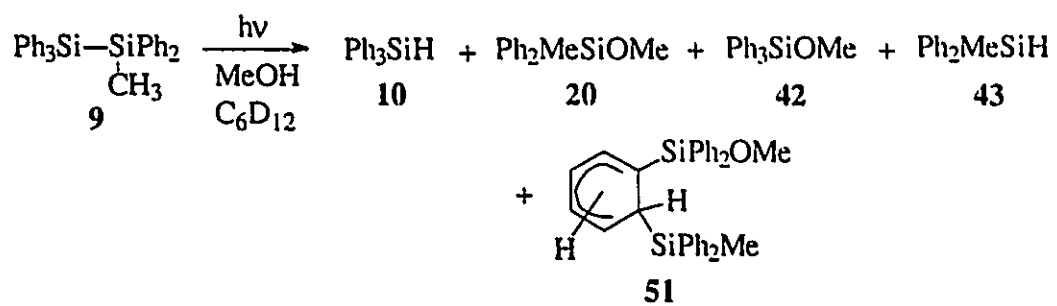
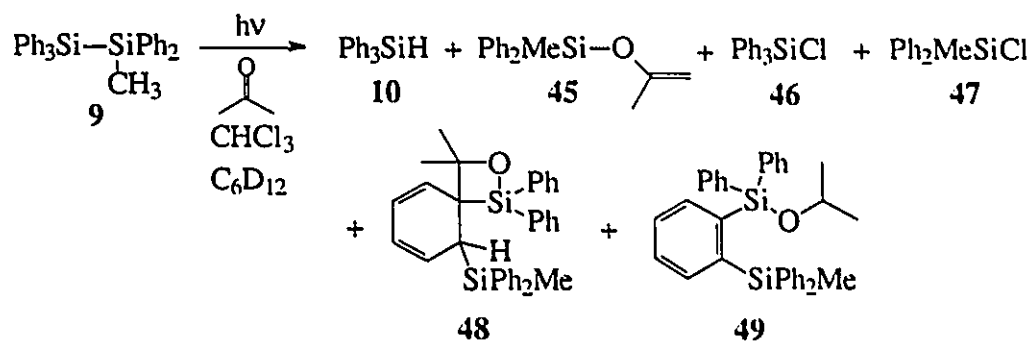
2.2 **Results**

Direct photolysis (254 nm) of deoxygenated 0.02 M solutions of **9** in cyclohexane or cyclohexane-*d*₁₂ containing 0.05 M acetone and 0.05 M chloroform affords the products shown in equation 2.2. Products **10**, **46**, and **47** were identified by gas chromatography (GC) and by coinjection of the photolysate with authentic samples. Silyl enol ether **45** was isolated by semi-preparative VPC and characterized by NMR, IR, and mass spectrometry. Small amounts of a product consistent with the addition of acetone to silatriene **50** were detected by GC and GC/MS, but its yield was too low (*ca.* 4-8%) to enable isolation. The ¹H NMR spectrum of the crude photolysis mixture after *ca.* 30% conversion, shown in Figure 2.1(a), shows prominent absorptions in the δ 5.6-6.0 range, a doublet at δ 3.61, along with other singlets in the δ 1.2-2.1 range and at δ 0.41. The spectral features are similar to those observed in the NMR spectra of the crude mixtures obtained from the

photolysis of several other aryl-disilanes in the presence of acetone¹⁰⁸ (see Chapter 4), and they are tentatively assigned as due to the 1,2-siloxetane **48**.

Product yields were determined by a combination of ¹H NMR and GC analyses of the crude photolysates and are collected in Table 2.1. The mass balance was 90-95% after 30% conversion of **9**. The ¹H NMR spectrum also exhibited minor absorptions which are assigned to silyl ether **49**, derived from formal ene reaction of acetone with silatriene **50** (eq 2.3). The mass spectral fragmentation pattern of the high molecular weight species detected by GC is consistent with a product of this type.^{102,108} 1,1,2,2-Tetrachloroethane was also detected by NMR spectroscopy and GC/MS analysis.





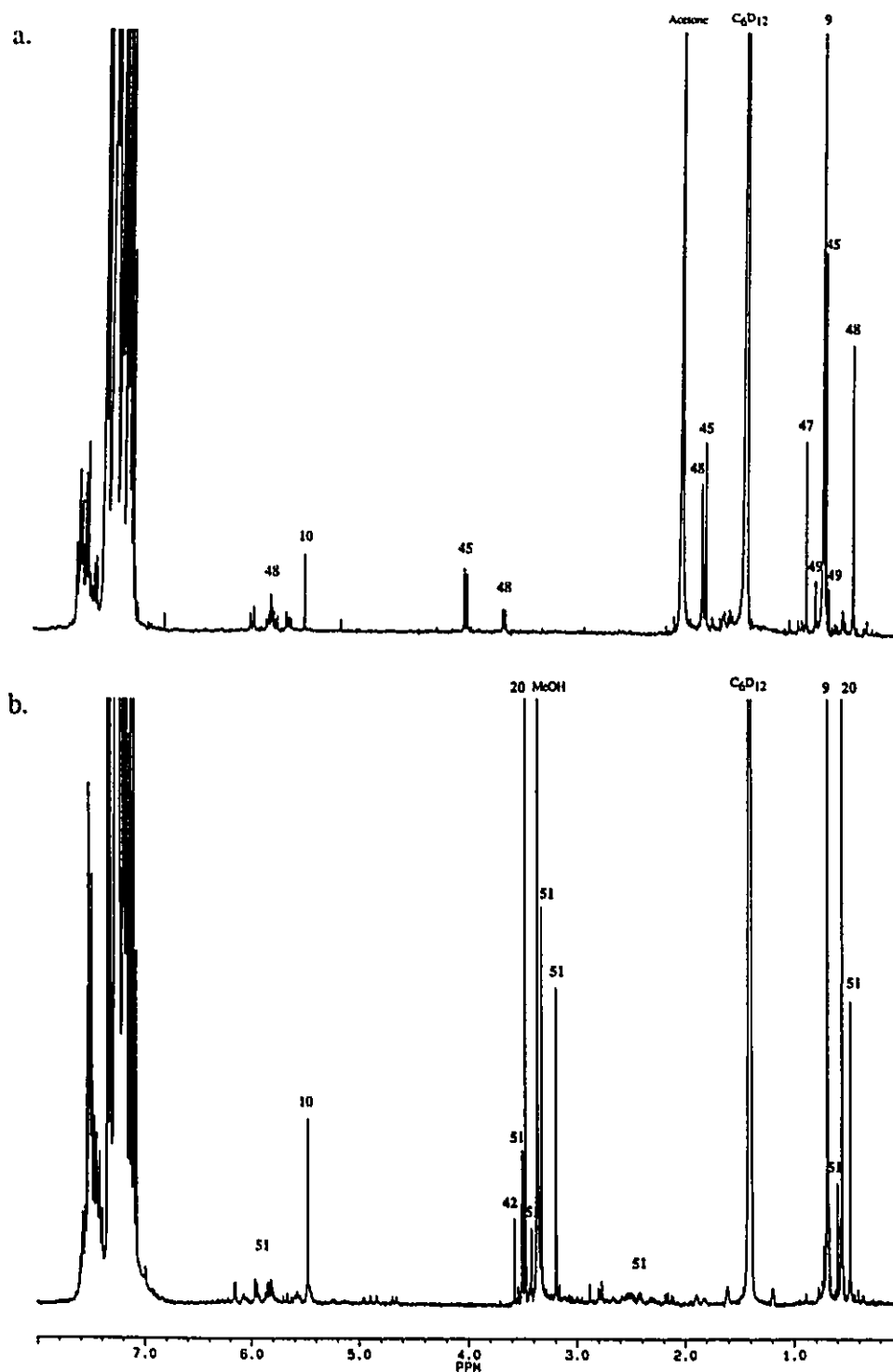


Figure 2.1 ^1H NMR spectra of crude mixtures from photolysis of deoxygenated 0.02 M solutions of 9 in cyclohexane- d_{12} , in the presence of (a) 0.05 M acetone and 0.05 M chloroform, and (b) 0.05 M methanol, at 23 °C to *ca.* 30% and 50% conversion, respectively. Resonances due to the various products are labelled in the spectra.

Table 2.1 Product Yields from the Photolysis of Methylpentaphenyldisilane (**9**) in the Presence of 0.05 M Acetone and Various Additives.^a

Solvent	Additive	10 (%)	45 (%)	47 (%) ^b	48 (%)
C ₆ D ₁₂	none	29	29	-	37 ^c
C ₆ D ₁₂	CHCl ₃ (0.05 M)	32	34	17	34 ^c
C ₆ D ₁₂	CHCl ₃ (0.5 M)	30	37	23	<i>nd</i>
C ₆ D ₁₂	CCl ₄ (1.0 M)	5	-	88	-
C ₆ D ₁₂	CHCl ₃ (0.2 M) <i>trans</i> -piperylene (0.1 M)	38	38	8	38 ^c
CD ₃ CN	CHCl ₃ (0.05 M)	7	-	66 ^d	-
CDCl ₃	none	13	-	79	-
CDCl ₃	chloranil	-	-	65	-

- a. Determined by ¹H NMR spectroscopy, relative to consumed **9**, after 30-50% conversion. Errors are *ca.* 10%. *nd* = not detected.
- b. The photolysate also contained **46**, in similar yield to **47**, as estimated by GC.
- c. The photolysate also contained small amounts (*ca.* 5%) of **49**.
- d. Yield is the sum of that of **47** and the corresponding silanol.

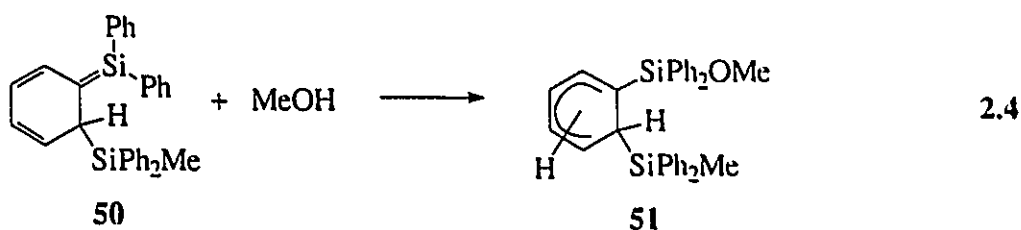
Photolysis of a deoxygenated 0.02 M solution of **9** in C₆D₁₂ containing 0.05 M acetone, but without added chloroform, yielded **10**, **45**, **48**, and **49** in similar chemical yields to those obtained in the presence of halocarbon. Methyl-diphenylsilane (**43**) was also detected in a chemical yield of *ca.* 2%. The mass balance was estimated to be *ca.* 65% after 30% conversion of **9**. Photolysis of a 0.02 M solution of **9** in C₆D₁₂ containing 0.05

M acetone, 0.2 M chloroform, and 0.1 M *trans*-piperylene under similar conditions led to substantial reductions in the yields of chlorosilanes **46** and **47**, but had little effect on the yields of **10** and **45** compared to the photolyses performed in the absence of diene (Table 2.1). The quantum yield for disappearance of **9** in cyclohexane-*d*₁₂ containing 0.05 M acetone was determined to be $\phi_{\text{dis}} = 0.33 \pm 0.05$, and was independent of the presence of chloroform.

Irradiation of a deoxygenated 0.005 M solution of **9** in acetonitrile-*d*₃ containing acetone (0.10 M) and chloroform (0.05 M) yields chlorosilanes (**46** and **47**) as the major products along with minor amounts of triphenylsilane (**10**) on the basis of ¹H NMR, GC, and GC/MS analysis of the crude photolysate after *ca.* 30% conversion. The ¹H NMR spectrum exhibited evidence for the formation of at least two other unidentified products in < 10% yield each. None of the silyl enol ether (**45**) could be detected under these conditions.

Steady-state photolysis (254 nm) of deoxygenated 0.02 M solutions of **9** in cyclohexane-*d*₁₂ containing 0.05 methanol at 25 °C affords **10** (43%), **20** (34%), **42** (3%), and **43** (4%) in significantly different yields than those reported previously by Sommer and coworkers (eq 2.1).³⁶ The ¹H NMR spectrum (shown in Figure 2.1(b)), and gas chromatographic and GC/MS analyses of the crude photolysate reveal the presence of isomeric products (**51**) consistent with the addition of methanol to **50** in 38% chemical yield. Adduct **51** exists as five isomers and is characterized by NMR absorptions in the vinylic, methoxy- and silylmethyl regions of the spectrum. The two major isomers, characterized by their methoxy absorptions, are formed in 16% and 12% yield while the other three minor isomers are formed in a combined yield of 10%. Capillary GC and

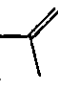
GC/MS analyses show the formation of at least four isomers which elute after the starting material (**9**) and exhibit molecular ions and fragmentation patterns consistent with **51** (eq 2.4). Unfortunately, as is common for most silatriene-alcohol adducts,^{94,95} **51** elutes as a single broad peak under megabore capillary or packed column GC conditions, precluding isolation of the individual isomers. Heating the crude, room temperature photolysis mixture at 100 °C for 16 h resulted in no apparent change in the product distribution. Photolysis of a similar solution at 55-60 °C to *ca.* 50% conversion yields the same products in similar yields to those obtained in the room temperature photolysis.



Merry-go-round photolysis (254 nm) of deoxygenated 0.01 M solutions of **9** in cyclohexane containing 0.05 M acetone and between 0.02 and 12.5 M chloroform to *ca.* 10% conversion, followed by GC analysis reveal that the quantum yields for formation of **10** and **45-47** are independent of chloroform concentration over the range 0.02-0.5 M (Table 2.2). The yield of **45** drops off dramatically to zero at chloroform concentrations higher than 0.5 M while the yields of the chlorosilanes **46** and **47** increase steadily. The quantum yield for formation of triphenylsilane **10** also decreases with increasing chloroform concentrations above 0.50 M, but does not drop to zero even in neat chloroform. A Stern-Volmer plot showing the decrease in the yield of **10** with increasing chloroform concentration and a plot of the relative quantum yield of **46** versus chloroform concentration are listed in Figure 2.2. Least squares analysis of the Stern-Volmer plot

over the 1.0-12.5 M range affords a $k_q\tau$ value of 0.06 ± 0.02 . The quantum yield for disappearance of **9** in the presence of 0.05 M acetone in neat CDCl_3 solution was determined to be 0.41 ± 0.07 .

Table 2.2 Relative Quantum Yields for Formation of **10**, **45**, **46**, and **47** from the Photolysis of Deoxygenated Solutions of **9** in Chloroform/Cyclohexane Mixtures Containing 0.05 M Acetone.^a

$[\text{CHCl}_3] / \text{M}$	Ph_3SiH (10)	Ph_2MeSiO  (45)	Ph_3SiCl (46)	Ph_2MeSiCl (47)
0	1.1	1.0	0	0
0.02	1.2	1.3	0.53	0.48
0.10	1.0	1.1	0.50	0.45
0.20	0.92	1.0	0.50	<i>nd</i>
0.50	0.97	0.91	0.64	0.61
1.0	0.91	0.05	0.75	0.70
3.0	0.94	0	1.5	1.3
6.0	0.75	0	2.0	2.1
12.5	0.61	0	3.6	3.6

- a. Errors are *ca.* $\pm 10\%$. Quantum yields for product for formation have been normalized relative to the quantum yield for formation of **45** in the absence of chloroform. *nd* = not determined.

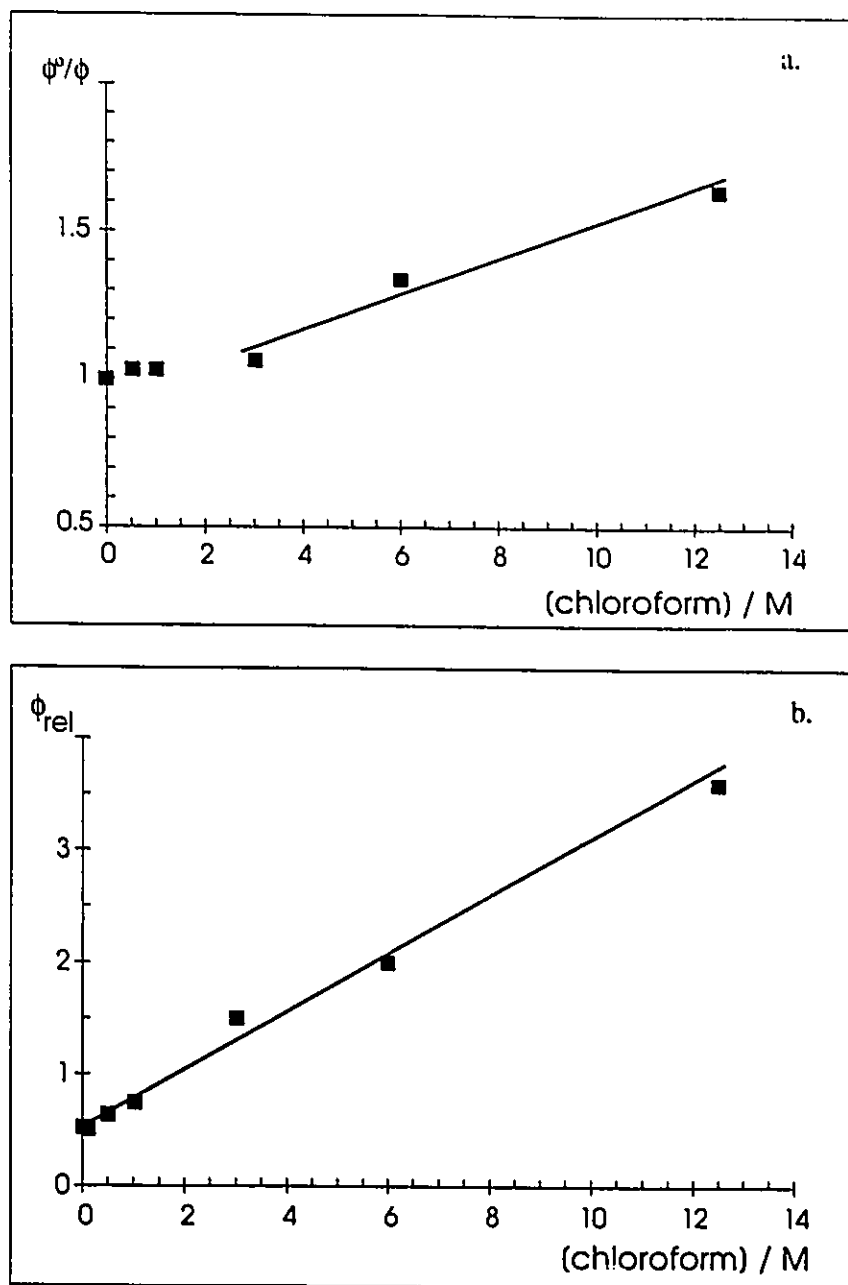


Figure 2.2 Photolysis of deoxygenated cyclohexane solutions of **9** (0.01 M) containing acetone (0.05 M) and varying concentrations of chloroform. (a) Stern-Volmer plot for product **10**. (b) Plot of relative quantum yield for formation of **46** versus chloroform concentration.

Steady-state photolysis of a 0.02 M solution of **9** in C₆D₁₂ containing acetone (0.05 M) and carbon tetrachloride (1.0 M) affords **10**, **46**, and **47** as the only detectable products by ¹H NMR and GC analysis.

Methylpentaphenyldisilane (**9**) exhibits a weak diffuse fluorescence emission band at room temperature centred at *ca.* 395 nm in hydrocarbon and ACN solutions. Figure 2.3 shows the absorption and emission spectra recorded with a solution of **9** in OCT at 23 °C. The behaviour of **9** contrasts that reported for **12** which exhibits dual fluorescence emission in OCT solution and a *ca.* 40 nm blue-shift in the CT emission band relative to that in ACN^{38,81,83,87,88} (see Figure 1.1). In order to verify that the spectra observed for solutions of **9** are not due to the formation of triphenylsilane (**10**) from photolysis of **9** by the spectrometer excitation source, fluorescence emission spectra were recorded for solutions of **10** in the same solvent. Solutions of **9** which were photolyzed for extended periods of time in the emission spectrometer exhibited spectra consisting of superimposed emission from both **9** and **10**.

Fluorescence emission from **9** is quenched inefficiently by the addition of chloroform to cyclohexane solutions of **9** at 23 ± 2 °C. Analysis of the data between 1.0 and 12.5 M chloroform according to the Stern-Volmer equation (eq 2.5) affords a linear plot with a $k_q\tau$ value of 0.06 ± 0.02 M⁻¹. Dichloromethane, on the other hand, does not quench the fluorescence of **9** detectably up to 15 M halocarbon, while carbon tetrachloride quenches the fluorescence fairly efficiently and exhibits linear Stern-Volmer behaviour. The $k_q\tau$ value was determined to be 1.6 ± 0.2 M⁻¹. Figure 2.4 shows the Stern-Volmer plots for fluorescence quenching of **9** by chloroform and carbon tetrachloride. The relative quantum yield for fluorescence emission of **9** in ACN relative to that in cyclohexane was estimated to be $\phi_F(\text{ACN})/\phi_F(\text{C}_6\text{H}_{12}) = 0.74$.

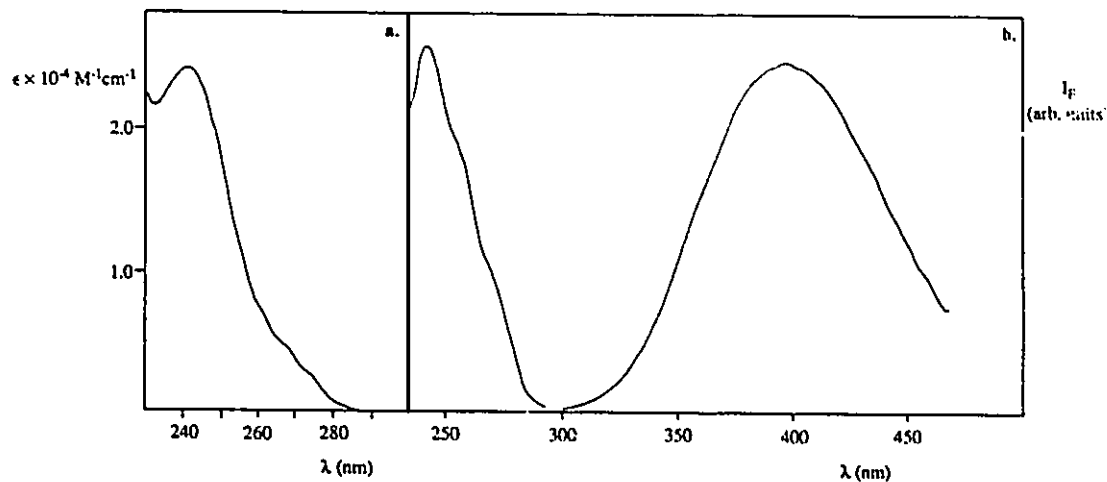


Figure 2.3 (a) Ultraviolet absorption spectrum and (b) fluorescence emission and excitation spectra of **9** in isooctane solution at 23 ± 2 °C.

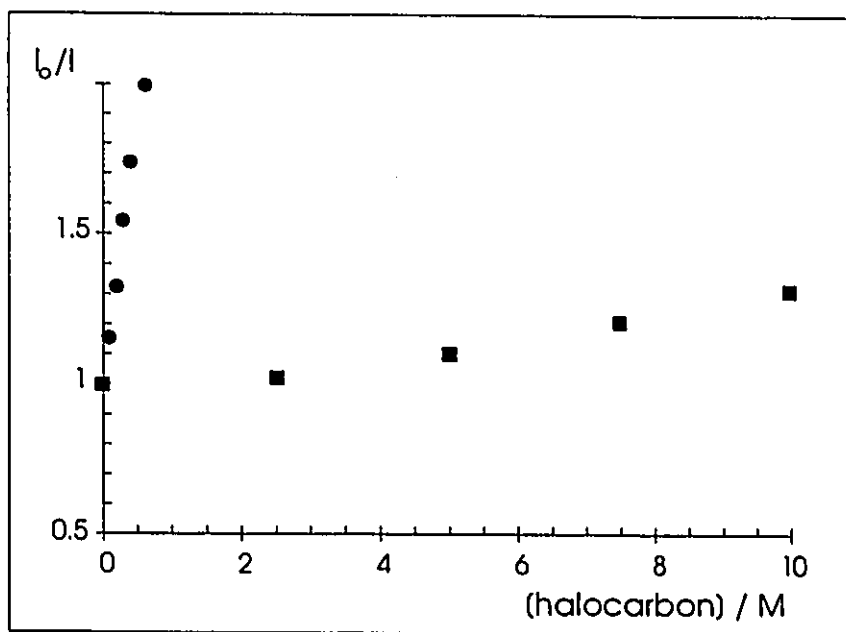


Figure 2.4 Stern-Volmer plots for quenching of fluorescence of **9** in cyclohexane solution at 23 ± 2 °C by chloroform (■) and carbon tetrachloride (●).

$$I^0/I = 1 + k_q\tau[Q] \quad 2.5$$

Photolysis of a deoxygenated chloroform solution of **9** (0.05 M) containing chloranil (≈ 0.001 M) as a sensitizer with 360 nm light yields chlorosilanes **46** and **47** as the only detectable silicon-containing products by GC. The ^1H NMR spectrum showed the formation of one additional product in *ca.* 10% yield, but it was not identified. The material balance was estimated to be *ca.* 75% after 50% conversion of **9**.

NLFP experiments employed a flow system containing deoxygenated solutions of **9** (*ca.* 2×10^{-4} M) in dried acetonitrile (ACN) or isooctane (OCT), the pulses (248 nm, *ca.* 16 ns, 80-120 mJ) from a KrF excimer laser, and a microcomputer-controlled detection system.^{109,110} The time-resolved UV absorption spectra recorded 70-90 ns and 2.8-3.2 μs after flash photolysis of a 1.7×10^{-4} M solution of **9** in ACN are shown in Figure 2.5. Representative decay traces recorded at 330 and 490 nm are shown in Figure 2.6.

The short-wavelength absorption region (300-340 nm) of the transient UV absorption spectrum (Figure 2.5) is quite complex. The decay traces in ACN solution show mixed first- and second-order kinetics with *ca.* 15% residual absorption (Figure 2.6 (a)). The residual absorption is long-lived on the timescale of these experiments ($\tau > 1$ ms) but is not present in static UV absorption spectra recorded within minutes after photolysis to 40-50% conversion. The addition of oxygen quenches the short-lived component of the 330 nm transient absorption in ACN while methanol has little effect on either. Although it is known that **11** has an absorption maximum in the 320-325 nm range,^{63,111} the sharp absorption band centred at 325 nm is due mainly to triphenylsilyl (**33**) and methyldiphenylsilyl radicals (**44**). This can be demonstrated by comparing the spectrum in Figure 2.5 to those recorded by laser flash photolysis (337 nm) of solutions of

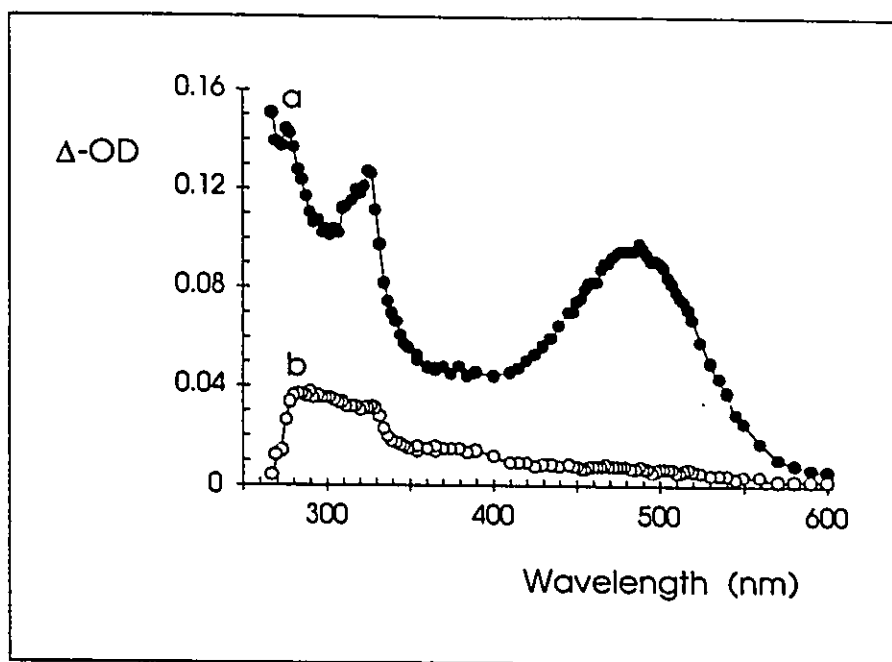


Figure 2.5 Time-resolved UV absorption spectra recorded (a) 70-90 ns and (b) 2.8-3.2 μ s after 248 nm nanosecond laser flash photolysis of a deoxygenated 1.8×10^{-4} M solution of **9** in acetonitrile at 23 ± 2 °C.

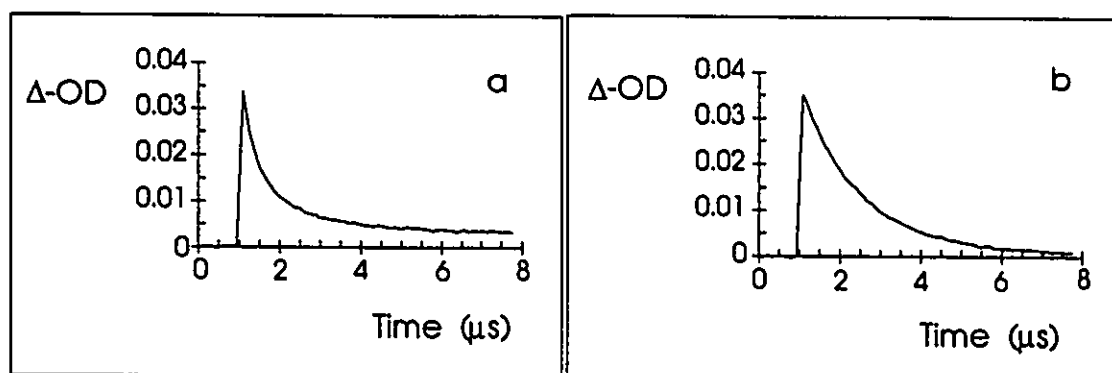
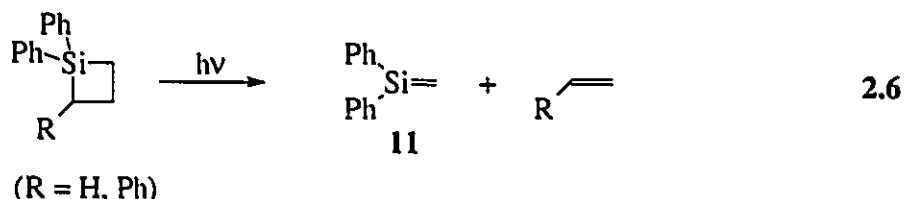


Figure 2.6 Transient decay traces recorded at (a) 330 nm and (b) 490 nm from 248 nm nanosecond laser flash photolysis of a 1.8×10^{-4} M solution of **9** in acetonitrile at 23 ± 2 °C.

silanes **10** and **43** in 1:4 BOOB/isooctane (Figure 2.7). The spectrum of **33** is in excellent agreement with those previously reported.⁷² Furthermore, this component of the spectrum from **9** is quenched by the addition of 0.1 M 2-bromopropane, which is known to react with arylsilyl radicals with rate constants in the 10^8 - 10^9 $M^{-1}s^{-1}$ range¹¹² (see Chapter 3). The transient absorption spectrum, recorded 120-160 ns following the laser pulse under these conditions, is shown in Figure 2.8.

The transient absorption spectrum recorded 40-80 ns following NLFP of a 0.003 M solution of 1,1-diphenylsilacyclobutane in ACN solution shown in Figure 2.9 demonstrates the absorption due to **11** centred at *ca.* 320-325 nm (see eq 2.6).¹¹¹ Similar spectra are obtained from NLFP of ACN and OCT solutions of 1,1,2-triphenylsilacyclobutane.⁶³



The decay kinetics of the transient centred at 490 nm are sensitive to the amount of trace water in the ACN. In rigorously dried ACN, the 490 nm transient decays with mixed first- and second-order kinetics and has a lifetime of 1.7 ± 0.2 μs . In less carefully dried ACN, the transient decays with clean first-order kinetics with lifetimes in the 300-900 ns range (Figure 2.6(b)). The transient decays with mixed first- and second-order kinetics and is much longer lived ($\tau > 10$ μs) in OCT solution. The lifetime of the 490 nm transient was shortened only slightly by the addition of 0.05 M 2,3-dimethyl-1,3-butadiene (DMB),

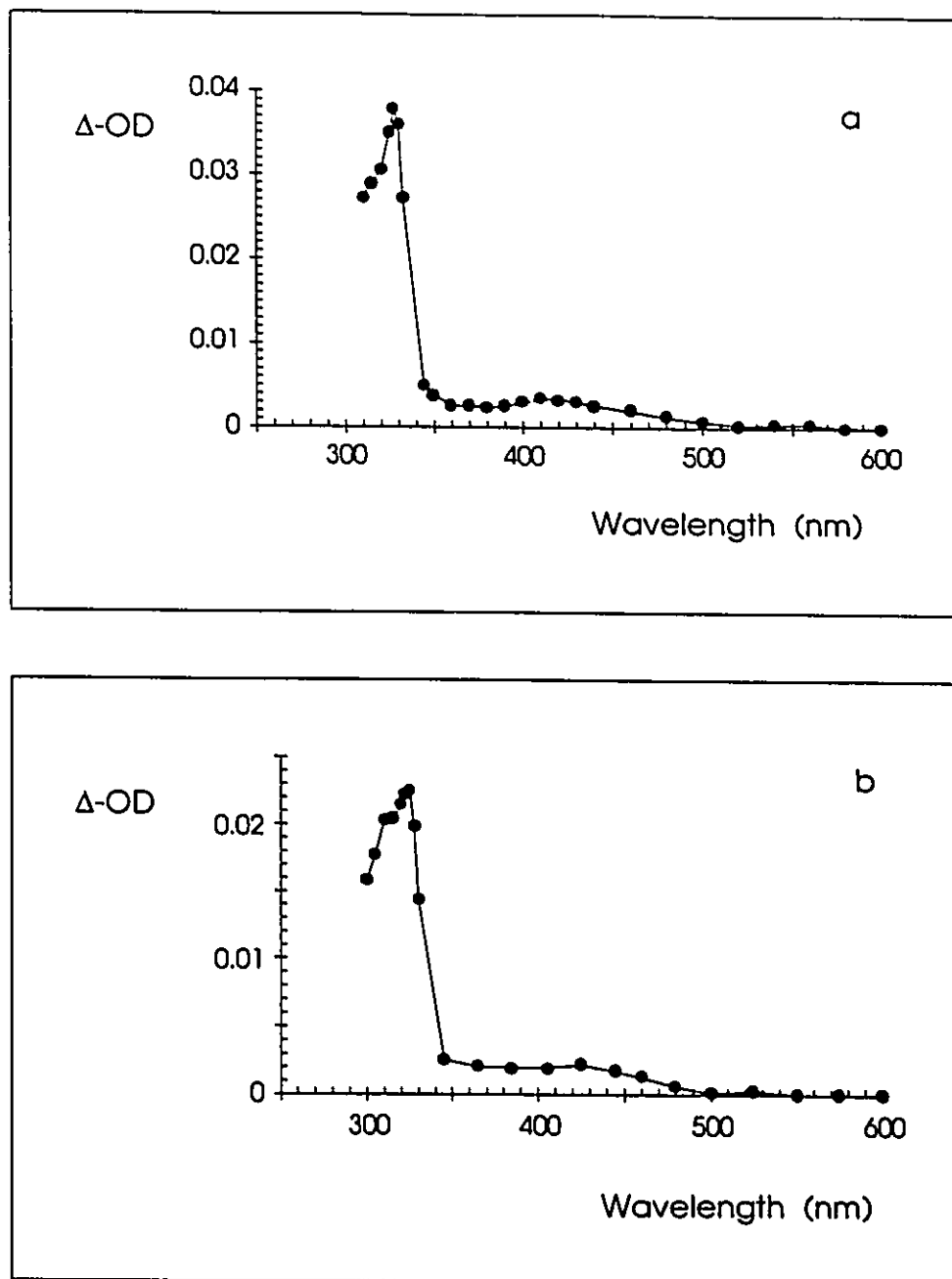


Figure 2.7 Transient absorption spectra of (a) triphenylsilyl- (33) and (b) methyl-diphenylsilyl radicals (44), from nanosecond laser flash photolysis (337 nm) of solutions of triphenylsilane (10) and methyl-diphenylsilane (43), respectively in 1:4 BOOB/isooctane at 23 ± 2 °C.

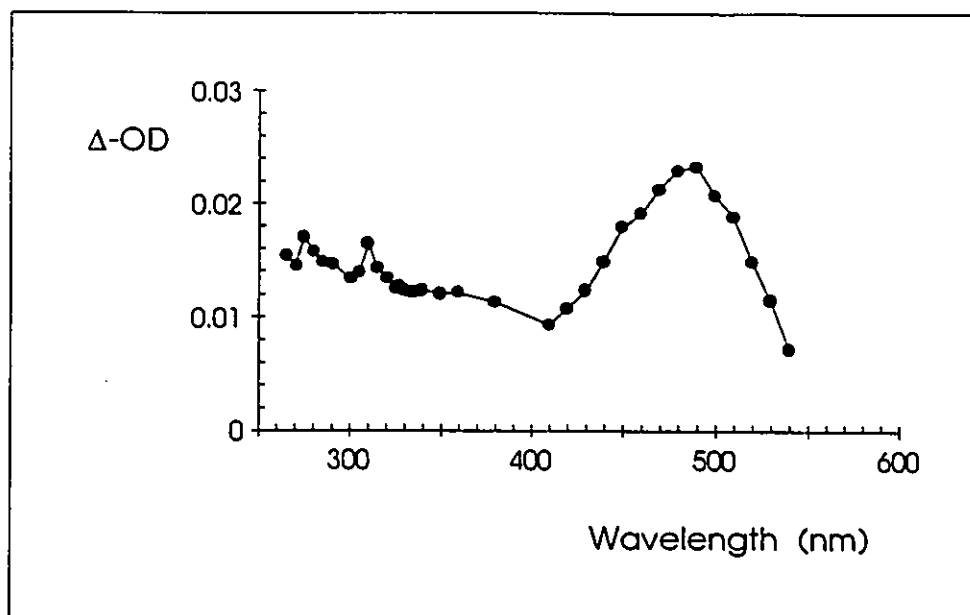


Figure 2.8 Time-resolved absorption spectrum recorded 120-160 ns following NLFP (248 nm) of a 1.7×10^{-4} M solution of **9** in ACN containing 0.1 M 2-bromopropane.

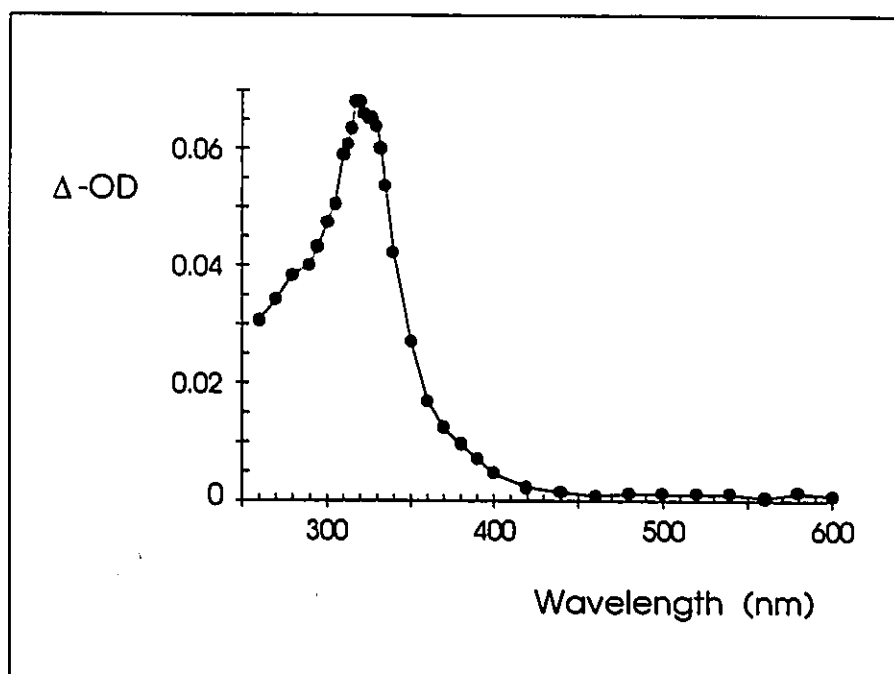
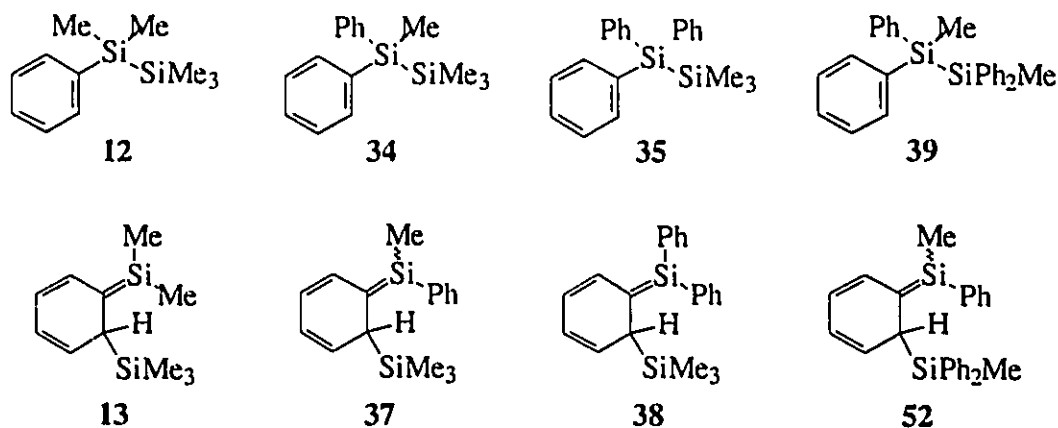


Figure 2.9 Transient absorption spectrum recorded 40-80 ns following laser excitation from NLFP of an oxygen saturated 3.1×10^{-3} M solution of 1,1-diphenylsilacyclobutane in ACN solution at 23 ± 2 °C.

indicating that it is not a triplet-state species of triplet energy greater than *ca.* 55 kcal/mol. The addition of up to 0.3 M triethylsilane had no effect on the lifetime, suggesting that the transient is not a silylene. Trialkylsilanes react with silylenes with rate constants in the 10^8 - 10^9 M⁻¹s⁻¹ range.¹¹³⁻¹¹⁷ The lifetime of the 490 nm transient is shortened by the addition of known silene trapping reagents such as oxygen, water, alcohols, acetic acid, alkenes, ethyl acetate, and acetone. These experiments suggest that the transient species contains a silicon-carbon double bond.

The 490 nm transient is assigned to silatriene **50** on the basis of the similarities in the UV absorption spectra and quenching behaviour with similar long-wavelength transients obtained from the photolysis of pentamethylphenyl- (**12**), 1,1,1,2-tetramethyl-1,1-diphenyl- (**34**), 1,1,1-trimethyl-2,2,2-triphenyl- (**35**), and 1,2-dimethyl-1,1,2,2-tetraphenyldisilane (**39**). Nanosecond laser flash photolysis (248 nm) of deoxygenated, continuously flowing, *ca.* 10⁻³ M solutions of **12**, **34**, **35**, and **39** in dried ACN or OCT solutions led to strong transient absorptions in the 270-600 nm range. Transient absorption spectra were recorded in a point-by-point manner as the average transient optical density in a selected time window following NLFP of the three disilanes. Figure 2.10 shows transient absorption spectra recorded within a few hundred nanoseconds after laser excitation for OCT and ACN solutions of **12**, **34**, and **35**. The transient absorption spectrum from NLFP of an n-pentane solution of **35** was virtually identical to that recorded in OCT solution. The transient absorption centred at 425 nm from flash photolysis of **12** has been previously assigned to silatriene **13**.^{14,82}



The short-wavelength transient absorptions (300-340 nm) from NLFP of **12**, **34**, and **35** decay with first-order kinetics in ACN solution with lifetimes in the 500-700 ns range. The decay traces show significant long-lived residual absorptions which total *ca.* 30% of the initial transient absorbances (Figure 2.11(a)). These short-lived transients have been assigned to the corresponding arylsilyl radicals on the basis of their absorption maxima,^{72,109} and the fact that they are quenched rapidly by carbon tetrachloride and oxygen, but not by acetone.

The absorptions centred at 460 and 490 nm from NLFP of **34** and **35** are assigned to silatrienes **37** and **38**, respectively. The red-shifts in the silatriene absorption maxima are consistent with increasing phenyl substitution at the trivalent silicon atom. The transient absorption spectrum recorded from NLFP of an OCT solution of **39** (Figure 2.12) shows a similar 460 nm absorption to **37** due to the same methylphenylsilatrienyl chromophore in silatriene **52**. In this case, the transient absorption in the 300-340 nm range is reasonably broad and matches the reported spectrum of 1,1-diphenylsilene (**II**) in OCT solution fairly precisely.⁶³ Since arylsilyl radicals are generally formed in low yields from the photolysis of arylsilylanes in hydrocarbon solvents (Table 2.1; Chapter 3), it is likely that this

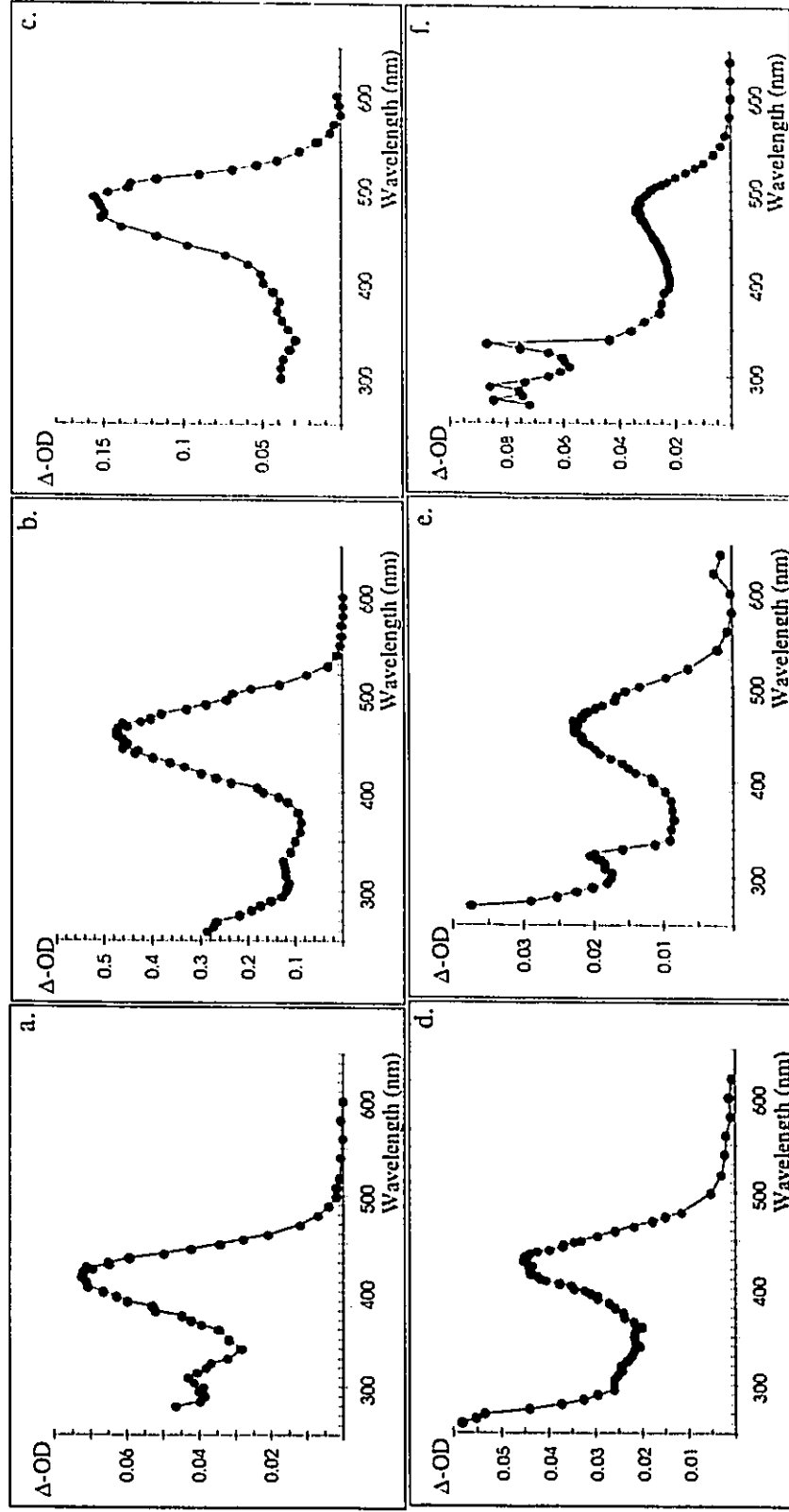


Figure 2.10 Transient absorption spectra recorded by NLFP, 10-200 ns after 248 nm laser excitation of deoxygenated OCT (a-c) and ACN (d-f) solutions of 12, 34, and 35.

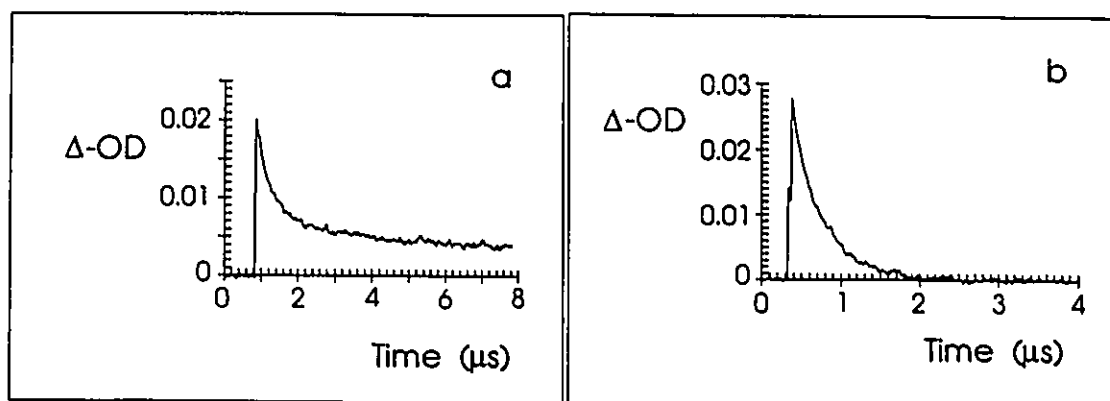


Figure 2.11 Transient decay traces recorded at (a) 320 and (b) 460 nm following NLFP (248 nm) of a *ca.* 0.001 M solution of **34** in deoxygenated acetonitrile at 23 ± 2 °C.

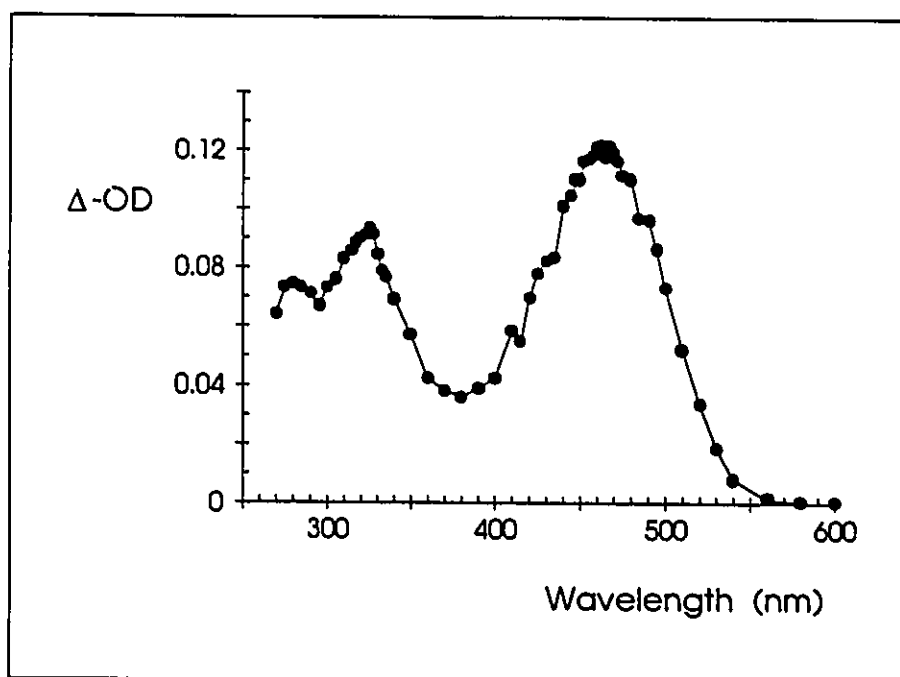
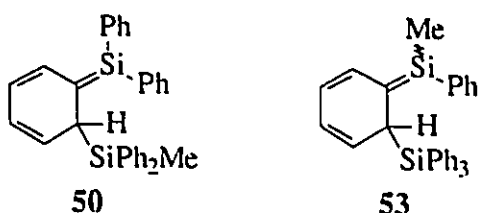


Figure 2.12 Transient absorption spectrum recorded 160-320 ns after laser excitation (248 nm) from NLFP of a deoxygenated 1.3×10^{-4} M solution of **39** in isooctane at 23 ± 2 °C.

absorption band is due mainly to **11** with only minor contributions from the corresponding methyldiphenylsilyl radicals (**44**).



The high degree of symmetry of the 490-nm absorption band in Figure 2.5 indicates that the other possible silatriene (**53**), which would be formed by formal [1,3] migration of a triphenylsilyl group into a phenyl ring on the other silicon atom, is not formed or is formed in much lower yield than **50**. Silatriene **53** contains the methylphenylsilatrienyl chromophore and would be expected to exhibit an absorption centred at *ca.* 460 nm by analogy with the absorption spectra obtained for silatrienes **37** and **52**. Further evidence for the assignment of **50** comes from the fact that the transient absorption spectrum of silatriene **38**, generated from flash photolysis of **35**, is very similar ($\lambda_{\text{max}} = 490 \text{ nm}$).

In a similar manner to **50**, the long-wavelength transient absorptions from NLFP of **12**, **34**, and **35** decay with clean first-order kinetics in dried ACN ($\tau = 1.1, 1.7, \text{ and } 2.7 \mu\text{s}$, respectively), while in OCT the transients are much longer lived ($\tau > 4 \mu\text{s}$) and decay with mixed first- and second-order kinetics (see Figure 2.11(b)). The addition of oxygen, alcohols, acetic acid, acetone, DMB, dimethyl sulfoxide (DMSO), carbon tetrachloride, and chloroform leads to reductions in the transient lifetimes but not in their initial yields. In OCT solution, the transients decay with pseudo first-order kinetics in the presence of these quenchers. Bimolecular quenching rate constants were determined by least squares analysis of the data according to equation 2.7 where k_q is the bimolecular quenching rate

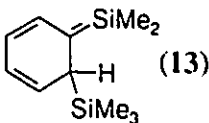
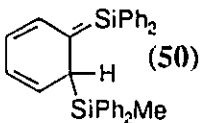
constant and k_0 is the rate constant for silatriene decay in the absence of any added quencher. In each case the rate constant is two to five times smaller for quenching of **50** than **13** (Table 2.3) which is consistent with the higher steric bulk at the trivalent silicon atom in **50**.

$$k_{\text{decay}} = k_0 + k_q[\text{Q}] \quad 2.7$$

The transient UV spectrum recorded from NLFP of a deoxygenated OCT solution of **9** under similar conditions to those employed above also shows two transient absorptions centred at 490 and 325 nm (Figure 2.13(a)). While the spectra recorded in ACN and OCT solutions are quite similar, there are subtle differences. In OCT solution, the absorption in the 300-340 nm range is slightly weaker than the 490 nm band, whereas in ACN, the short-wavelength absorption is sharper and more intense than the long-wavelength transient. Similar spectra were recorded from OCT solutions of **9** in the presence of 0.05 M chloroform (Figure 2.13(b)), in oxygen-saturated solution (Figure 2.13(c)), and in the presence of 0.06 M acetone (Figure 2.13(d)).

The rate constant for the reaction of 1,1-diphenylsilene (**11**) with chloroform in OCT solution was estimated to be $< 10^4 \text{ M}^{-1}\text{s}^{-1}$, from the lifetime of **11** (generated from the photolysis of 1,1,2-triphenylsilacyclobutane⁶³) in OCT containing 2 M chloroform. The rate constant for reaction of silatriene **50** with chloroform is estimated to be $< 10^6 \text{ M}^{-1}\text{s}^{-1}$, based on the rate constant for chloroform reaction with silatriene **13** in OCT solution ($k_q = 1.1 \times 10^6 \text{ M}^{-1}\text{s}^{-1}$). The rate constant for quenching of *tert*-butyldiphenylsilyl radicals (**41**) (generated from the photolysis of disilane **40**; see Chapter 3) with *trans*-piperylene in OCT solution was determined to be $(6.2 \pm 0.4) \times 10^7 \text{ M}^{-1}\text{s}^{-1}$.

Table 2.3 Rate Constants for Bimolecular Quenching of Silatrienes **13** and **50** by Oxygen, Acetone, Ethyl Acetate, Cyclohexene, DMB, 1,1,1-Trifluoroethanol, and Acetic Acid in ACN Solution at 23 ± 2 °C.^a

Reagent	k_q ($\times 10^{-8}$ Ms)	
	 (13)	 (50)
O ₂ (ACN) ^b	8.5 ± 0.8	3.8 ± 0.3
O ₂ (OCT) ^c	6.9 ± 0.4	1.52 ± 0.09
Acetone	7.7 ± 0.2	2.54 ± 0.15
Ethyl Acetate	0.033 ± 0.003	d
Cyclohexene	0.012 ± 0.002	0.009 ± 0.001
DMB ^e	1.28 ± 0.03	0.23 ± 0.01
CF ₃ CH ₂ OH	0.236 ± 0.004	0.039 ± 0.002
CH ₃ COOH	2.9 ± 0.1	0.97 ± 0.03

- Errors reported as twice the standard deviation from least squares of the data according to equation 2.7.
- Calculated assuming a value of 0.0085 M for the concentration of oxygen in O₂-saturated ACN.¹¹⁸
- Calculated assuming a value of 0.015 M for the concentration of oxygen in O₂-saturated OCT.¹¹⁹
- Not determined.
- Recorded in OCT solution.

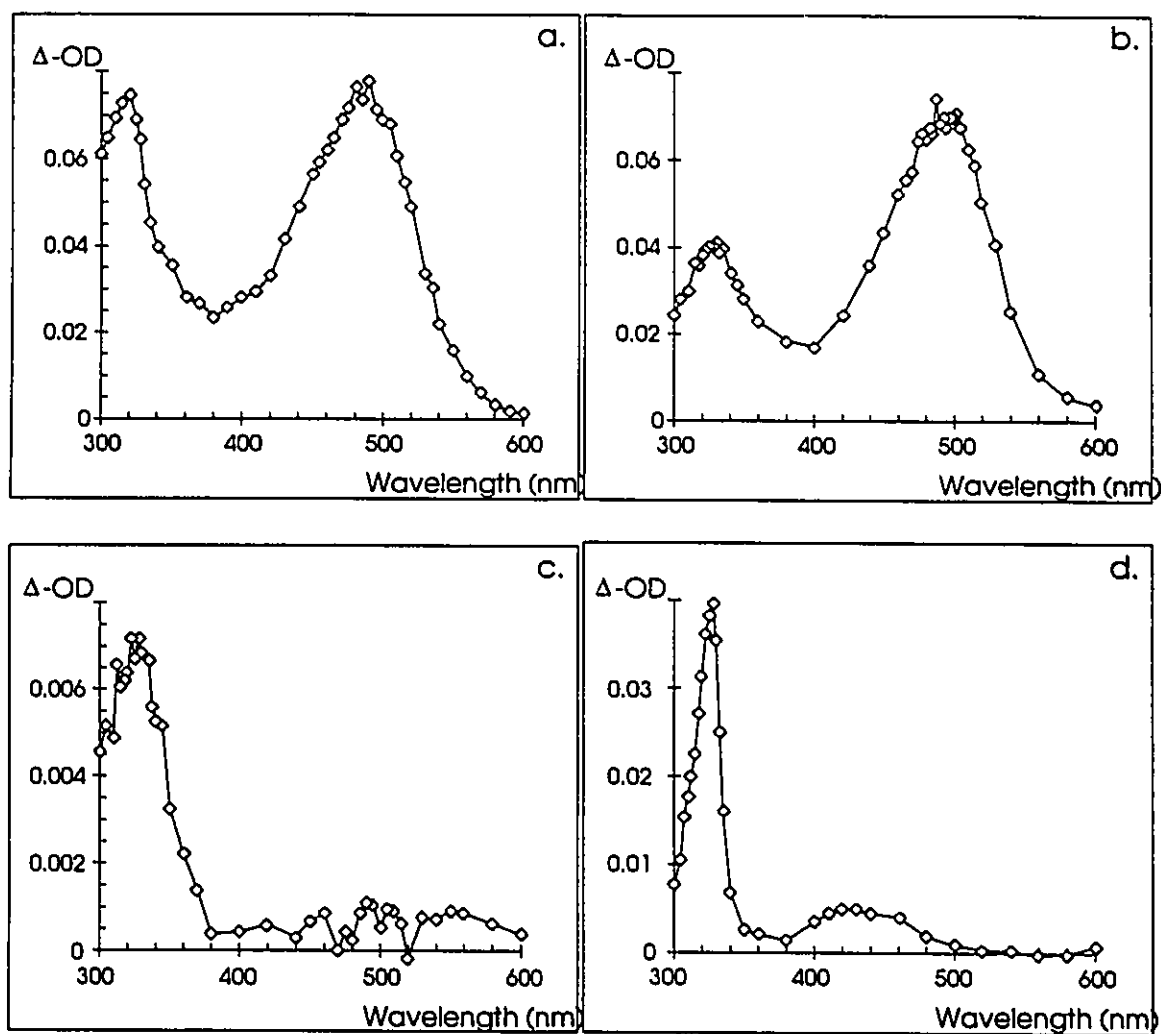


Figure 2.13 Transient UV absorption spectra, recorded by nanosecond laser flash photolysis of 1.8×10^{-4} M solutions of **9** in OCT under the following conditions: (a) deoxygenated solution; (b) partially oxygenated solution containing 0.05 M chloroform; (c) oxygenated solution; (d) deoxygenated solution containing 0.06 M acetone. The spectra were recorded 100-500 ns after 248 nm laser excitation, and were corrected for corrected for minor, long-lived residual absorption at $\lambda < 320$ nm.

2.3 Discussion

The photochemistry of methylpentaphenyldisilane (**9**) has been reinvestigated in attempts to detect 1,1-diphenylsilene (**11**) directly by NLFP techniques, to evaluate the relative yields of silatrienes, **11**, and free silyl radicals **33** and **44**, and to determine the role of silyl radicals in simple silene and silatriene formation.¹²⁰ Sommer has suggested previously that **11** is the major transient species produced upon photolysis of **9** in non-polar solvents (see eq 2.1);³⁶ however, the formation of silatriene- or silyl radical-derived products has not been reported. We have found that the photochemistry of **9** is *considerably* more complex than previously reported. We are able to detect significant amounts of silyl radical- and silatriene-derived products, in addition to triphenylsilane (**10**) and those derived from **11**, upon irradiation of cyclohexane solutions of **9** containing acetone and chloroform as silene and radical trapping agents, respectively.

Indeed, NLFP experiments employing OCT solutions of **9** have revealed that silyl radicals **33** and **44**, 1,1-diphenylsilene (**11**), and silatriene **50** can be detected *selectively* by the addition of the appropriate trapping agents (or combination thereof) to the solution (Figure 2.13). In general, the intense silyl radical absorptions overlap those due to **11**, thus, **9** is not a suitable substrate for the characterization **11** by NLFP techniques. The transient absorption spectrum of the deoxygenated OCT solution (Figure 2.13(a)) is the sum of those due to silene **11**, silatriene **50**, and silyl radicals **33** and **44**, and is similar to the spectrum recorded in ACN solution under similar conditions (Figure 2.5) except that the absorption band in the 300-340 nm range is weaker and broader in OCT solution due to higher relative yield of **11** versus silyl radicals compared to that obtained in ACN solution. The addition of 0.06 M acetone to the deoxygenated solution causes very fast

decay rates for **11** and **50**,^{108,109} and affords a transient spectrum consisting of absorptions due solely to silyl radicals **33** and **44** (Figure 2.13(d)). This spectrum agrees well with the previously published spectra of these radicals^{72,109} and with those shown in Figure 2.7. The addition of chloroform (0.05 M) to partially oxygenated OCT solutions quenches only the silyl radicals and affords a spectrum consisting of absorptions due to **11** ($\lambda_{\text{max}} = 325 \text{ nm}$)⁶³ and silatriene **50** ($\lambda_{\text{max}} = 490 \text{ nm}$) (Figure 2.13(b)). 1,1-Diphenylsilene (**11**) reacts sluggishly with oxygen;⁶³ thus, saturation of an OCT solution with oxygen results in selective quenching of silyl radicals (**33** and **44**) and silatriene **50**, affording a spectrum which is assigned to the simple silene (Figure 2.13(c)).

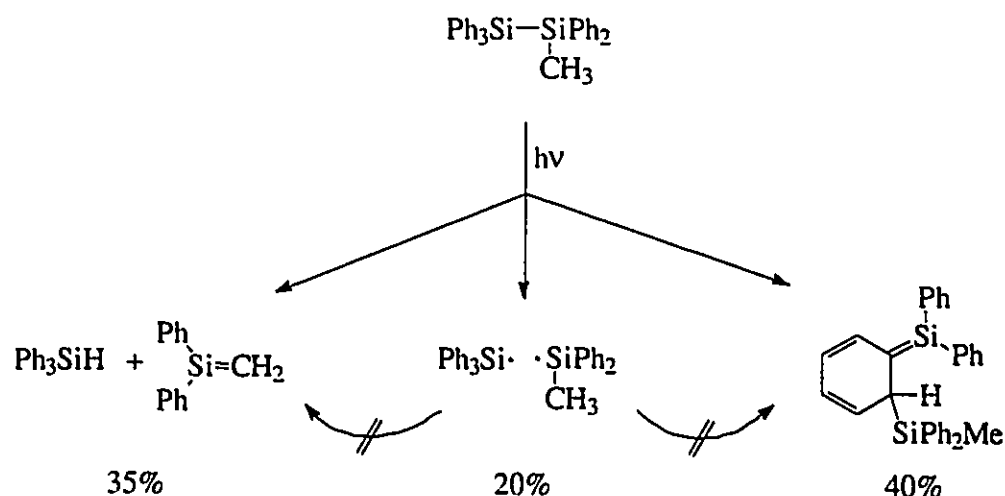
Photolysis of cyclohexane solutions of **9** in the presence of acetone affords two products consistent with acetone trapping of silatriene **50**: the expected silyl ether^{96,102} (**49**) from formal ene reaction of acetone with silatriene **50** in low chemical yields (*ca.* 5%), and the 1,2-siloxetane (**48**) which arises from formal [2+2]-cycloaddition of acetone to **50**. The formation of **48** contrasts with Ishikawa's results^{96,102} obtained for the photolysis of several phenyldisilanes in the presence of carbonyl compounds. They reported that, in each case, silyl ethers analogous to **49** were the exclusive silicon-containing products formed. Siloxetanes such as **48** are thermally and hydrolytically unstable, thus eluding detection by GC analysis or separation by vacuum distillation or chromatographic techniques (see Chapter 4). We are, therefore, only able to detect **48** in the NMR spectra of the crude photolysates.

An examination of the mechanism of formation of **11** and **50** has been undertaken in order to establish the role of the silyl radicals and the photochemical partitioning of **9**. Sommer initially proposed that **11** may be formed by a concerted dehydrosilylation reaction from a disilane excited state;³⁶ however, Brook has recently suggested that **11** is

more likely formed by disproportionation of silyl free radicals (**33** and **44**) produced by Si-Si bond homolysis.⁵ Several years ago, Sakurai also suggested that simple silenes and silatrienes likely arise by silyl radical disproportionation and recombination reactions, respectively.^{40,106} Acetone and chloroform were selected as silene and radical trapping agents, respectively, since the resulting silyl enol ether (**45**) and chlorosilanes (**46** and **47**) are stable under these conditions, and these reagents react rapidly and specifically with silenes and arylsilyl radicals, respectively ($k_q \approx 10^8\text{-}10^9 \text{ M}^{-1}\text{s}^{-1}$),^{63,69,107-109,112} ensuring that they are trapped quantitatively at the concentrations employed in these experiments. Furthermore, these reagents do not interact significantly with the disilane singlet excited state at concentrations up to *ca.* 0.5 M. The chemical yields and relative quantum yields for product formation for photolysis of **9** in the presence of 0.05 M acetone and from 0 to 12.5 M chloroform, listed in Tables 2.1 and 2.2, respectively, provide significant mechanistic insight. The lack of reduction in the yield of silene-derived products, **10** and **45**, or increase in the yield of the silyl radical-derived products, **46** and **47**, between 0.02 and 0.50 M chloroform indicates that the formation of 1,1-diphenylsilene (**11**) occurs directly from the lowest excited singlet state and not from disproportionation of free arylsilyl radicals **33** and **44** (see Scheme 2.1). Likewise, the chemical yields of the silatriene-derived products (**48** and **49**) are unaffected by the presence of 0.05 M chloroform indicating that they are not radical-derived. In the absence of added halocarbon, **33** and **44** presumably form higher molecular weight oligomers by addition reactions with the disilane.⁷² The lower material balance observed for photolyses in the absence of chloroform compared to those in the presence of the halocarbon is consistent with this proposal. The data in Table 2.1 also provides the photochemical partitioning of reaction from the excited state(s) of **9**. Dehydrosilylation leading to the formation of **10**

and **11** accounts for *ca.* 35% of the photoreactivity of **9**, while free arylsilyl radical and silatriene formation account for *ca.* 20% and 40%, respectively.

Scheme 2.1 The Photochemical Reactivity of Methylpentaphenyldisilane in Hydrocarbon Solution



The yields of the chlorosilanes (**46** and **47**) are substantially reduced when the photolysis of **9** is carried out in the presence of 0.1 M *trans*-piperylene compared to the photolysis in the absence of diene, which indicates that silyl free radicals (**33** and **44**) arise from the disilane lowest triplet excited state.¹²¹ (A more complete discussion of the triplet-state photoreactivity of phenyldisilanes appears in Chapter 3.) The possibility of silyl radical reactions with the added diene ($k_q = 6.2 \times 10^7 \text{ M}^{-1}\text{s}^{-1}$) in these experiments was ruled out by the use of sufficient chloroform (0.2 M) to trap greater than 90% of the silyl radicals which are formed. The yields of silene-derived products (**45**, **48**, and **49**), formed from photolysis of **9** in the presence of acetone, are unaffected by the addition of

0.05 M chloroform or 0.1 M *trans*-piperylene which indicates that simple silene and silatriene formation occurs from direct dehydrosilylation and [1,3]-silyl migration, respectively, in the disilane lowest excited singlet state. NLFP experiments are also consistent with this observation in that they have demonstrated that the formation of both **50** and silyl radicals occurs within a timescale shorter than the duration of the laser pulse (*ca.* 10 ns).

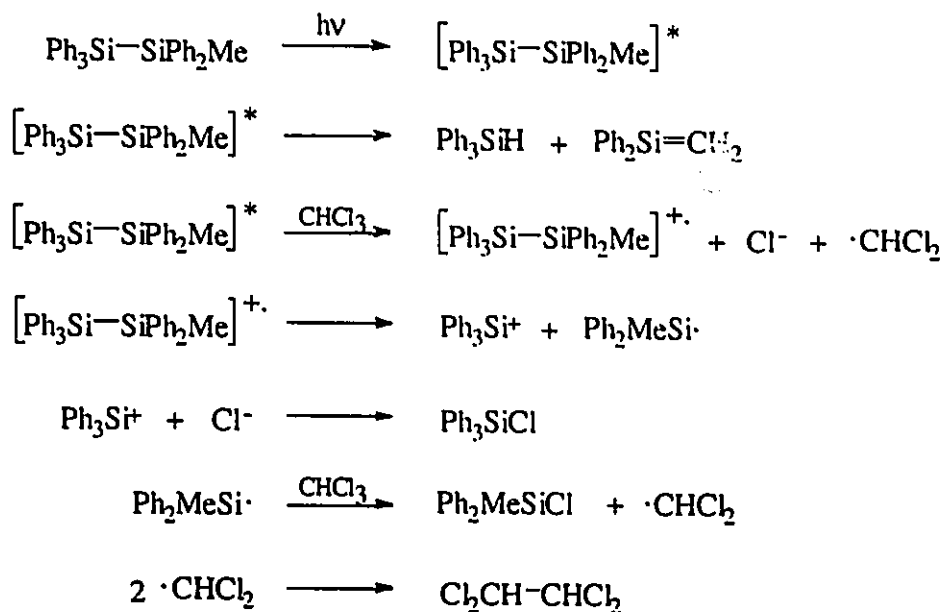
The photochemistry of **9** at high chloroform concentrations is markedly different than in neat cyclohexane. The yields of the chlorosilanes increase dramatically at chloroform concentrations higher than 0.50 M while the yield of **45** drops off to zero above 3.0 M chloroform. The yield of triphenylsilane (**10**) decreases only slightly up to 12.5 M chloroform as does the fluorescence emission from **9** (see Figures 2.2, 2.4). Although it is known that silenes react with alkyl halides,^{1,5,108} the decrease in yield of **45** is *not* due to competitive trapping of 1,1-diphenylsilene (**11**) with chloroform. The rate constants for quenching of **11** by acetone⁶³ and chloroform in OCT solution are $(3.3 \pm 0.2) \times 10^8 \text{ M}^{-1}\text{s}^{-1}$ and $< 10^4 \text{ M}^{-1}\text{s}^{-1}$, respectively, so even in neat chloroform solution, **11** reacts at least 100 times faster with acetone than with chloroform. Thus, the persistent formation of triphenylsilane (**10**), which is coupled with 1,1-diphenylsilene (**11**) production, even at high chloroform concentrations is curious. Our failure to detect **45** at high chloroform concentrations is, therefore, attributed to thermal or secondary photochemical decomposition. The $k_q\tau$ values obtained for quenching of the formation of **10** and fluorescence emission from **9** by chloroform are in excellent agreement, indicating that the two processes are related. Assuming that **9** has a similar excited singlet state lifetime as **12** at room temperature ($\tau \approx 30 \text{ ps}$),⁸² allows an estimate of the rate constant for fluorescence quenching by chloroform as $k_q \approx 10^9 \text{ M}^{-1}\text{s}^{-1}$.

At high concentrations, chloroform quenches the disilane fluorescence via direct reaction with the excited singlet state or by catalysis of intersystem crossing to the disilane lowest excited triplet state. It is possible that the efficiency of intersystem crossing in the disilane is enhanced by an increase in solvent polarity^{38,121} at high chloroform concentrations or a heavy-atom effect may be involved (see Chapter 3). Several disilanes are known to undergo efficient photoinduced electron transfer reactions with reagents such as 9,10-dicyanoanthracene^{122,123}, quinones,¹²⁴ or electron deficient benzenes.⁹¹ The oxidation potential of **9** is < 1.7 volts versus Ag/AgCl in ACN solution;¹²⁵ therefore, it is quite likely that at high chloroform concentrations, the singlet excited state of **9** reacts by electron transfer to yield the radical cation of **9**, the dichloromethyl radical, and chloride ion (Scheme 2.2). Unfortunately, electron transfer to chloroform is dissociative, so application of the Weller equation to estimate the free energy of electron transfer is not possible.^{126,127} Cleavage of the radical cation of **9** to the triphenylsilyl cation and methyl-diphenylsilyl radical (**44**) would then yield **46** by reaction of the cation with chloride and **47** by chlorine atom abstraction from solvent by **44**. The chloranil-sensitized photolysis of **9** confirms that: generation of the radical cation of **9** in chloroform ultimately leads to the formation of **46** and **47**. In this case, chloranil absorbs the light (360 nm) and efficiently oxidizes **9**, while chloroform acts solely as a trap for the silyl radicals produced by cleavage of disilane radical cation. Thus, the products which arise from electron transfer quenching of the singlet excited state of **9** by chloroform are the same as those derived from the halogen atom abstraction reactions of the corresponding triplet-derived silyl free radicals.

The electron transfer mechanism for the reaction of the singlet excited state of **9** with chloroform is supported by fluorescence quenching experiments with dichloromethane and

carbon tetrachloride. Dichloromethane, which has a higher reduction potential than chloroform,¹²⁸ does not quench the fluorescence of **9** up to 15 M halocarbon, while carbon tetrachloride, which has a lower reduction potential than chloroform,¹²⁸ quenches the fluorescence of **9** over twenty times more efficiently ($k_q\tau = 1.6 \pm 0.2 \text{ M}^{-1}$). This result is confirmed by the fact that photolysis of a cyclohexane solution of **9** containing 1.0 M carbon tetrachloride yields only **10**, **46**, and **47**, with the yield of triphenylsilane (**10**) substantially lower than that obtained in the photolysis of **9** under the same conditions but in the presence of 1.0 M chloroform.

Scheme 2.2 Electron Transfer Quenching of Methylpentaphenyldisilane



The photolysis of **9** in ACN (or ACN-*d*₃) solution in the presence of acetone and chloroform affords much higher yields of radical-derived products. While this indicates

that the yields of triplet-derived silyl radicals are increased substantially due to enhanced intersystem crossing in the disilane,^{38,121} it is also possible that direct electron transfer quenching contributes to chlorosilane formation under these conditions, even at the low chloroform concentrations employed in these experiments. However, higher yields of silyl radicals are observed in the transient absorption spectra obtained in ACN solution without any added trapping reagents (Figure 2.5, 2.10), so the conclusion that the photolysis of arylidisilanes in polar solvents affords significantly higher yields of silyl radicals than are obtained in hydrocarbon solvents is valid.

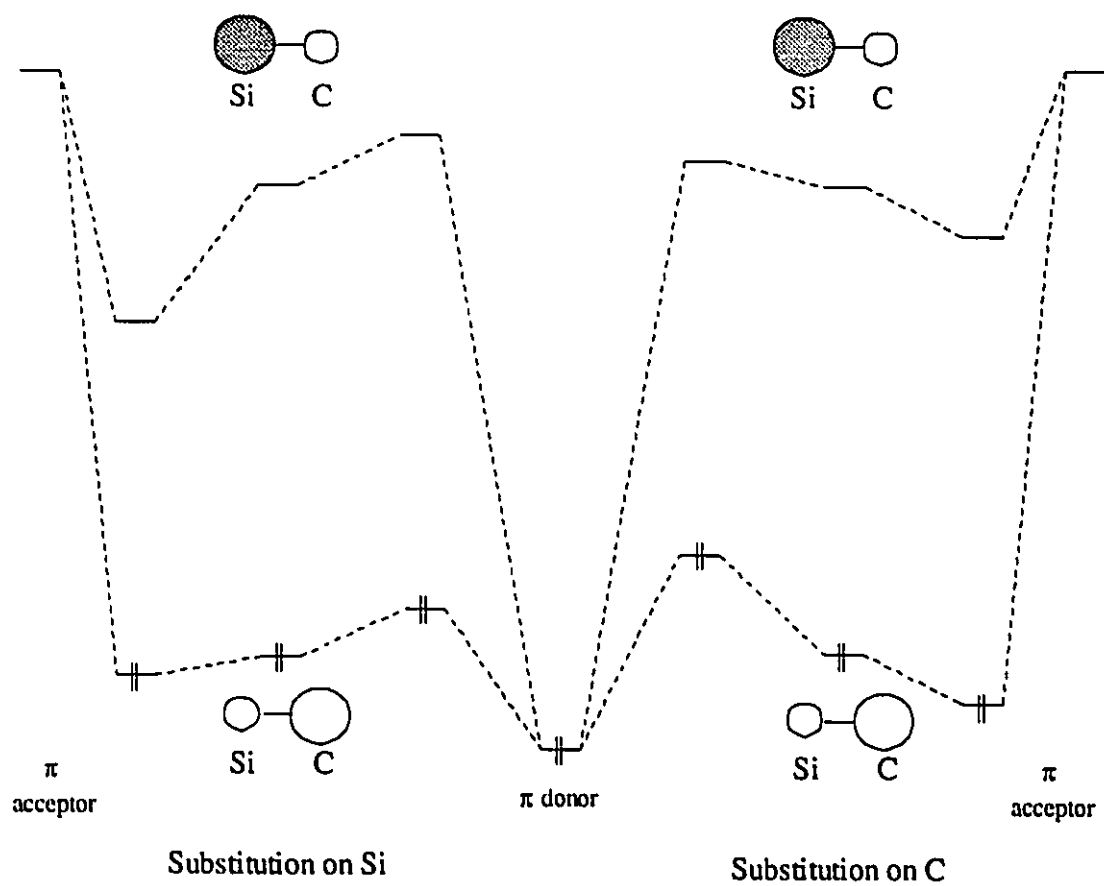
We have reinvestigated the photochemistry of **9** in the presence of methanol and found that products of the addition of the alcohol to silatriene **50** are formed in a combined yield of about 40%, while triphenylsilane (**10**) and methoxymethyldiphenylsilane (**20**) are each formed in about 40% yield. The yield of methanol/silatriene adducts **51** are in good agreement with the combined yields of the silatriene-derived products (**48** and **49**) from the photolysis in the presence of acetone. Sommer and coworkers reported the formation of significant yields of methoxytriphenylsilane (**42**) and methyldiphenylsilane (**43**). However it is unlikely that they arise from reaction of the corresponding silyl radicals with the alcohol as they suggested.³⁶ In our hands, **42** and **43** are formed in yields of less than 5% in the photolysis of **9** at room temperature. We suspected that the higher reported yields of **42** and **43** might be due to thermal decomposition of **51**, but photolysis of **9** in methanolic cyclohexane at 55-60 °C afforded a similar product distribution as that obtained at room temperature. Finally, heating the crude, room temperature photolysate at 100 °C for 16 hours resulted in no apparent change in the product distribution.

Transient absorption spectra recorded from NLFP of disilanes **12**, **34**, **35**, and **39** (Figure 2.10, 2.11) demonstrate the effect of increasing phenyl substitution on the corresponding silatriene absorption. Successive substitution of a methyl with a phenyl group causes the silatriene absorption maxima to shift from 425 nm (**13**) to 460 nm (**37**, **52**) to 490 nm (**38**, **50**), consistent with increasing conjugation in the silatrienyl chromophore. The transient absorption spectra from each disilane are virtually identical above 400 nm in OCT and ACN solutions indicating that silatriene absorption maxima are independent of solvent polarity.

It is interesting to compare the effect of phenyl substitution on silatriene absorption maxima with arylsilyl radical absorptions. The triphenylsilyl (**33**), methyldiphenylsilyl (**44**), and dimethylphenylsilyl (**54**) radicals exhibit transient absorptions in the 305-330 nm range.⁷² It is likely that only one phenyl group can be in direct conjugation with the radical centre at any one time due to the non-planar structure of silyl radicals,¹⁹ thus the inductive effects of increasing phenyl substitution appear to have little effect on their absorptions. Silatrienes, on the other hand, are more sensitive to substituents on the trivalent silicon and carbon atoms which can act as π acceptors and donors, respectively. The replacement of a methyl with a phenyl group on a silatriene causes a *ca.* 30-35 nm red-shift in the absorption and the effect is additive.

Michl has explained the effects of substitution on silene UV absorption spectra by considering the π system alone¹ according to Scheme 2.3 since it is generally accepted that simple silene absorptions are of (π , π^*) character. Recall that simple silenes are polarized species and as a result the magnitudes of the orbital coefficients on silicon and carbon are quite different in the HOMO and LUMO. A π -acceptor substituent on the silicon atom should lower the energy of the LUMO (π^* orbital) due to the large orbital

Scheme 2.3 Effects of π -Donor and π -Acceptor Substituents on the HOMO and LUMO Energies of Silenes



coefficient on Si, whereas the energy of the HOMO (π orbital) should only be lowered slightly. This small HOMO-LUMO gap results in red-shifts in the UV absorption spectra of π -acceptor substituted silenes. Likewise, a π donor substituent on carbon should raise the HOMO without affecting the LUMO and cause a red-shift in the UV absorption. A π -acceptor substituent at carbon should cause only a small red-shift in the (π , π^*) transition since the LUMO will not be lowered much due to the small coefficient on C.

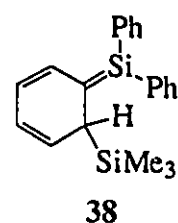
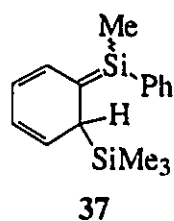
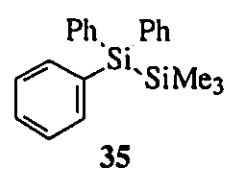
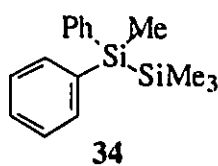
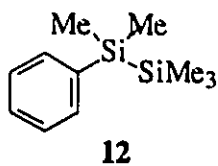
The lifetime of silatriene **50** is shortened by the addition of silene trapping agents such as carbonyl compounds, alcohols, acetic acid, alkenes, dienes, and oxygen with rate constants in the 10^6 - 10^8 $\text{M}^{-1}\text{s}^{-1}$ range.¹⁰⁹ The bimolecular rate constants (Table 2.3) are a factor of 2-5 smaller for the reaction of **50** with these reagents compared to **13** consistent with its assignment. The increased steric bulk in **50** due to phenyl substitution slows down the attack by these reagents at the silenic silicon atom in (or during a fast equilibrium to) the rate-determining step. The mechanistic aspects of silatriene reactions are discussed in greater detail in Chapter 4.

CHAPTER 3

SOLVENT AND SUBSTITUENT EFFECTS ON THE PHOTOREACTIVITY OF PHENYLDISILANES

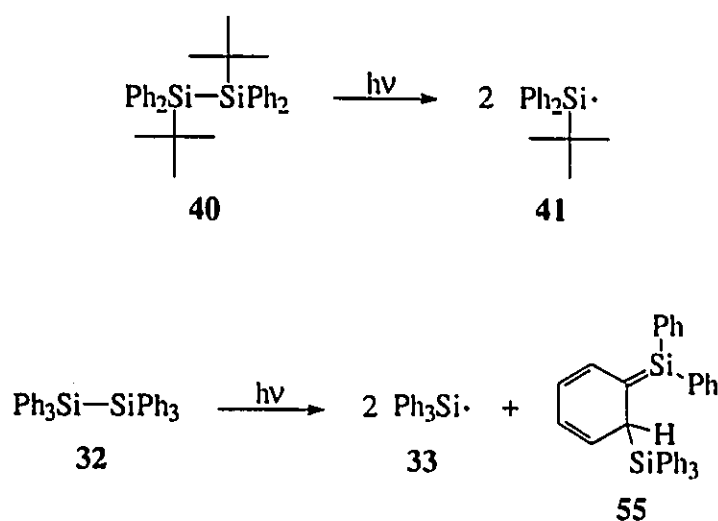
3.1 Introduction

The examination of the photochemistry of disilanes **12**, **34**, and **35** has been undertaken to probe the effects of phenyl substitution and solvent polarity on disilane photoreactivity. Nanosecond laser flash photolysis (NLFP) experiments on these disilanes reveal a significant solvent dependence on the relative yields of silatrienes (**13**, **37**, **38**) versus the corresponding silyl radicals. The transient absorption spectra for **34** and **35**



(Figure 2.10) demonstrate that the silyl radical absorptions between 300-340 nm are much more intense in acetonitrile (ACN) than in isooctane (OCT) solution. Steady-state photolyses of the three disilanes have been carried out in hydrocarbon and ACN solutions to confirm this solvent effect and quantify the effects of disilane structure on the yields of simple silenes, silatrienes, and silyl radicals. The excited states responsible for silene and silyl radical formation have been determined through triplet sensitization and quenching experiments. Likewise, the role of silyl free radicals in silatriene formation has been examined by competitive trapping experiments.

As a test of our understanding of the factors which control disilane photoreactivity, 1,2-di-*tert*-butyl-1,1,2,2-tetraphenyldisilane (**40**) has been synthesized as a potential high-yield source of *tert*-butyldiphenylsilyl radicals (**41**). The photochemistry of **40** has been investigated by steady-state and NLFP techniques, and rate constants for reaction of **41** with several known silyl radical trapping agents have been determined. The photochemistry of hexaphenyldisilane (**32**), a reported source of triphenylsilyl radicals (**33**),¹⁰⁷ has been reexamined by NLFP techniques to determine the extent of silatriene (**55**) formation.



3.2 Results

3.2.1 The Photochemistry of Phenylidisilanes in Non-Polar and Polar Solvents

Disilanes **12**, **34**, and **35** are known compounds and were synthesized from the corresponding chlorosilanes and lithium according to published procedures.^{129,130} Compounds **34** and **35** exhibit weak fluorescence emission in ACN or OCT solution at room temperature (Figure 3.1), similar to that reported previously for **12**.^{38,81,83,87,88} The emission maxima for all three disilanes are blue-shifted by *ca.* 35 nm in hydrocarbon solvents relative to those in ACN and decrease in energy with increasing phenyl substitution on the disilane (Table 3.1). Oxygen has no discernible effect on the intensity of fluorescence emission from **12** or **34**. Thus, it is likely that emission from **34** and **35** occurs from a charge-transfer (CT) excited state by analogy with that reported for **12**.

Steady-state photolysis (254 nm) of deoxygenated 0.05 M solutions of **12**, **34**, and **35** in cyclohexane-*d*₁₂ containing 0.05 M acetone to *ca.* 80% conversion affords the product mixtures shown in equation 3.1. Silyl ethers **56** and silyl enol ether **45** were isolated by semi-preparative VPC and fully characterized. The other products were identified by GC/MS, and/or by ¹H and ¹³C NMR analyses of the crude photolysates. Chemical yields, determined by ¹H spectroscopy, are listed in Table 3.2. Ishikawa and coworkers have reported that the photolysis of **12** in the presence of acetone yields the silatriene ene-adduct (**56a**) exclusively in 59% yield.¹⁰² However, we have been able to detect significant amounts of trimethylsilane, silyl enol ether **58**, and the 1,2-siloxetane **57a**, in addition to **56a**. Significant amounts of siloxetanes **57b,c** are detected from the photolysis of disilanes **34** and **35** under similar conditions. Siloxetanes **57** are formal silatriene/acetone [2+2] cycloaddition products^{108,121} while silyl enol ethers (**45** and **58**)

Table 3.1 Charge-Transfer Fluorescence Emission Maxima from OCT and ACN Solutions of 12, 34, and 35 at 23 ± 2 °C.

Disilane	$\lambda_{\text{max}}^{\text{F}}$ (nm) OCT	$\lambda_{\text{max}}^{\text{F}}$ (nm) ACN
PhMe ₂ Si-SiMe ₃ (12)	345	380
Ph ₂ MeSi-SiMe ₃ (34)	355	390
Ph ₃ Si-SiMe ₃ (35)	360	390

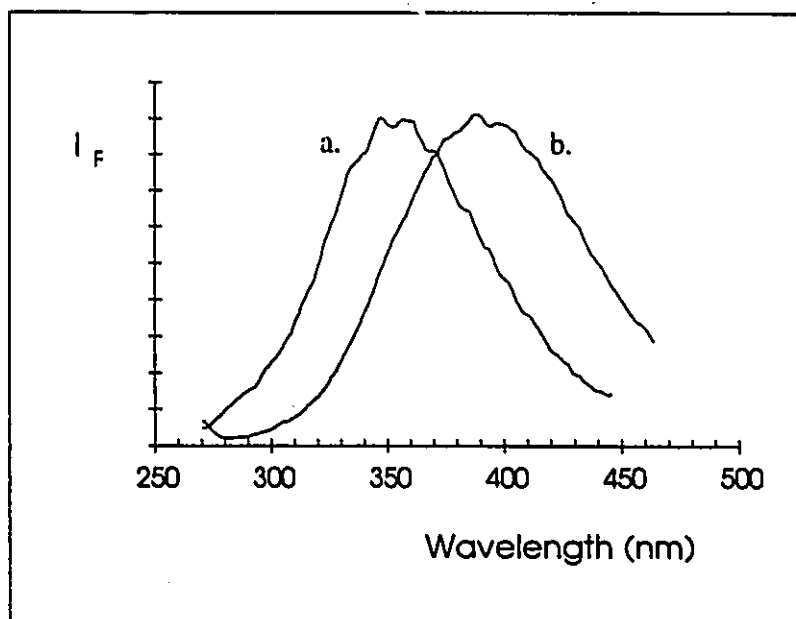


Figure 3.1 Fluorescence emission spectra recorded from (a) OCT and (b) ACN solutions of 34 at 23 ± 2 °C.

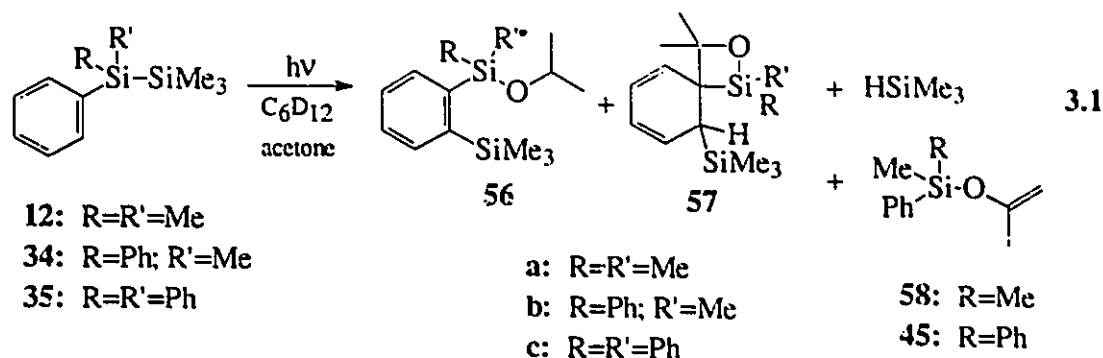


Table 3.2 Product Yields from the Photolysis of 0.05 M Cyclohexane- d_{12} Solutions of Disilanes 12, 34, and 35 in the Presence of Acetone (0.05 M).^a

Disilane		56	57	PhMeRSiO-C(=C)Me	Me ₃ SiH
12	a	41%	21%	13%	19%
34	b	54%	28%	14%	18%
35	c	33%	69%	-	nd

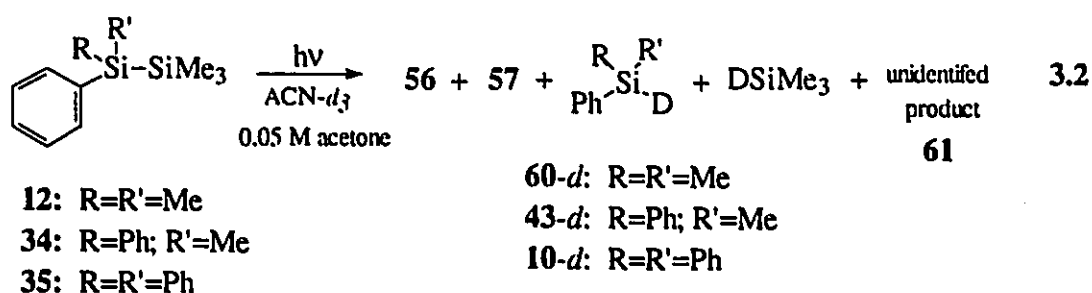
- a. Determined by ¹H NMR spectroscopy, after *ca.* 80% conversion. Integrated against dichloromethane as the internal standard. Errors are considered to be *ca.* 5%.
nd = not detectable.

are acetone ene adducts of 1,1-diphenylsilene (11)^{63,120} and 1-methyl-1-phenylsilene (36),¹³¹ respectively. The spectroscopic evidence for siloxetanes and a discussion of their mechanistic implications in silatriene reactions with acetone appear in Chapter 4.

Photolysis of 35 under similar conditions but with 0.1 M CHCl₃ added as a silyl radical trap results in the formation of chlorotriphenylsilane (46) and trimethylsilylchloride (59) in

3 and 4% yield, respectively, in addition to **56c** and **57c** in similar yields as those obtained in the absence of halocarbon.

Photolysis (254 nm) of deoxygenated 0.05 M solutions of **12**, **34**, and **35** in dried acetonitrile (or acetonitrile- d_3) containing acetone (0.05 M) yields the products shown in equation 3.2. The product yields, determined by a combination of ^1H NMR spectroscopy and GC analysis of the crude photolysates, are listed in Table 3.3. The major product (**61**), characterized by a singlet at δ 0.053 ppm in the ^1H NMR spectra of the crude mixtures, has not yet been identified; however, hexamethyldisilane and hexamethyldisiloxane have been excluded as possibilities. The two silanes formed from photolysis of each disilane in ACN- d_3 solution (trimethylsilane and **60-d**, **43-d**, or **10-d**) were > 90 % deuterated as estimated by GC/MS and from the absence of Si-H resonances in the ^1H NMR spectra. The silyl enol ethers **45** and **58** were not detected in these photolyses. Merry-go-round photolyses indicate that the quantum yields for disappearance of **35** are at most *ca.* 20% higher in hydrocarbon solution than in acetonitrile.

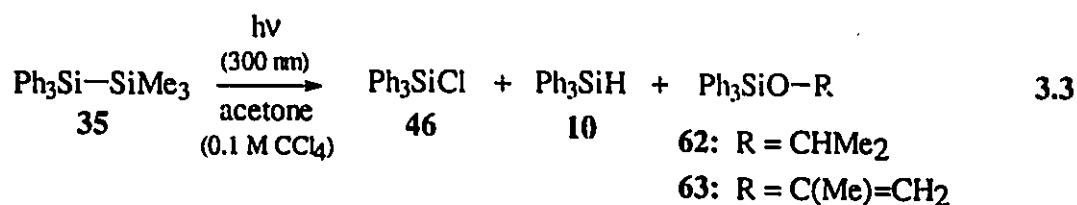


Steady-state photolysis of **12**, **34**, and **35** (0.05 M) in deoxygenated dried acetonitrile (or acetonitrile- d_3) containing acetone (0.05 M) and chloroform (0.05-0.1 M) as a silyl radical trap results in extremely complex product mixtures in the case of **12** and

34, whereas the photolysis of 35 is considerably cleaner. In all three cases, trimethylsilyl chloride (59), the corresponding phenylchlorosilane, and 1,1,2,2-tetrachloroethane are detected in addition to the products shown in equation 3.2. Product yields were determined by integration of the ^1H NMR spectra of the crude photolysates after *ca.* 40% conversion and are listed in Table 3.3. They are independent of the concentrations of both acetone and chloroform over a range of 0.02-0.1 M.

3.2.2 Triplet Quenching and Sensitization Experiments

Photolysis (300 nm) of deoxygenated 0.01 M solutions of 35 in acetone under conditions where the solvent absorbs the light, and in the presence (0.01-0.1 M) or absence of CCl_4 , yields only the silyl radical derived products shown in equation 3.3. No silatriene derived products are detected by GC or GC/MS analyses of the crude photolysates. Product yields are listed in Table 3.4.



Benzene sensitization experiments were performed to rule out the possibility that the silyl radicals produced from the acetone sensitization experiments arise from electron transfer sensitization (the oxidation potential of 35 is < 1.8 volts versus Ag/AgCl in ACN).¹²⁵ Steady-state photolysis (254 nm) of 0.05 M and 0.001 M deoxygenated

Table 3.3 Product Yields from Photolysis of 0.05 M ACN- d_3 Solutions of **12**, **34**, and **35** Containing 0.05 M Acetone in the Presence and Absence of Chloroform.^a

Disilane		[CHCl ₃] / M	56	57	DSiMe ₃	Me ₃ SiCl	PhRR'SiD	PhRR'SiCl	61 ^b
12	a	0	18%	16%	9%	-	8%	-	25%
		0.05 ^c	5%	<i>nd</i>	3%	41%	1%	34%	<i>nd</i>
34	b	0	6%	<i>nd</i>	4%	-	8%	-	34%
		0.05 ^c	5%	<i>nd</i>	5%	73%	6%	78%	<i>nd</i>
35	c	0	5%	<i>nd</i>	48%	-	25%	-	43%
		0.1 ^c	5%	<i>nd</i>	13%	85%	10%	70%	<i>nd</i>

- a. Determined by ¹H NMR spectroscopy, after *ca.* 40% conversion. Errors are considered to be about 5%. *nd* = not detectable.
- b. Unidentified product with singlet at δ 0.053 ppm. Its yield was calculated assuming that this resonance is due to a -Si(CH₃)₃ group.
- c. Yields of the silyl chlorides include those of the corresponding siloxanes. 1,1,2,2-Tetrachloroethane is also formed as a photolysis product.

benzene solutions of **35** containing 0.1 M methanol and 0.02 M CCl₄ (or CHCl₃), as silene and silyl radical traps, respectively, to *ca.* 30% conversion yields the product mixture shown in equation 3.4. The solvent is the primary absorber of the 254 nm irradiation at these disilane concentrations ($\epsilon_{254}(\text{C}_6\text{H}_6) = 90 \text{ M}^{-1}\text{cm}^{-1}$,¹¹⁹ $\epsilon_{254}(\text{35}) =$

4400 M⁻¹cm⁻¹). The product yields of these experiments along with those from the acetone sensitization experiments are collected in Table 3.4.

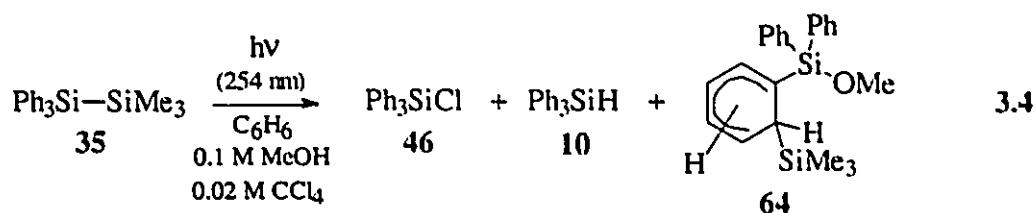


Table 3.4 Product Yields from Acetone- and Benzene-Sensitized Photolyses of 1,1,1-Trimethyl-2,2,2-triphenyldisilane (35).^a

Solvent	[CCl ₄] /M	[35] /M	46 ^b	10	62 + 63	64
acetone ^c	0	0.01	-	11%	32%	-
	0.1	0.01	45%	2%	<i>nd</i>	-
benzene ^d	0.02	0.001	12%	2%	-	35%
	0.02	0.05	< 1%	< 1%	-	56%

- Irradiations were carried out in deoxygenated solutions to *ca.* 30% conversion. Product yields were determined by GC analyses relative to the disappearance of 35 using an internal standard and are considered accurate to $\pm 10\%$. *nd* = not detectable.
- Yields calculated as the sum of the chlorosilane and corresponding silanol.
- 300 nm excitation.
- 254 nm excitation. Solutions also contained 0.1 M methanol.

Triplet quenching experiments employing NLFP techniques to monitor the relative yields of silyl radicals and silatrienes directly have also been carried out to verify the steady-state results. Saturation of ACN solutions of **35** with *trans*-piperylene ($E_T = 60$ kcal/mol)¹¹⁹ as a triplet quencher leads to a reduction in the triphenylsilyl radical (**33**) absorption centred at 328 nm compared to that of silatriene **38** ($\lambda_{\text{max}} = 490$ nm). However, the solubility of this diene in ACN is too low to completely quench silyl radical formation or to enable an accurate Stern-Volmer analysis of the data. Therefore, quenching studies were carried out in tetrahydrofuran (THF) solution. Transient absorption spectra recorded from NLFP of deoxygenated THF solutions of **35** in the presence and absence of 0.067 M *trans*-piperylene are shown in Figure 3.2. The relative transient absorbances at 328 and 490 nm were taken as a measure of the yield of **33** between 0 and 0.067 M diene. This procedure is necessary in order to account for screening of the disilane by *trans*-piperylene ($\epsilon = \text{ca. } 100 \text{ M}^{-1}\text{cm}^{-1}$ at 248 nm) and variations in the laser intensity during the experiment. The formation of **38** is not quenched by the diene over the concentration range employed in this experiment since the reduction in the silatriene transient absorbance is accounted for by the increase in the static optical density of the solution at 248 nm. Stern-Volmer analysis of the data (Figure 3.3) according to equation 3.5 yielded a $k_q\tau$ value of $52 \pm 23 \text{ M}^{-1}$ where k_q is the rate constant for quenching of the disilane triplet excited state by *trans*-piperylene and τ is the disilane triplet lifetime. The value of k_q has been estimated to be $8.5 \times 10^9 \text{ M}^{-1}\text{s}^{-1}$ by measurement of the rate constant for quenching of 4-methoxy-acetophenone triplets by *trans*-piperylene in THF solution at 23 °C. This value of k_q gives an estimate of 6 ± 3 ns for the lifetime of the triplet state of **35** under these conditions.

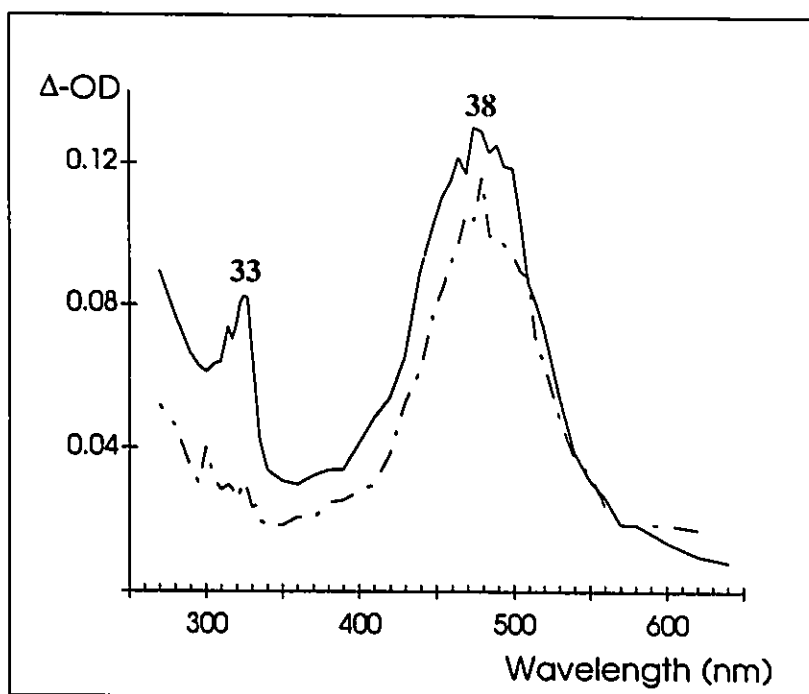


Figure 3.2 Transient absorption spectra recorded 0-40 ns after 248 nm laser excitation of deoxygenated 5.5×10^{-4} M THF solutions of **35** in the absence (—) and presence (---) of *trans*-piperylene (0.067 M). The absorption bands due to silatriene **38** and triphenylsilyl radical **33** are labelled. The latter spectrum is actually *ca.* 3.5 times less intense than is shown, but this is accounted for by screening of the laser excitation light by the diene.

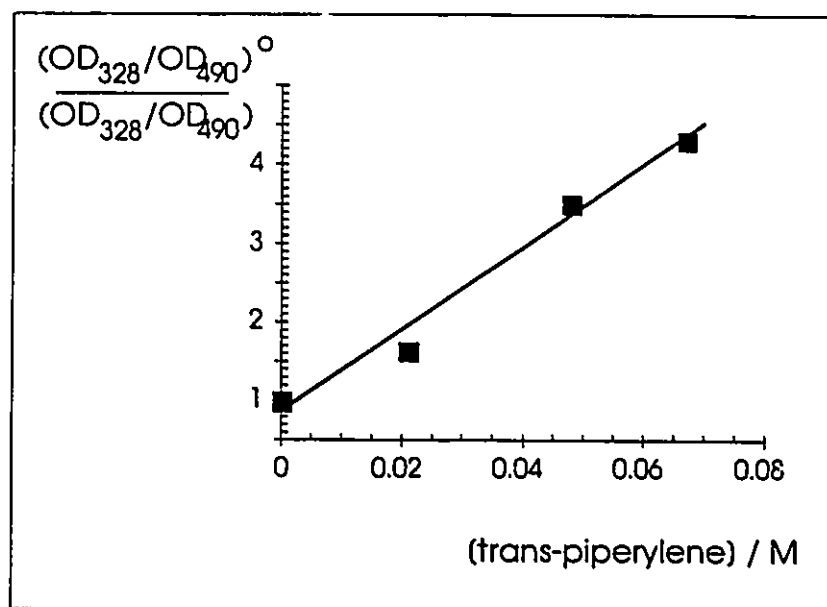


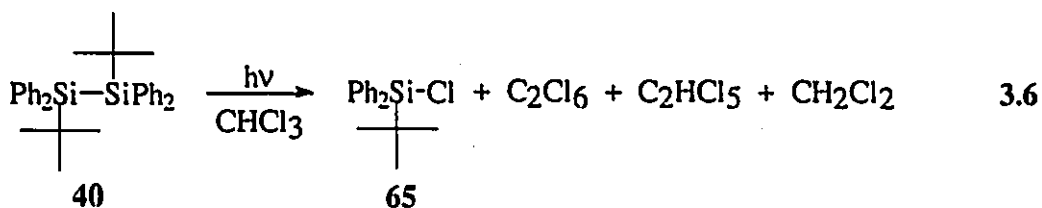
Figure 3.3 Stern-Volmer quenching plot of the yield of triphenylsilyl radicals (33), measured by the relative optical densities at 328 and 490 nm, obtained by NLFP of THF solutions of 35 containing different concentrations of *trans*-piperylene.

$$\frac{(OD^{328}/OD^{490})_0}{(OD^{328}/OD^{490})} = 1 + k_q \tau [\text{diene}] \quad 3.5$$

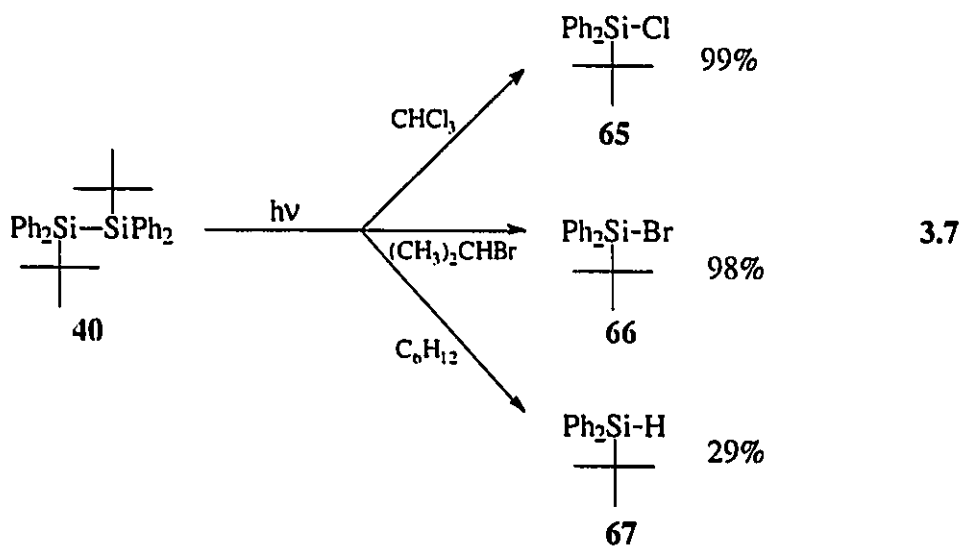
3.2.3 The Photochemistry of 1,2-Di-*tert*-butyl-1,1,2,2-tetraphenyldisilane and Hexaphenyldisilane

Disilane **40** was synthesized from *tert*-butylchlorodiphenylsilane (**65**) and lithium in dry THF following Gilman's general method for phenyldisilane preparation.^{129,130} It exhibits weak fluorescence emission in solution at room temperature. The emission maxima are 350 nm and 363 nm in cyclohexane and acetonitrile (or chloroform) solutions, respectively. The position and magnitude of these solvent shifts indicates that the lowest excited singlet state in **40** is a charge-transfer state, similar to that reported previously for **12**.^{38,81,83,87,88}

Steady-state photolysis (254 nm) of a deoxygenated 0.005 M solution of **40** in chloroform to *ca.* 74% conversion afforded *tert*-butyldiphenylsilyl chloride (**65**) as the exclusive silicon-containing product in $99 \pm 5\%$ yield along with minor amounts of hexachloroethane, dichloromethane, and pentachloroethane (see eq 3.6). The yield of **65** was linear with photolysis time up to at least 10% conversion. The quantum yields for disappearance of **40** and formation of **65** in chloroform solution, determined by potassium ferrioxalate actinometry,¹³² are 0.35 ± 0.07 and 0.64 ± 0.10 , respectively.



Irradiation (254 nm) of a deoxygenated 0.005 M solution of **40** in cyclohexane containing 0.10 M 2-bromopropane to *ca.* 60% conversion afforded *tert*-butyl-diphenylsilyl bromide (**66**) as the sole silicon-containing product in $98 \pm 5\%$ yield (eq 3.7). The photolysis of a deoxygenated 0.002 M cyclohexane solution of **40** to *ca.* 60% conversion, without any added halocarbon quencher, yielded *tert*-butyldiphenylsilane (**67**) in $29 \pm 5\%$ chemical yield as the only detectable product by GC. Compound **67** was not detected when **40** was photolyzed in the presence of an alkyl halide. These results are consistent with the generation of the *tert*-butyldiphenylsilyl radical (**41**) upon photolysis of **40** which then reacts by halogen atom abstraction with any halocarbon present in solution to yield the corresponding halosilane.



The quantum yield for disappearance of **40** in cyclohexane solution was found to be approximately half that for photolysis in chloroform solution. Simultaneous photolysis of deoxygenated 0.006 M solutions of **40** in THF and cyclohexane (HEX) containing 0.1 M chloroform using a merry-go-round apparatus revealed that the relative quantum yield for

silyl radical formation in THF versus cyclohexane solution is $\phi_{\text{THF}}/\phi_{\text{HEX}} = 1.4 \pm 0.1$ based on the relative yields of chlorosilane **65**. Steady-state photolysis ($\lambda > 265$ nm) of deoxygenated 0.01 M solutions of **40** in cyclohexane containing 0.1 M chloroform and varying amounts of *trans*-piperylene (0-0.1 M) were carried out using a merry-go-round apparatus. Stern-Volmer analysis of the data according to equation 3.8 led to a linear plot and a $k_{\text{q}}\tau$ value of $9.5 \pm 1.9 \text{ M}^{-1}$. Using an estimate of k_{q} of $7 \times 10^9 \text{ M}^{-1}\text{s}^{-1}$,¹³³ yields a value of $\tau = 1.4 \pm 0.3$ ns for the triplet lifetime of **40**.

$$\frac{[\text{65}]^0}{[\text{65}]} = 1 + k_{\text{q}}\tau[\text{diene}] \quad 3.8$$

Subsequent to the Stern-Volmer quenching experiments we discovered that **41** reacts at an appreciable rate with *trans*-piperylene ($k_{\text{q}} = 6.2 \times 10^7 \text{ M}^{-1}\text{s}^{-1}$). This leads to complications in the interpretation of the steady-state triplet quenching experiments described above since the observed reduction in yield of silyl chloride (**65**) was also due to competitive quenching of the silyl free radical (**41**) in addition to the contribution from the quenching of the disilane triplet excited state. This resulted in an *overestimation* of the lifetime of the triplet excited state. Reanalysis of the data (Figure 3.4), taking into consideration the contribution of radical quenching by diene, affords a $k_{\text{q}}\tau$ value of $6.2 \pm 1.9 \text{ M}^{-1}$ and a corresponding triplet lifetime of 0.9 ± 0.3 ns.

Nanosecond laser flash photolysis (248 nm) of deoxygenated *ca.* 10^{-4} M solutions of **40** in OCT or ACN leads to intense transient absorptions in the 290-320 nm range which decay with mixed first- and second-order kinetics ($\tau = 3\text{-}5 \mu\text{s}$). The transient absorption spectrum recorded 40-80 ns following laser excitation of an OCT solution of **40** and a representative decay trace recorded at 305 nm are shown in Figure 3.5. This spectrum is similar to the spectra of arylsilyl radicals **33** and **44** (Figure 2.7), both of which exhibit

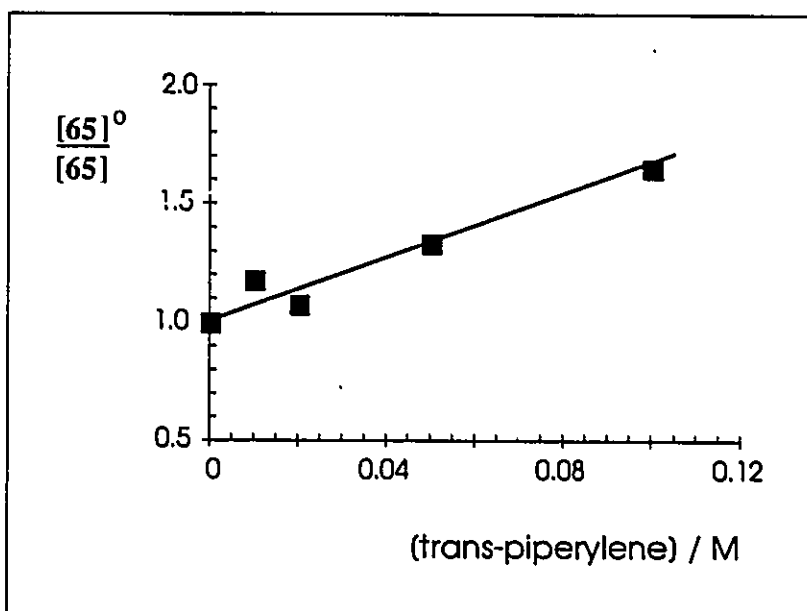


Figure 3.4 Stern-Volmer quenching plot from the photolysis ($\lambda > 265$ nm) of deoxygenated 0.01 M solutions of **40** in cyclohexane containing 0.1 M chloroform and *trans*-piperylene (0-0.1 M).

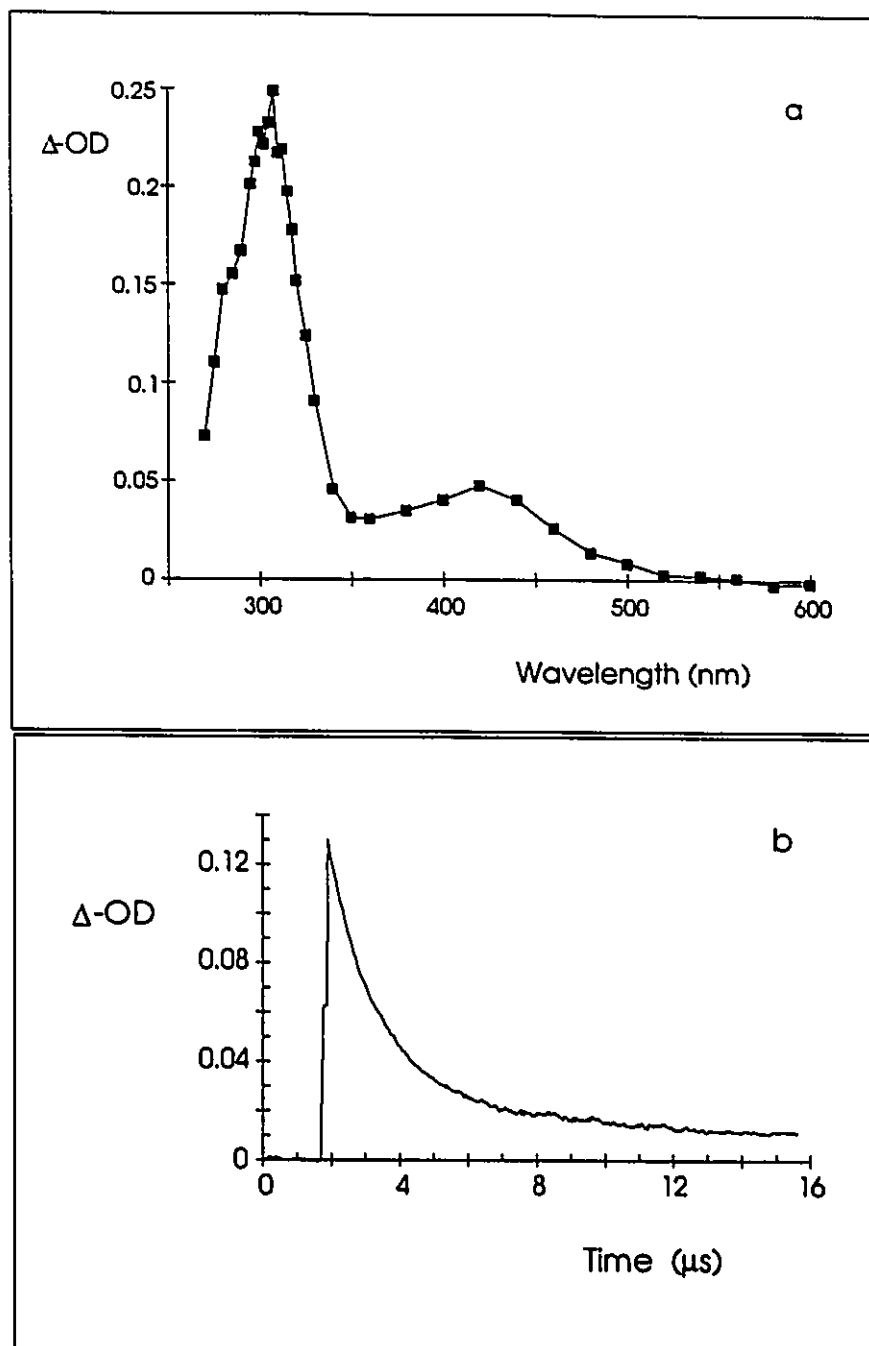
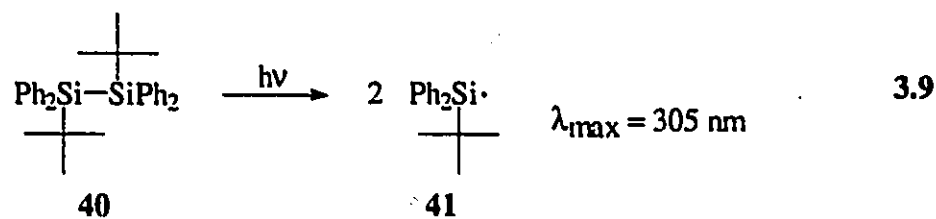


Figure 3.5 (a) Transient absorption spectrum, recorded 40-80 ns after the laser pulse, from NLFP of a deoxygenated 1.2×10^{-4} M solution of **40** in isooctane solution at 23 ± 2 °C. (b) A representative transient decay trace recorded at 305 nm under the same conditions.

strong absorptions in the 300-340 nm range and additional weak absorptions between 380 and 450 nm. The transient absorption spectrum from NLFP of **40** recorded under similar conditions in dried ACN solution was indistinguishable from that recorded in isooctane (Figure 3.5(a)). The addition of 0.7 M acetone or 0.02 M methanol had no effect on the lifetime of the transient (monitored at 305 or 420 nm) which indicates that it is not a silene or a silylene species. Silenes^{63,108,109,111,134} and silylenes^{14,113-117} are known to be quenched by acetone and alcohols with rate constants in the 10^8 - 10^{10} $M^{-1}s^{-1}$ range. The addition of alkyl halides, alkenes, or oxygen to solutions of **40** shortens the lifetime of the transient and leads to clean pseudo first-order decay kinetics. Thus, the transient absorption spectrum shown in Figure 3.5(a) is assigned to the *tert*-butyldiphenylsilyl radical (**41**) (eq 3.9). The product of the extinction coefficient of **41** at 305 nm and its quantum yield for formation ($\epsilon_{305}\phi$) has been estimated by benzophenone actinometry to be $9100 M^{-1}cm^{-1}$, which leads to a value of $\epsilon_{305} = 14000 M^{-1}cm^{-1}$ for the extinction coefficient of silyl radical **41**. Unfortunately, the extinction coefficients of triphenylsilyl (**33**) and methyldiphenylsilyl radicals (**44**), have not been reported so the significance of this result is not obvious. However, the extinction coefficient of the triethylsilyl radical has been estimated⁶⁷ as $1100 \pm 600 M^{-1} cm^{-1}$ which, as expected, is significantly smaller than that of **41**.



Bimolecular rate constants for quenching of **41** with several alkyl halides, alkenes, DMSO, and acetone have been determined by NLFP techniques. Plots of k_{decay} versus quencher concentration are linear in every case allowing calculation of the bimolecular rate constants by least squares analysis of the data according to equation 3.10 where k_0 is the estimated first-order rate constant for radical decay in the absence of added quencher. Typical quenching plots of this type are shown in Figure 3.6. Rate constants for quenching of **41** by several alkyl halides, alkenes, and acetone are listed in Table 3.5 along with reported rate constants for the reaction of triethylsilyl and triphenylsilyl radicals (**33**) with some of the reagents employed in this study.^{69,107} The lifetime of **41** was not affected significantly by the addition of up to 0.7 M acetone or up to 1.8 M DMSO, allowing an estimate of the upper limit of $k_q < 10^5 \text{ M}^{-1}\text{cm}^{-1}$ for the quenching rate constant in both cases. Addition of greater amounts of acetone or DMSO was not feasible due to competing absorption of the excitation light by the quenchers at these concentrations. The rate constant for quenching of **41** with chloroform in ACN is $(3.1 \pm 0.1) \times 10^8 \text{ M}^{-1}\text{s}^{-1}$, identical to that obtained for quenching in OCT solution under similar conditions.

$$k_{\text{decay}} = k_0 + k_q[\text{Q}] \quad 3.10$$

While this work was in progress, Ito and coworkers reported the results of a study of the photochemistry of hexaphenyldisilane (**32**) by microsecond flash photolysis.¹⁰⁷ The reported transient spectrum from flash photolysis of **32** consisted of an intense absorption band at 325-330 nm due to **33** and a relatively weak absorption band centred at 490 nm which we believe should be assigned to silatriene **55** (eq 3.11) by analogy with the NLFP results for **9** and **35**.

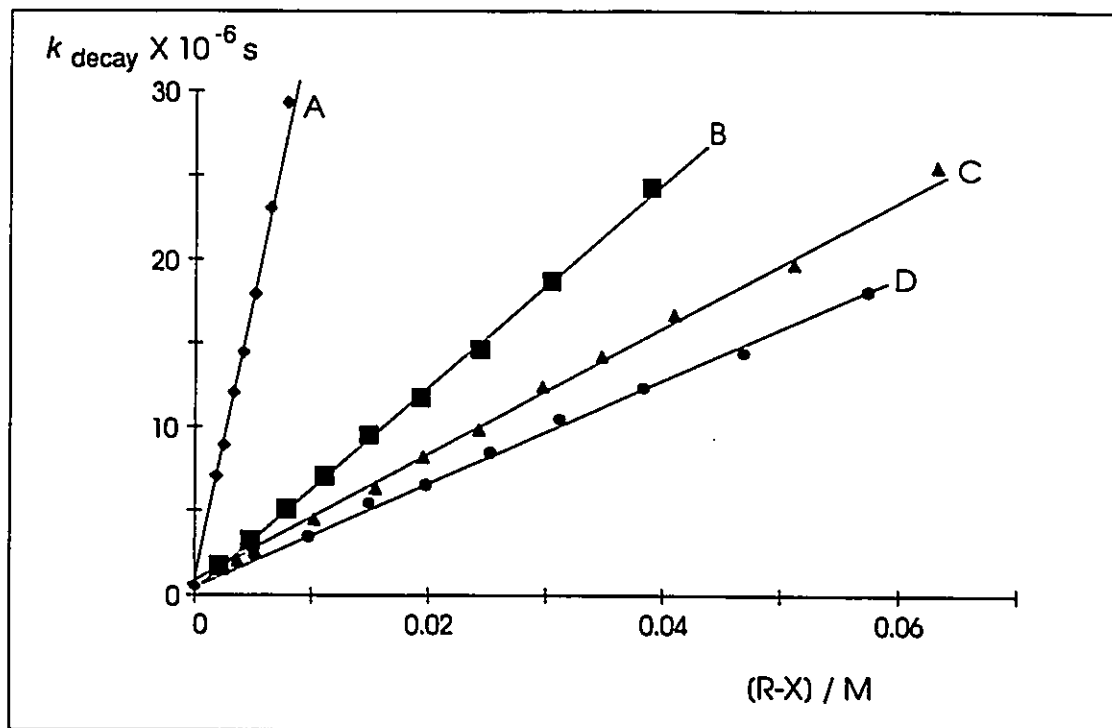
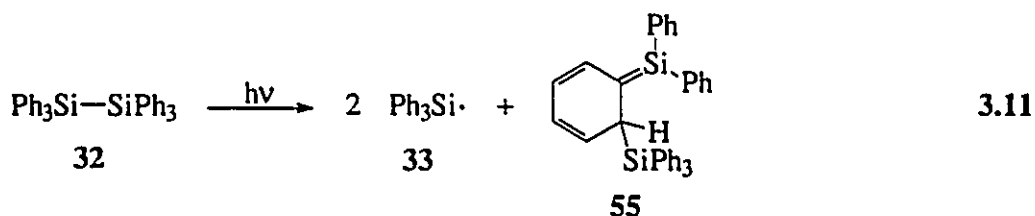


Figure 3.6 Plots of k_{decay} of radical 41 versus quencher concentration, for reaction of several alkyl halides listed in Table 3.5: A, CCl_4 ; B, *tert*-butyl bromide; C, 2-bromopropane; D, chloroform.

Table 3.5 Bimolecular Rate Constants for Quenching of *tert*-Butyldiphenylsilyl (41), Triethylsilyl, and Triphenylsilyl (33) Radicals by Alkyl Halides, Alkenes, and Acetone in Deoxygenated Isooctane (OCT) solution at 23 ± 2 °C.^a

Reagent	k_q ($\times 10^{-8}$ Ms)		
	<i>t</i> -BuPh ₂ Si· (41)	Et ₃ Si·	Ph ₃ Si· (33)
(CH ₃) ₃ CBr	6.0 ± 0.1	11.0 ± 0.5 ^b	-
(CH ₃) ₂ CHBr	3.9 ± 0.1	-	-
CH ₃ (CH ₂) ₃ CH ₂ Br	2.9 ± 0.1	5.4 ± 0.1 ^b	-
CCl ₄	36 ± 2	46 ± 8 ^b	-
CHCl ₃	3.0 ± 0.1	2.5 ^c	1.1 ± 0.1 ^f
CH ₂ Cl ₂	0.054 ± 0.002	0.71 ^c	0.034 ± 0.002 ^f
(CH ₃) ₃ CCl	0.0079 ± 0.0007	0.025 ± 0.002 ^b	0.0080 ± 0.0004 ^f
1-hexene	0.038 ± 0.004	0.048 ± 0.005 ^d	-
cyclopentene	0.019 ± 0.001	0.022 ± 0.003 ^d	-
<i>trans</i> -piperylene	0.62 ± 0.04	-	-
acetone	< 0.001	0.0028 ± 0.0008 ^e	-
DMSO	< 0.001	-	-

- Errors are reported as twice the standard deviation of least squares analysis of the data according to equation 3.10.
- Data from reference 69.
- Data from reference 135.
- Data from reference 71.
- Rate constant for quenching by 3-pentanone; data from reference 70.
- Data from reference 107.



The transient absorption spectrum obtained after NLFP of a deoxygenated *ca.* 10^{-4} M solution of **32** in isooctane is shown in Figure 3.7(a). The long- and short-wavelength transients decay with mixed first- and second-order kinetics but with different lifetimes. The lifetime of the short-wavelength transient is estimated to be *ca.* 2.5 μs while that of the long-wavelength species is $> 8 \mu\text{s}$. The addition of 0.07 M acetone quenches the long-wavelength absorption but has no effect on the short-wavelength region. The transient absorption spectrum recorded under these conditions, shown in Figure 3.7(b), is very similar to the spectrum of the triphenylsilyl radical (**33**) recorded by us (Figure 2.7(a)) and reported previously by other workers.^{72,107} The quenching of the long-wavelength transient is consistent with its assignment to silatriene **55** since these silenes are known to react with acetone with rate constants in the 10^8 - $10^9 \text{ M}^{-1}\text{s}^{-1}$ range^{108,109} (see Chapter 4).

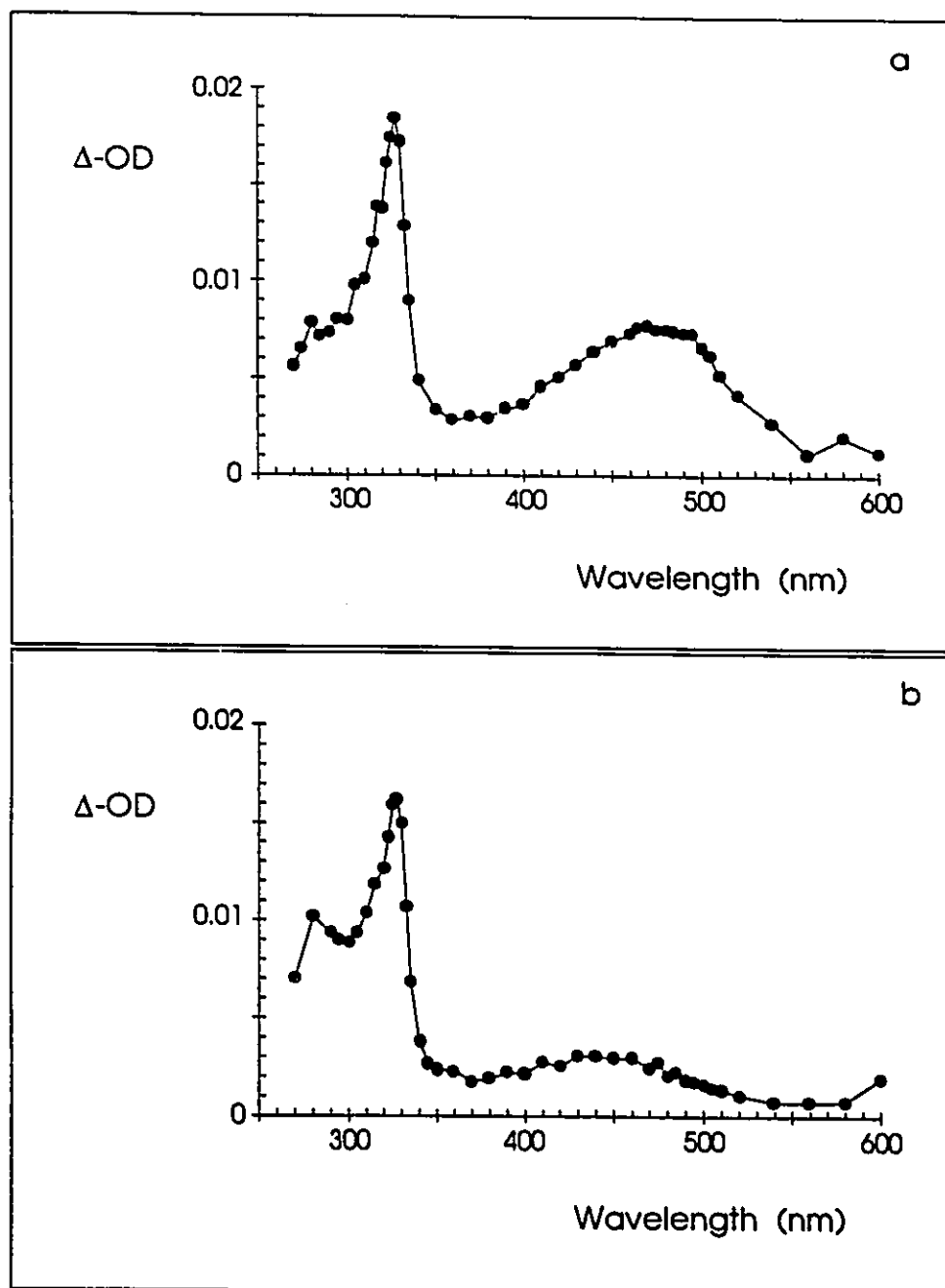
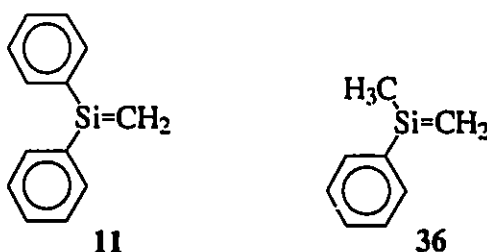


Figure 3.7 (a) Transient absorption spectrum, recorded 150-400 ns after the laser pulse, from NLFP of a deoxygenated 8×10^{-5} M solution of hexaphenyldisilane (32) in isoctane at 23 ± 2 °C. (b) Transient absorption spectrum recorded under similar conditions in the presence of 0.07 M acetone.

3.3 Discussion

Solvent polarity and phenyldisilane structure play dramatic roles in the photochemistry of these compounds. Direct photolysis of phenyldisilanes results in competitive [1,3]-silyl migration (yielding silatrienes), dehydrosilylation (yielding simple silenes **11** and **36**, along with the corresponding silanes), and Si-Si bond homolysis (yielding the corresponding silyl radicals). The formation of these three types of intermediates is evident from the steady-state photolysis of these compounds in the presence of acetone (as a silatriene/silene trap) and chloroform (as a silyl radical trap). NLFP experiments have shown that silatrienes and silyl radicals are easily detected as strong absorptions in the 390-520 nm and 300-340 nm ranges, respectively. The steady-state product studies have confirmed the silatriene and silyl radical assignments in the transient UV absorption spectra (Figure 2.10). Simple silenes **11** and **36** are not detected in these spectra, however, due to their low yields, low extinction coefficients, and the fact that they absorb in the same region as the arylsilyl radicals.



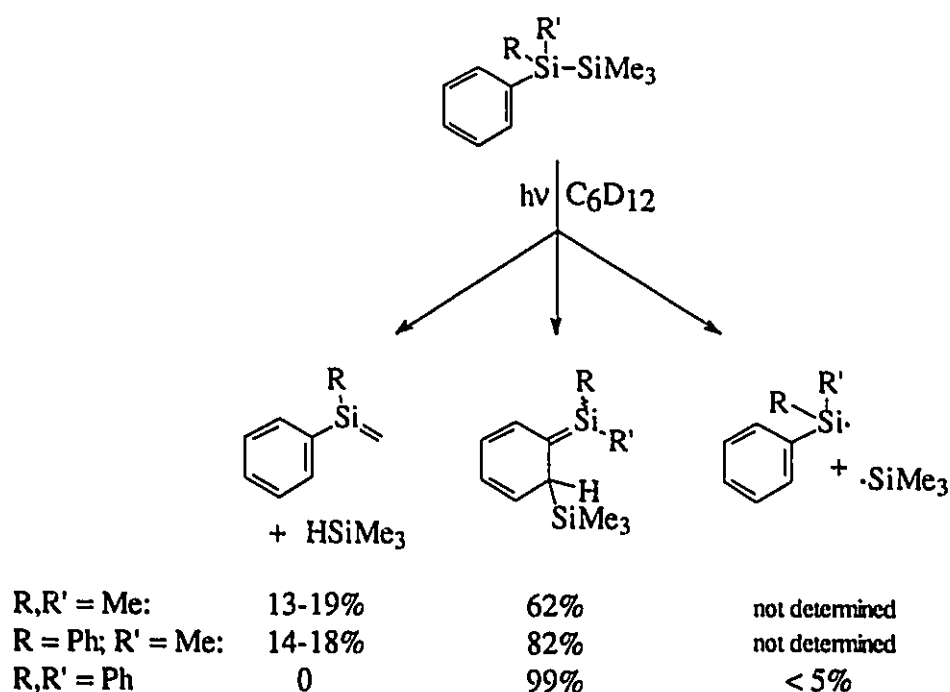
The photochemistry of the three trimethylsilyl-substituted phenyldisilanes (**12**, **34**, and **35**) is relatively straightforward in non-polar solvents such as cyclohexane or isooctane, although it is much more complex than prior reports of the photochemistry of **12** and **34** suggest.³⁹⁻⁴¹ The present experiments employed acetone at concentrations

(0.05 M) sufficient to trap the simple silenes⁶³ and silatrienes^{108,109} quantitatively ($k_q = 10^8$ - 10^9 M⁻¹s⁻¹). Previous studies of the photolysis of **12** in the presence of acetone in non-polar solvents have suggested that silatriene **13** is the sole silicon-containing reactive intermediate produced based on the isolation of acetone ene adduct **56a**.¹⁰² In partial agreement with these studies, we have detected significant amounts of the silatriene/acetone ene adducts (**56a-c**; 30-55%) from the photolysis of **12**, **34**, and **35**. However, we have also detected significant yields of the formal acetone/silatriene [2+2]-cycloadducts (**47a-c**; 20-70%), and silyl enol ethers (**45**, **58**; *ca.* 15%), consistent with the formation of simple silenes (**11** and **36**). We conclude that the major transient photoproduct from the photolysis of these compounds is the corresponding silatriene (**13**, **37**, and **38**), but it accounts for only 60-80% of the product mixture for **12** and **34** (Scheme 3.1). The formation of **45** and **58** from the photolysis of **34** and **12**, respectively, is accompanied by the formation of undeuterated trimethylsilane. No products consistent with the formation of 1,1-dimethylsilene and the corresponding arylsilane are detected from the photolyses of these three disilanes. Dehydrosilylation from **35** yielding 1,1-dimethylsilene and triphenylsilane is not observed which accounts for the almost quantitative formation of silatriene-derived products. Apparently, the formation of the more highly conjugated phenylsilene is favoured substantially over 1,1-dimethylsilene.

Silyl radical derived products are detected as chlorosilanes in yields of < 5% when the disilanes are photolyzed in the presence of sufficient chloroform (0.05 M) to trap any silyl radicals quantitatively ($k_q \approx 3 \times 10^8$ M⁻¹s⁻¹).^{69,107,112} The yields of the silatriene-derived products are unaffected by the presence of chloroform which indicates that silatriene formation occurs from direct [1,3]-silyl rearrangement in a disilane excited state and not from recombination of the two free silyl radicals formed from Si-Si bond homolysis. Also, the fact that the transient UV absorption spectrum obtained from NLFP

of 35 in n-pentane solution is essentially the same as the spectrum recorded in OCT rules out the possibility that silatriene formation occurs via recombination of singlet derived in-cage silyl radicals. If this mechanism were valid, the yield of free silyl radicals, reflected by the intensity of transient absorptions in the 300-340 nm range, would be expected to be higher in n-pentane since its relatively low viscosity would allow more facile cage escape than OCT.

Scheme 3.1 Phenyldisilane Photochemical Partitioning in Non-Polar Solvents



The photochemistry of the trimethylsilyl-substituted disilanes is dramatically different in ACN solution, showing that the relative yields of the silatriene- and radical-derived products are remarkably dependent upon solvent polarity. Steady-state photolysis experiments show that the formation of free silyl radicals predominates and that silatriene

formation becomes a minor pathway by the increased yields of deuteriosilanes and chlorosilanes in the absence and presence of chloroform in ACN, respectively (Table 3.3). The photolysis of ACN solutions **12**, **34**, and **35** in the absence of chloroform yields small amounts of the corresponding silatriene/acetone adducts (Table 3.3). The yields of the silatriene-derived products are *ca.* 35% for photolysis of **12** but are much lower for **34** and **35**. Products consistent with acetone trapping of simple silenes **11** and **36** are not detected, but this is not unexpected since they are formed in much lower yields than the silatriene-derived products in hydrocarbon solution.

Photolysis of these disilanes in the presence of chloroform in ACN solution results in the formation of the corresponding chlorosilanes and reductions in the yields of trimethylsilane-*d*, the corresponding phenylsilane-*d*, and unidentified product **61**. The yields of silatriene ene adducts **56b** and **56c** from the photolysis of **34** and **35**, respectively, are unaffected by the presence of chloroform compared to the values obtained in the absence of halocarbon. This indicates that silatrienes **37** and **38** are formed by concerted rearrangement as opposed to silyl radical recombination. On the other hand, the formation of silatriene-derived products (**56a** and **57a**) from the photolysis of **12** is partially quenched by the addition of chloroform. However, this quenching is not due to a reaction of the halocarbon with the charge-transfer excited state of **12** since there is no reduction in the fluorescence emission intensity from this disilane up to 0.2 M chloroform. Neither are the reduction in yield of **56a** and **57a** due to competitive silatriene quenching by the halocarbon when **12** is photolyzed in the presence of chloroform. Although chloroform does quench silatriene **13** in ACN solution ($k_q = (1.1 \pm 0.1) \times 10^6 \text{ M}^{-1}\text{s}^{-1}$), the rate constant for quenching by acetone is *ca.* 800 times faster ($k_q = (7.7 \pm 0.2) \times 10^8 \text{ M}^{-1}\text{s}^{-1}$) under these conditions. Therefore, silatriene **13** *may* be formed, in part, by a silyl radical recombination process. One inconsistency with this conclusion is our inability to detect

hexamethyldisilane as a co-product in the photolyses of ACN solutions of **12**, **34**, and **35** in the absence of chloroform; hexamethyldisilane would be expected to be formed if the silatrienes are formed to any extent by recombination of free silyl radicals.

We have been unable to identify the major product **61** from the photolyses of ACN-*d*₃ solutions of **12**, **34**, and **35** in the absence of chloroform. It is detected in the ¹H NMR spectra of the crude photolysates but is undetectable by gas chromatography (GC) under our conditions; however, GC spiking experiments indicate that **61** is not hexamethyldisilane or hexamethyldisiloxane. The formation of **61** is quenched by the addition of chloroform indicating that it is probably radical-derived. Despite the fact that **61** remains unidentified our conclusions remain the same: silyl radical formation is the predominant photochemical process in ACN solution.

The formation of the corresponding deuterated silanes in the photolyses of **12**, **34**, and **35** in ACN-*d*₃ in the presence of 0.05 M chloroform is a particularly intriguing result. Deuterated silanes cannot arise by deuterium atom abstraction from ACN-*d*₃ by silyl radicals since the estimated rate of this reaction ($k < 7 \times 10^4 \text{ M}^{-1}\text{s}^{-1}$; estimated from the lifetime of the triphenylsilyl radical in ACN) is at least ten times slower than reaction with chloroform ($k_{\text{q}} \approx 3 \times 10^8 \text{ M}^{-1}\text{s}^{-1}$)^{69,107,112} under these conditions. This indicates that the solvent (ACN-*d*₃) must play some direct role in the photochemistry of these compounds. The possibility that deuterated silanes are formed by the interaction of trace amounts of D₂O with the phenyldisilane excited singlet or triplet states can be ruled out since the concentration of D₂O in the ACN-*d*₃ employed in these experiments ($\leq 0.005 \text{ M}$; estimated from the lifetime of 1,1-diphenylsilene)¹¹¹ is too low for excited state quenching to occur. The only observable effect of the trace amounts of D₂O present is the partial hydrolysis of the corresponding chlorosilanes formed in the photolyses in the presence of chloroform. The silanols which are produced from hydrolysis of the

chlorosilanes are also formed in too low of a concentration to quench the disilane excited states directly. Thus, it appears unlikely that they play a role in the formation of the deuterated silanes either.

The transient UV absorption spectra obtained from NLFP of **12**, **34**, and **35** (Figure 2.10) also demonstrate the increase in yield of silyl radicals in ACN compared to hydrocarbon solution. It has been suggested that silene formation from aryldisilanes occurs from a singlet excited state^{37,82,89} and that intersystem crossing in aryldisilanes is enhanced in polar media.³⁸ Thus, these results are consistent with silatriene and silyl radical formation from excited states of different multiplicities, with the latter being triplet-derived.

Triplet sensitization and quenching experiments have confirmed that silyl radical formation occurs from an aryldisilane triplet excited state. Acetone sensitized photolysis of **35** yields *only* radical-derived products. The triplet state of acetone ($\phi_{isc} = 0.90$, $E_{T1} = 80$ kcal/mol)¹¹⁹ can be expected to be quenched by **35**, by an energy transfer process, at close to the diffusion-controlled rate since phenyldisilane triplet energies are on the order of 80 kcal/mol or less.³⁸ The product yields from benzene-sensitized irradiation of **35** also confirm the triplet origin of silyl radicals. The yields of silyl radical and silatriene-derived products in benzene solution are dependent upon the concentration of disilane **35**. At high concentrations of **35** (*ca.* 0.05 M) silatriene formation predominates due to efficient quenching of the benzene singlet excited state ($E_{S1} = 109$ kcal/mol; $\tau_{S1} = 30$ ns)¹³⁶ by the disilane. At low disilane concentration singlet quenching is less efficient, benzene intersystem crossing to the triplet excited state can occur ($\phi_{isc} = 0.23$; $E_{T1} = 84$ kcal/mol; $\tau > 6$ μ s),¹³⁶ and the yield of radical-derived products (**10** and **46**) increases dramatically due to more efficient formation of the phenyldisilane triplet excited state. NLFP experiments with THF solutions of **35** have allowed direct estimation of the yields

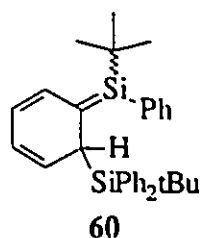
of the triphenylsilyl radical (33) relative to those of silatriene 38 at varying concentrations of *trans*-piperylene, and confirm that silyl radicals do indeed arise from a triplet excited state. Stern-Volmer analysis of the data reveals that the triplet excited state of 35 is very short-lived ($\tau \approx 6$ ns), which precludes its direct detection by NLFP techniques and indicates that deactivation of this excited state, presumably by Si-Si homolysis, is very rapid.¹²¹

The study of the photochemistry of 12, 34, and 35 in hydrocarbon and ACN solutions has clearly demonstrated that the photochemical behaviour of phenyldisilanes can be controlled to a large extent by solvent polarity. However, all three of these disilanes exhibit surprisingly similar behaviour and show little sensitivity to changes in the degree of phenyl substitution. In general, silene formation predominates in hydrocarbon solution while free silyl radicals are the major products in polar solvents such as ACN.

On the other hand, the photochemistry of 1,2-di-*tert*-butyl-1,1,2,2,-tetraphenyl-disilane (40) clearly demonstrates that phenyldisilane structure can also play a major role. The photolysis of 40 in hydrocarbon *and* polar solvents (CHCl₃, THF, ACN) is remarkably clean, yielding *only* products consistent with the trapping of *tert*-butyldiphenylsilyl radicals (41). NLFP experiments have also provided direct evidence for the sole formation of 41 based on its characteristic UV absorption spectrum (Figure 3.5) and reactions with alkyl halides, alkenes, and oxygen.

The short- and long-wavelength transient absorptions in Figure 3.5 exhibit identical kinetic behaviour in the presence and absence of silyl radical and silene trapping reagents. Similar weak long-wavelength absorptions have been observed in the spectra of triphenylsilyl⁷² (33) and methyldiphenylsilyl radicals (44) (Figure 2.7). Thus, the transient absorption from 40 centred at 420 nm is attributed to weak absorption by radical 41. The formation of silatriene (68) from 40 would be expected to result in intense transient

absorption centred at *ca.* 460 nm, by analogy with silatrienes **37** and **52**, with different kinetic behaviour towards silene and silyl radical scavengers.



The short-wavelength component in Figure 3.5 ($\lambda_{\text{max}} = 305 \text{ nm}$) is blue-shifted relative to that in the spectrum of the methyldiphenylsilyl radical (**44**) ($\lambda_{\text{max}} = 325 \text{ nm}$) and is closer to that of the phenylsilyl radical ($\lambda_{\text{max}} = 297 \text{ nm}$).⁷² This may be due to a steric effect of the bulky *tert*-butyl group which causes one of the phenyl rings to twist out of conjugation with the radical centre. The *tert*-butyl substituent may force **41** to adopt a more pyramidal geometry than the methyldiphenylsilyl radical (**44**), although inductive effects may also play a role.

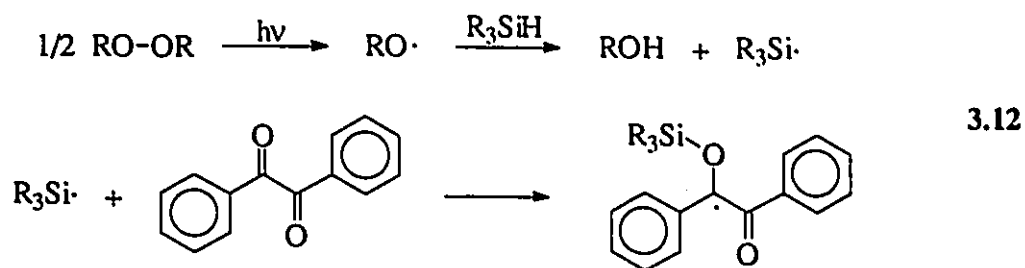
The reaction quantum yield for **40** is dependent upon solvent polarity. The quantum yield for disappearance of **40** in cyclohexane is about one-half that in chloroform solution. Likewise, the quantum yield for silyl radical production (detected as chlorosilane **65**) is 1.4 times higher in THF compared to cyclohexane solution. We originally suggested that the lower disappearance quantum yield in cyclohexane versus chloroform solution was due to silyl radical recombination in hydrocarbon solution in the absence of trapping agents.¹¹² However, in light of the triplet origin of silyl radicals, it is possible that these observations are attributable to a solvent effect on the efficiency of intersystem crossing in this disilene. Another possibility is direct electron-transfer quenching of the singlet excited state of **40** by chloroform solvent which should yield the same products as those derived from

reactions of triplet-derived silyl free radicals¹²⁰ (Chapter 2). Conclusive evidence for the triplet photoreactivity of **40** has been obtained from the Stern-Volmer quenching of chlorosilane formation with *trans*-piperylene (Figure 3.4). No curvature is observed in the Stern-Volmer plot, indicating that radical formation from the photolysis of this compound is *entirely* triplet-derived.

The clean formation of silyl radicals from the photolysis of **40** in polar *and* non-polar solvents is remarkable considering the general complexity of the product mixtures obtained with the other disilanes employed in this study. Thus, the structure of this disilane is the major factor which determines its photochemistry; simple silene formation is blocked by the absence of a methyl group attached to silicon and the phenyl and *tert*-butyl substituents have sufficient steric bulk that silatriene formation is suppressed. We have demonstrated that silyl radicals arise from the disilane triplet excited state; therefore, the unique structure of **40** must result in low singlet state reactivity (silatriene formation) allowing intersystem crossing to the triplet excited state to occur. The triplet state of **40** reacts rapidly by Si-Si homolysis ($\tau = 1\text{-}2$ ns) in a similar manner to that of **35**.

The generation of arylsilyl radicals **41** cleanly and directly in a single photochemical step has several advantages to the classical "indirect" methods which involve a photochemically or thermally generated radical initiator. While rate constants have been determined for several silyl radical reactions, most of the data is qualitative and has been obtained by competition kinetics using product studies or ESR spectroscopy. There are a few reports of the use of kinetic ESR spectroscopy^{70,71,137} or laser flash photolysis techniques^{67,69-72,138-140} to determine absolute rate constants but they have been mostly limited to reactions of trialkylsilyl radicals. Prior to our investigation there existed only a single report of the measurement of absolute rate constants for the reactions of arylsilyl radicals.¹⁰⁷ The majority of the absolute bimolecular rate constants for silyl

radical reactions has been obtained by monitoring the decay of the silyl radical directly, as in the case of **33**,¹⁰⁷ or by monitoring the growth of the product of the reaction of the radical with either the substrate or a secondary probe (e.g. benzil; eq 3.12) as a function of added substrate.^{69-71,139,140} Although these methods are extremely useful, one limitation is the requirement of the use of high (> 1 M) concentrations of precursor silane and peroxide initiator. This is because hydrogen abstraction from silanes is relatively slow ($k = 10^7 \text{ M}^{-1}\text{s}^{-1}$),⁶⁷ and the extinction coefficient of dialkyl peroxides is low above 300 nm.¹⁴¹



Although the rates of reaction of **41** with the substrates listed in Table 3.5 are generally slightly slower than those reported for the triethylsilyl radical, they follow the same trends in magnitude. The only major discrepancies are the reactions with dichloromethane and *tert*-butyl chloride. The reported rate constants for the triethylsilyl radical are *ca.* 13 and 3 times faster,⁶⁹ respectively, than the present ones reported for **41**. On the other hand, the rate constant for reaction of **41** with dichloromethane is identical with that reported for the reaction of the triphenylsilyl radical (**33**) with this reagent.¹⁰⁷ We also note that the reported rate constant for the reaction of triethylsilyl with dichloromethane was calculated⁶⁹ from a relative value determined from competition experiments,¹³⁵ which may be less accurate than the others.

Transient absorption spectra recorded by NLFPS of hexaphenyldisilane (32) in the absence and presence of acetone (Figure 3.7) have demonstrated that silatriene 55 is formed in appreciable amounts in addition to the triphenylsilyl radical (33). Thus, disilane 40 is the only phenyldisilane reported to date which generates a *single* type of silicon reactive intermediate upon photolysis in solution at room temperature.

CHAPTER 4

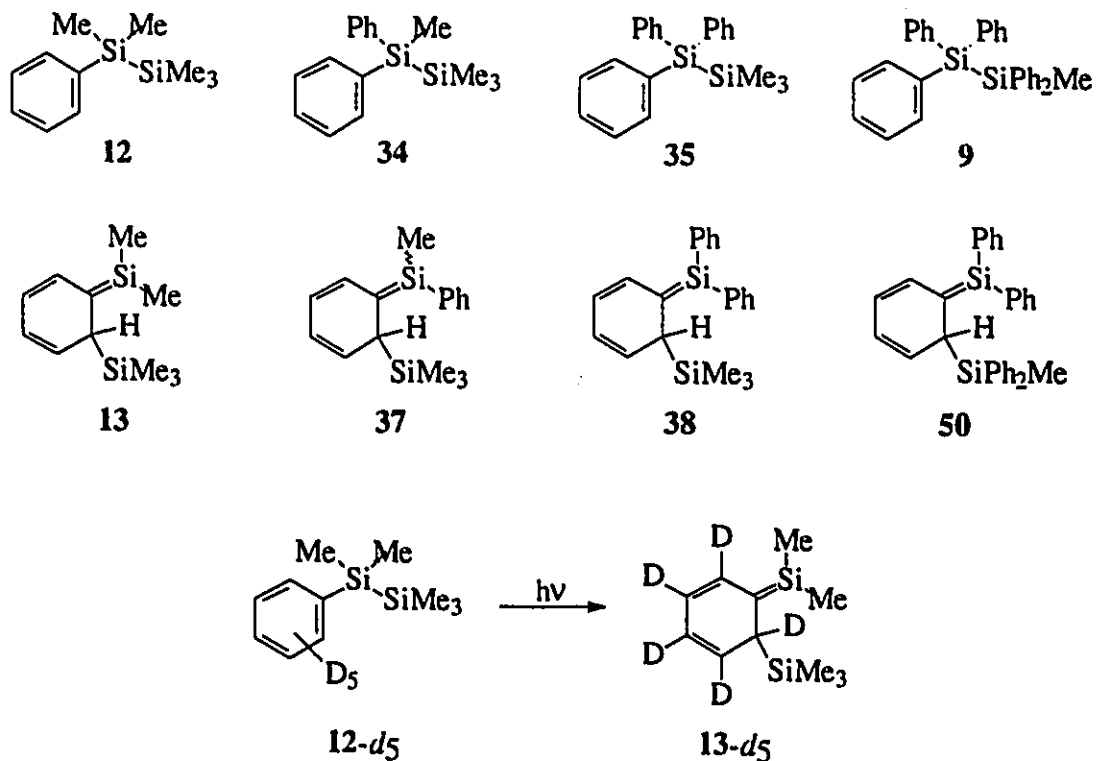
SOLVENT AND SUBSTITUENT EFFECTS ON THE REACTIVITY OF SILATRIENES

4.1 Introduction

Although there are reports of the relative rates of reactions of stabilized silenes with reagents such as alcohols, amines, and dienes,² little quantitative data on silene reactivity exists. For this reason, the mechanisms of silene reactions are very poorly understood. Little is known about the effects of solvent polarity or substitution at silicon on the kinetics and mechanisms of silene reactions. We have demonstrated the generality of 1,3,5-(1-sila)hexatriene (silatriene) formation from photolysis of phenyldisilanes (**9**, **12**, **34**, **35**) and the ease with which they can be detected by nanosecond laser flash photolysis (NLFP) techniques even when they are formed in relatively low yields (see Chapters 2 and 3). Thus, these phenyldisilanes have been employed as precursors in the study of solvent and substituent effects on silatriene reactivity.

This chapter represents a study of the reactions of silatrienes (**13**, **37**, **38**), generated by photolysis of disilanes **12**, **34**, and **35**, respectively, with acetone, 2,3-dimethyl-1,3-butadiene (DMB), oxygen, alkyl halides, methoxytrimethylsilane (MTMS) and alcohols by steady-state and NLFP techniques. The reactions of silatriene **50**, generated from photolysis of **9**, with several reagents are also briefly discussed. Silatriene formation from

disilanes **12**, **34**, and **35** involves a [1,3]-migration of a trimethylsilyl group in each case generating a homologous series of silatrienes (**13**, **37**, **38**) which differ only in substitution at the trivalent silicon atom. Absolute rate constants for reactions of these silatrienes with the reagents listed above have been determined in acetonitrile, isooctane, and tetrahydrofuran solution. Kinetic deuterium isotope effects on the rates of reaction of silatriene **13** with acetone, oxygen, and DMB have been determined using the phenyl- d_5 analog (**12- d_5**) which generates silatriene **13- d_5** upon irradiation. The products (and chemical yields) from the photolysis of **12**, **34**, and **35** in the presence of acetone, DMB, oxygen, carbon tetrachloride, MTMS, and methanol in hydrocarbon and ACN solvents have been identified. UV absorption spectra of silatrienes **13**, **37**, and **38** in tetrahydrofuran are reported and compared to those obtained in ACN and OCT solutions.



4.2 Results

4.2.1 Silatriene UV Absorption and THF Complexation

The positions of the silatriene (13, 37, 38) absorption maxima, obtained by NLFP of disilanes 12, 34, 35, respectively, are virtually the same in ACN and OCT solutions (Figure 2.10); however, the transient absorption spectra recorded in THF solution (see Figure 4.1) are significantly different. The absorption maximum of the long-wavelength transient (13), observed from NLFP of 12, shifts by *ca.* 35 nm from 425 nm in ACN and OCT solution to 460 nm in THF solution. The long-wavelength absorption from 34 shifts by *ca.* 10 nm from 460 in ACN and OCT to 470 nm in THF solution, while the position of the transient absorption from 35 is the same in all three solvents ($\lambda_{\text{max}} = 490 \text{ nm}$).

The short-wavelength absorption bands (300-340 nm) from NLFP of 34 and 35 are very weak in OCT solution and are approximately half as intense in THF compared to ACN solution. The addition of up to *ca.* 12% THF to ACN solutions of 12 results in increasing red-shifts and broadening of the long-wavelength absorption band. Transient absorption spectra recorded from NLFP of optically matched solutions (at 248 nm) of 12 in ACN, THF, and 5% THF/ACN are shown in Figure 4.2. The spectra were normalized by measurement of the initial optical density at 425 and 460 nm after NLFP of the three solutions.

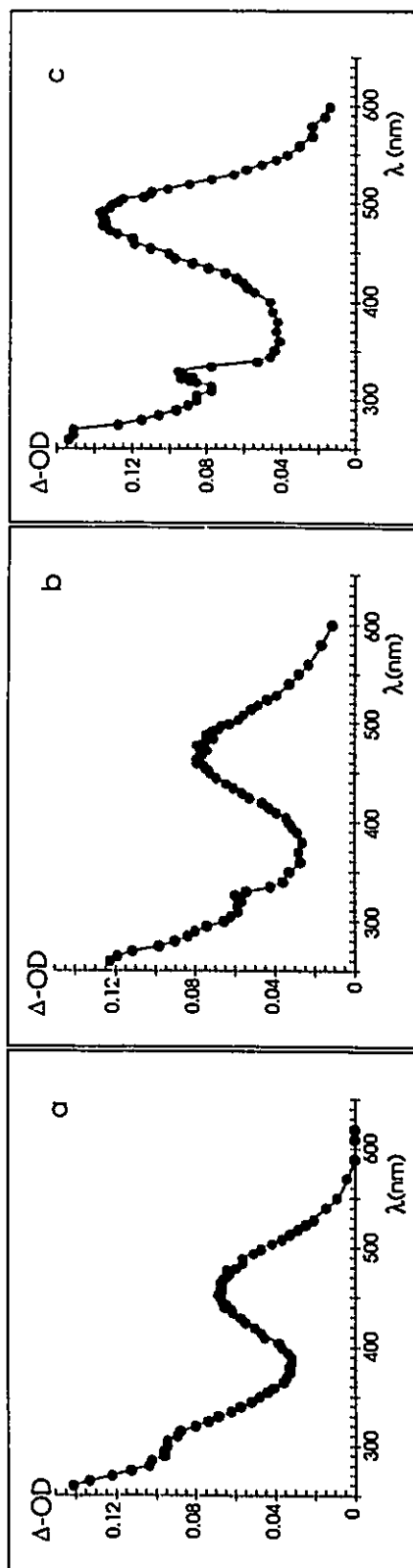


Figure 4.1 Transient absorption spectra recorded by NLFP, 10-200 ns after 248 nm laser excitation of deoxygenated THF solutions of (a) **12**, (b) **34**, (c) **35** at 23 ± 2 °C.

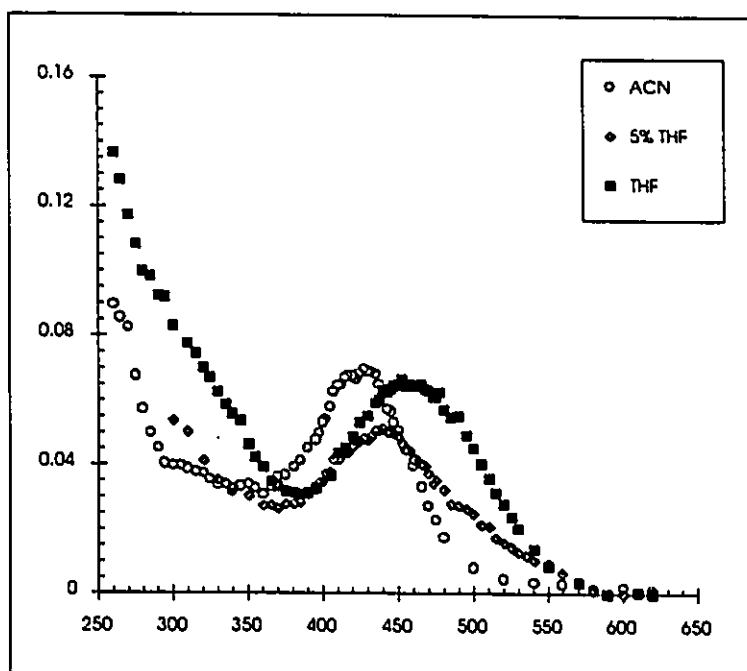
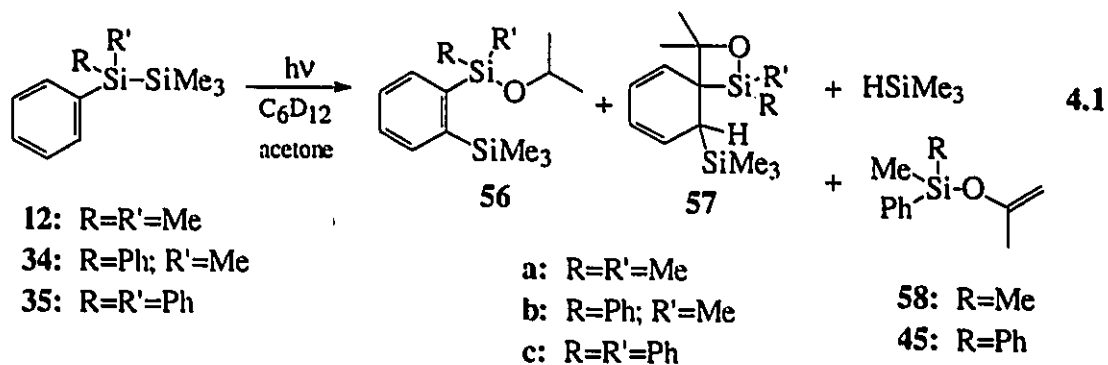


Figure 4.2 Transient absorption spectra from NLFP of deoxygenated solutions of **12** in ACN, THF, and 5% THF/ACN at 23 ± 2 °C.

4.2.2 Silatriene Reactions with Carbonyl Compounds

Steady-state photolysis (254 nm) of deoxygenated 0.05 M solutions of **12**, **34**, and **35** in cyclohexane-*d*₁₂ containing 0.05 M acetone to *ca.* 80% conversion yields the products shown in equation 4.1. The two types of silatriene/acetone adducts, **56** and **57**, are the major products in each case, while trimethylsilane and silyl enol ethers **45** and **58** are formed in low yields from the photolysis of **34** and **12**, respectively (see Chapter 3; Table 3.2). Photolysis of ACN solutions of the three disilanes yields smaller amounts of silatriene-derived products due to markedly higher yields of the corresponding silyl radicals in this solvent.



The 1,2-siloxetanes **57** are thermally and hydrolytically unstable and, therefore, have been characterized by detailed NMR spectroscopic analysis of the crude photolysates. They are not detectable by GC analyses of the crude mixtures and decompose upon attempted vacuum distillation and either normal or reverse-phase chromatography. Siloxetane **57a** is highly unstable as it decomposed during an overnight NMR experiment in C₆D₁₂ solution at room temperature. The other two siloxetanes survived for several days at room temperature in C₆D₁₂ solution. Siloxetane **57c** decomposed within 4 hours

at 115 °C in C₆D₁₂ and within 12 hours at room temperature in the presence of one equivalent of methanol in C₆D₁₂ solution. The products of decomposition of **57** have not yet been identified.

The structures of siloxetanes **57** have been assigned through ¹³C, nOe, spin-decoupling, and ¹H-¹³C heteronuclear shift correlation NMR experiments on the crude photolysates after *ca.* 50% conversion. The chemical shifts were similar in C₆D₁₂ and CDCl₃ so the spectra of **57a** and **57b** were recorded in the former solvent for convenience and to minimize decomposition. The ¹H NMR spectrum of the crude photolysate obtained after *ca.* 50% conversion of **35** is shown in Figure 4.3. The initial ¹H and ¹³C assignments of **57c** were made by subtraction of the resonances due to authentic samples of **35** and **56c**. The ¹H NMR assignments were verified by ¹H-¹H spin decoupling and nOe experiments while the ¹³C NMR assignments were verified by the ¹H-¹³C heteronuclear shift correlation spectrum of the mixture which is shown in Figure 4.4.

The nOe experiments not only verify that the ¹H resonances assigned to **57c** belong to the same molecule but they also allow the assignment of the stereochemistry of the molecule. The two possible structures of **57c** from molecular mechanics (MMX) calculations are shown below. Irradiation of the methyl group at δ 1.41 caused enhancements in the other methyl group (δ 1.84), a vinyl proton at δ 5.74, and one of the phenyl protons. Irradiation of the methyl group at δ 1.84 resulted in enhancements of the other methyl group (δ 1.41), the allylic proton resonance (δ 2.93), one vinyl proton at δ 5.89, and one phenyl proton. ¹H-¹H spin decoupling experiments demonstrated that the vinyl proton resonance at δ 5.89 was vicinal to the allylic proton. Finally, irradiation of the trimethylsilyl singlet at δ -0.17 caused enhancements of the allylic, vinyl, and phenyl resonances. Thus, the stereochemistry of siloxetane **57c** is assigned as *syn-57c*.

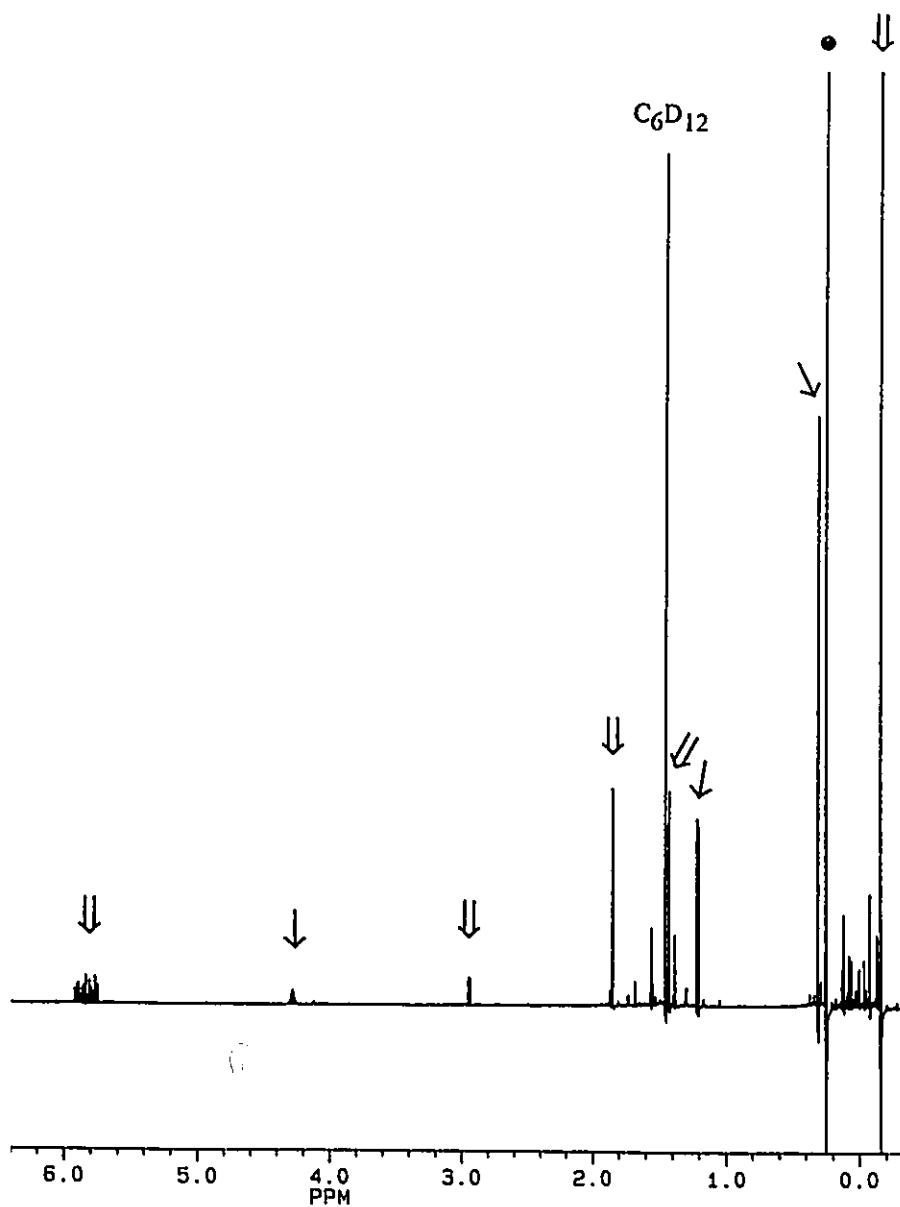


Figure 4.3 ^1H NMR spectrum (500 MHz; δ -0.4-6.4 region) of a crude mixture from photolysis of a deoxygenated, 0.05 M solution of **35** in cyclohexane containing 0.05 M acetone to *ca.* 50% conversion, after evaporation of solvent and redissolution in CDCl_3 . Resonances due to protons in **35** (\bullet), **56c** (\downarrow), and **57c** (\Downarrow) are labelled. The spectrum has been expanded to reveal the weak signals in the δ 2.9-6.0 region.

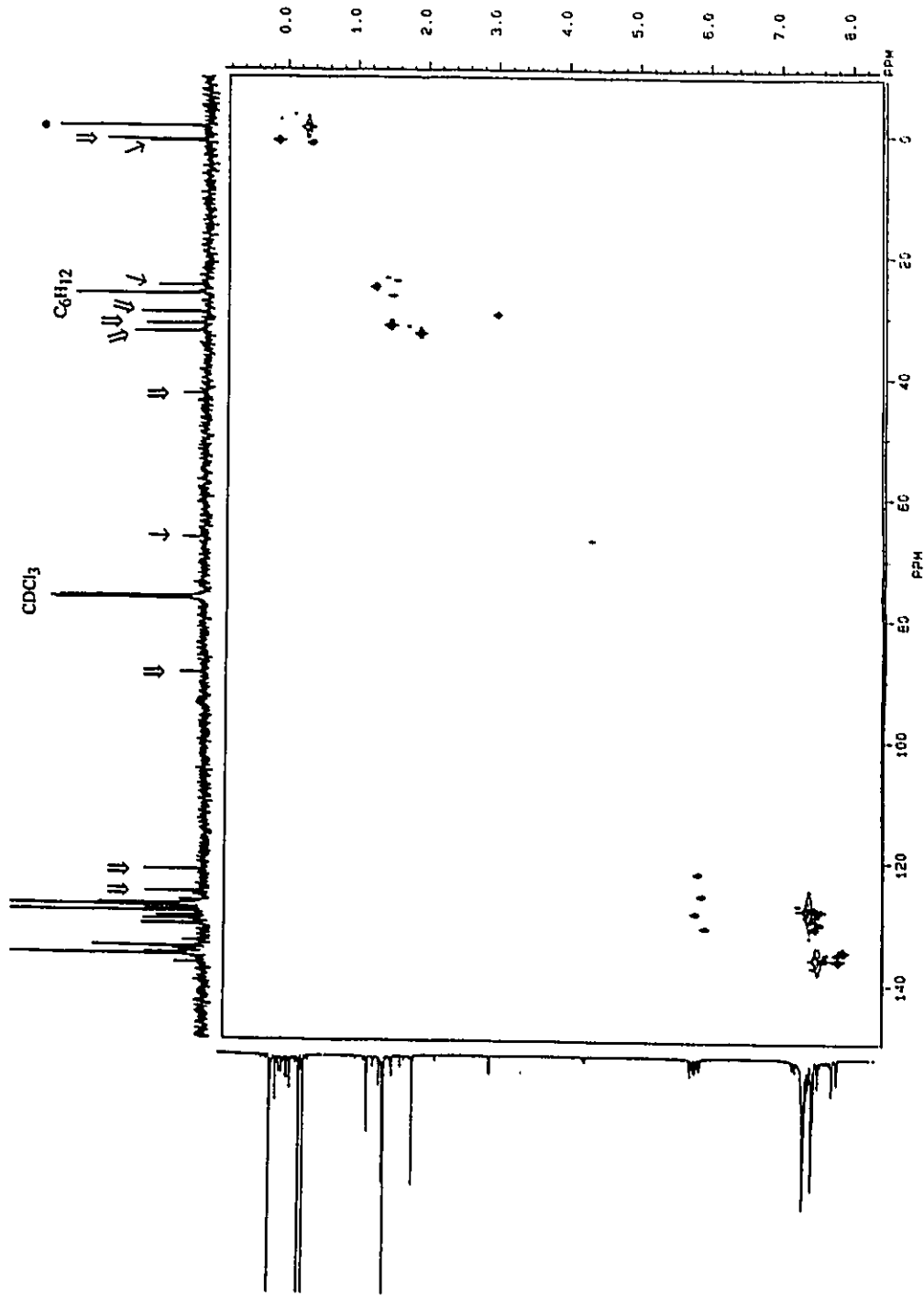
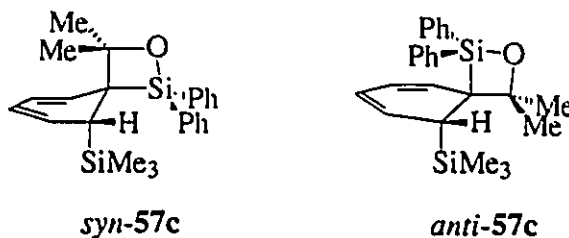


Figure 4.4 ^1H - ^{13}C Heteronuclear shift correlation NMR spectrum of the same photolysis sample used in Figure 4.3. Resonances due to carbons in 35 (●), 56c (↓), and 57c (⇓) are labelled.

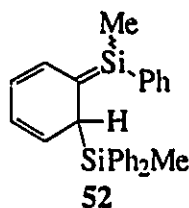


Additional evidence for the structure of **57c** has been obtained from the ^{13}C NMR, ^{29}Si NMR, and infrared spectra of the crude photolysis mixtures. Quaternary carbon resonances were observed at δ 44.4 and δ 89.4 which have been assigned to C_4 and C_3 of the siloxetane ring, respectively. The latter resonance compares to a value of δ 67.1 for the ketyl carbon in **56c**. The ^{29}Si NMR spectrum exhibited resonances at δ 2.2 and δ 12.4 which have been assigned to the trimethylsilyl and siloxetane ring silicon atoms, respectively. The siloxetane ring silicon resonance is shielded by *ca.* 5 ppm compared to the ^{29}Si resonance in 1,1-diphenylsilacyclobutane¹⁴² due to the presence of the ring oxygen atom and additional alkyl substitution on the ring carbon atoms in **57c**. The infrared spectrum showed a strong absorption band at 1057 cm^{-1} , which is characteristic of the siloxetane Si-O stretching vibration in 1,2-siloxetanes.⁶²

Although the yields of siloxetanes **57a** and **57b** from the photolysis of **12** and **34** are much lower than the yield of **57c** from **35**, their presence is evident in the ^1H NMR spectra of the crude photolysates in C_6D_{12} solutions. The TMS regions of these spectra are very complex; however, the allylic and vinylic proton resonances attributed to **57a,b** are quite prominent. The ^1H and ^{13}C NMR spectra of these two siloxetanes have been assigned tentatively by a similar procedure employed for **57c** and are listed in Chapter 6. ^{29}Si NMR spectra of **57a,b** were not recorded due to their low yields.

NLFP experiments demonstrate that the addition of acetone (or acetone- d_6) to solutions of **9**, **12**, **12- d_5** , **34**, **35**, and **39** results in a reduction of the silatriene lifetime in each case with no decrease in the initial yield of the transient. Likewise, addition of ethyl acetate to ACN solutions of **12** shortens the lifetime of silatriene **13**. Plots of k_{decay} versus quencher concentration are linear in every case. Representative plots of this type for quenching of silatrienes **13**, **37**, and **38** with acetone in deoxygenated OCT solution are shown in Figure 4.5. Quenching rate constants for reactions of acetone, acetone- d_6 , and ethyl acetate with **13**, **13- d_5** , **37**, and **38** are listed in Table 4.1. These rate constants were determined by linear least squares analysis of the data according to equation 4.2, where k_0 is the pseudo-first order rate constant for transient decay in the absence of quencher and k_q is the second order rate constant for transient quenching with quencher, Q. The rate constant for quenching of **52** (generated from photolysis of 1,2-dimethyl-1,1,2,2-tetra-phenyldisilane (**39**)) with acetone in OCT solution was determined to be $(1.96 \pm 0.03) \times 10^9 \text{ M}^{-1}\text{s}^{-1}$ while that for acetone quenching of **50** in ACN solution is $(2.54 \pm 0.15) \times 10^8 \text{ M}^{-1}\text{s}^{-1}$ (see Table 2.3).

$$k_{\text{decay}} = k_0 + k_q[\text{Q}] \quad 4.2$$



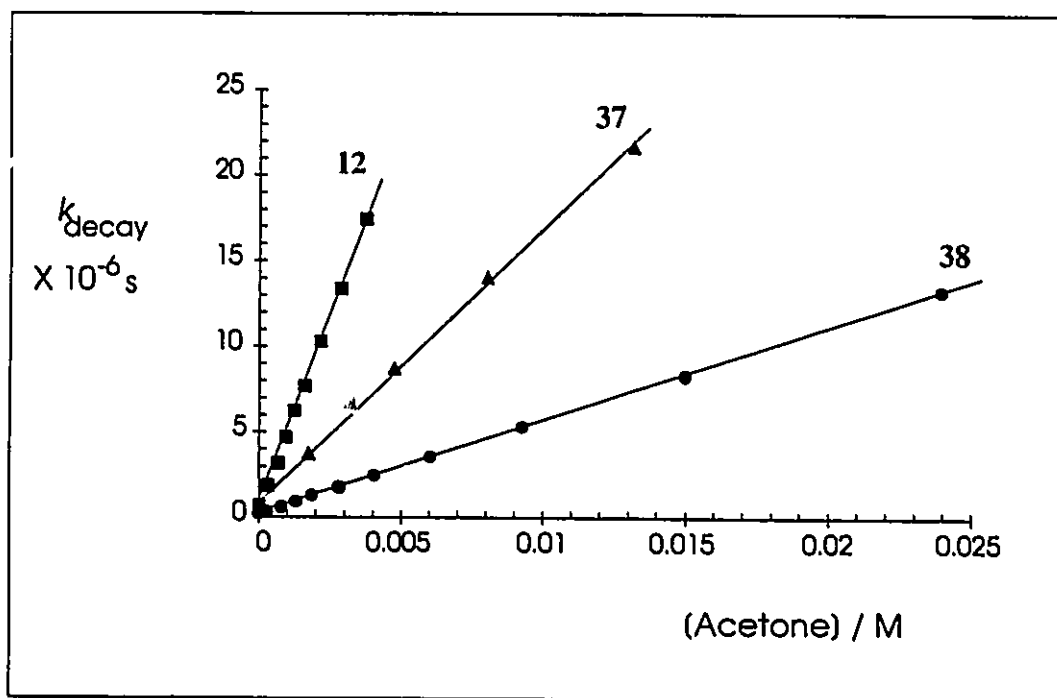
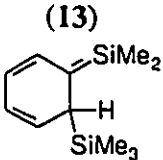
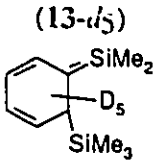
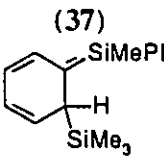
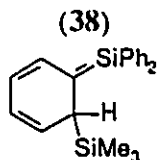


Figure 4.5 Plots of k_{decay} versus quencher concentration for reactions of silatrienes 12, 37, and 38 with acetone in isooctane (OCT) solution at 23 ± 2 °C.

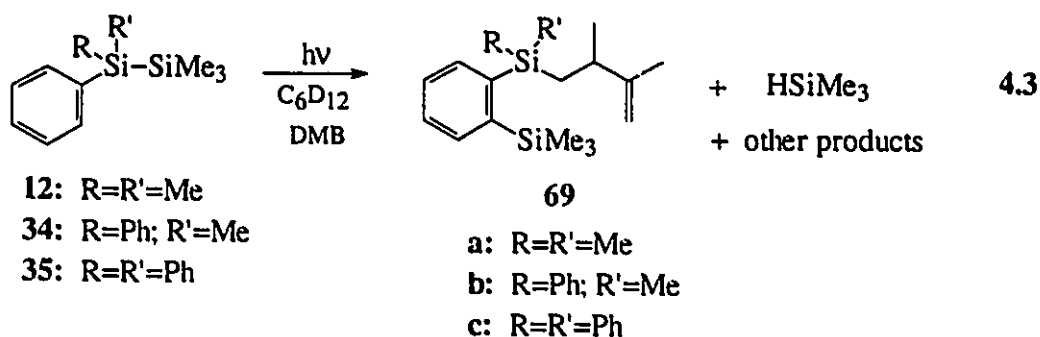
Table 4.1 Rate Constants for Reaction of Silatrienes **13**, **13-*d*₅**, **37**, and **38** with Acetone, Acetone-*d*₆, and Ethyl Acetate (EtOAc) in Acetonitrile (ACN), Tetrahydrofuran (THF), and Isooctane (OCT) solution at 23 ± 2°C.^a

Reagent	Solvent	k_q (X 10 ⁻⁸ Ms)			
		(13) 	(13-<i>d</i>₅) 	(37) 	(38) 
Acetone	ACN	7.7 ± 0.2	7.7 ± 0.1	3.1 ± 0.2	1.5 ± 0.1
	THF	2.46 ± 0.05	b	1.62 ± 0.02	1.22 ± 0.03
	OCT	45.0 ± 0.6	45.1 ± 0.5	15.8 ± 0.6	5.42 ± 0.05
Acetone- <i>d</i> ₆	OCT	44.1 ± 0.8	b	b	b
EtOAc	ACN	0.033 ± 0.003	b	b	b

- a. Errors reported as twice the standard deviation from least squares analysis of the data according to equation 4.2.
- b. Not determined.

4.2.3 Reactions with Alkenes and Dienes

Photolysis (254 nm) of deoxygenated 0.05 M solutions of **12**, **34**, and **35** in cyclohexane-*d*₁₂ containing 0.06 M DMB to *ca.* 80% conversion affords the product mixtures shown in equation 4.3. Product yields, determined by integration of the ¹H NMR (300 MHz) spectra versus an internal standard, are listed in Table 4.2. Silatriene ene-adducts **69** were identified by ¹H NMR, GC/MS, and GC/FTIR analyses of the crude photolysates. The ¹H NMR and mass spectra of **69a** and **69b** were similar to those reported previously.¹⁰⁰ Ene-adduct **69b** exists as equal amounts of two diastereomers; the trimethylsilyl (TMS) groups of the two diastereomers were separated by 0.005 ppm.



Trimethylsilane is detected by ¹H NMR as a minor product from the photolyses of **12** and **34** on the basis of the Si-H multiplet at δ 4.00 ($J = 3.6$ Hz) and the methyl doublet at δ 0.08.¹⁴³ Small amounts of minor products are also detected by the presence of additional TMS resonances in the ¹H NMR spectra but could not be identified due to their low yield and the complexity of the spectra. Some evidence was observed for the presence of cyclohexadienyl protons in very low yield (< 5%). Explicit evidence for Diels-Alder or ene DMB adducts of simple silenes (**11**, **36**) could not be obtained, however.

Table 4.2 Product Yields from the Photolysis of 0.05 M Cyclohexane-*d*₁₂ Solutions of Disilanes **12**, **34**, and **35** in the Presence of DMB (0.06 M) to *ca.* 80% Conversion.^a

Disilane		69	Me ₃ SiH	others ^b
12	a	60%	17%	9% (2)
34	b	72%	10%	5% (1)
35	c	34%	< 2%	62% (5)

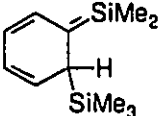
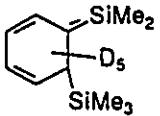
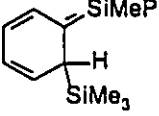
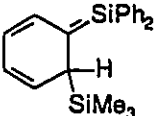
- a. Determined by ¹H NMR spectroscopy, after *ca.* 80% conversion. Integrated against dichloromethane as the internal standard. Errors are considered to be *ca.* 5%.
- b. Unidentified additional products, for which the number and combined yields are listed.

The product mixture from the photolysis of **35** in DMB/cyclohexane-*d*₁₂ was exceedingly complex and contained at least five products in addition to the silatriene ene-adduct **69c**. The ¹H NMR spectrum of the crude mixture shows substantial absorption in the vinylic region, which indicates that at least one of the minor products is likely a [2+2]- or [4+2]-adduct of DMB with **38**.

NLFP experiments have demonstrated that the addition of DMB to solutions of **9**, **12**, **12-*d*₅**, **34**, and **35** results in reductions of the corresponding silatriene lifetimes with no decrease in the initial yield of the transients. Likewise, addition of cyclohexene to ACN solutions of **9** and **12** shortens the lifetimes of the corresponding silatrienes (**50** and **13**).

Plots of k_{decay} versus quencher concentration are linear in every case. The quenching rate constants for reactions of cyclohexene and DMB with **13**, **13-*d*₅**, **37**, and **38** were determined by linear least squares analysis of the data according to equation 4.2 and are listed in Table 4.3. The rate constant for cyclohexene quenching of silatriene **50** in ACN solution is $(9 \pm 1) \times 10^5 \text{ M}^{-1}\text{s}^{-1}$, while that for quenching of **13** by DMSO in dioxane solution is $(3.0 \pm 0.2) \times 10^9 \text{ M}^{-1}\text{s}^{-1}$.

Table 4.3 Rate Constants for Reaction of Silatrienes **13**, **13-*d*₅**, **37**, and **38** with DMB and Cyclohexene in Tetrahydrofuran (THF), and Isooctane (OCT) solution at $23 \pm 2^\circ\text{C}$.^a

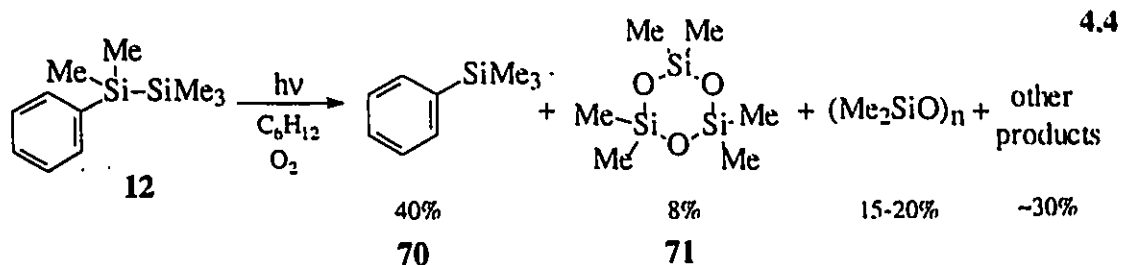
Reagent	Solvent	k_q ($\times 10^{-8} \text{ Ms}$)			
		(13) 	(13-<i>d</i>₅) 	(37) 	(38) 
DMB	THF	0.09 ± 0.01	b	0.07 ± 0.01	b
	OCT	1.28 ± 0.03	1.15 ± 0.05	0.68 ± 0.01	0.30 ± 0.01
Cyclohexene	ACN	0.012 ± 0.002	b	b	b

a. Errors reported as twice the standard deviation from least squares analysis of the data according to equation 4.2.

b. Not determined.

4.2.4 Reactions with Oxygen

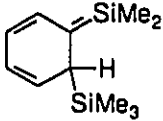
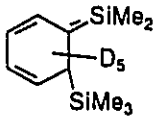

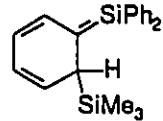
Steady-state photolysis (254 nm) of a 0.005 M solution of **12** in oxygen-saturated cyclohexane ($[O_2] = ca. 0.01 M$)¹¹⁹ to *ca.* 80% conversion yields phenyltrimethylsilane (**70**), hexamethyl-1,3,5-cyclotrisiloxane (**71**), and at least eight other relatively minor products, which include cyclohexanol, cyclohexanone, dimethylphenylsilanol, and octamethyl-1,3,5,7-cyclotetrasiloxane as identified by GC/MS analysis (eq. 4.4). A similar product composition is obtained when the solution was photolyzed to *ca.* 10% conversion, indicating that **70** and **71** are true primary photoproducts of the reaction. Photolysis of **12-d₅** in oxygen-saturated cyclohexane to *ca.* 30% conversion under identical conditions results in the formation of **70-d₅** and the other products listed below, according to GC/MS analysis of the crude photolysate. Steady-state photolysis of **35** under similar conditions affords **70** (69%) and a mixture of least seven other minor products which included cyclohexanol, cyclohexanone, and triphenylsilanol.



Addition of oxygen shortens the lifetimes of the silatrienes generated by NLFP of phenyldisilanes, **9**, **12**, **12-d₅**, **34**, **35**, and **39**, but has no effect on their initial yields following laser excitation. Plots of k_{decay} versus quencher concentration are linear in every case; thus, the second order quenching rate constants were calculated as the slopes

of these plots according to equation 4.2. Quenching rate constants for silatriene reactions with oxygen are listed in Table 4.4. The rate constant for quenching of silatriene **13-d₅** with oxygen in OCT solution is the same, within experimental error, as that for quenching of **13** under the same conditions. The rate constants for oxygen quenching of **50** in ACN and OCT solutions are $(3.8 \pm 0.3) \times 10^8 \text{ M}^{-1}\text{s}^{-1}$ and $(1.52 \pm 0.09) \times 10^8 \text{ M}^{-1}\text{s}^{-1}$, respectively (Table 2.3).

Table 4.4 Rate Constants for Reaction of Silatrienes **13**, **13-d₅**, **37**, and **38** with Oxygen in Acetonitrile (ACN), Tetrahydrofuran (THF), and Isooctane (OCT) solution at $23 \pm 2^\circ\text{C}$.^a

Reagent	Solvent	k_q ($\times 10^{-8}$ Ms)			
		(13) 	(13-d₅) 	(37) 	(38) 
O ₂	ACN	8.5 ± 0.8	b	4.8 ± 0.6	2.6 ± 0.5
	THF	5.0 ± 0.5	b	b	b
	OCT	6.9 ± 0.4	6.8 ± 0.6	3.5 ± 0.1	1.9 ± 0.2

- a. Errors reported as twice the standard deviation from least squares analysis of the data according to equation 4.2.
- b. Not determined.

4.2.5 Reactions with Alkyl Halides

Steady-state photolysis (254 nm) of a deoxygenated 0.03 M solution of **12** in cyclohexane-*d*₁₂ containing 0.03 M CCl₄ yields small amounts of chlorotrimethylsilane (**59**), chlorodimethylphenylsilane (**72**), and hexachloroethane in addition to several other minor products which have not been identified. Similarly, photolysis of a solution of **35** under these conditions affords a complex mixture of products which include **59** and chlorotriphenylsilane (**46**) in *ca.* 5% yield each, according to ¹H NMR analysis of the crude photolysate.

Addition of CCl₄ or CHCl₃ (up to *ca.* 0.05 M and 0.5 M, respectively) to ACN or OCT solutions of **12**, **34**, and **35** leads to reductions in the silatriene lifetimes but not their initial yields. Plots of k_{decay} versus quencher concentration are linear in every case; thus, the second order quenching rate constants were calculated as the slopes of these plots according to equation 4.2. Representative plots of this type for quenching of silatrienes **13** and **37** with CCl₄ in deoxygenated ACN solution are shown in Figure 4.6. Quenching rate constants for silatriene reactions with CCl₄ and CHCl₃ are listed in Table 4.5.

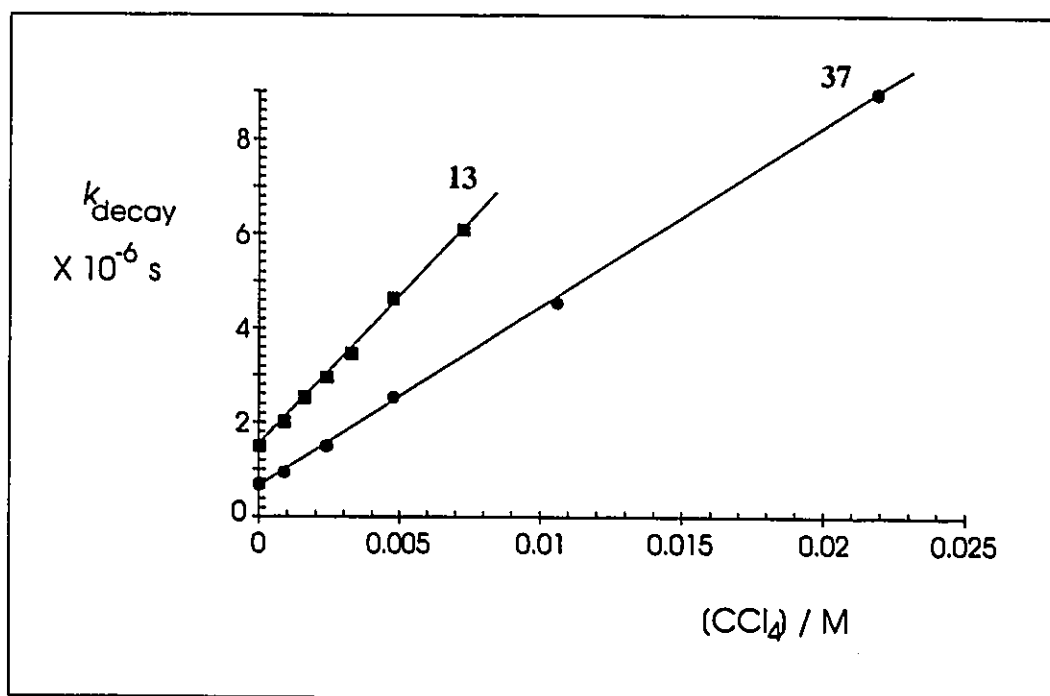
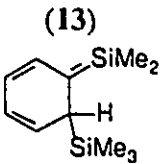
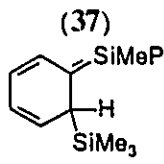
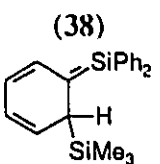


Figure 4.6 Plots of k_{decay} versus quencher concentration for reactions of 13 and 37 with CCl_4 in acetonitrile (ACN) solution at 23 ± 2 °C.

Table 4.5 Rate Constants for Reaction of Silatrienes **13**, **37**, and **38** with Carbon Tetrachloride (CCl₄) and Chloroform (CHCl₃) in Acetonitrile (ACN) and Isooctane (OCT) Solution at 23 ± 2°C.^a

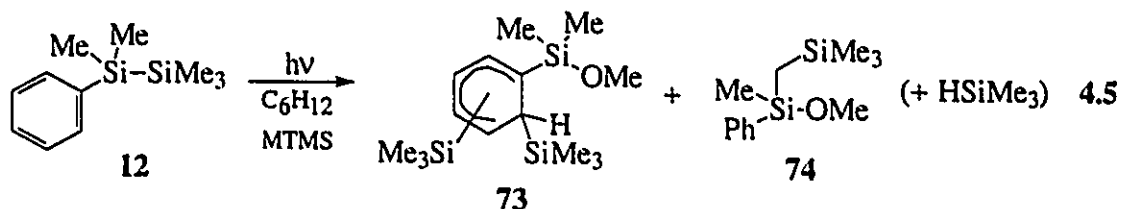
Reagent	Solvent	k_q (X 10 ⁻⁸ Ms)		
		(13) 	(37) 	(38) 
CCl ₄	ACN	6.4 ± 0.2	3.8 ± 0.1	b
	OCT	4.4 ± 0.1	1.6 ± 0.1	1.1 ± 0.1
CHCl ₃	OCT	0.011 ± 0.001	b	b

a. Errors reported as twice the standard deviation from least squares analysis of the data according to equation 4.2.

b. Not determined.

4.2.6 Reactions with Methoxytrimethylsilane (MTMS)

Steady-state photolysis (254 nm) of a deoxygenated 0.01 M solution of **12** in neat methoxytrimethylsilane (MTMS) affords a mixture of five products which we have tentatively identified by GC/MS (eq 4.5). Four of the products exhibit identical mass spectra (**73**) which are consistent with MTMS addition to silatriene **13**. Unfortunately, they could not be isolated due to their similar GC retention times. The fifth compound (**74**) exhibits a mass spectrum consistent with the addition of MTMS to 1-methyl-1-phenylsilene (**36**). The chemical yields of **73** and **74** were not determined quantitatively, however, their relative yields were similar to the silatriene and silene adducts in the acetone trapping experiments.



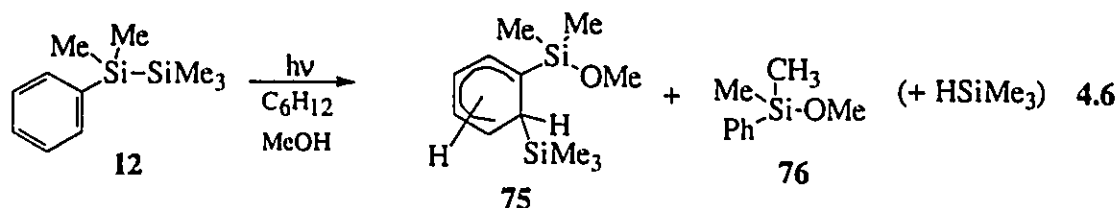
The addition of up to 0.6 M dried MTMS to a deoxygenated ACN solution of **12** caused no observable reduction in the lifetime of silatriene **13**. This allows an estimation of the upper limit for the rate constant for the reaction of **13** with MTMS as $k_q < 10^5 \text{ M}^{-1}\text{s}^{-1}$.

4.2.7 Silatriene Reactions with Alcohols

Steady-state photolysis (254 nm) of a deoxygenated 0.01 M cyclohexane solution of **12** containing 0.1 M methanol leads to the formation of a mixture of products which become increasingly more complex with greater conversion. Photolysis to *ca.* 10% conversion yields a mixture of five primary products detectable by capillary GC (see eq 4.6). One of the components, methoxydimethylphenylsilane (**76**), is the product of addition of methanol to 1-methyl-1-phenylsilene (**36**), and was formed in 15% yield. Analysis of the crude photolysate by GC/MS demonstrated that the other five compounds (**75**) were isomers consistent with the addition of methanol to silatriene **13**, and were formed in estimated yields of 8%, 38%, 7%, and 32% (assuming equal FID response factors). Photolysis of **12** to high conversion (*ca.* 90%) under these conditions leads to the formation of at least nine products owing, presumably, to the secondary photolysis of one or more of the primary photoproducts. GC/MS analysis of the crude photolysates obtained from irradiation of 0.01 M ACN solutions of **12** containing 0.5 M methanol and 0.5 M methanol-*Od* to *ca.* 50% conversion revealed a deuterium KIE of $k_{\text{H}}/k_{\text{D}} = 1.7 \pm 0.3$, based on the relative yields of the methanol and methanol-*Od* silatriene adducts (**75** and **75-d**). Similarly, photolysis of 0.001 M ACN solutions of **12** under similar conditions but containing 0.005 M methanol and 0.005 M methanol-*Od* afforded a deuterium KIE of $k_{\text{H}}/k_{\text{D}} = 1.4 \pm 0.2$.

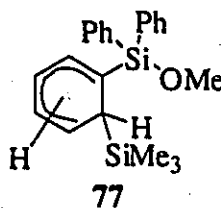
Steady-state photolysis of deoxygenated 0.005 M ACN (or cyclohexane) solutions containing between 0.001 and 0.20 M methanol to *ca.* 10% conversion did not result in detectable changes in the relative yields of the silatriene/methanol adducts (**75**) based on

GC/MS analysis of the crude mixtures. Variation of the GC injector port temperature between 150 and 250 °C resulted in no detectable changes in the adduct yields.



Steady-state of photolysis of ACN solutions of **12** in the presence of 2,2,2-trifluoroethanol (TFE), acetic acid (HOAc), ethylene glycol, and 1,3-propanediol under similar conditions affords complex mixtures in each case consistent with alcohol addition to silatriene **13** and simple silene **36**.

Irradiation of a deoxygenated 0.05 M C_6D_{12} solution of **35** in the presence of methanol (0.05 M) to *ca.* 40% conversion results in similar behaviour. The formation of at least four isomers (**77**) consistent with methanol addition to silatriene **38** is evident in the ^1H NMR spectrum of the crude photolysate due to the presence of trimethylsilyl (δ 0.2-0.1), allylic (δ 1.9-2.8), methoxy (δ 3.4-3.6), and vinyl (δ 4.7-6.4) absorptions (see Figure 4.7). GC/MS analysis of the crude mixture also reveals the formation of products which elute after the starting disilane and which exhibit mass spectra consistent with **77**.



The lifetimes of silatrienes **13**, **37**, **38**, and **50** are shortened by the addition of alcohols and acetic acid to solutions (ACN, OCT, or THF) of disilanes **12**, **34**, **35**, and **9**, respectively. In every case, the silatrienes decay with clean pseudo-first order decay kinetics and with no reduction in their initial yields in the presence of added alcohol. Plots of k_{decay} versus quencher concentration are linear for acetic acid (HOAc), acetic acid-*d* (DOAc), and 1,1,1-trifluoroethanol (TFE) in ACN and THF solutions. In these cases the data were analyzed according to equation 4.2. Representative quenching plots for the reaction of **38** with HOAc and TFE in ACN solution are shown in Figure 4.8.

Non-linear plots of k_{decay} versus quencher concentration are obtained for quenching by MeOH, MeOD, H₂O, D₂O, ethanol (EtOH), and *tert*-butyl alcohol (*t*-BuOH) in all three solvents, and by TFE and 1-pentanol (C₅H₁₁OH) in OCT solution. In these cases the data were analyzed according to equation 4.7 where $k_{\text{q}}^{(2)}$ is the third order rate constant corresponding to transient quenching with two molecules of quencher Q. Representative plots for the quenching of silatriene **37** with MeOH and MeOD in ACN solution are shown in Figure 4.9. Rate constants for quenching of **13**, **37**, **38**, and **50** by MeOH, MeOD, H₂O, D₂O, EtOH, *t*-BuOH, TFE, HOAc, and DOAc in ACN solution are listed in Tables 4.6 and 4.7, while rate constants for quenching of **13**, **37**, and **38** by MeOH, TFE, HOAc, and C₅H₁₁OH in OCT and THF solutions are listed in Table 4.8.

$$k_{\text{decay}} = k_0 + k_{\text{q}}[\text{Q}] + k_{\text{q}}^{(2)}[\text{Q}]^2 \quad 4.7$$

Bimolecular rate constants for reaction of silatriene **13** with ethylene glycol and 1,3-propanediol in ACN and THF solutions have been determined in a similar manner by NLFP methods. Non-linear plots of k_{decay} versus quencher concentration are obtained

for ethylene glycol in both solvents, while quenching by 1,3-propanediol yields linear plots. The rate constants were determined by analysis of the data according to equations 4.7 and 4.2, respectively, and are listed in Table 4.9.

In attempts to identify the third-order process which results in curvature in the alcohol quenching plots, we have measured the rate constant for methanol quenching of **13** in the presence of an acid (trifluoroacetic acid) and a base (triethylamine). The quenching plots for the reaction of **13** with methanol in the presence of 0.003 M or 0.017 M trifluoroacetic acid (TFA) and 0.002 M triethylamine show considerable upward curvature; the rate constants are listed in Table 4.10. The rate constant for TFA quenching of **13** is estimated to be $7 \times 10^7 \text{ M}^{-1}\text{s}^{-1}$, based on the lifetime of **13** in the presence of 0.017 M TFA in ACN solution.

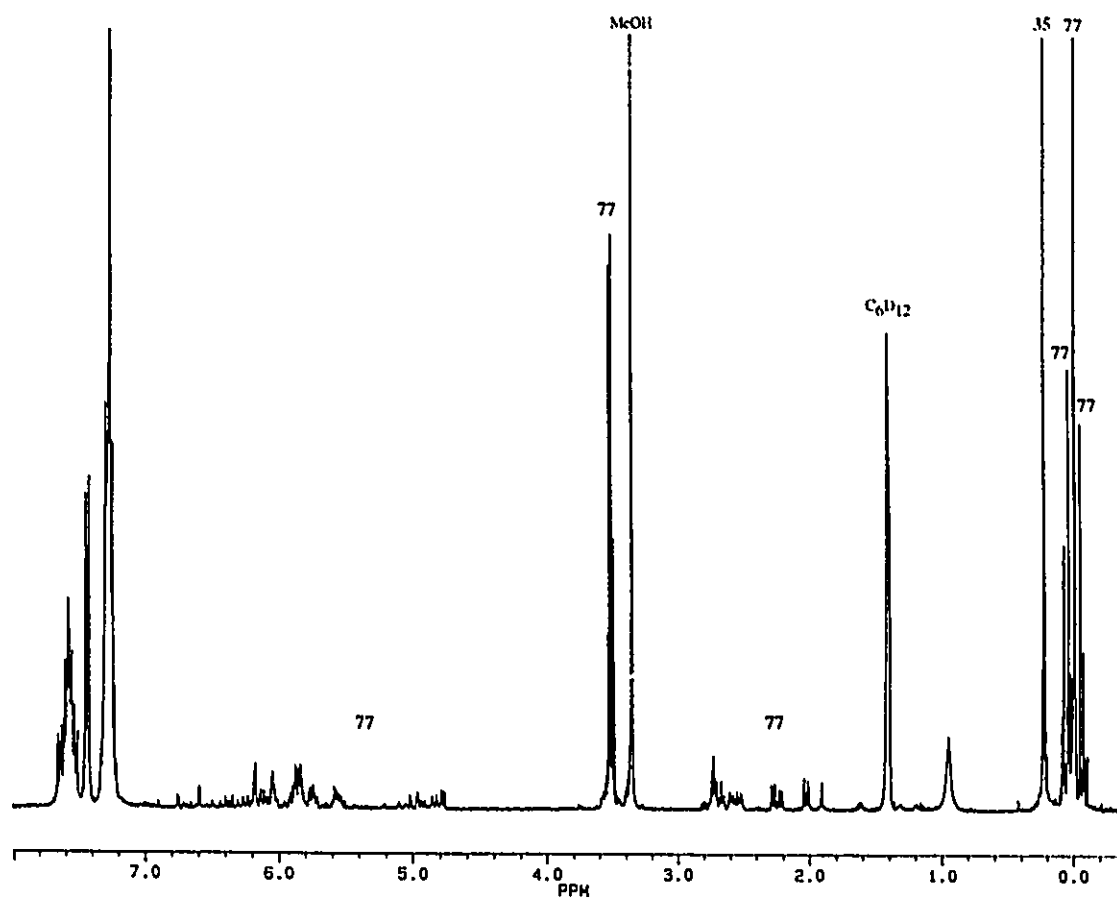


Figure 4.7 ^1H NMR spectrum of the crude mixture from photolysis of a deoxygenated 0.05 M C_6D_{12} solution of **35** containing 0.05 M methanol to *ca.* 50% conversion. Resonances due to protons in **35** and **77** are labelled.

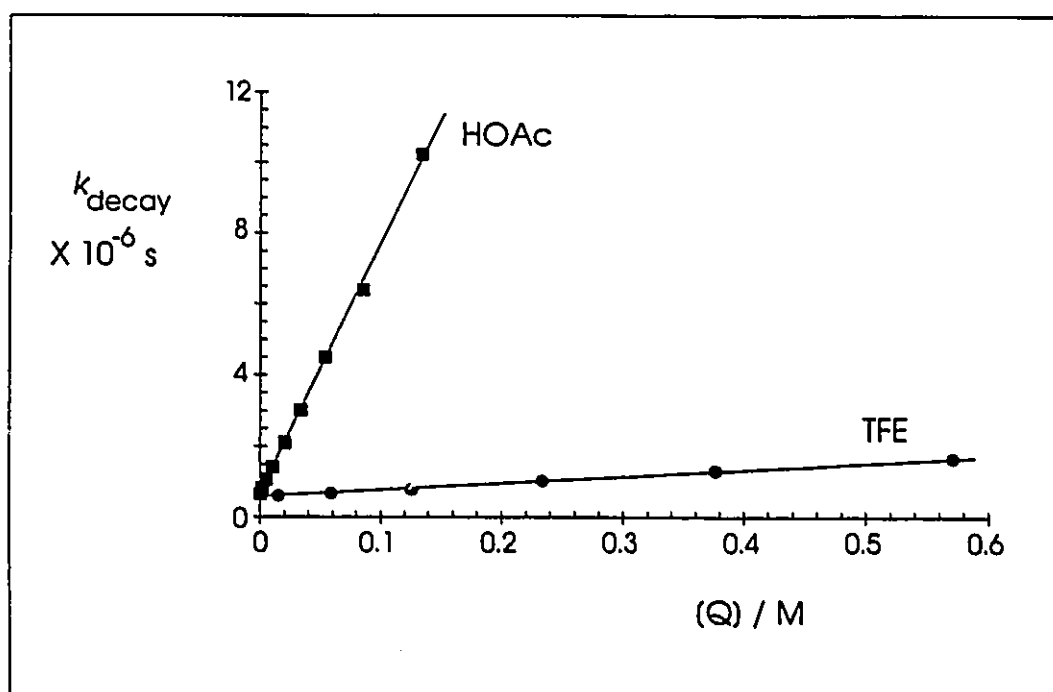


Figure 4.8 Plots of k_{decay} versus quencher concentration for quenching of **38** with acetic acid (HOAc) and trifluoroethanol (TFE) in acetonitrile (ACN) solution at 23 ± 2 °C.

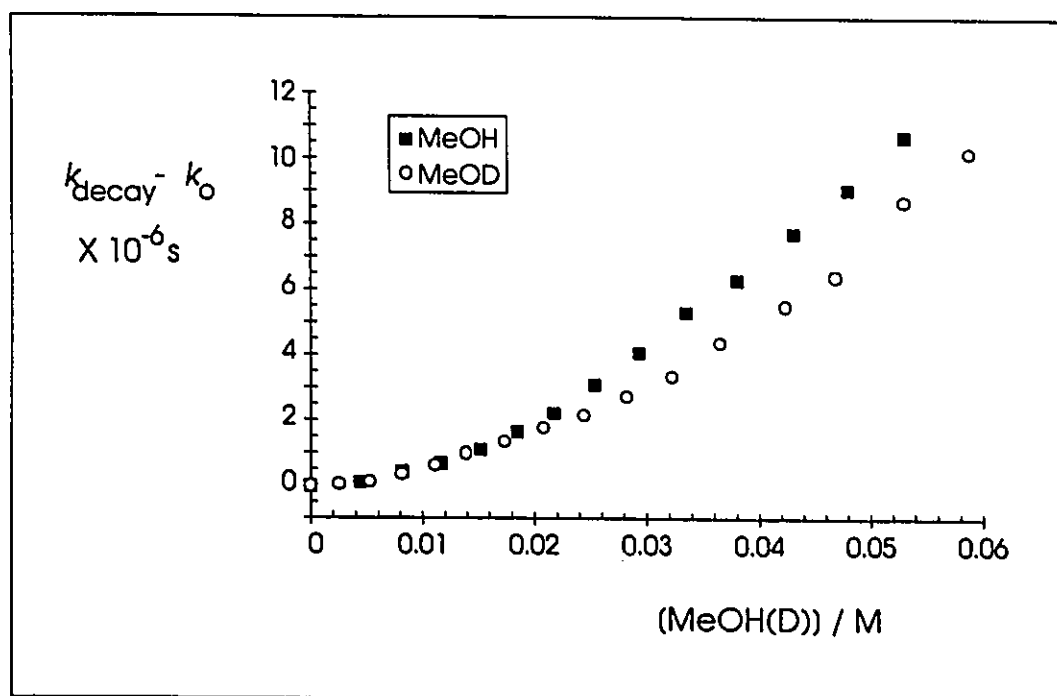

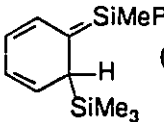
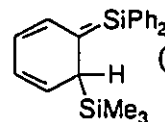


Figure 4.9 Plots of k_{decay} versus quencher concentration for reactions of 37 with methanol (MeOH) and methanol-*Od* (MeOD) in acetonitrile (ACN) solution at 23 ± 2 °C.

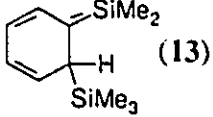
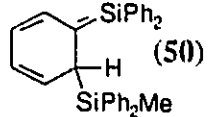
Table 4.6 Rate Constants for Reaction of Silatrienes **13**, **37**, and **38** with Methanol (MeOH), Methanol-*Od* (MeOD), Trifluoroethanol (TFE), Acetic Acid (HOAc), and Acetic Acid-*d* (DOAc) in ACN Solution at 23 ± 2 °C. ^a

Reagent		 (13)	 (37)	 (38)
MeOH	$10^{-8}k_q$	2.3 ± 0.7	0.60 ± 0.25	0.17 ± 0.10
	$10^{-8}k_q^{(2)}$	49 ± 10	28 ± 5	11 ± 4
MeOD	$10^{-8}k_q$	1.2 ± 0.2	0.34 ± 0.08	0.09 ± 0.04
	$10^{-8}k_q^{(2)}$	51 ± 4	23 ± 2	7.9 ± 0.7
TFE	$10^{-8}k_q$	0.236 ± 0.004	0.056 ± 0.001	0.017 ± 0.001
HOAc	$10^{-8}k_q$	2.9 ± 0.1	1.41 ± 0.05	0.70 ± 0.02
DOAc	$10^{-8}k_q$	2.8 ± 0.1	b	b

a. Errors are reported as twice the standard deviation from least squares analysis of the data according to equations 4.2 or 4.7.

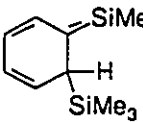


b. Not determined.

Table 4.7 Rate Constants for Quenching of Silatrienes **13** and **50** with H₂O, D₂O, Methanol (MeOH), Ethanol (EtOH), and *tert*-Butyl Alcohol (*t*-BuOH) in Acetonitrile (ACN) Solution at 23 ± 2 °C.^a

Reagent		 (13)	 (50)
H ₂ O	10 ⁻⁸ k _q	4.4 ± 1.3	2.2 ± 0.3
	10 ⁻⁸ k _q ⁽²⁾	46 ± 60	13 ± 5
D ₂ O	10 ⁻⁸ k _q	2.6 ± 0.8	1.3 ± 0.2
	10 ⁻⁸ k _q ⁽²⁾	71 ± 36	21 ± 5
MeOH	10 ⁻⁸ k _q	2.3 ± 0.7	1.7 ± 0.3
	10 ⁻⁸ k _q ⁽²⁾	49 ± 10	7 ± 7
EtOH	10 ⁻⁸ k _q	1.5 ± 0.3	0.67 ± 0.09
	10 ⁻⁸ k _q ⁽²⁾	32 ± 6	9.5 ± 1.6
<i>t</i> -BuOH	10 ⁻⁸ k _q	0.37 ± 0.08	0.25 ± 0.04
	10 ⁻⁸ k _q ⁽²⁾	1 ± 1	2.1 ± 0.4

a. Errors are reported as twice the standard deviation from least squares analysis of the data according to equation 4.7.

Table 4.8 Rate Constants for Reaction of Silatrienes **13**, **37**, and **38** with MeOH, 1-Pentanol (C₅H₁₁OH), Trifluoroethanol (TFE), and Acetic Acid (HOAc) in THF and OCT Solution.^a

Reagent	Solvent		 (13)	 (37)	 (38)
			k_q		
MeOH	THF	k_q	1.2 ± 0.1	0.95 ± 0.05	0.7 ± 0.1
		$k_q^{(2)}$	12 ± 2	11 ± 1	6.4 ± 1.3
	OCT	k_q	3.0 ± 0.8	1.8 ± 0.5	1.1 ± 0.4
		$k_q^{(2)}$	130 ± 20	100 ± 15	64 ± 12
C ₅ H ₁₁ OH	OCT	k_q	1.9 ± 0.7	1.2 ± 0.3	0.5 ± 0.2
		$k_q^{(2)}$	116 ± 14	80 ± 8	54 ± 5
TFE	THF	k_q	0.168 ± 0.003	0.063 ± 0.002	0.051 ± 0.003
		$k_q^{(2)}$			
	OCT	k_q	2.3 ± 0.6	b	b
		$k_q^{(2)}$	88 ± 14	b	b
HOAc	THF	k_q	0.61 ± 0.01	b	b

a. Second- and third-order rate constants are reported in units of 10⁸ M⁻¹s⁻¹ and 10⁸ M⁻²s⁻², respectively. Errors are reported as twice the standard deviation of least squares analysis of the data according to equations 4.2 or 4.7.

b. Not determined.

Table 4.9 Rate Constants for Reaction of Silatriene **13** with Ethylene Glycol and 1,3-Propanediol in Acetonitrile (ACN) and Tetrahydrofuran (THF) Solution at 23 ± 2 °C.^a

Reagent		ACN	THF
HOCH ₂ CH ₂ OH	$10^{-8}k_q$	0.6 ± 0.4	0.87 ± 0.16
	$10^{-8}k_q^{(2)}$	80 ± 10	8.0 ± 1.6
HOCH ₂ CH ₂ CH ₂ OH	$10^{-8}k_q$	16.9 ± 0.8	3.2 ± 0.1

- a. Errors are reported as twice the standard deviation of least squares analysis of the data according to equations 4.2 or 4.7.

Table 4.10 Rate Constants for Quenching of Silatriene **13** with Methanol (MeOH) in Acetonitrile (ACN) Solution in the Presence of Trifluoroacetic Acid (TFA) or Triethylamine at 23 ± 2 °C.^a

Solvent	k_q (X 10^{-8} Ms)	$k_q^{(2)}$ (X 10^{-8} M ² s ²)
ACN	2.3 ± 0.7	49 ± 10
0.003 M TFA / ACN	2.0 ± 0.2	83 ± 5
0.017 M TFA / ACN	1.2 ± 0.5	100 ± 20
0.002 M Et ₃ N / ACN	1.8 ± 0.5	80 ± 10

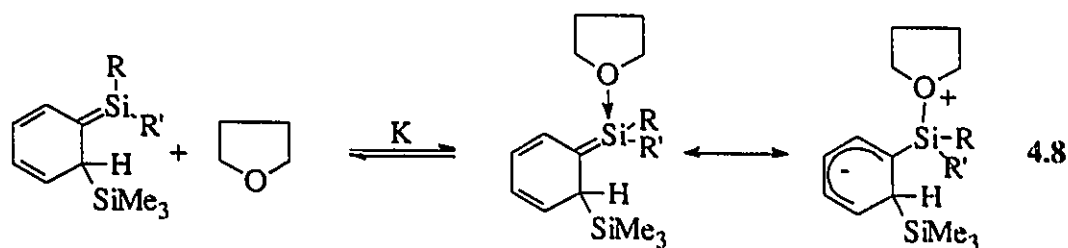
- a. Errors are reported as twice the standard deviation of least squares analysis of the data according to equation 4.7.

4.3 Discussion

The transient UV absorption spectra of silatrienes **13**, **37**, and **38** are virtually identical in ACN and OCT solutions in each case. However, the absorption maximum of **13** shifts from 425 nm in ACN and OCT to 460 nm in THF solution (Figure 4.1). We attribute this shift to complexation of the silatriene with THF solvent molecules (eq 4.8) analogous to the silene/THF complex (**19**) reported by Wiberg.⁵² The THF/silatriene complex may be represented as a Lewis acid complex or as a formal zwitterion. Evidence for this complex formation is provided by the fact that transient spectra recorded in THF/ACN mixtures containing low concentrations of THF are *broadened* with respect to those recorded in either pure ACN or THF. The spectrum recorded in 5% THF/ACN can be interpreted as arising from roughly equal amounts of free and complexed silatriene (see Figure 4.2). The equilibrium constant for THF complex formation with **13** in ACN solution is estimated to be *ca.* 1.6 M^{-1} assuming that the extinction coefficients of the free and complexed silatriene are similar. The transient absorption due to silatriene **37** is red-shifted by only 10 nm in THF solution ($\lambda_{\text{max}} = 470 \text{ nm}$) compared to ACN and OCT solutions ($\lambda_{\text{max}} = 460 \text{ nm}$), while the absorption spectrum of silatriene **38** ($\lambda_{\text{max}} = 490 \text{ nm}$) is the same in all three solvents. These observations indicate that increasing phenyl substitution at the trivalent silicon atom leads to a smaller equilibrium constant for complex formation or leads to a "looser" complex.

The variations in the rate constants for quenching of **13**, **37** and **38** by acetone and oxygen in ACN and THF solution indicate that the reactions involve the free silene in each case, as has been suggested previously by Wiberg.⁵² The rates of reaction of **13** and **37** with acetone are *ca.* 3 and 2 times slower in THF versus ACN solution, respectively, while

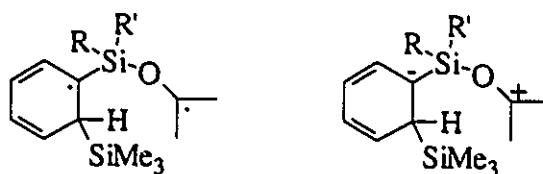
the rate constant for quenching of **13** by oxygen in THF is about one-half that in ACN solution, indicative of THF complexation of both silatrienes. The rate constants for quenching of silatriene **38** by acetone are the same in ACN and THF, consistent with the absence of spectral shifts in the absorption spectrum of **38** in THF solution. These results support the conclusion that the equilibrium constant for silatriene/THF complex formation decreases with increasing phenyl substitution.



The reduction in the rate constants for quenching of **13** in THF solution are not as large as expected based on the estimated equilibrium constant for complex formation. Application of a correction term for the equilibrium formation of the silatriene/THF complex $(K_{\text{THF}}[\text{THF}] + 1)^{-1}$ leads to the prediction that the rate constant for acetone quenching should be *ca.* 20 times slower in THF versus ACN solution. The main reason for this discrepancy is that the equilibrium constant used in this calculation is only a crude estimate based on a single transient UV absorption spectrum (Figure 4.2). Another factor to consider is the effect of solvent polarity on the reaction of silatrienes with acetone and oxygen. The reactions of silatrienes with acetone are significantly faster in OCT ($\epsilon = 1.94$)¹⁴⁴ than in ACN ($\epsilon = 35.94$)¹⁴⁴ solution which is ascribable to stabilization of the carbonyl *n*-orbital (and/or the silatriene) in the more polar solvent.¹⁴⁵ THF ($\epsilon = 7.58$)¹⁴⁴

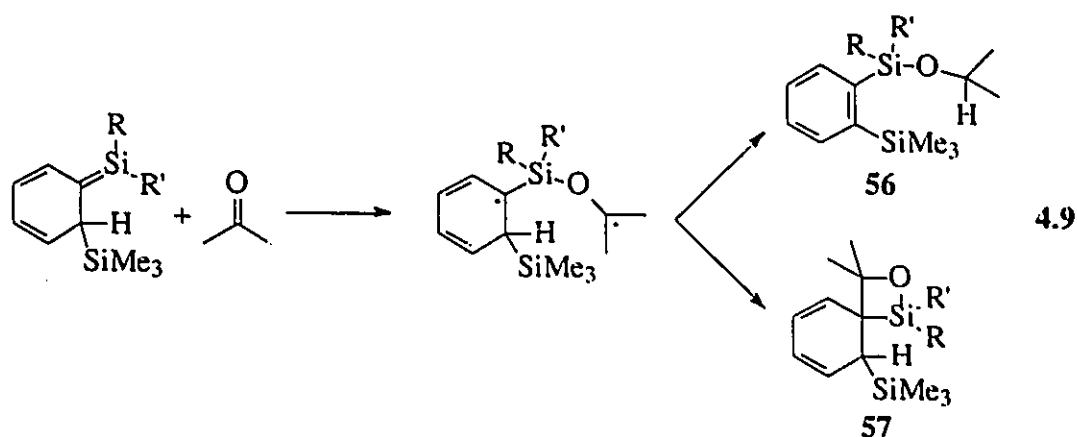
is less polar than ACN; thus, it is conceivable that the reduction in rate constant due to complex formation is partially offset by an increase due to lower solvent polarity.

The reactions of silatrienes **13**, **37**, and **38** with acetone are much more complex than that reported previously for **13**.¹⁰² The products of these reactions, ethers **56** and siloxetanes **57**, suggest that they proceed in a stepwise manner involving biradical or zwitterionic intermediates. Additional evidence for a stepwise mechanism comes from the



lack of observable kinetic isotope effects (KIE) on the reactions of **13-d₅** with acetone in ACN or OCT solutions, which indicates that migration of the allylic hydrogen (or deuterium) is not involved in the rate-determining step for ether formation. The absence of a detectable KIE on the reaction of **13** with acetone-*d*₆ ($k_{\text{H}}/k_{\text{D}} = 1.0 \pm 0.1$ in OCT) is not consistent with the formation of a zwitterionic intermediate with positive charge on the ketyl carbon. Cation formation should be susceptible to significant secondary KIE's due to the cumulative effects of the six alpha deuteriums;¹⁴⁶ however, the magnitude of the secondary KIE for radical formation under these conditions is not known. More convincing evidence for biradical intermediates is the fact that acetone quenching of silatrienes is faster in OCT than in ACN solution. The rate-determining formation of a polar intermediate would be expected to be faster in a polar solvent such as ACN. Therefore, the mechanism most likely involves initial rate-determining nucleophilic attack at silicon by the carbonyl oxygen atom to yield a biradical intermediate which cyclizes to

the corresponding siloxetane (57) or undergoes H-migration to yield the corresponding ether (56) (eq 4.9).



The driving force for the reactions between silatrienes and carbonyl compounds is, presumably, the formation of a strong Si-O bond (BDE = 120 kcal/mol;⁶⁸ see Table 1.3). Leigh and coworkers have recently demonstrated that the rate of reaction of 1,1-diphenylsilene (11) with carbonyl compounds correlates roughly with the calculated (AM1) energies of the carbonyl nonbonding molecular orbitals or with the *n*-ionization potentials (IP).⁶³ The rate of reaction of 13 with ethyl acetate (*n*-IP = 10.4 eV)¹⁴⁷ is *ca.* 200 times slower than reaction with acetone (*n*-IP = 9.7 eV)¹⁴⁸ in ACN solution, consistent with these observations. Similar results have been reported by Ishikawa and coworkers,¹⁰² who noted that methyl acetate is a substantially less efficient trap for 13 than acetone, on the basis of the results of steady-state photolysis of 12 in the presence of a slight excess of trapping agent.

The rate constants for acetone quenching of silatrienes are dependent upon the degree of phenyl substitution. In all three solvents, the rate constants for reaction of

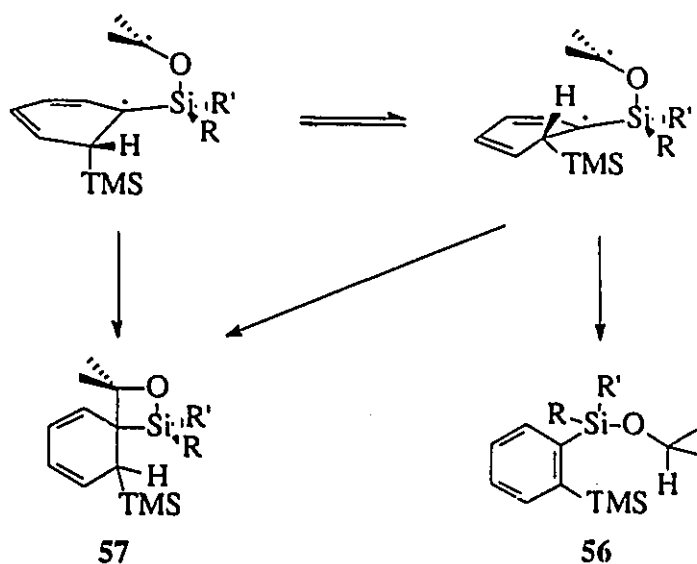
acetone with silatrienes **13**, **37**, and **38** decrease by a factor of 2-8 throughout the series **13** > **37** > **38**. Similar substituent effects on the rate constants for silatriene quenching by DMB, oxygen, alkyl halides, and alcohols are observed. These results support the conclusion that increasing phenyl substitution at trivalent silicon slows down the rate of attack of the silatriene trapping reagent.

The variation in the relative yields of the silatriene/acetone adducts (**56** and **57**) from photolysis of the three disilanes is quite intriguing. The photolysis of **35** yields about twice as much siloxetane **57c** as silyl ether **56c**, whereas the formation of ethers **56a,b** predominates in the photolyses of **12** and **34**. These differences can be ascribed to conformational effects in the biradical intermediate formed initially from nucleophilic attack of the carbonyl oxygen atom on the silatriene (Scheme 4.1). In the two possible biradical conformers, the allylic hydrogen atom or the trimethylsilyl group occupy a pseudo-axial position. Both conformers can generate the corresponding siloxetane (**57**); however, only the conformer with the axial allylic hydrogen atom can yield the silyl ether adduct (**56**).^{149,150} Increasing the phenyl substitution tends to force the trimethylsilyl group into the pseudo-axial position, thereby inhibiting silyl ether formation.

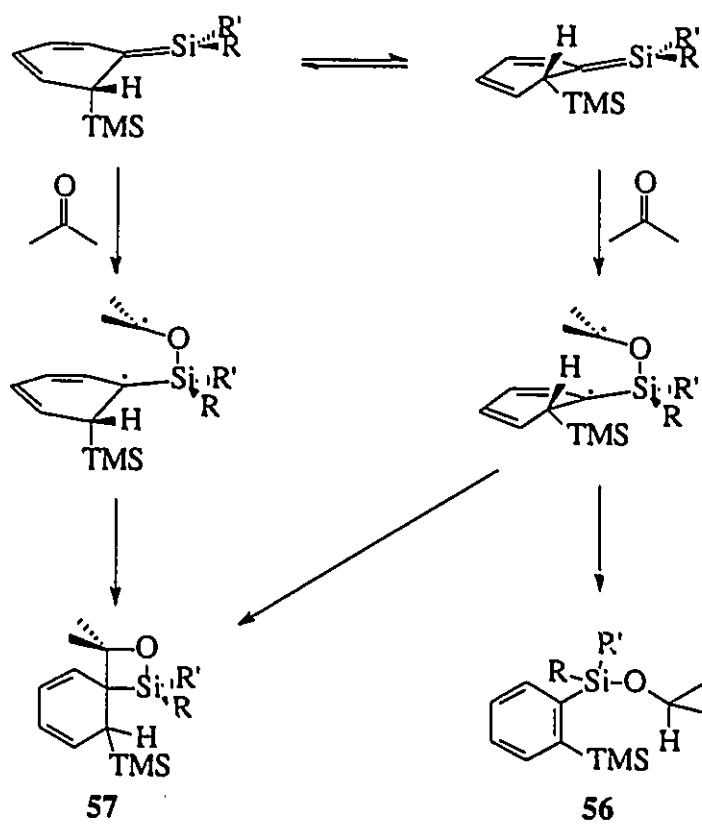
It is possible that the singlet biradicals in Scheme 4.1 are too short-lived to attain conformational equilibrium. Alternatively, the differences in the siloxetane and silyl ether yields may be ascribable to conformational effects in the silatriene *prior* to attack of the acetone molecule (Scheme 4.2). In this case, the silatriene conformer with the trimethylsilyl group in the pseudo-axial position would be expected to yield mainly the siloxetane (**57**), while the silatriene conformer with the pseudo-axial allylic hydrogen atom would yield both siloxetane (**57**) and silyl ether (**56**). Increasing steric bulk at the trivalent

silicon atom in the silatriene should favour the pseudo-axial trimethylsilyl conformation and lead to higher yields of the siloxetane adduct (**57**).

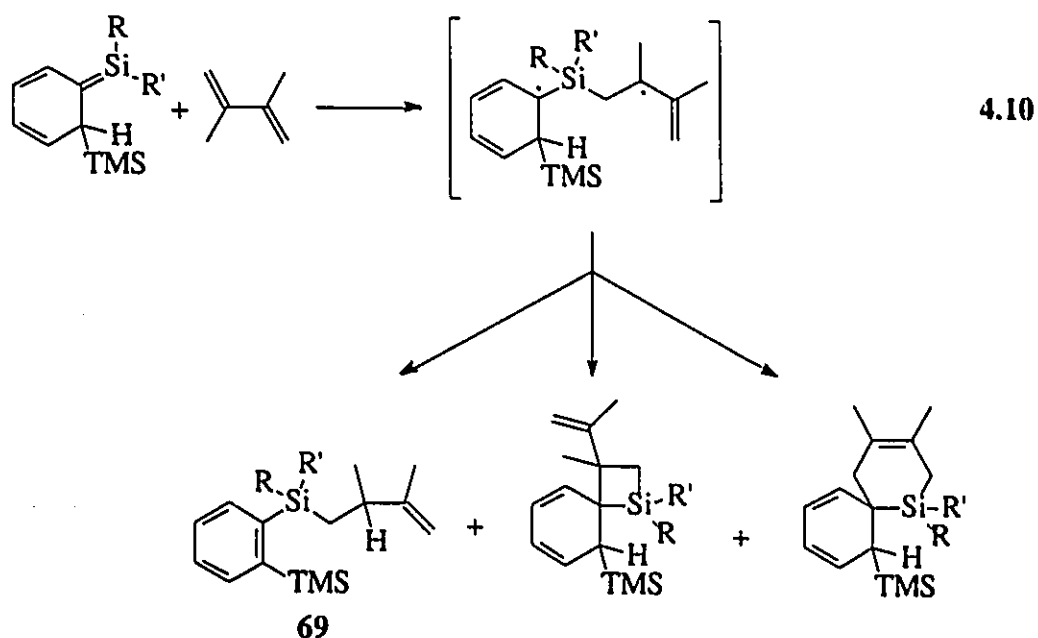
Scheme 4.1 Biradical Conformational Effects on Silatriene/Acetone Adduct Yields



The complex product mixtures obtained from the photolyses of disilanes **12**, **34**, and **35** in the presence of DMB indicate that the reactions of the corresponding silatrienes with alkenes also proceed in a stepwise fashion. It has been suggested previously that simple silenes react with dienes by a stepwise mechanism due to the common formation of both [4+2]- and ene-addition products.^{1,5} The major product from the photolyses of **12** and **34** is the corresponding ene adduct **69** along with one or two minor products. However,

Scheme 4.2 Silatriene Conformational Effects on Silatriene/Acetone Adduct Yields

69c is formed in much lower yield from **35** and at least five other products, of which at least one possesses cyclohexadienyl protons, are detected. The other unidentified products presumably arise from cyclization of a biradical intermediate analogous to that formed in the acetone trapping reaction (eq 4.10). The yields of the cyclized adducts are highest from **35** indicating that conformational effects on the biradical reactivity are important, similar to that proposed for acetone quenching. Additional evidence for a stepwise mechanism is provided by the lack of an observable KIE on the reaction of DMB with **13-d5**.



In general, the rates of silatriene quenching by DMB are a factor of *ca.* 20-40 times slower than silatriene quenching by acetone. This is presumably due to the smaller driving force associated with the formation of a silicon-carbon bond (BDE = 90 kcal/mol)⁶⁸ versus a silicon-oxygen bond. The rate of cyclohexene quenching of **13** in ACN solution

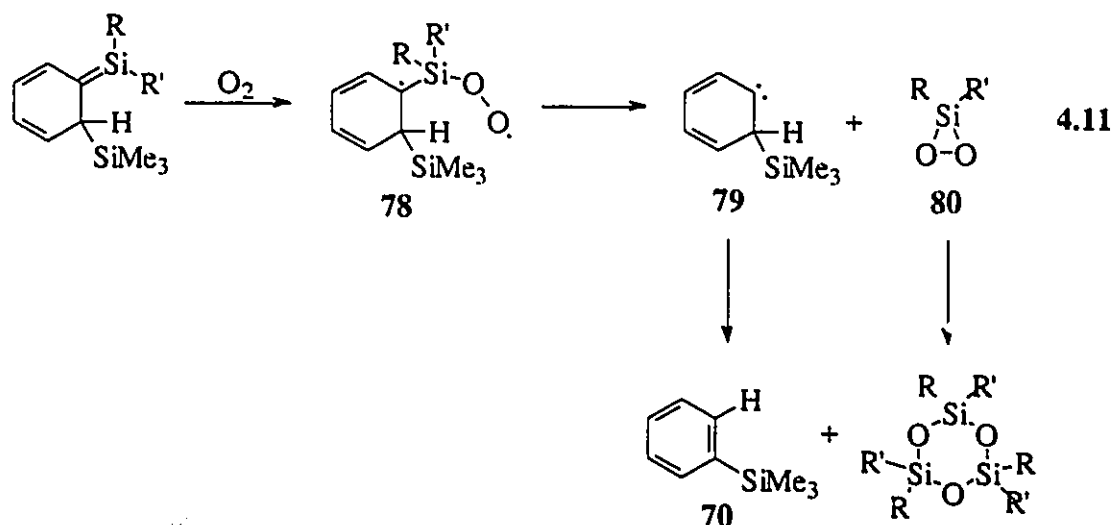
is a factor of 100 times slower than the rate of reaction of DMB with 13 in OCT solution. While solvent polarity will play some role in accounting for the large differences in the two rate constants, it is more likely that they are ascribable to steric effects on the attack of the two alkenes on the silatriene or to the relative stabilities of the biradical intermediates. Initial attack on the silatriene by cyclohexene is expected to be slower than DMB due to greater alkyl substitution on the carbon-carbon double bond. Statistical factors may also be important since DMB contains two carbon-carbon double bonds compared to one in cyclohexene. Furthermore, the reaction of silatrienes with cyclohexene generates a secondary alkyl radical centre in the cyclohexyl moiety while DMB yields a much more stable allylic radical (eq 4.10).

It is generally accepted that silenes are highly reactive toward oxygen based on the oxygen-sensitivity of stabilized silenes,^{45,46} the trapping of simple silenes by oxygen at high temperatures,^{64,65} and the reaction of simple silenes with oxygen in frozen matrices.⁶⁶ However, there is no evidence that simple or stabilized silenes react with molecular oxygen at measurable rates by NLFP techniques ($k > 10^5 \text{ M}^{-1}\text{s}^{-1}$) in fluid solution at room temperature. Furthermore, our group has recently reported that 1,1-diphenylsilene (11) does not react with oxygen at a measurable rate.⁶³ Thus, the demonstration that silatrienes react rapidly with oxygen with rate constants in the 10^8 - $10^9 \text{ M}^{-1}\text{s}^{-1}$ range^{14,108,109} (Table 4.4) is quite remarkable. The presence of oxygen has no effect on the initial yields of the silatrienes, indicating that the silatrienes, not the disilane excited states, are the reactive species with oxygen.

The products from disilane photolyses in the presence of oxygen are those consistent with formal silylene ($\text{R}'\text{RSi:}$) extrusion to yield phenyltrimethylsilane, although the reaction clearly does not proceed via this mechanism. The products ultimately arise from one or

more intermediates formed after initial attack of oxygen on the silatriene. By analogy with the proposed stepwise mechanisms for silatriene reactions with carbonyl compounds and alkenes, we suggest that the reaction proceeds by a mechanism involving the initial formation of biradical **78** (eq 4.11). The cyclohexadienyl moiety stabilizes **78** by conjugation with one of the radical centres which accounts for the high reactivity of silatrienes with oxygen compared to simple silenes.⁶³ Additional evidence for a stepwise mechanism is provided by the lack of an observable deuterium KIE on the reaction of oxygen with **13-*d*₅**. The small solvent dependence on the rate constants for silatriene quenching by oxygen is also consistent with the formation of a non-polar intermediate. In fact, silatriene quenching by oxygen is one of the few reactions that is faster in ACN than in OCT solution. It is proposed that biradical **78** reacts by the loss of the corresponding dioxasilirane to yield a cyclohexadienyl-carbene intermediate (**79**) which gives **70** following [1,2]-hydrogen or trimethylsilyl migration. The dioxasilirane (**80**) can be expected to yield the corresponding silanone upon thermal decomposition by analogy with the behaviour of carbonyl oxides.¹⁵¹ Dimethylsilanone is itself a highly reactive species which is known to yield silanone oligomers^{1,11,12,64,152} such as those reported in this case. The photolysis of **12-*d*₅** under similar conditions yields **70-*d*₅** with no loss of deuterium which effectively rules out the possibility that **70** arises via abstraction of hydrogen atoms from solvent by trimethylsilylphenyl radicals. We do not have any explicit evidence for the formation of any intermediates other than the silatrienes; thus, we are unable to rule out the possibility of the involvement of other intermediates such as the corresponding siladioxetane or hydroperoxide. However, it seems unlikely that the siladioxetane or hydroperoxide would yield **70** and silanone-derived products upon

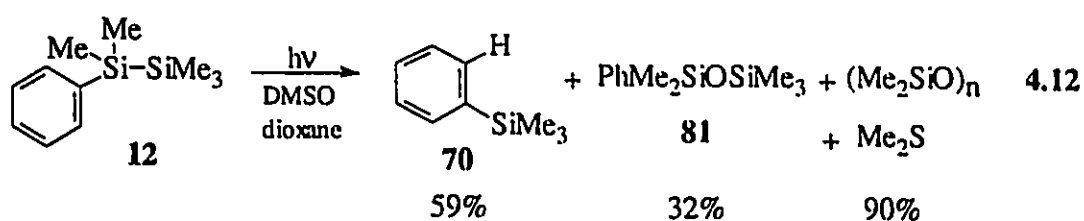
thermal decomposition. Furthermore, we have not been able to detect 2-trimethylsilylphenol as a product in the crude photolysates.



Gaspar and coworkers have previously reported a rate constant for oxygen quenching of 13^{14} which is a factor of four times higher than our value. However, our rate constants were determined from the silatriene decay rates for a minimum of five different oxygen concentrations, and are likely more accurate.

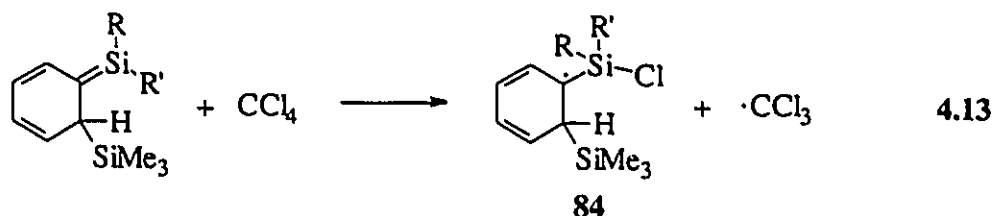
It is interesting to note that Weber and coworkers have reported that photolysis of **12** in the presence of dimethyl sulfoxide (DMSO) also yields **70** and dimethylsilanone-derived oligomers (eq 4.12).^{153,154} While they initially considered a mechanism similar to that shown in equation 4.10 involving carbene **78**, it was ruled out in favour of one involving direct nucleophilic attack by DMSO on the disilane excited singlet state. Their rationale for excluding the mechanism involving the intermediacy of **78** was the fact that photolysis of pentamethyl(4-tolyl)disilane (**82**) under the same conditions yields 4-trimethylsilyl-toluene (**83**), and none of the meta-substituted isomer. Weber suggested that the allylic

hydrogen in carbene **78** should undergo more facile [1,2] migration than the trimethylsilyl group to yield 3-trimethylsilyltoluene if this mechanism were valid.^{153,154} However, [1,2]-silyl migrations are known to occur in α -silylcarbenes (eq 1.18)^{49,50} and in β -trialkylsilylaminyll radicals.¹⁵⁵ Ando has successfully exploited facile [1,2]-silyl migrations from silicon to carbene centres in the synthesis of numerous silenes.^{49,50} Furthermore, the silicon-carbon bond (BDE = 90 kcal/mol) is significantly weaker than the carbon-hydrogen bond (BDE = 105 kcal/mol).⁶⁸ Thus, the possibility that **77** undergoes preferential [1,2]-trimethylsilyl migration cannot be ruled out. The mechanism involving DMSO quenching of the disilane excited singlet state can be excluded since the excited singlet state lifetime of **12** is only *ca.* 30 ps in solution at room temperature.⁸² NLFP experiments have shown that DMSO quenches silatriene **13** at close to the diffusion-controlled rate in dioxane solution at room temperature ($k_q = 3.0 \times 10^9 \text{ M}^{-1}\text{s}^{-1}$), with no reduction in its initial yield. We initially suspected that disiloxane **81** arose from the reaction of dimethylphenyl- and trimethylsilyl radicals with DMSO; however, this reaction is quite slow in the case of *tert*-butyldiphenylsilyl radicals (**41**) ($k_q < 10^5 \text{ M}^{-1}\text{s}^{-1}$).



Although Brook has reported that stabilized silenes "get hot in carbon tetrachloride or chloroform",⁵ there are no reports of similar reactions of transient silenes. Silatrienes **13**, **37**, and **38** are quenched at substantial rates by carbon tetrachloride in ACN and OCT solution. The trend of decreasing rate constant with increasing phenyl substitution is the

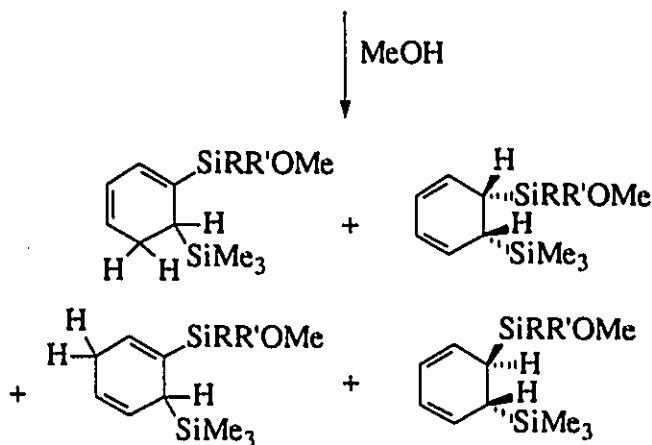
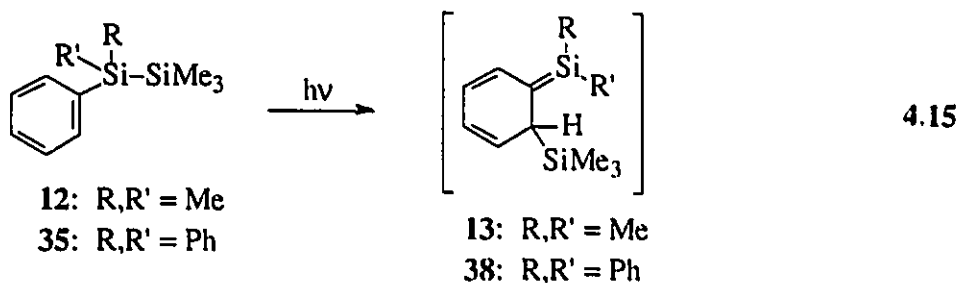
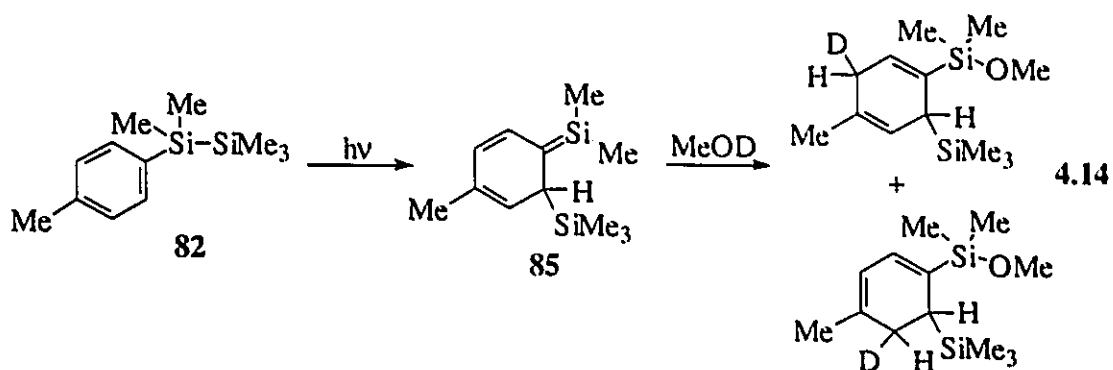
same as that observed for the other trapping reagents employed in this study. The product mixtures obtained from the photolysis of **12** or **35** in the presence of CCl_4 are so complex that we are unable to identify many of the products and determine the course of the reaction. The rate constants are slightly faster in ACN versus OCT solution indicating that polar intermediates *may* be involved in these reactions. However, it is also reasonable to suggest, by analogy with the oxygen reaction, that the first step of the reaction is chlorine atom abstraction to yield radical intermediate **84** (eq 4.13).



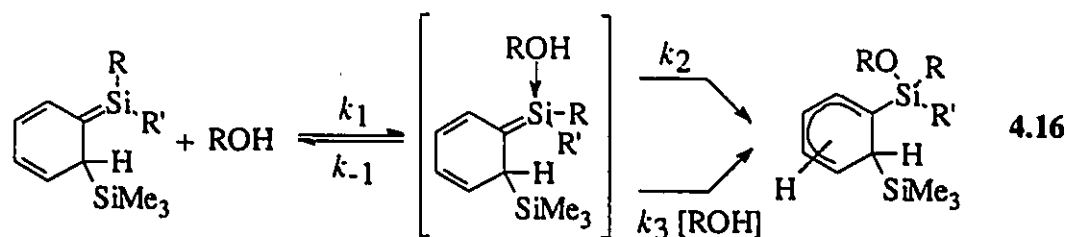
Although the addition of alcohols to silenes is often considered a "classic" silene trapping reaction, very little is known about the mechanism. Wiberg has suggested a stepwise mechanism involving rate-determining nucleophilic attack by the alcohol oxygen atom² (eq 1.14), while Sakurai has proposed a similar mechanism involving oxygen atom attack followed by rate-determining proton transfer (eq 1.15).⁵⁸ Conversely, Jones has reported the stereospecific syn-addition of methanol to a silene, suggesting a concerted addition in this case.³⁰

The photolysis of aryldisilanes in the presence of alcohols generally leads to the formation of several isomers consistent with alcohol addition to the corresponding silatrienes.^{89,94,95} Ishikawa has reported that the photolysis of benzene solutions of pentamethyl(4-tolyl)disilane (**82**) in the presence of methanol-*Od* affords two isomers, consistent with 1,4- and 1,6-addition of the alcohol to silatriene **85** (eq 4.14).⁹⁵ Curiously, the products arising from 1,2-alcohol addition were not detected in this case.

Steady-state photolysis of cyclohexane solutions of pentamethylphenyldisilane (**12**) or 1,1,1-trimethyl-2,2,2-triphenyldisilane (**35**) containing 0.1 M (or 0.05 M) methanol to *ca.* 10% conversion affords four products, based on GC and GC/MS analysis, consistent with alcohol addition to silatrienes **13** and **39**, respectively (eq 4.15).



The curved quenching plots for water, methanol, ethanol, *tert*-butanol, and ethylene glycol reactions with silatrienes **13**, **37**, **38**, and **50** (Figure 4.9) in ACN and THF solutions are consistent with a stepwise addition mechanism involving rapid, reversible formation of an alcohol/silatriene complex, followed by competing intracomplex and bimolecular proton transfer, the latter involving a second molecule of alcohol (eq 4.16). Application of the equilibrium assumption to the alcohol/silatriene complex in equation 4.16 leads to the expression for the pseudo-first order rate constant for decay of the silatriene (k_{decay}) shown in equation 4.17, where k_0 is the rate constant for decay in the absence of added trapping agent and the other rate constants correspond to those defined in equation 4.16. Thus, the second- and third-order rate constants listed in Tables 4.6, 4.7, and 4.8 can be equated with k_1k_2/k_{-1} and k_1k_3/k_{-1} , respectively. The general trend in the data listed in Table 4.6 is that both k_q and $k_q^{(2)}$ decrease throughout the series $\text{H}_2\text{O} > \text{MeOH} > \text{EtOH} > t\text{-BuOH}$. Although the acidities of these alcohols follows this trend, it appears that the nucleophilicity of the alcohol may have a significant effect on the equilibrium constant for silatriene/alcohol complex formation.



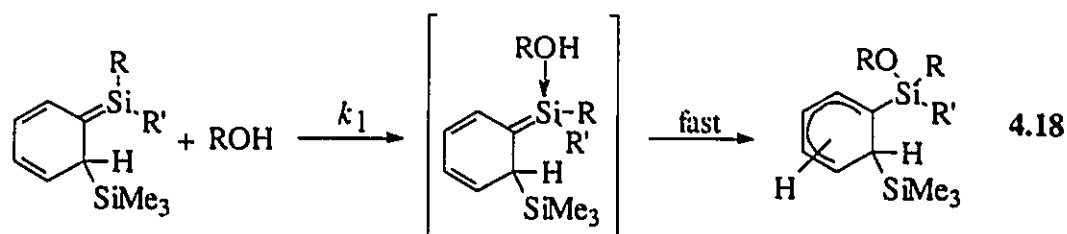
$$k_{\text{decay}} = k_0 + (k_1k_2/k_{-1})[\text{ROH}] + (k_1k_3/k_{-1})[\text{ROH}]^2 \quad 4.17$$

The second-order component of the reactions of silatrienes **13**, **37**, and **38** with methanol in ACN solution are subject to a small kinetic isotope effect (KIE) of $k_{\text{H}}/k_{\text{D}} \approx 1.8$ - 1.9 . Likewise, the second-order component of the reactions of **13** and **50** with water in ACN solution are subject to a KIE of $k_{\text{H}}/k_{\text{D}} = 1.7$. The magnitude of the KIE on the second-order rate constant for the reaction of methanol with **13** was confirmed by GC/MS analysis of the crude mixture obtained from steady-state photolysis of **12** in the presence of equimolar amounts of methanol and methanol-*O**d* (at low total alcohol concentration where the second-order process predominates) which revealed $k_{\text{H}}/k_{\text{D}} = 1.4 \pm 0.2$. These results provide the first clear examples that proton transfer is involved in the rate-determining step in the reactions of alcohols with silicon-carbon double bonds. Unfortunately, due to the comparatively large errors associated with the determination of the third-order rate constants, the KIE's on these rate constants are not detectable; however, steady-state photolysis of **12** under similar conditions to those employed above but at high total alcohol concentration, where the third-order process should predominate, revealed a KIE of $k_{\text{H}}/k_{\text{D}} = 1.7 \pm 0.3$.

The examination of the relative yields of the alcohol adducts of silatriene **13** as a function of total alcohol concentration has been carried out in an attempt to obtain additional evidence for the mechanism outlined in equation 4.16. If our mechanism is correct (eq 4.16), second-order intracomplex proton transfer should predominate at low alcohol concentration, while the third-order process should be more important at high alcohol concentration. Intracomplex proton transfer should yield mainly the 1,2-alcohol addition products, whereas bimolecular proton transfer should yield a mixture of all four isomers (eq 4.15). Unfortunately, GC/MS analysis of the crude mixtures obtained from photolysis of ACN (or cyclohexane) solutions of **12** in the presence of between 0.001 M

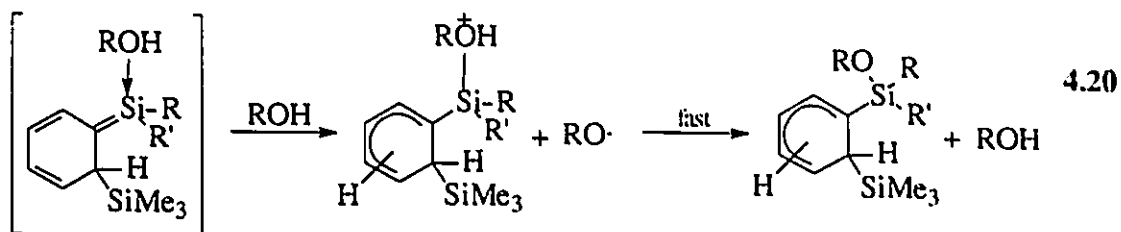
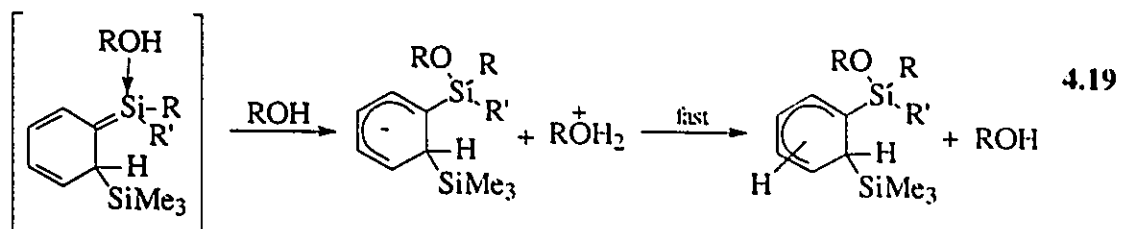
and 0.2 M methanol failed to reveal any changes in the relative yields of silatriene adducts **75**. The reasons for these observations are not obvious, although it is possible that the silatriene/alcohol adducts (**75**) thermally equilibrate at room temperature or in the heated injector port in the GC.

Linear quenching plots are obtained for the reactions of silatrienes **13**, **37**, **38**, and **50** with 2,2,2-trifluoroethanol (TFE) and acetic acid (HOAc) in ACN and THF solutions (see Figure 4.8). In these cases, the alcohols are substantially more acidic and less nucleophilic than water and "normal" alcohols like methanol, ethanol, and *tert*-butanol, such that the formation of the silatriene/alcohol complex, described by k_1 , becomes rate-determining (eq 4.18). Furthermore, the reaction of HOAc with **13** in ACN solution does not exhibit an observable KIE ($k_H/k_D = 1.0 \pm 0.1$), consistent with this mechanism. Steady-state photolysis of ACN solutions of **12** in the presence of either TFE or HOAc affords a complex mixture of at least four isomers in both cases, consistent with the addition of the alcohol to silatriene **13**.



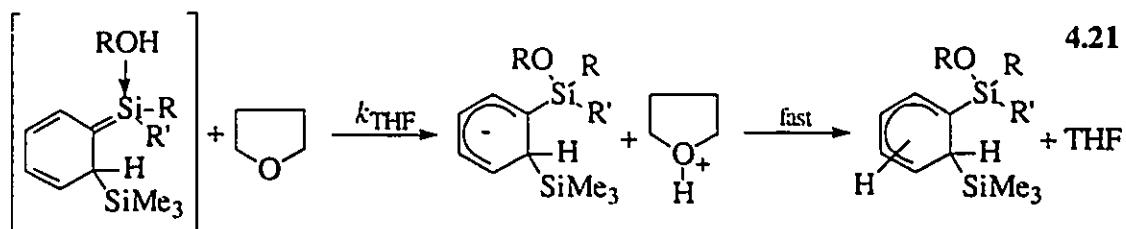
The kinetic scheme for alcohol quenching of silatrienes outlined in equation 4.16 does not specify the mode of interaction of the second alcohol molecule in the third-order proton transfer process. The two possible mechanisms are: (i) rate-determining deprotonation of the silatriene/alcohol complex followed by rapid reprotonation (eq 4.19),

or (ii) rate-determining protonation of the complex followed by rapid deprotonation (eq 4.20).



The quenching kinetics are somewhat more complicated in THF than in ACN solution due to the formation of silatriene/THF complexes and the possible involvement of THF in bimolecular proton transfer reactions. THF has the potential to act as a base (eq 4.21), and would be expected to affect the observed kinetics *only* if the third-order process involves rate-determining deprotonation followed by rapid reprotonation (eq 4.19). In order to simplify the interpretation of alcohol quenching in THF solution, it is useful to begin with silatriene **38** which does not exhibit spectral evidence for silatriene/THF complex formation. If we assume that the equilibrium constant for silatriene/alcohol complex formation is similar in THF and ACN solutions, deprotonation of the complex by THF would be expected to *increase* the observed second-order quenching rate constants relative to those obtained in ACN. The effects of THF on the

observed third-order rate constants are not as easy to predict; however, the rate constants are potentially sensitive to solvent effects on the equilibrium constants for silatriene-alcohol complex formation and to solvation effects on the alcohol.



The involvement of THF in bimolecular proton transfer according to equation 4.21 leads to the expression shown in equation 4.22 for the observed pseudo-first order rate of silatriene decay in THF as a function of added methanol, where K_{THF} is the equilibrium constant for silatriene/THF complex formation and the rate constants are those defined in equations 4.16 and 4.21. If the third-order process involves protonation/deprotonation (eq 4.20), THF would be expected to have relatively small effects on the observed rate constants compared to those measured in ACN solution.

$$k_{\text{decay}} = k_0 + \frac{k_1}{k_{-1}} * \frac{1}{(K_{\text{THF}}[\text{THF}] + 1)} * (k_2[\text{ROH}] + k_{\text{THF}}[\text{THF}][\text{ROH}] + k_3[\text{ROH}]^2) \quad 4.22$$

The rate constants for methanol quenching of 38 in ACN and THF solution are more consistent with the deprotonation/reprotonation mechanism (eq 4.19) for the third-order process. The second-order rate constant (k_q) is *ca.* three times *larger* in THF compared to ACN solution, whereas the third-order rate constants ($k_q^{(2)}$) are the same within the error. The small variation in $k_q^{(2)}$ indicates that the assumptions that silatriene/THF

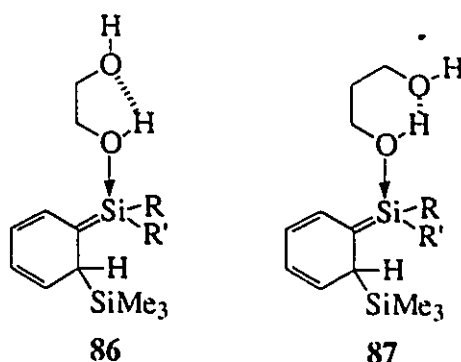
complex formation is insignificant for **38** and the equilibrium constant for silatriene/alcohol complex formation is similar in THF and ACN, are valid.

Tentative identification of the third-order process allows a comparison of the rate constants for methanol quenching of **13** and **37** in THF and ACN solutions. The second-order rate constant for methanol quenching of **13** in THF is about one-half that observed in ACN solution. However, as in the case of acetone quenching (*vide infra*), the observed reduction in the second-order rate constant is not as large as predicted by the estimated equilibrium constant for formation of the silatriene/THF complex. The expected reduction in the second-order rate constant for quenching of **13** in THF versus ACN solution is presumably offset by an increase in the rate due to the contribution of deprotonation of the silatriene/alcohol complex by THF (eq 4.21). On the other hand, the second-order rate constant for methanol quenching of **37** is *larger* in THF compared to ACN due to a significantly lower equilibrium constant for THF complex formation, in this case. The third-order rate constants for methanol quenching of **13** and **37** are *ca.* four and three times smaller in THF versus ACN solution, respectively, which *may* be attributable to silatriene/THF complex formation.

Methanol quenching of **13** in ACN solution in the presence of 0.017 M (and 0.003 M) trifluoroacetic acid and in the presence of 0.002 M triethylamine has been carried out in attempts to identify the third-order process. It was expected that if acid or base catalysis occurred under these conditions, the observed rate constant for silatriene decay (k_{obs}) would exhibit a linear (second-order) dependence upon alcohol concentration. Unfortunately, there are only small changes in the second- and third-order quenching rate constants under these conditions (Table 4.10). However, the interpretation of these results is somewhat complicated. In the presence of high concentrations of strong acid

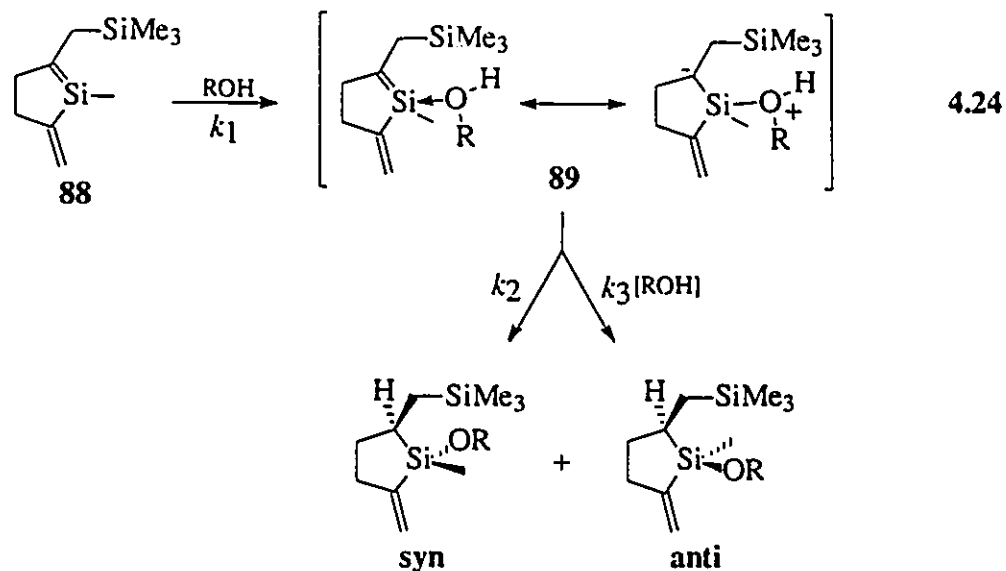
(TFA), a fraction of the methanol molecules are protonated, leading to reductions in the concentration of free methanol available for initial complex formation with the silatriene. Nevertheless, we can state that the results of the acid catalysis experiments are *not* consistent with the mechanism which involves rate-determining protonation of the silatriene/alcohol complex followed by rapid deprotonation (eq 4.20). A significant increase in the observed second-order rate constant is expected when methanol quenching is carried out in the presence of triethylamine based on the tentative assignment of the third-order process as deprotonation/reprotonation (eq 4.19); however, the kinetics of triethylamine catalyzed methanol quenching is complicated by the potential formation of amine/silatriene complexes.

The reaction of silatriene **13** with diols in ACN and THF solution is quite interesting. Curved quenching plots are obtained for the reaction of ethylene glycol, whereas *linear* second-order plots are observed for 1,3-propanediol. The observed second-order quenching rate constants in this case are intermediate in magnitude between the second- and third-order terms obtained from ethylene glycol quenching. These results are more consistent with the deprotonation/protonation mechanism (eq 4.19) than with protonation/deprotonation (eq. 4.20). Deprotonation of the silatriene/alcohol complex by the free hydroxyl group in ethylene glycol must occur via a five-membered transition state (**86**), while the same process involving 1,3-propanediol can occur via a more favourable six-membered transition state (**87**). Both diols would be expected to exhibit linear quenching plots if the protonation/deprotonation mechanism were operative since they both have long enough alkyl chains to facilitate protonation at carbon 2 in the silatriene.

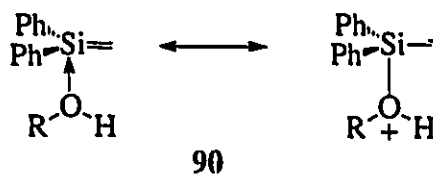


The mechanism outlined in equation 4.16 is qualitatively similar to that proposed by Sakurai for alcohol addition to a cyclic silene (88)⁵⁸ (eq 4.24); however, Sakurai did not specify that alcohol/silene complex formation was reversible. A comparison of the ratios k_2/k_3 measured by Sakurai with our values of $k_q/k_q^{(2)}$ ($= k_2/k_3$) is worthwhile. The k_2/k_3 values for silatriene quenching are all considerably less than unity and vary only slightly throughout the series of "normal" alcohols. Conversely, the corresponding values obtained by Sakurai vary from 4.6 for methanol to infinity for *tert*-butanol.⁵⁸ This indicates that proton transfer within the alcohol/silatriene complex is much slower relative to the intermolecular process than it is for 89.

The discrepancies between Sakurai's results and our results are ascribable to several factors. The main factor which may explain the large differences in the k_2/k_3 values is the inherent structure of the two silenes. Silatriene/alcohol complexes are expected to be stabilized by the cyclohexadienyl moiety by analogy with biradical stabilization in ketone, alkene, and oxygen trapping reactions. In contrast, the zwitterionic silene/alcohol complex (89) has a highly unstable, localized tertiary carbanion centre and would be expected to undergo much more rapid intramolecular proton transfer. Sakurai's results are perhaps more consistent with what we have learned about the mechanism of alcohol



addition to 1,1-diphenylsilene (**11**).¹³⁴ While we have obtained explicit kinetic evidence for a stepwise mechanism involving competing, rate determining, intra- and intermolecular proton transfer for the reactions of alcohols with silatrienes, we have been unable to obtain kinetic evidence for a similar stepwise mechanism for the reaction of **11**. Alcohol quenching of **11** follows strict second-order kinetics and exhibits small, but significant, deuterium KIE's.¹¹¹ The alcohol/1,1-diphenylsilene complex (**90**) would have a primary carbanion centre and would be expected to be significantly less stable than a similar silatriene/alcohol complex. Thus, the preliminary indications are that the reaction of **11** with alcohols occurs via a concerted mechanism.



The interpretation of Sakurai's experiments is also complicated by the fact that they were carried out in alcohol/acetonitrile mixtures with the alcohol concentration varied between 1.5 and 20 M. At these high alcohol concentrations, the formation of alcohol oligomers is expected to be prevalent (eq 4.25), even in ACN solution.¹⁵⁶ Alcohol oligomers are typically more acidic than the monomers due to weakening of the O-H bond by hydrogen bonding interactions, and their presence affects the kinetics of carbene^{155,157} and cation¹⁵⁸ reactions in different ways depending on the alcohol. In the case of methanol, the formation of oligomers was detected by upward curvatures in the quenching plots.¹⁵⁶⁻¹⁵⁸ The oxygen atoms in alcohol oligomers are sometimes more sterically inaccessible to reaction (e.g. *tert*-butanol) leading to downward curvature in the quenching plots.^{156,157} However, the involvement of alcohol oligomers in the silatriene reactions in ACN and THF solution can be ruled out since the plots show noticeable curvature at alcohol concentrations below 0.01 M, concentrations at which oligomer formation should be insignificant. Furthermore, analogous reactions of 1,1-diphenylsilene in ACN solution exhibit strict second-order linear quenching plots up to at least 0.01 M alcohol¹¹¹ and the quenching plots for *tert*-butanol reactions with **13** and **50** are curved upwards in a similar manner to the methanol quenching plots.



CHAPTER 5

SUMMARY AND CONCLUSIONS

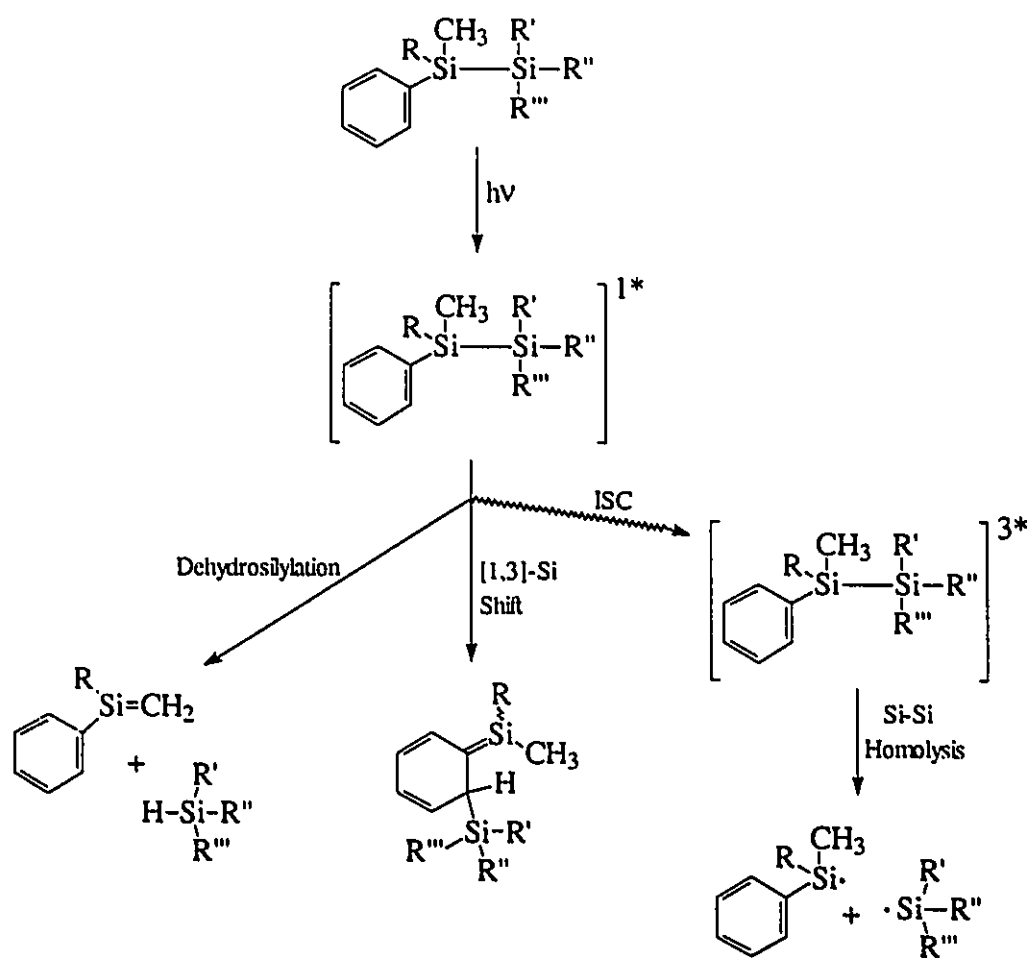
5.1 Contributions of the Study

While it has been known for over 20 years that the photolysis of arylsilylanes yields products consistent with the formation of simple silenes, 1,3,5-(1-sila)hexatrienes (silatrienes), and silyl free radicals, little was known about the mechanisms of formation of each type of reactive intermediate, prior to this study. Although each product type arises from formal disproportionation, recombination, or cage escape of silyl radicals generated from Si-Si bond homolysis,^{40,106} concerted singlet excited state rearrangements have also been proposed.^{37,38,82,89} Prior to this work, there existed several reports concerning the reactivity of silyl free radicals¹⁵⁻¹⁹ and stabilized silenes;^{1,5} however, there was surprisingly little information about the mechanistic aspects of the reactions of small, transient simple and conjugated silenes. The data which had been obtained was based mainly on product studies, and thus was largely qualitative. The properties of reactive silenes had been investigated at low temperature using matrix isolation techniques;¹ however, only two examples of the use of time-resolved spectroscopy to characterize such silenes in fluid solution at room temperature had been published.^{14,82}

The main goal of this study was to employ a *combination* of steady-state and time-resolved techniques (nanosecond laser flash photolysis (NLFP)) to characterize, in detail, the effects of solvent and substitution on the photochemistry of arylsilanes and the chemistry of the resulting transient silenes and silyl radicals. A second goal was to obtain sufficient information about arylsilane photochemistry and silene reactivity so that design and control over similar systems would be possible. The work described in this thesis has led to a significantly better understanding of the nature of the primary and secondary photochemical processes involved in the photolysis of arylsilanes. This is depicted in Scheme 5.1.

The initial aspect of this investigation was the attempted characterization of 1,1-diphenylsilene (**11**) by NLFP techniques employing methylpentaphenyldisilane (**9**)³⁶ as the precursor. It was subsequently discovered that silyl radicals (**33** and **44**) and silatriene **50** are easily detected by NLFP, the former overlapping with the expected absorption due to **11**. However, we have been able to obtain transient absorption spectra of each of the three types of silicon reactive intermediates *selectively* by the addition of the appropriate trapping agents to the solution of **9** (Figure 2.13). These observations led to a reinvestigation of the photochemistry of **9** in the presence of acetone or methanol as the silene trap, and chloroform as the silyl radical trapping agent. We discovered that, contrary to Sommer's report,³⁶ products consistent with the formation of **11** are formed in only 40% yield in hydrocarbon solution, while those consistent with silatriene **50** and silyl radicals (**33** and **44**) are formed in 40%, and 20% yields, respectively. In general, the photochemistry of phenyldisilanes (**9**, **12**, **32**, and **34**) is *considerably* more complicated than previously reported.^{36,39-41}

Scheme 5.1 The Photoreactivity of Aryldisilanes



NLFP and steady-state photolysis experiments using the homologous series of aryldisilanes **9**, **12**, **34**, and **35** have revealed a dramatic solvent effect on the photochemistry of phenyldisilanes. Transient UV absorption spectra obtained from NLFP of these disilanes demonstrate that the yields of the corresponding silyl radicals (characterized by absorptions in the 300-340 nm range) are much higher in acetonitrile (ACN) than in isooctane (OCT) solution. Likewise, the yields of the corresponding silatrienes (characterized by absorptions in the 400-520 nm range) are significantly lower in ACN solution. Steady-state product studies have confirmed this solvent effect. Products consistent with the intermediacy of silatrienes and simple silenes are formed in yields of 60-95% and 15-40%, respectively, in hydrocarbon solvents, while silyl radical-derived products are formed in yields of 5-20% (Table 5.1). However, in ACN solution, silyl radical-derived products are formed in 60-95% yield while silene-derived products are formed in < 15% yield. We have attributed this solvent effect to enhancement of intersystem crossing to the disilane lowest triplet excited state in polar solvents. Triplet sensitization and quenching experiments have conclusively demonstrated that silyl free radicals are triplet-derived,¹²¹ while simple silenes and silatrienes arise from the disilane lowest singlet excited state.¹²⁰ The triplet lifetime of **35** is quite short ($\tau = 6$ ns) due to rapid deactivation by Si-Si bond homolysis. Competitive photolyses of **9** and **35** in the presence of acetone and chloroform, as silene and silyl radical trapping agents, respectively, have demonstrated convincingly that simple silene and silatriene are formed by concerted rearrangements in the disilane singlet excited state and not from disproportionation or recombination of triplet-derived silyl free radicals.

Steady-state photolysis and fluorescence studies of **9** in the presence of high concentrations of carbon tetrachloride or chloroform in cyclohexane solution have demonstrated that aryldisilane singlet excited states can react directly with suitable

oxidants by electron transfer processes. Chloranil-sensitized photolysis of **9** in chloroform has confirmed that the products which arise from these reactions are indistinguishable from those derived from reactions of the corresponding silyl free radicals with the halocarbon solvent.

We have also been successful in the design and synthesis of an aryldisilane (**40**) which affords only the corresponding *tert*-butyldiphenylsilyl radicals (**41**) in a single chemical step (Si-Si bond homolysis) upon direct irradiation in ACN, chloroform, and hydrocarbon solvents. This is quite a remarkable achievement considering the general complexity of the photoreactivity of the other disilanes examined. The absence of hydrogens on the carbon atoms adjacent to the two silicons precludes dehydrosilylation, while the bulky *tert*-butyl groups block the [1,3]-silyl migration leading to silatriene formation. Triplet quenching experiments have confirmed that the silyl radicals are triplet-derived in this case as well, and have allowed the triplet lifetime to be estimated as 0.9 ± 0.3 ns. Absolute rate constants for the reactions of **41** with several alkyl halides, alkenes, and acetone have been measured by NLFP techniques. The rate constants are generally very similar to those reported previously for the reactions of triethylsilyl radicals.¹¹²

In a given solvent, disilane structure is the key factor which determines the relative yields of simple silene, silatriene, and silyl free radicals (Table 5.1). Silatrienes are formed in particularly high yields from **12**, **34**, and **35** in hydrocarbon solution when the migrating group is the relatively small trimethylsilyl moiety. The migrating group in methylpentaphenyldisilane (**9**) is the more sterically bulky methyldiphenylsilyl moiety leading to lower yields of the corresponding silatriene (**50**). Steric inhibition of [1,3]-silyl migration in **9** enhances the apparent efficiency of the competing processes: dehydrosilylation (generating **11**) and intersystem crossing leading to silyl free radical formation. The most striking example of the effects of disilane structure is observed for

1,2-di-*tert*-butyl-1,1,2,2-tetraphenyldisilane (**40**) which affords the corresponding silyl radicals exclusively in hydrocarbon and polar solvents. In the cases of **12** and **34**, dehydrosilylation competes. While two dehydrosilylation pathways are possible, the reaction shows a high preference for the one leading to the more thermodynamically stable silene.

Table 5.1 Chemical Yields of Silatriene, Simple Silene, and Silyl Radicals from the Photolysis of Disilanes **9**, **12**, **34**, **35**, and **40** in Hydrocarbon Solution^a

Disilane	Silatriene %	Simple Silene %	Silyl Radicals %
PhMe ₂ Si-SiMe ₃ (12)	70	19	b
Ph ₂ MeSi-SiMe ₃ (34)	80	18	b
Ph ₃ Si-SiMe ₃ (35)	95	0	5
Ph ₃ Si-SiPh ₂ Me (9)	45	35	20
<i>t</i> BuPh ₂ Si-SiPh ₂ <i>t</i> Bu (40)	0	0	100

- a. Yields taken from aryldisilane photolyses in cyclohexane-*d*₁₂ employing 2,3-dimethyl-1,3-butadiene (DMB) or acetone as silene traps and chloroform as the silyl radical trap.
- b. Not determined.

This work also represents the first systematic study of the effects of solvent polarity and substitution at the silenic silicon atom on the UV absorption and reactivity of conjugated silenes. We have developed a large library of absolute rate constants for reactions of silatrienes with classical silene trapping agents such as carbonyl compounds,

alkenes, dienes, oxygen, alkyl halides, and alcohols which, in conjunction with product studies, have provided significant mechanistic details of these reactions. In general, increasing phenyl substitution at the trivalent silicon atom leads to decreasing rate constants for reaction with silene trapping agents and to increasing red-shifts in the UV absorption maximum. Phenyl substitution increases the steric bulk at the silenic silicon atom resulting in reductions in the rate of attack of trapping reagents, and increases the conjugation in the chromophore causing red-shifts in the UV absorption maxima.

Solvent polarity has a minimal effect on the UV-visible absorptions of silatrienes; however, we have obtained the first evidence for the formation of a THF complex with a *transient silene*, analogous to the stabilized silene/THF complex (19) reported by Wiberg.⁵² The absorption maximum of silatriene 13 is red-shifted from 425 nm in OCT or ACN solutions to 460 nm in THF. Likewise, the rate constants for reaction of 13 with the reagents listed above are substantially reduced in THF solution, consistent with formation of a complex which is significantly less reactive towards silene traps than the free silatriene. Increasing phenyl substitution leads to smaller spectral shifts and smaller reductions in the quenching rate constants in THF solution due to reduced equilibrium constants for complex formation.

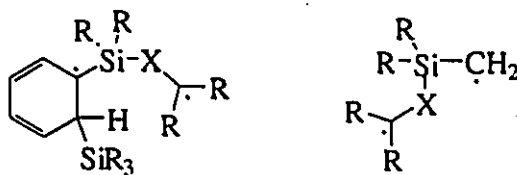
The isolated products of the reactions of transient silenes with carbonyl compounds are frequently the corresponding alkene and silanone oligomers,^{64,66} which are suggested to arise from thermal decomposition of 1,2-siloxetane intermediates formed by formal [2+2]-cycloaddition of the silene and the carbonyl compounds. Although there are a couple of examples of the isolation of 1,2-siloxetanes derived from reactions of stabilized silenes,⁶² the characterization of siloxetanes formed from reactions of transient silenes with carbonyl compounds had been elusive prior to this study.^{49,159,160} We have obtained the first spectroscopic evidence for the formation of 1,2-siloxetanes from the

reactions of acetone with aryldisilane-derived silatrienes (13, 37, 38, 50).^{108,120,121} Unfortunately, these siloxetanes are thermally and hydrolytically unstable so we have been unable to isolate them and are limited to spectroscopic characterization of the crude photolysis mixtures. Attempts to isolate 1,2-siloxetanes are currently underway in our laboratory.

We have formulated detailed mechanisms for the reactions of silatrienes with ketones, alkenes, and oxygen. The identification of 1,2-siloxetanes (57) and silyl ethers (56) as products suggests that the ketone reactions proceed via a stepwise mechanism. NLFP experiments have also demonstrated that 13-*d*₅ reacts with acetone, 2,3-dimethyl-1,3-butadiene (DMB), and oxygen at the same rates as 13, implying that migration of the allylic hydrogen is not involved in the rate-determining step. Thus, these reactions occur via stepwise mechanisms involving biradical intermediates.

The reactions of non-acidic alcohols with silatrienes afford curved quenching plots and are susceptible to small but significant deuterium kinetic isotope effects (KIE's). We have also detected four isomeric addition products, consistent with addition of the alcohol to the corresponding silatriene in each case. These observations indicate that the reaction of alcohols with silatrienes proceeds by a multistep mechanism involving rapid, reversible silatriene/alcohol complex formation followed by rate-determining uni- or bimolecular proton transfer (eq 4.16). This is the first clear demonstration of the involvement of proton transfer in the rate-determining step in the addition of alcohols to silicon-carbon double bonds. More acidic and less nucleophilic alcohols such as 2,2,2-trifluoroethanol and acetic acid follow strict second order kinetics in their reactions with silatrienes and do not exhibit observable KIE's. This is consistent with rate-determining complex formation followed by rapid proton transfer (eq 4.18).

In general, the reactions of silatrienes yield products which appear to be quite different from analogous reactions of simple silenes. However, our results demonstrate that the reactivity of silatrienes is consistent with what is known of silene behaviour, if the silatriene is viewed as a silene with an excellent radical- or anion-stabilizing substituent on the silenic carbon atom. Our group has recently reported evidence that carbonyl compounds add to 1,1-diphenylsilene (**11**) in a concerted, asynchronous ene reaction in which Si-O bond formation precedes hydrogen atom transfer.⁶³ The hexadienyl moiety in silatrienes is able to stabilize biradical intermediates such that the reaction changes from a concerted mechanism for **11** to a stepwise mechanism for silatrienes. The stepwise reaction of **11** would generate a considerably less stable primary alkyl radical centre in the analogous biradical.



The present work suggests that similar factors are operative in reactions with alkenes, oxygen, alkyl halides, and alcohols. 1,1-Diphenylsilene (**11**) reacts rather sluggishly with oxygen and alkyl halides ($k_q < 10^6 \text{ M}^{-1}\text{s}^{-1}$), whereas silatrienes react with these reagents with rate constants in the 10^7 - $10^9 \text{ M}^{-1}\text{s}^{-1}$ range (Chapter 4). Alcohol quenching of **11** affords linear quenching plots indicative of second-order kinetics and small, but detectable, deuterium KIE's.¹¹¹ These observations *may* be consistent with concerted addition of the alcohol molecule to the silicon-carbon double bond in **11**, in contrast with the proposed stepwise mechanism for alcohol quenching of silatrienes (eq

4.16). The dienyl substituent on the silenic carbon atom presumably stabilizes the silatriene/alcohol complex in an analogous manner in which biradical stabilization occurs.

5.2 Future Work

Related work which is currently underway in our laboratory includes the attempted isolation of 1,2-siloxetanes from the reaction of ketones with silatrienes, a detailed investigation of the reactions of alcohols and other classic silene trapping agents with 1,1-diphenylsilene (**11**), and an examination of the effects of para-substitution on the reactivity of **11** with carbonyl compounds and other silene traps. At this stage, our knowledge of the reactivity of silatrienes exceeds that of simple silenes. Thus, it is a high priority to elucidate the mechanistic details of simple silene reactions. Another study which is worthwhile to investigate is the examination of photoinduced electron-transfer reactions of arylsilanes by NLFPS techniques with the ultimate goal of direct characterization of transient silyl cations. Finally, examination of the *photochemistry* of silatrienes by two-colour, two-laser flash photolysis techniques is an intriguing possibility.

CHAPTER 6

EXPERIMENTAL

6.1 General

^1H NMR spectra were recorded on Bruker AM500 (500 MHz), AC300 (300 MHz), AC200 (200 MHz), or Varian EM390 (90 MHz) spectrometers in deuteriochloroform, cyclohexane- d_{12} , or acetonitrile- d_3 solution, and are reported in parts per million downfield from tetramethylsilane using the residual solvent resonances as the internal standard. ^{13}C NMR spectra were recorded on the Bruker AM500 (125.5 MHz), AC300 (75.5 MHz), or AC200 (50.3 MHz) spectrometers. ^{29}Si NMR were recorded on the Bruker AC300 spectrometer at 59.6 MHz using the DEPT pulse sequence.¹⁶¹ Ultraviolet absorption spectra were recorded on a Hewlett-Packard HP8451 UV spectrometer or a Perkin-Elmer Lambda 9 spectrometer interfaced to an IBM-PC. Fluorescence emission and excitation spectra were recorded on a Perkin-Elmer LS5 spectrofluorometer. High resolution mass spectra were recorded on a VG Analytical ZABE mass spectrometer employing a mass of 12.0000 for carbon. Infrared spectra were recorded on a Bio-Rad FTS-40 FTIR spectrometer and are reported in wavenumbers (cm^{-1}). Melting points were determined using a Mettler FP82 hot stage (controlled by a Mettler FP80 central processor) mounted on an Olympus BH-2 microscope and are uncorrected. Combustion analyses were performed by Dr. D.S. Mitchell (Uniroyal, Inc.;

Guelph, Ontario) using a Perkin-Elmer Model 240C elemental analyzer, calibrated with acetanilide. Molecular mechanics (MMX) calculations were carried out using PCMODEL3 (Serena Software).

Gas chromatographic analyses were carried out using a Hewlett-Packard 5890 gas chromatograph equipped with a flame ionization detector, a Hewlett-Packard 3396A recording integrator, and one of the following fused silica capillary columns: (a) 12 m x 0.53 mm HP-1; Hewlett-Packard, Inc.; (b) 5 m x 0.53 mm HP-1; Hewlett-Packard, Inc.; (c) 15 m x 0.20 mm DB-1; Chromatographic Specialties, Inc. A conventional heated splitless injector port (200-250 °C) was used in conjunction with columns (a) and (b) while cold on-column injection was used with column (c). Semi-preparative VPC separations employed a Varian 3300 gas chromatograph equipped with a thermal conductivity detector and a 6' x 0.25" OV-101 stainless steel packed column (Chromatographic Specialties, Inc.). GC/MS analyses were carried out using a Hewlett-Packard 5890 gas chromatograph equipped with a HP-5971A mass selective detector and a DB-1 capillary column (12 m x 0.2 mm; Chromatographic Specialties, Inc.). GC-FTIR analyses employed a Hewlett-Packard 5890 gas chromatograph equipped with an HP-1 megabore capillary column (5 m x 0.53 mm; Hewlett-Packard, Inc.) and a Bio-Rad GC/32 interface to the Bio-Rad FTS-40 FTIR spectrometer.

6.2 Commercial Solvents and Reagents

Cyclohexane (BDH Omnisolv), 2,2,4-trimethylpentane (isooctane; Baker HPLC), water (Caledon HPLC), deuterium oxide (MSD Isotopes), chloroform-*d* (MSD Isotopes),

glacial acetic acid (Fisher reagent), acetic acid-*d* (Aldrich), methanol-*Od* (Aldrich), 2,2,2-trifluoroethanol (Aldrich NMR grade), trifluoroacetic acid (BDH), ethylene glycol (Aldrich spectrograde), 1,3-propanediol (Aldrich), absolute ethanol, cyclopentene (Aldrich), 1-hexene (Aldrich), *trans*-piperylene (Aldrich), 1-bromopentane (Aldrich), 2-bromo-2-methylpropane (Aldrich), 2-chloro-2-methylpropane (BDH), bromobenzene-*d*₅ (Aldrich), triethylsilane (Aldrich), triphenylsilane (Aldrich), triphenylsilanol (Aldrich), 1,2-dimethyl-1,1,2,2-tetraphenyldisilane (Petrarch), hexamethyldisilane (Aldrich), hexamethyldisiloxane (Aldrich), methyldiphenylsilane (Aldrich), dimethylphenylsilane (Aldrich), chlorotrimethylsilane (Aldrich), chlorodiphenylmethylsilane (Aldrich), chlorodimethylphenylsilane (Aldrich), chlorotriphenylsilane (Aldrich), *tert*-butyldiphenylsilyl chloride (Aldrich) were used as received from the suppliers. Cyclohexane-*d*₁₂ and acetonitrile-*d*₃ were used as received from Isotec, Inc. The water content (presumably as D₂O) in the latter was estimated as *ca.* 0.005 M from the lifetime of 1,1-diphenylsilene in oxygenated acetonitrile-*d*₃ at 24 °C.¹¹¹

Acetonitrile (BDH Omnisolv) was refluxed over calcium hydride for several days and distilled under nitrogen immediately prior to use. Tetrahydrofuran (Caledon HPLC) and dioxane (BDH reagent) were refluxed over sodium and distilled under nitrogen. Methanol (Fisher HPLC) was predried with calcium hydride, distilled from magnesium under nitrogen, and stored over molecular sieves (3Å). *tert*-Butyl alcohol (Fisher reagent) was distilled from calcium oxide and stored over molecular sieves (4Å). Benzene (Fisher reagent) was extracted with concentrated sulfuric acid and distilled before use. Methoxytrimethylsilane (Aldrich) was stored over activated molecular sieves (4Å). 2,3-Dimethyl-1,3-butadiene (DMB; Aldrich Gold Label) and di-*tert*-butyl peroxide (BOOB; Aldrich) were passed through activated alumina. Cyclohexene (Aldrich Gold Label) and 2-bromopropane (Matheson Coleman and Bell) were distilled before use. Acetone (Baker

reagent), carbon tetrachloride (Matheson Coleman and Bell spectrograde), chloroform (BDH Omnisolv), and dichloromethane (Fisher HPLC) were distilled from anhydrous potassium carbonate and stored over molecular sieves (4Å). Dimethyl sulfoxide (BDH reagent) was fractionally distilled twice from calcium hydride under nitrogen and stored over molecular sieves (4Å). Ethyl acetate (BDH reagent) was distilled from phosphorous pentoxide under nitrogen. Triethylamine (Fisher reagent) was distilled from sodium hydroxide under nitrogen prior to use. 1-Pentanol (Baker reagent) was distilled under nitrogen and stored over molecular sieves (3Å). Chloranil (Aldrich) was recrystallized twice from ethanol.

6.3 Nanosecond Laser Flash Photolysis

Nanosecond laser flash photolysis experiments employed the pulses from a Lumonics 510 excimer laser filled with F₂/Kr/He (248 nm, *ca.* 16 ns, *ca.* 4 mJ) or a Lumonics TE-861M excimer laser filled with N₂/He (337 nm, 6 ns, *ca.* 4 mJ) and a microcomputer-controlled detection system.^{109,110} Disilane solutions were prepared at concentrations such that the absorbance at the excitation wavelength (248 nm) was *ca.* 0.7-0.8 (10⁻³-10⁻⁴ M), and were flowed continuously through a 3 x 7 mm Suprasil flow cell connected to a calibrated 50 mL, 100 mL, or 250 mL reservoir. The solutions were deoxygenated continuously with a stream of dry nitrogen. Quenchers were added directly to the reservoir by microlitre syringe as aliquots of neat liquids or standard solutions. Oxygen quenching studies were carried out using a Matheson 600 gas proportioner to regulate the composition of oxygen/nitrogen mixtures which were bubbled continuously through the solution contained in the reservoir. The concentrations of oxygen in oxygen-saturated

isooctane,¹¹⁹ acetonitrile,¹¹⁸ and tetrahydrofuran¹⁶² are 0.015 M, 0.0085 M, and 0.010 M, respectively. Rate constants were calculated by least squares analysis of decay rate-concentration (6-20 points) which spanned at least one order of magnitude in the transient decay rate. Errors are reported as twice the standard deviation obtained from the least squares analysis in each case.

6.4 Preparation and Characterization of Compounds

Disilanes **9**, **12**, **12-*d*₅**, **32**, **34**, and **35** have been prepared according to the literature procedures and exhibited melting or boiling points and spectral data which agreed with those reported in each case. 1,2-Di-*tert*-butyl-1,1,2,2-tetraphenyldisilane (**40**) was synthesized using a modification of Gilman's procedure for the synthesis of arylsilanes^{129,130} and is the same general method used for the synthesis of the other disilanes except for **12-*d*₅**.¹⁶³ Methoxytriphenylsilane (**42**)¹⁶⁴ and methoxymethyldiphenylsilane (**20**)¹⁶⁵ were prepared from the corresponding silyl chlorides following minor modifications of the literature procedures. Chloropentamethyldisilane used in the synthesis of **12-*d*₅** was prepared from hexamethyldisilane following Sakurai's method.¹⁶⁶

1,2-Di-tert-butyl-1,1,2,2-tetraphenyldisilane (40): *tert*-Butyldiphenylsilyl chloride (**65**) (3.17 g, 0.012 mol) was dissolved in dry THF (40 mL), and the solution was added dropwise to a 100 mL round-bottom flask equipped with a reflux condenser, nitrogen inlet, and magnetic stirrer and containing lithium powder (approximately 0.4 g, 0.06 mol; obtained by washing the appropriate quantity of a 25% mineral oil dispersion with dry THF on a glass frit). The resulting suspension gradually turned a bright red-brown colour

as it was stirred under a nitrogen atmosphere for 8 h at room temperature indicating the formation of *tert*-butyldiphenylsilyl lithium. This suspension was filtered through glass wool and added dropwise to neat silyl chloride (**65**) (3.17 g, 0.012 mol) contained in a similar apparatus. The resulting suspension was stirred at room temperature for 15 h, hydrolyzed with 0.02 M aqueous sulfuric acid (50 mL), and extracted with diethyl ether (2 x 30 mL). The combined ether extracts were dried with anhydrous sodium sulfate, and the solvent was removed on the rotary evaporator, yielding a light yellow solid.

Recrystallization from ethyl acetate yielded the product (2.2 g, 2.4 mmol, 40%) as colourless cubes.

m.p. = 210-211 °C. ^1H NMR (CDCl_3 , 200 MHz): δ = 0.84 (s, 18H, CH_3), 7.25-7.70 (m, 20H, Ph). ^{13}C NMR (CDCl_3 , 50.3 MHz): δ = 20.4, 29.1, 127.2, 128.7, 136.6, 137.5. ^{29}Si NMR (CDCl_3 , 59.6 MHz): δ = -12.9. IR (CDCl_3): 3073 (m), 3052 (m), 2970 (s), 2858 (s), 1652 (m), 1427 (s), 1096 (s), 700 (m). UV: λ_{max} = 250 nm (ϵ = $21700 \text{ M}^{-1}\text{cm}^{-1}$). MS: m/z (I) = 478 (1), 421 (45), 365 (15), 343 (13), 265 (36), 259 (40), 197 (87), 135 (100), 105 (27). Exact mass: calcd for $\text{C}_{20}\text{H}_{38}\text{Si}_2$, m/z 478.2512; found, 478.2496. Anal. calcd for $\text{C}_{20}\text{H}_{38}\text{Si}_2$: C, 80.29; H, 8.01. Found: C, 80.29; H, 7.80.

Pentamethylphenyldisilane (**12**):¹²⁹ b.p. = 53-55 °C (2 mbar). ^1H NMR (C_6D_{12} , 300 MHz): δ = 0.06 (s, 9H, SiMe_3), 0.33 (s, 6H, SiMe_2), 7.2-7.4 (m, 5H, Ph). ^{13}C NMR (C_6D_{12} , 125 MHz): δ = -3.8, -2.1, 128.2, 128.8, 133.3, 134.2. IR (CCl_4): 3067 (w), 2964 (m), 2928 (s), 2853 (w), 1597 (w), 1452 (w), 1250 (s), 1098 (s), 1015 (s), 864 (w), 827 (m). MS: m/z (I) = 208 (15), 193 (12), 135 (100), 105 (10), 73 (32). Exact mass: calcd for $\text{C}_{11}\text{H}_{20}\text{Si}_2$, m/z 208.1104; found, 208.1106.

Pentamethyl(pentadeuteriophenyl)disilane (12-d₅) was prepared by a modification of Weber's procedure.¹⁶³ A THF solution (10 mL) of chloropentamethyldisilane¹⁶⁶ (3.5 mL, 0.019 mol) and bromobenzene-d₅ (2 mL, 0.019 mol) was added dropwise over 1.5 h to a suspension of Mg (0.466 g, 0.02 mol) in THF (10 mL). The resulting suspension was refluxed for 1 h, hydrolyzed with water (20 mL), and extracted with diethyl ether (2 x 20 mL). The combined organic extracts were dried with anhydrous magnesium sulfate and the solvent was removed on a rotary evaporator yielding a clear light yellow oil. The resulting oil was distilled under reduced pressure to yield 12-d₅ as a clear colourless oil (2.0 g, 0.009 mol, 49%).

b.p. = 139-141 °C (55 mm). ¹H NMR (CDCl₃, 200 MHz): δ = 0.06 (s, 9H, SiMe₃), 0.34 (s, 6H, SiMe₂). ¹³C NMR (CDCl₃, 50.3 MHz): δ = -4.1, -2.3. IR (CDCl₃): 2954 (s), 2893 (m), 2274 (w), 2241 (w), 1602 (s), 1300 (m), 1246 (s), 1054 (m), 836 (s), 802 (m). MS: *m/z* (I) = 213 (12), 198 (12), 140 (100), 73 (12). Exact mass: calcd for C₁₁H₁₅D₅Si₂, *m/z* 213.1417; found, 213.1403.

Methylpentaphenyldisilane (9)^{129,130} was recrystallized three times from ethanol. m.p. = 146-148 °C. ¹H NMR (CDCl₃, 200 MHz): δ = 0.80 (s, 3H, SiMe), 7.2-7.5 (m, 25H, Ph). ¹³C NMR (CDCl₃, 50.3 MHz): δ = -3.2, 127.8, 127.9, 129.0, 129.2, 134.8, 135.5, 136.3. ²⁹Si NMR (CDCl₃, 59.6 MHz): δ = -23.0, -23.4. IR (CCl₄): 3070 (s), 3052 (s), 2998 (w), 2959 (w), 1967 (w), 1897 (w), 1822 (w), 1486 (m), 1428 (s), 1248 (m), 1104 (s), 999 (w), 700 (s). MS: *m/z* (I) = 456 (15), 441 (5), 379 (5), 259 (100), 197 (45), 181 (15), 105 (10). Exact mass: calcd for C₃₁H₂₈Si₂, *m/z* 456.1730; found, 456.1742.

*Hexaphenyldisilane (32)*¹⁶⁷ was synthesized from chlorotriphenylsilane and sodium in dry xylenes according to published procedures and was recrystallized several times from

toluene. m.p. = 365-368 °C. lit. m.p. = 361-362 °C.¹⁴⁷ MS: m/z (I) = 518 (15), 379 (2), 259 (100), 181 (15), 105 (12).

1,1,1,2-Tetramethyl-2,2-diphenyldisilane (34):¹²⁹ b.p. = 95-96 °C (0.2 mm). ¹H NMR (CDCl₃, 200 MHz): δ = 0.13 (s, 9H, SiMe₃), 0.58 (s, 3H, SiMe), 7.3-7.5 (m, 10H, Ph). ¹³C NMR (CDCl₃, 50.3 MHz): δ = -4.9, -1.7, 127.8, 128.7, 134.8. IR (CCl₄): 3069 (m), 3053 (w), 2954 (s), 2929 (m), 2897 (m), 2855 (w), 1965 (w), 1428 (s), 1247 (s), 1105 (s), 859 (s), 835 (s), 699 (s). MS: m/z (I) = 270 (25), 255 (10), 197 (100), 135 (30), 105 (20), 73 (10). Exact mass: calcd for C₁₆H₂₂Si₂, m/z 270.1260; found, 270.1276.

1,1,1-Trimethyl-2,2,2-triphenyldisilane (35)^{129,130} was recrystallized four times from ethanol. m.p. = 107-109 °C. ¹H NMR (CDCl₃, 200 MHz): δ = 0.23 (s, 9H, SiMe₃), 7.3-7.5 (m, 15H, Ph). ¹³C NMR (CDCl₃, 50.3 MHz): δ = -0.9, 127.9, 128.9, 135.6, 135.9. ²⁹Si NMR (CDCl₃, 59.6 MHz): δ = -18.9, -20.9. IR (CCl₄): 3069 (s), 3052 (m), 2998 (w), 2955 (m), 2895 (w), 1953 (w), 1882 (w), 1820 (w), 1485 (w), 1428 (s), 1246 (s), 1103 (s), 852 (s), 836 (s), 701 (s). MS: m/z (I) = 332 (20), 317 (10), 259 (100), 197 (25), 181 (20), 135 (10), 105 (15), 73 (10). Exact mass: calcd for C₂₁H₂₄Si₂, m/z 332.1417; found, 332.1439.

Methoxymethyldiphenylsilane (20):¹⁶⁴ b.p. = 180 °C (50 mm). ¹H NMR (CDCl₃, 200 MHz): δ = 0.68 (s, 3H, SiCH₃), 3.57 (s, 3H, SiOCH₃), 7.3-7.6 (m, 10H, Ph). ¹³C NMR (CDCl₃, 50.3 MHz): δ = -3.6, 51.2, 127.9, 129.9, 134.0, 134.3. GC/MS: m/z (I) = 228 (20), 213 (100), 183 (40), 151 (23), 121 (63), 105 (43), 91 (23), 77 (20), 59 (40).

Methoxytriphenylsilane (42)¹⁶⁵ was recrystallized from methanol. m.p. = 52-53 °C. ¹H NMR (CDCl₃, 200 MHz): δ = 3.64 (s, 3H, SiOCH₃), 7.3-7.6 (m, 15H, Ph). ¹³C NMR

(CDCl₃, 50.3 MHz): δ = 51.9, 127.9, 130.1, 133.9, 135.4. MS: m/z (I) = 290 (55), 213 (100), 183 (43), 136 (70), 105 (30), 91 (8), 77 (11).

6.5 Steady-State Photolyses

6.5.1 General Methods

Steady-state photolysis experiments were carried out in a Rayonet photochemical reactor equipped with a merry-go-round and one to twelve RPR-254 (254 nm), RPR-300 (300 nm), or RPR-350 (350 nm) lamps. Experiments in which the disilane was irradiated directly employed the 254 nm lamps, except for those carried out in the presence of *trans*-piperylene or carbon tetrachloride, which employed the 300 nm lamps and a Pyrex filter. The acetone-sensitized photolyses employed the 300 nm lamps, while the chloranil-sensitized photolysis employed the 350 nm lamps and a Pyrex filter. Photolysis solutions were contained in 5 x 75 mm or 9 x 100 mm quartz tubes, or 5 mm quartz NMR tubes, which were sealed with rubber septa and deoxygenated with a stream of dry nitrogen prior to photolysis. Chemical yields were determined by integration of the ¹H NMR (300 MHz) spectra of the crude photolysates from small scale (*ca.* 10 mg disilane) runs in deuterated solvents and/or by GC analyses relative to the disappearance of the starting disilane using an appropriate internal standard (usually dodecane, hexadecane, or eicosane). For the NMR experiments, a known amount of dichloromethane or methyl *tert*-butyl ether was included as an internal integration standard. The response of the FID detector was calibrated relative to the internal standards by the construction of working curves.

6.5.2 Quantum Yield Determinations

For quantum yield measurements in the photolysis of 0.005 M chloroform or cyclohexane solutions of **40**, the solutions also contained 10^{-4} M hexadecane and 0.005 M eicosane as internal standards for the quantitation of products and starting material, respectively. The disappearance of **40** and the formation of **65** were monitored between 0 and 10% conversion and employed potassium ferrioxalate actinometry,¹³² following Bunce's method for the use of Rayonet reactors.¹⁶⁸ Quantum yields are the averages of triplicate determinations.

6.5.3 Photoproduct Identification

Compounds (**45** and **56**) were isolated by semi-preparative VPC and fully characterized. Siloxetanes **48** and **57** were identified by NMR analysis of the crude photolysates. The remaining photoproducts were identified by a combination of GC/MS, GC/FTIR, ¹H NMR spectroscopy, and/or by GC coinjection of the photolysates with authentic samples.

2-Diphenylmethylsiloxypene (45): ¹H NMR (500 MHz; CDCl₃): δ = 0.72 (s; 3H), 1.79 (s; 3H), 4.02 (d, J = 6.8 Hz; 2H), 7.4-7.6 (m; 10H). ¹³C NMR (125 MHz; CDCl₃): δ = -2.7, 22.8, 92.3, 127.9, 129.9, 134.2, 135.8, 155.7. GC/IR: 3062 (m), 2970 (w), 1638 (w), 1376 (w), 1273 (s), 1116 (s), 1056 (s), 934 (w), 894 (w), 795 (s). GC/MS: *m/z* (I) = 254 (10), 239 (50), 197 (70), 161 (15), 137 (100), 105 (25), 91 (15), 51 (14).

3,3-Dimethyl-2-oxa-1,1-diphenyl-1-sila-9-methyldiphenylsilylspiro[3.5]nona-5,7-diene (48): ^1H NMR (300 MHz; CDCl_3): δ = 0.41 (s, 3H), 1.79 (s, 3H), 2.08 (s, 3H), 3.61 (d, J = 6.1 Hz; 1H), 5.6-6.0 (m, 4H).

Diphenyl(2-methyldiphenylsilylphenyl)(2-propoxy)silane (49): ^1H NMR (300 MHz; CDCl_3): δ = 0.61 (d, J = 6.1 Hz; 6H), 0.79 (s, 3H), 3.92 (sept, J = 6.1 Hz, 1H). GC/MS: m/z (I) = 514 (1), 499 (2), 457 (4), 437 (6), 395 (23), 379 (30), 317 (100), 257 (18), 199 (28), 105 (7), 77 (4).

Dimethyl(2-trimethylsilylphenyl)(2-propoxy)silane (56a):¹⁰² ^1H NMR (300 MHz; C_6D_{12}): δ (multiplicity; integral; identification) = 0.375 (s; 9H; $\text{Si}(\text{CH}_3)_3$), 0.380 (s; 6H; $\text{Si}(\text{CH}_3)_2$), 1.22 (d, J = 6.1 Hz; 6H; CH_3), 4.13 (sept, J = 6.1 Hz; 1H; OCHMe_2), 7.20-7.60 (m; 4H; Ph). ^{13}C NMR (75.5 MHz; C_6D_{12}): δ = 1.4 ($\text{Si}(\text{CH}_3)_2$), 1.9 ($\text{Si}(\text{CH}_3)_3$), 26.1 (CH_3), 66.2 (OCHMe_2), 127.9, 128.5, 134.9, 135.5, 145.1, 146.6 (Ph). GC/FTIR: 3077 (w), 3055 (m), 2979 (s), 2890 (m), 1385 (m), 1256 (s), 1172 (m), 1129 (s), 1022 (s), 846 (s), 738 (m). MS: m/z (I) = 266 (2), 251 (2), 209 (30), 193 (100), 147 (14), 116 (12), 75 (15).

Methylphenyl(2-trimethylsilylphenyl)(2-propoxy)silane (56b): ^1H NMR (300 MHz; C_6D_{12}): δ (multiplicity; integral; identification) = 0.32 (s; 9H; $\text{Si}(\text{CH}_3)_3$), 0.63 (s; 3H; SiCH_3), 1.09 (d, J = 6.1 Hz; 3H; CH_3), 1.21 (d, J = 6.1 Hz; 3H; CH_3), 4.07 (sept, J = 6.1 Hz; 1H; OCHMe_2), 7.10-7.70 (m; 9H; Ph). ^{13}C NMR (75.5 MHz; C_6D_{12}): δ = -0.3 (SiCH_3), 1.9 ($\text{Si}(\text{CH}_3)_3$), 25.7 (CH_3), 26.0 (CH_3), 66.8 (OCHMe_2), 127.7, 128.1, 128.7, 129.8, 135.2, 135.5, 136.5, 139.3, 143.1, 147.5 (Ph). GC/FTIR: 3116 (w), 3076 (m), 3057 (s), 2978 (s), 2907 (m), 1430 (m), 1385 (m), 1256 (s), 1118 (s), 1019 (s), 850 (s), 796 (s). MS: m/z (I) = 328 (2), 313 (2), 271 (12), 255 (11), 209 (21), 193 (100), 178

(45), 137 (33), 105 (6), 73 (6). Exact mass: calcd for $C_{19}H_{28}OSi_2$, 328.1679; found, 328.1686.

Diphenyl(2-trimethylsilylphenyl)(2-propoxy)silane (56c): 1H NMR (200 MHz; $CDCl_3$): δ (multiplicity; integral; identification) = 0.30 (s; 9H; $Si(CH_3)_3$), 1.20 (d, $J = 6.1$ Hz; 6H; CH_3), 4.25 (sept, $J = 6.1$ Hz; 1H; $OCHMe_2$), 7.20-7.70 (m; 14H; Ph). ^{13}C NMR (50.3 MHz; $CDCl_3$): $\delta = 1.6$ ($Si(CH_3)_3$), 25.5 (CH_3), 67.1 ($OCHMe_2$), 127.1, 127.6, 128.4, 129.7, 135.1, 135.9, 136.4, 137.2, 140.7, (Ph). ^{29}Si NMR (59.6 MHz; $CDCl_3$): $\delta = -2.1$ ($SiMe_3$), -12.2 ($OSiPh_2Ar$). GC/FTIR: 3074 (m), 3058 (s), 2978 (m), 2904 (w), 1429 (m), 1386 (m), 1252 (m), 1116 (s), 1021 (s), 843 (s), 791 (s), 765 (s). MS: *m/e* (I) = 390 (5), 375 (3), 333 (10), 317 (16), 271 (20), 255 (100), 240 (72), 199 (78), 165 (10), 135 (15), 105 (23), 73 (60). Exact mass: calcd for $C_{24}H_{30}OSi_2$, 390.1835; found, 390.1853.

1,1,3,3-Tetramethyl-2-oxa-1-sila-9-trimethylsilylspiro[3.5]nona-5,7-diene (57a): 1H NMR (500 MHz; C_6D_{12}): δ (multiplicity; integral; identification; nOe enhancements) = 0.03 (s; 9H; $Si(CH_3)_3$), 0.41 (s; 6H; $Si(CH_3)_2$), 1.26 (s; 3H; CH_3 ; δ 5.97), 1.47 (s; 3H; CH_3 ; δ 1.26, δ 2.57, δ 5.77, δ 7.2-7.4), 2.57 (d; $J = 6.3$ Hz; allyl; δ 1.47, δ 5.77, δ 7.3-7.4), 5.7-6.0 (cmplx m; 4H; vinyl). ^{13}C NMR (125 MHz; C_6D_{12}): $\delta = 0.6$ ($Si(CH_3)_2$), 1.3 ($Si(CH_3)_3$), 30.4 (allyl), 31.8 (CH_3), 33.4 (CH_3), 41.4, 87.2 (C-O).

1,3,3-Trimethyl-2-oxa-1-phenyl-1-sila-9-trimethylsilylspiro[3.5]nona-5,7-diene (57b): 1H NMR (500 MHz; C_6D_{12}): δ (multiplicity; integral; identification; nOe enhancements) = 0.05 (s; 9H; $Si(CH_3)_3$); 0.68 (s; 3H; $SiCH_3$), 1.40 (s; 3H; CH_3 ; δ 1.61, δ 5.74, δ 7.7), 1.61 (s; 3H; CH_3 ; δ 2.68, δ 5.79, δ 7.2-7.4), 2.69 (d; $J = 6.3$ Hz; allyl; δ 1.61, δ 5.79), 5.7-6.0 (cmplx m; 4H; vinyl). ^{13}C NMR (125 MHz; C_6D_{12}): $\delta = 1.2$ ($Si(CH_3)_3$), 1.8

(SiCH₃), 30.7 (allyl), 31.7 (CH₃), 33.8 (CH₃), 42.4, 87.7 (C3), 123.5, 126.4, 130.0, 130.3 (C5-C8).

syn-3,3-Dimethyl-2-oxa-1,1-diphenyl-1-sila-9-trimethylsilylspiro[3.5]nona-5,7-diene (57c): ¹H NMR (500 MHz; CDCl₃): δ (multiplicity; integral; identification; nOe enhancements) = -0.17 (s; 9H; Si(CH₃)₃; δ2.93, δ5.7-5.9, phenyl), 1.41 (s; 3H; CH₃; δ 1.84, δ5.74, phenyl), 1.84 (s; 3H; CH₃; δ1.41, δ2.93, δ5.89, phenyl), 2.93 (d; J = 6.3 Hz; allyl), 5.74 (d; 1H; J = 9.3 Hz; H5), 5.78 (dd; 1 H; J = 4.9; 9.15 Hz; H7), 5.84 (dd; 1H; J = 4.9, 9.3 Hz; H6), 5.89 (dd; 1H; J = 6.3, 9.15 Hz; H8). ¹³C NMR (125 MHz; CDCl₃): δ = 1.3 (Si(CH₃)₃), 29.9 (allyl), 31.8 (CH₃), 33.2 (CH₃), 44.4, 89.4 (C-O), 122.0 (C7), 125.7 (C6), 129.0 (C5), 131.0 (C8). ²⁹Si NMR (59.6 MHz; CDCl₃): δ = 2.2 (SiMe₃), 12.4 (siloxetane Si). IR (CDCl₃): 3071 (m), 2930 (s), 2853 (s), 1590 (m), 1429 (s), 1248 (s), 1122 (s), 1057 (s).

1-Trimethylsilyl-2-(4-(2,3-dimethyl-1-butenyl)dimethylsilyl)benzene (69a):¹⁰⁰ ¹H NMR (300 MHz; C₆D₁₂): δ (multiplicity; integral; identification) = 0.37 (s; 9H; Si(CH₃)₃), 0.39 (s; 3H; Si(CH₃)), 0.41 (s; 3H; Si(CH₃)), 0.91 (dd, J = 7.5, 14.9 Hz; 1H; CH₂), 1.07 (dd, J = 6.8, 14.9 Hz; 1H; CH₂), 1.00 (d, J = 6.8 Hz; 3H; CH₃), 1.63 (s; 3H; CH₃), 2.39 (m; 1H; allyl), 4.60 (m; 2H; vinyl). GC/MS: *m/e* (I) = 290 (2), 275 (5), 217 (29), 207 (18), 191 (100), 160 (36), 135 (32), 73 (64), 59 (20). GC/FTIR: 3077 (m), 3054 (m), 2968 (s), 2909 (m), 1646 (m), 1454 (m), 1415 (m), 1377 (m), 1255 (s), 1117 (m), 1040 (m), 891 (m), 840 (s), 734 (s).

1-Trimethylsilyl-2-(4-(2,3-dimethyl-1-butenyl)methylphenylsilyl)benzene (69b):¹⁰⁰ ¹H NMR (300 MHz; C₆D₁₂): δ (multiplicity; integral; identification) = 0.108 (s; 4.5H; Si(CH₃)₃), 0.113 (s; 4.5H; Si(CH₃)₃), 0.615 (s; 1.5H; SiCH₃), 0.627 (s; 1.5H; SiCH₃), 0.93 (d, J = 6.8 Hz; 1.5H; CH₃), 0.95 (d, J = 6.8 Hz; 1.5H; CH₃), 1.21 (cmplx m; 2H;

CH₂), 1.60 (s; 1.5H; CH₃), 1.61 (s; 1.5H; CH₃), 2.40 (m; J = 6.8 Hz; 1H; allyl), 4.61 (m; 2H; vinyl). GC/MS: *m/z* (I) = 352 (2), 337 (1), 279 (31), 269 (62), 253 (24), 191 (100), 160 (33), 135 (55), 121 (31), 73 (44), 59 (7), 55 (16). GC/FTIR: 3116 (w), 3075 (m), 3057 (s), 2968 (s), 2907 (m), 1646 (m), 1454 (m), 1430 (m), 1376 (m), 1255 (s), 1109 (s), 1053 (m), 891 (m), 843 (s), 796 (s), 734 (s).

1-Trimethylsilyl-2-(4-(2,3-dimethyl-1-butenyl)diphenylsilyl)benzene (69c): ¹H NMR (300 MHz; C₆D₁₂): δ (multiplicity; integral; identification) = -0.02 (s; 9H; Si(CH₃)₃), 0.87 (d, J = 6.8 Hz; 3H; CH₃), 1.35 (m; 2H; CH₂), 1.62 (s; 3H; CH₃), 2.40 (m; 1H; allyl), 4.56 (m; 2H; vinyl). GC/MS: *m/z* (I) = 414 (12), 399 (2), 341 (24), 331 (76), 315 (10), 301 (11), 253 (100), 222 (39), 195 (42), 135 (25), 105 (32), 73 (32), 55 (16). GC/FTIR: 3075 (s), 3058 (s), 2966 (s), 2905 (m), 1644 (m), 1429 (m), 1375 (m), 1264 (s), 1108 (s), 890 (m), 842 (s), 735 (s).

Photolysis of 9 in methanolic cyclohexane: A deoxygenated cyclohexane-*d*₁₂ solution of **9** (0.02 M) containing methanol (0.05 M) was irradiated to *ca.* 50% conversion and monitored by ¹H NMR spectroscopy and GC. GC/MS analysis of the crude photolysate verified the formation of **10**, **20**, **42**, and **43**, and showed four other isomeric products which elute after **9**, and which have been tentatively assigned to **51**: GC/MS *m/z* (I) = 488 (10), 473 (38), 395 (6), 317 (13), 259 (40), 213 (100), 197 (94), 183 (74), 104 (40), 59 (14). The resonances in the ¹H NMR spectrum assigned to **51** are labelled in Figure 2.1(b).

Photolysis of 12 in methoxytrimethylsilane: A deoxygenated solution of **12** (0.01 M) in distilled methoxytrimethylsilane was photolyzed to *ca.* 80% conversion with 254 nm light. GC and GC/MS analysis revealed the formation of five major products. The one with the shortest retention time is identified as **74** on the basis of its mass spectrum: *m/z* (I) = 238

(1), 223 (100), 191 (18), 177 (9), 151 (10), 135 (11), 121 (19), 105 (9), 73 (10), 59 (16), 43 (9). The other four products eluted within 0.6 minutes of each other (but 3-4 min after 74) under the same conditions, and were identified as isomers of 73 on the basis of their virtually identical mass spectra: m/z (I) = 312 (1), 297 (3), 239 (28), 209 (7), 193 (7), 151 (30), 135 (100), 121 (12), 89 (43), 73 (67), 59 (12), 45 (22).

Photolysis of 12 in methanolic cyclohexane: Irradiation (254 nm) of a deoxygenated cyclohexane solution of 12 (0.01 M) containing 0.1 M methanol to *ca.* 10% conversion afforded five products on the basis of capillary GC and GC/MS analysis of the crude photolysate. The one with the shortest retention time is identified as dimethylmethoxyphenylsilane (76) on the basis of its mass spectrum: m/z (I) = 166 (11), 151 (100), 121 (50), 105 (11), 91 (13), 77 (8), 59 (22). The other four products eluted within 1 minute of each other but after 12 under the same conditions, and were identified as isomers of 75 on the basis of their similar mass spectra: m/z (I) = 240 (17), 239 (28), 225 (7), 151 (84), 135 (75), 121 (52), 89 (84), 73 (100), 59 (75).

Photolysis of 35 methanolic cyclohexane: A deoxygenated cyclohexane- d_{12} solution of 35 (0.05 M) containing methanol (0.05 M) was irradiated to *ca.* 40% conversion and monitored by ^1H NMR spectroscopy and GC. GC/MS analysis of the crude photolysate showed the formation of four isomeric products which elute after 35 which have been tentatively assigned to 77: GC/MS m/z (I) = 364 (6), 363 (5), 349 (3), 259 (16), 213 (100), 183 (47), 105 (16), 73 (22), 59 (6). The resonances in the ^1H NMR spectrum assigned to 77 are labelled in Figure 4.7.

REFERENCES

- (1) Raabe, G.; Michl, J. *Chem. Rev.* **1985**, *85*, 419.
- (2) Wiberg, N. *J. Organomet. Chem.* **1984**, *273*, 141.
- (3) Gusel'nikov, L.E.; Nametkin, N.S. *Chem. Rev.* **1979**, *79*, 529.
- (4) Brook, A.G. In *The Chemistry of Organic Silicon Compounds*; Patai, S. , Rappoport, Z. , Eds.; John Wiley & Sons: New York, 1989; pp 965-1005.
- (5) Brook, A.G.; Baines, K.M. *Adv. Organomet. Chem.* **1986**, *25*, 1.
- (6) Coleman, B.; Jones, M. *Rev. Chem. Intermed.* **1981**, *4*, 297.
- (7) Gusel'nikov, L.E.; Nametkin, N.S.; Vdovin, V.M. *Acc. Chem. Res.* **1975**, *8*, 18.
- (8) Corey, J.Y. In *The Chemistry of Organic Silicon Compounds*; Rappoport, Z. , Patai, S. , Eds.; John Wiley & Sons Ltd.: 1989; pp 1-56.
- (9) West, R. *Science* **1984**, *225*, 1109.
- (10) Barton, T.J.; Ijadi-Maghsoodi, S.; Magrum, G.R.; Paul, G.; Robinson, L.R.; Yeh, M.H. In *Silicon Chemistry*; Corey, E. Y., Corey, J. Y., Gaspar, P. P., Eds.; Ellis Horwood: Chichester, 1988; pp 201-210.
- (11) Maltsev, A.K.; Khabashesku, V.N.; Nefedov, O.N.; Zelinsky, N.D. In *Silicon Chemistry*; Corey, E. Y., Corey, J. Y., Gaspar, P. P., Eds.; Ellis Horwood: Chichester, 1988; pp 211-223.
- (12) Barton, T.J. *Pure Appl. Chem.* **1980**, *52*, 615.
- (13) Davidson, I.M.T. In *Silicon chemistry*; Corey, E. Y., Corey, J. Y., Gaspar, P. P., Eds.; Ellis Horwood: Chichester, 1988; pp 175-182.
- (14) Gaspar, P.P.; Holten, D.; Konieczny, S.; Corey, J.Y. *Acc. Chem. Res.* **1987**, *20*, 329.
- (15) Jackson, R.A. *Adv. Free Radical Chem.* **1969**, *3*, 231.

- (16) Alberti, A.; Pedulli, G.F. *Rev. Chem. Intermed.* **1987**, *8*, 207.
- (17) Milaev, A.G.; Okhlobystin, O.Y. *Russ. Chem. Rev.* **1980**, *49*, 1829.
- (18) Chatgililoglu, C. *Acc. Chem. Res.* **1992**, *25*, 188.
- (19) Sakurai, H. In *Free Radicals, Vol. II*; Kochi, J. K., Ed.; Wiley & Sons: New York, 1973; pp 741-808.
- (20) Lambert, J.B.; Schulz, W.J., Jr.; McConnell, J.A.; Schilf, W. In *Silicon Chemistry*; Corey, E. Y., Corey, J. Y., Gaspar, P. P., Eds.; Ellis Horwood: Chichester, 1988; pp 183-190.
- (21) Gusel'nikov, L.E.; Flowers, M.C. *J. Chem. Soc., Chem. Commun.* **1967**, 864.
- (22) Mulliken, R.S. *J. Am. Chem. Soc.* **1950**, *72*, 4493.
- (23) Valkovich, P.B.; Ito, T.I.; Weber, W.P. *J. Org. Chem.* **1974**, *39*, 3543.
- (24) Golino, C.M.; Bush, R.D.; Roark, D.N.; Sommer, L.H. *J. Organomet. Chem.* **1974**, *66*, 29.
- (25) Jutzi, P.; Langer, P. *J. Organomet. Chem.* **1980**, *202*, 401.
- (26) Brix, T.; Arthur, N.L.; Potzinger, P. *J. Phys. Chem.* **1989**, *93*, 8193.
- (27) Boudjouk, P.; Sommer, L.H. *J. Chem. Soc., Chem. Commun.* **1973**, 54.
- (28) Elsheikh, M.; Pearson, N.R.; Sommer, L.H. *J. Am. Chem. Soc.* **1979**, *101*, 2491.
- (29) Jones, P.R.; Bates, T.F.; Cowley, A.F.; Arif, A.M. *J. Am. Chem. Soc.* **1986**, *108*, 3122.
- (30) Jones, P.R.; Bates, T.F. *J. Am. Chem. Soc.* **1987**, *109*, 913.
- (31) Cheng, A.H.-B.; Jones, P.R.; Lee, M.E.; Roussi, P. *Organometallics* **1985**, *4*, 581.
- (32) Maier, G.; Mihm, G.; Reisenauer, H.P. *Angew. Chem. Int. Ed. Engl.* **1981**, *20*, 597.
- (33) Jones, P.R.; Lim, T.F.O.; Pierce, R.A. *J. Am. Chem. Soc.* **1980**, *102*, 4970.
- (34) Barton, T.J.; Burns, S.A.; Burns, G.T. *Organometallics* **1982**, *1*, 210.
- (35) Wiberg, N.; Preiner, G.; Schieda, O. *Chem. Ber.* **1981**, *114*, 3518.

- (36) Boudjouk, P.; Roberts, J.R.; Golino, C.M.; Sommer, L.H. *J. Am. Chem. Soc.* **1972**, *94*, 7926.
- (37) Sakurai, H. In *Silicon Chemistry*; Corey, J. Y., Corey, E. Y., Gaspar, P. P., Eds.; Ellis Horwood: Chichester, 1988; pp 163-172.
- (38) Shizuka, H.; Hiratsuka, H. *Res. Chem. Intermed.* **1992**, *18*, 131.
- (39) Ishikawa, M. *Pure Appl. Chem.* **1978**, *50*, 11.
- (40) Sakurai, H. *J. Organomet. Chem.* **1980**, *200*, 261.
- (41) Ishikawa, M.; Kumada, M. *Adv. Organomet. Chem.* **1981**, *19*, 51.
- (42) Ishikawa, M.; Fuchikami, T.; Kumada, M. *J. Organomet. Chem.* **1976**, *117*, C58.
- (43) Ishikawa, M.; Fuchikami, T.; Kumada, M. *J. Organomet. Chem.* **1978**, *149*, 37.
- (44) Sakurai, H.; Kamiyama, Y.; Nakadaira, Y. *J. Am. Chem. Soc.* **1976**, *98*, 7424.
- (45) Brook, A.G.; Kallury, R.K.M.R.; Poon, Y.C. *Organometallics* **1982**, *1*, 987.
- (46) Brook, A.G.; Nyburg, S.C.; Abdesaken, F.; Gutekunst, B.; Gutekunst, G.; Kallury, R.K.M.R.; Poon, Y.C.; Chang, Y.; Wong-Ng, W. *J. Am. Chem. Soc.* **1982**, *104*, 5667.
- (47) Brook, A.G.; Nyburg, S.C.; Reynolds, W.F.; Poon, Y.C.; Chang, Y.; Lee, J.S. *J. Am. Chem. Soc.* **1979**, *101*, 6750.
- (48) Brook, A.G.; Harris, J.W.; Lennon, J.; El Sheikh, M. *J. Am. Chem. Soc.* **1979**, *101*, 83.
- (49) Ando, W.; Sekiguchi, A.; Sato, T. *J. Am. Chem. Soc.* **1982**, *104*, 6830.
- (50) Ando, W.; Sekiguchi, A.; Sato, T. *J. Am. Chem. Soc.* **1981**, *103*, 5573.
- (51) Arrington, C.A.; Klingensmith, K.A.; West, R.; Michl, J. *J. Am. Chem. Soc.* **1984**, *106*, 525.
- (52) Wiberg, N.; Wagner, G.; Muller, G.; Riede, J. *J. Organomet. Chem.* **1984**, *271*, 381.
- (53) Wiberg, N.; Wagner, G. *Chem. Ber.* **1986**, *119*, 1467.

- (54) Jones, P.R.; Cheng, A.H.; Albanesi, T.E. *Organometallics* **1984**, *3*, 78.
- (55) Bernardi, F.; Bottoni, A.; Olivucci, M.; Robb, M.A.; Venturini, A. *J. Am. Chem. Soc.* **1993**, *115*, 3322.
- (56) Apeloig, Y.; Karni, M. *J. Am. Chem. Soc.* **1984**, *106*, 6676.
- (57) Cooper, J.; Hudson, A.; Jackson, R.A. *J. Chem. Soc., Perkin Trans. II.* **1973**, 1933.
- (58) Kira, M.; Maruyama, T.; Sakurai, H. *J. Am. Chem. Soc.* **1991**, *113*, 3986.
- (59) Brook, A.G.; Safa, K.D.; Lickiss, P.D.; Baines, K.M. *J. Am. Chem. Soc.* **1985**, *107*, 4338.
- (60) Bush, R.D.; Golino, C.M.; Homer, G.D.; Sommer, L.H. *J. Organomet. Chem.* **1974**, *80*, 37.
- (61) Roark, D.N.; Sommer, L.H. *J. Chem. Soc., Chem. Commun.* **1973**, 167.
- (62) Brook, A.G.; Chatterton, W.J.; Sawyer, J.F.; Hughes, D.W.; Vorspohl, K. *Organometallics* **1987**, *6*, 1246.
- (63) Leigh, W.J.; Bradaric, C.J.; Sluggett, G.W. *J. Am. Chem. Soc.* **1993**, *115*, 5332.
- (64) Davidson, I.M.T.; Dean, C.E.; Lawrence, F.T. *J. Chem. Soc., Chem. Commun.* **1981**, *1981*, 52.
- (65) Davidson, M.T.; Wood, I.T. *J. Chem. Soc., Chem. Commun.* **1982**, 550.
- (66) Sander, W.; Trommer, M. *Chem. Ber.* **1992**, *125*, 2813.
- (67) Chatgililoglu, C.; Scaiano, J.C.; Ingold, K.U. *Organometallics* **1982**, *1*, 466.
- (68) Walsh, R. In *The Chemistry of Organic Silicon Compounds*; Patai, S., Rappoport, Z., Eds.; John Wiley & Sons Ltd.: 1989; pp 371-391.
- (69) Chatgililoglu, C.; Ingold, K.U.; Scaiano, J.C. *J. Am. Chem. Soc.* **1982**, *104*, 5123.
- (70) Chatgililoglu, C.; Ingold, K.U.; Scaiano, J.C. *J. Am. Chem. Soc.* **1982**, *104*, 5119.
- (71) Chatgililoglu, C.; Ingold, K.U.; Scaiano, J.C. *J. Am. Chem. Soc.* **1983**, *105*, 3292.

- (72) Chatgililoglu, C.; Ingold, K.U.; Lusztyk, J.; Nazran, A.S.; Scaiano, J.C. *Organometallics* **1983**, *2*, 1332.
- (73) Kopping, B.; Chatgililoglu, C.; Zehnder, M.; Giese, B. *J. Org. Chem.* **1992**, *57*, 3994.
- (74) Speier, J.L. *Adv. Organomet. Chem.* **1979**, *17*, 407.
- (75) Hague, D.N.; Prince, R.H. *J. Chem. Soc.* **1965**, *1965*, 4690.
- (76) Gilman, H.; Atwell, W.H.; Schwebke, G.L. *J. Organomet. Chem.* **1964**, *2*, 369.
- (77) Hague, D.N.; Prince, R.H. *Chem. Ind.* **1964**, *1964*, 1492.
- (78) Sakurai, H.; Kumada, M. *Bull. Chem. Soc. Jpn.* **1964**, *37*, 1894.
- (79) Pitt, C.G.; Bock, H. *J. Chem. Soc., Chem. Commun.* **1972**, *1972*, 28.
- (80) Sakurai, H.; Tasaka, S.; Kira, M. *J. Am. Chem. Soc.* **1972**, *94*, 9285.
- (81) Sakurai, H.; Sugiyama, H.; Kira, M. *J. Phys. Chem.* **1990**, *94*, 1837.
- (82) Shizuka, H.; Okazaki, K.; Tanaka, M.; Ishikawa, M.; Sumitani, M.; Yoshihara, K. *Chem. Phys. Lett.* **1985**, *113*, 89.
- (83) Shizuka, H.; Sato, Y.; Ishikawa, M.; Kumada, M. *J. Chem. Soc., Chem. Commun.* **1982**, 439.
- (84) Shizuka, H.; Obuchi, H.; Ishikawa, M.; Kumada, M. *J. Chem. Soc., Chem. Commun.* **1981**, 405.
- (85) Shizuka, H.; Sato, Y.; Ueki, Y.; Ishikawa, M.; Kumada, M. *J. Chem. Soc., Far. Trans. 1* **1984**, *80*, 341.
- (86) Shizuka, H.; Obuchi, H.; Ishikawa, M.; Kumada, M. *J. Chem. Soc., Far. Trans. 1* **1984**, *80*, 383.
- (87) Hiratsuka, H.; Mori, Y.; Ishikawa, M.; Okazaki, K.; Shizuka, H. *J. Chem. Soc., Far. Trans. 2* **1985**, *81*, 1665.
- (88) Shizuka, H. *Pure Appl. Chem.* **1993**, *65*, 1635.
- (89) Kira, M.; Miyazawa, T.; Sugiyama, H.; Yamaguchi, M.; Sakurai, H. *J. Am. Chem. Soc.* **1993**, *115*, 3116.

- (90) Rettig, W. *Angew. Chem. Int. Ed. Engl.* **1986**, *25*, 971.
- (91) Horn, K.A.; Whitenack, A.A. *J. Phys. Chem.* **1988**, *92*, 3875.
- (92) Sakurai, H.; Kira, M. *J. Am. Chem. Soc.* **1974**, *96*, 791.
- (93) Sakurai, H.; Kira, M. *J. Am. Chem. Soc.* **1975**, *97*, 4879.
- (94) Ishikawa, M.; Oda, M.; Nishimura, K.; Kumada, M. *Bull. Chem. Soc. Jpn.* **1983**, *56*, 2795.
- (95) Ishikawa, M.; Fuchikami, T.; Kumada, M. *J. Organomet. Chem.* **1976**, *118*, 155.
- (96) Ishikawa, M.; Sakamoto, H. *J. Organomet. Chem.* **1991**, *414*, 1.
- (97) Ishikawa, M.; Fuchikami, T.; Sugaya, T.; Kumada, M. *J. Am. Chem. Soc.* **1975**, *97*, 5923.
- (98) Ishikawa, M.; Fuchikami, T.; Kumada, M. *J. Organomet. Chem.* **1978**, *162*, 223.
- (99) Ishikawa, M.; Fuchikami, T.; Kumada, M. *J. Organomet. Chem.* **1977**, *127*, 261.
- (100) Ishikawa, M.; Fuchikami, T.; Kumada, M. *J. Organomet. Chem.* **1976**, *118*, 139.
- (101) Ishikawa, M.; Nakagawa, K.; Enokida, R.; Kumada, M. *J. Organomet. Chem.* **1980**, *201*, 151.
- (102) Ishikawa, M.; Fuchikami, T.; Kumada, M. *J. Organomet. Chem.* **1977**, *133*, 19.
- (103) Ishikawa, M.; Fuchikami, T.; Kumada, M. *J. Organomet. Chem.* **1979**, *173*, 117.
- (104) Ishikawa, M.; Kikuchi, M.; Watanabe, K.; Sakamoto, H.; Kunai, A. *J. Organomet. Chem.* **1993**, *443*, C3.
- (105) Ishikawa, M.; Kikuchi, M.; Kunai, A.; Takeuchi, T.; Tsukihara, T.; Kido, M. *Organometallics* **1993**, *12*, 3474.
- (106) Sakurai, H.; Nakadaira, Y.; Kira, M.; Sugiyama, H.; Yoshida, K.; Takiguchi, T. *J. Organomet. Chem.* **1980**, *184*, C36.
- (107) Ito, O.; Hoteiya, K.; Watanabe, A.; Matsuda, M. *Bull. Chem. Soc. Jpn.* **1991**, *64*, 962.
- (108) Leigh, W. J.; Sluggett, G. W. *Organometallics* **1993**, in press.

- (109) Sluggett, G.W.; Leigh, W.J. *J. Am. Chem. Soc.* **1992**, *114*, 1195.
- (110) Leigh, W.J.; Workentin, M.S.; Andrew, D. *J. Photochem. Photobiol. A: Chem.* **1991**, *57*, 97.
- (111) Leigh, W.J.; Banisch, J.H., unpublished results.
- (112) Sluggett, G.W.; Leigh, W.J. *Organometallics* **1992**, *11*, 3731.
- (113) Levin, G.; Das, P.K.; Bilgrien, C.; Lee, C.L. *Organometallics* **1989**, *8*, 1206.
- (114) Gaspar, P.P.; Boo, B.H.; Chari, S.; Ghosh, A.K.; Holten, D.; Kirmaier, C.; Konieczny, S. *Chem. Phys. Lett.* **1984**, *105*, 153.
- (115) Conlin, R.T.; Netto-Ferreira, J.C.; Zhang, S.; Scaiano, J.C. *Organometallics* **1990**, *9*, 1332.
- (116) Shizuka, H.; Tanaka, H.; Tonokura, K.; Murata, K.; Hiratsuka, H.; Ohshita, J.; Ishikawa, M. *Chem. Phys. Lett.* **1988**, *143*, 225.
- (117) Levin, G.; Das, P.K.; Lee, C.L. *Organometallics* **1988**, *7*, 1231.
- (118) Smith, G.J. *J. Photochem.* **1983**, *22*, 51.
- (119) Murov, S.L. *Handbook of Photochemistry*; Dekker: New York, 1973;
- (120) Sluggett, G. W.; Leigh, W. J. *Organometallics* **1993**, in press.
- (121) Leigh, W.J.; Sluggett, G.W. *J. Am. Chem. Soc.* **1993**, *115*, 7531.
- (122) Nakadaira, Y.; Sekiguchi, A.; Funada, Y.; Sakurai, H. *Chem. Lett.* **1991**, 327.
- (123) Nakadaira, Y.; Komatsu, N.; Sakurai, H. *Chem. Lett.* **1985**, 1781.
- (124) Igarashi, M.; Ueda, T.; Wakasa, M.; Sakaguchi, Y. *J. Organomet. Chem.* **1991**, *421*, 9.
- (125) Workentin, M.S., unpublished results.
- (126) Andrieux, C.P.; Le Gorande, A.; Saveant, J.-M. *J. Am. Chem. Soc.* **1992**, *114*, 6892.
- (127) Saveant, J.-M. *Adv. Phys. Org. Chem.* **1990**, *26*, 1.

- (128) Mann, C.K.; Barnes, K.K. *Reactions of the Carbon-Halogen Bond*; Marcel Dekker, Inc.: New York, 1970; pp 201-244.
- (129) Gilman, H.; Lichtenwalter, G.D. *J. Am. Chem. Soc.* **1958**, *80*, 608.
- (130) Gilman, H.; Peterson, D.J.; Wittenberg, D. *Chem. Ind.* **1958**, 1479.
- (131) Ishikawa, M.; Nishimura, Y.; Sakamoto, H. *Organometallics* **1991**, *10*, 2701.
- (132) Hatchard, C.G.; Parker, C.A. *Proc. R. Soc.* **1956**, *235A*, 518.
- (133) Lissi, E.A.; Encinas, M.V. In *CRC Handbook of Photochemistry, Vol. II*; Scaiano, J. C., Ed.; CRC Press: Boca Raton, 1989; pp 111-176.
- (134) Leigh, W.J.; Banisch, J.H.; Sluggett, G.W., unpublished results.
- (135) Aloni, R.; Rajbenbach, L.A.; Horowitz, A. *Internat. J. Chem. Kinet.* **1979**, *11*, 899.
- (136) Wintgens, V. In *CRC Handbook of Organic Photochemistry, Vol. I*; Scaiano, J. C., Ed.; CRC Press: Boca Raton, 1989; pp 405-418.
- (137) Choo, K.Y.; Gaspar, P.P. *J. Am. Chem. Soc.* **1974**, *96*:5, 1284.
- (138) Ingold, K.U.; Luszyk, J.; Scaiano, J.C. *J. Am. Chem. Soc.* **1984**, *106*, 343.
- (139) Chatgililoglu, C.; Griller, D.; Lesage, M. *J. Org. Chem.* **1989**, *54*, 2492.
- (140) Chatgililoglu, C.; Ingold, K.U.; Scaiano, J.C. *J. Org. Chem.* **1987**, *52*, 938.
- (141) Chatgililoglu, C. In *CRC Handbook of Photochemistry, Vol II*; Scaiano, J. C., Ed.; CRC Press: Boca Raton, 1989; pp 3-11.
- (142) Krapivin, A.M.; Magi, M.; Svergun, V.I.; Zaharjan, R.Z.; Babich, E.D.; Ushakov, N.V. *J. Organomet. Chem.* **1980**, *190*, 9.
- (143) Webster, D.E. *J. Chem. Soc.* **1960**, 5132.
- (144) Scaiano, J.C. In *CRC Handbook of Photochemistry, Vol II*; Scaiano, J. C., Ed.; CRC Press: Boca Raton, 1989; pp 343-346.
- (145) Turro, N.J. *Modern Molecular Photochemistry*; Benjamin/Cummings: Menlo Park, 1978; pp 107-108.

- (146) Melander, L.; Saunders, W.H. *Reaction Rates of Isotopic Molecules*; Wiley-Interscience: New York, 1980
- (147) Klasnic, L. *Int. J. Quantum Chem.* **1978**, *5*, 373.
- (148) Young, V.Y.; Cheng, K.L. *J. Chem. Phys.* **1976**, *65*, 3187.
- (149) Agosta, W.C.; Wolff, S. *J. Am. Chem. Soc.* **1977**, *99*, 3355.
- (150) Beckwith, A.L.J. *Tetrahedron* **1981**, *37*, 3073.
- (151) Sander, W.W. *J. Org. Chem.* **1989**, *54*, 333.
- (152) Tomadze, A.V.; Yablokova, N.V.; Yablokov, V.A.; Razuvaev, G.A. *J. Organomet. Chem.* **1981**, *212*, 43.
- (153) Okinoshima, H.; Weber, W.P. *J. Organomet. Chem.* **1978**, *149*, 279.
- (154) Soysa, H.S.D.; Weber, W.P. *J. Organomet. Chem.* **1979**, *173*, 269.
- (155) Farris, J.M.; MacInnes, I.; Walton, J.C.; Maillard, B. *J. Organomet. Chem.* **1991**, *403*, C25.
- (156) Griller, D.; Liu, M.T.H.; Scaiano, J.C. *J. Am. Chem. Soc.* **1982**, *104*, 5549.
- (157) Moss, R.A.; Shen, S.; Hadel, L.M.; Kmieciak-Lawrynowicz, G.; Wlostowska, J.; Krogh-Jespersen, K. *J. Am. Chem. Soc.* **1987**, *109*, 4341.
- (158) McClelland, R.A.; Chan, C. *Angew. Chem. Int. Ed. Engl.* **1991**, *30*, 1337.
- (159) Bachrach, S.M.; Streitwieser, A., Jr. *J. Am. Chem. Soc.* **1985**, *107*, 1186.
- (160) Barton, T.J.; Hussmann, G.P. *Organometallics* **1983**, *2*, 692.
- (161) Blinka, T.A.; Helmer, B.J.; West, R. *Adv. Organomet. Chem.* **1984**, *23*, 193.
- (162) Battino, R.; Rettich, T.R.; Tominaga, T. *J. Phys. Chem. Ref. Data.* **1983**, *12*, 163.
- (163) Swaim, R.E.; Weber, W.P.; Boettger, H.G.; Evans, M.; Bockhoff, F.M. *Org. Mass. Spect.* **1980**, *15*, 304.
- (164) Brook, A.G.; Gilman, H. *J. Am. Chem. Soc.* **1955**, *77*, 2322.
- (165) Brook, A.G.; Dillon, P.J. *Can. J. Chem.* **1969**, *47*, 4347.
- (166) Sakurai, H.; Tominaga, K.; Watanabe, T.; Kumada, M. *Tet. Lett.* **1966**, 5493.

- (167) Gilman, H; Dunn, G.E. *J. Am. Chem. Soc.* **1951**, *73*, 5077.
- (168) Bunce, N.J.; LaMarre, J.; Vaish, S.P. *Photochemistry and Photobiology* **1984**, *39*, 531.